Proceedings of the 3. International Conference on Luminescence Dosimetry

Research Establishment Risø, Roskilde

Publication date:
1971

Document Version
Publisher's PDF, also known as Version of record

Risø Report No. 249
Part III (pp. 880 - 1229)

Risø Report No. 249
Part III (pp. 880 - 1229)

Danish Atomic Energy Commission
Research Establishment Risø

Proceedings of The Third International Conference on Luminescence Dosimetry, held at the Danish AEC Research Establishment Risø 11-14 October 1971

Sponsored by The Danish Atomic Energy Commission and
The International Atomic Energy Agency

December 1971

Sales distributors: Jul. Gjellerup, 87, Sølvgade, DK-1307 Copenhagen K, Denmark
Available on exchange from: Library, Danish Atomic Energy Commission, Risø, DK-4000 Roskilde, Denmark

December 1971

Risø Report No. 249
Part III (pp. 880-1229)

Proceedings of the Third International Conference on Luminescence Dosimetry

Held at

The Danish Atomic Energy Commission
Research Establishment Risø

October 11-14 1971

Sponsored by

The Danish Atomic Energy Commission

and

International Atomic Energy Agency

Editor

V. Mejdahl

ISBN 87 550 0120 3
ISBN 87 550 0124 6

CONTENTS

PART I

New Techniques of Thermoluminescent Dating of Ancient Pottery: I. The Subtraction Method

by

S.J. Fleming and D. Stoneham.

The Research Laboratory for Archaeology
and History of Art
6, Keble Road, Oxford.

ABSTRACT

Accurate thermoluminescent dating has been possible over the past three years, using two routine techniques termed the fine-grain and inclusion methods, provided a reasonable knowledge of the burial circumstances (i.e. soil radioactivity and water uptake) has been established from 'on site' measurements. The absence of that information has previously been a justification for rejection of some sites from attempts at dating. However the two routine methods differ in one essential feature. The source of dosage of fine-grains (around 1 micron in diameter) in pottery are all three forms of natural radiation, α , β and δ (and a small cosmic-ray component). Quartz grains (around 100 microns in diameter) embedded in the clay matrix only experience β and δ radiation as the α-radiation that originates in the matrix only partially penetrates such large crystals. Use of the two methods 'in tandem' allows the environmental component to be eliminated. The difference of the archaeological doses each method yields leaves a dose dependent only upon the single component of α-radiation, a parameter that is internal to the pottery.

The importance of factors such as sherd water uptake, radon emanation and pottery pore size are discussed with respect to the subtraction technique and exampled by material from the Roman Fort at Paginton, England. Applications of the new method are given for (i) pottery from Yotoco Ferry, Columbia, (ii) pottery from the Neolithic site of Hacilar in Turkey, and (iii) an Etruscan Bust in terracotta. Age determination here is estimated to have an accuracy of around $\pm 12\%$, but it is stressed that close note must be made of various pottery parameters that control that accuracy before the length process of the subtraction technique is embarked upon.

Introduction

The general principles of dating using the thermoluminescent (TL) method have already been extensively discussed.[3] Two TL techniques involving different approaches to sample preparation are now routinely used - the fine-grain method[15] and the inclusion method[4]. To understand the difference between the two techniques, which have been developed to overcome problems of two inhomogeneities found in pottery, it is necessary to briefly review the micro-dosimetry of pottery fabrics. As Plate 1 illustrates, the fabric of pottery may be described as a matrix of amorphous fired clay in which is embedded a variety of crystalline minerals (such as quartz and feldspars) in a whole range of grain sizes. The TL observed is dominantly emitted by the crystalline inclusions, while the matrix itself emits little or no TL.[6] However the inclusions are virtually free of internal self-radioactivity due to uranium and thorium, while in the specific case of quartz grains even the beta-emitting radioactive potassium (^{40}K) is absent.[7] Thus the pottery's radioactivity is carried by the fired clay matrix. Consequently alpha particles arising from radioactive disintegrations occurring at the inclusion/matrix interface will only penetrate around 25 microns on average, while particles originating from further away in the matrix will be appropriately less penetrating. Hence the radiation environment of each size of inclusion in the pottery fabric is different. Grains of around 1 micron diameter experience full alpha, beta and gamma radiation dosage; larger grains of 100 microns and more have large internal regions where little or no alpha radiation dosage occurs, so that their source of dosage is primarily the longer-ranged beta and gamma radiation.

By gentle, controlled, crushing of the pottery, grains from both size categories can be extracted as the adhesion between the crystals and their clay host seems to yield before grain damage occurs. The smaller grains are used in the fine-grain technique while the larger grains are used in the inclusion technique. For the former the sample is prepared by deposition of the 1-5 micron grains onto thin aluminium discs out of an acetone suspension. The uniform pottery powder layer is then in a convenient form for alpha-irradiation in the laboratory. This allows the efficiency of that radiation to be compared with the efficiency of beta or gamma radiation in inducing TL storage. This relative factor is usually termed the k-value.[1]

A crystalline extract in the 100 micron grain size range is obtained using the standard geological technique of magnetic separation. The next step is to reduce the extract to a quartz concentrate by etching with hydrofluoric acid, which removes less resistant minerals, like the feldspars present, while cleaning the quartz grains free of surface contamination.[7] Such contamination occurs as elements from the clay matrix diffuse into the outer regions of the quartz during kiln-firing and these impurities are able to form TL trapping sites. But their close proximity to the matrix radioactivity negates the inclusion dating principles, namely, that the alpha radiation dosage of these large quartz grains can be ignored compared with the dosage due to beta and gamma radiation that they 'see'.

The subtraction technique: some theoretical considerations

The difference between the radiation dosimetries of each grain size means, inevitably, that the archaeological dosages predicted by TL analysis using the two routine approaches differ. The difference is a direct reflection of the alpha radiation dose the fine-grains of quartz have received, so we may write down the following equations:

$$A + B + G = F \quad (1)$$

$$fB + G = I \quad (2)$$

$$\text{and} \quad \frac{A}{B} = \frac{\alpha T}{\beta T} \quad (3)$$

where A, B, and G are the archaeological dosages experienced by the pottery due to alpha, beta and environmental radiation respectively. F is then the fine-grain accumulated dosage and I is the inclusion accumulated dosage, both expressed in rads. f expresses the magnitude of beta radiation attenuation due to grain size, an effect similar to that discussed above for alpha radiation but an order of magnitude less severe. α and β are the annual dose-rates obtained from radioactive analysis, so that for T expressing the age, equation (3) acts as a link between A and B.

From equations (1) to (3) we obtain A through

$$A\left(1 + (1-f)\frac{\beta}{\alpha}\right) = F - I \quad (4)$$

$$\text{and Age} = A/\alpha \quad (5)$$

The important feature of equations (4), (5) is that the age determination they yield has no dependence upon the environmental dose component - dating is possible through knowledge only of internal parameters of the pottery.

A complicating factor in application of these simultaneous equations is the variation of α and β with the environmental conditions prevalent at any specific time. Firstly, during burial the pottery sherd takes up water in its fine pores to a level tending to fluctuate seasonally. The water acts as a radiation-absorber and so lowers the dose that the quartz grains in the pottery experience. Indeed it is more effective in stopping radiation than clay fabric by some 25% for beta radiation and close to 50% for alpha radiation.[4,5] A similar argument applies to ground water percolating through the soil of the burial context so that the gamma radiation environmental dose that arises from that context is also subject to seasonal variations, but the water is only 14% more effective than the soil constituents in radiation absorption.

Secondly, in the uranium decay series there is a gaseous emanation, radon-222 with a half-life of 3.84 days and an inert chemical nature that allows a high degree of mobility of the radioisotope through dry porous media like pottery and soil. Diffusion lengths of up to 2 metres have been recorded in sandy soil.[13] However, in soaking wet conditions the freedom of gas diffusion is drastically reduced (typically to ranges of travel of less than 2 cms) though displacement of radon is still possible over distances of as much as a metre by a direct transportation mechanism. Then with a view to estimation of annual dose-rate that the pottery experiences, close watch must be kept upon the two extreme conditions, (i) dry, radon-lossy and (ii) wet, radon-retaining. These considerations are particularly important in the soil as 98% of the gamma dose associated with the uranium decay series lies beyond radon while only 56% of the alpha and beta dose delivered by the uranium content of the pottery is after the gaseous decay. So it is anticipated that fluctuations, both long and short term, in the wetness of the archaeological context, will effect the environmental dose-rate more than the internal dose-rate, and make estimates of the former using present day knowledge of site less reliable than preferred.

The subtraction technique, based on equations (1) to (5) is the response to this lack of confidence in our present knowledge about burial conditions. However, before discussing application of this new approach it is

appropriate to introduce one further consequence of investigations of water uptake of pottery. In coarser pottery fabric we must anticipate the presence of many large pores and many thick clay walls of dimensions in the 10 microns plus range. Then it is necessary to reconsider the alpha radiation microdosimetry to some degree. A fine quartz grain embedded in the centre of a thick clay wall experiences an alpha dosage, from radioactivity in that wall, completely unaffected by the presence or absence of water in the adjoining pores. The enhanced dependence of the alpha dose-rate, α , in equation (5) upon the level of water uptake of the sherd (by virtue of the relatively higher stopping power of water for that type of radiation compared with beta or gamma radiation) enables the subtraction technique to be a suitable research tool in the investigation of this internal dosimetry problem.

Practical examples of the subtraction technique

Two sherds from the Roman site of Baginton in England (dating close to AD 70) and the soil samples from their associated burial contexts are used here as examples of the subtraction technique. The relevant data of the internal radioactivity of each sherd and of their TL analysis are given in Table 1, while Figs. 1, 2 illustrate the glow curves of the fine-grain and inclusion extracts of one of them (sherd 90e2). Details of the methods of determination of sherd saturation water uptake and radon emanation power in radioactive analysis and of methods of correction for supralinearity in radiation response in TL analysis are described elsewhere.[7,15]

Table 1

	Sherd 90e2	Sherd 90h15
Annual dose-rate (millirads per year)		
Saturation water uptake (% of dry sherd weight)	6.6	33.0
Measured k-value	0.145	0.138
Alpha radiation dose-rate: dry	181	204
wet	193	162
Preferred alpha dose-rate:	192	164
Beta radiation dose-rate: dry	163	240
wet	159	179
Preferred beta dose-rate	159	182

Archaeological dose (rads) from glow-curve analysis	(Sherd 90e2)	(Sherd 90h15)
Fine grain total	890	805
Including a supralinearity correction of	30	120
Inclusion total	500	465
Including a supralinearity correction of	15	0
Subtraction age (from equations (1) to (5) :	1960 years (AD 10)	1960 years (AD 10)

.....

The preferred dose-rates in this Table were chosen by assuming a retention of water during burial at the level of 95% of saturation with an uncertainty in that estimate of ±5%. This was expected in the climatic conditions of Britain and vindicated by measurement of the water held by both sherds immediately after their removal from burial. (In this respect the sherd 90h15 seemed particularly remarkable.)

The major sources of error in the dating method are (i) systematic errors in absolute calibration of the radioactive sources used in laboratory determination of the pottery's susceptibility to alpha and beta radiation (estimated at ±7.5% and ±5% respectively, in practice), and (ii) the random error obtained by combination of the error in archaeological dose estimated from each routine method, remembering that it is imposed on an alpha-dose value which is the difference of those quantities and usually smaller than either. Other smaller errors arise in statistical and reproducibility uncertainties in radioactivity analysis.[1]

For sherd 90e2 systematic errors amount to around ±8.3% and random errors to around ±8.2% yielding an overall uncertainty in age determination of ±11.7% (or ±230 years).

For sherd 90h15 systematic errors amount to around ±9.3% and random errors to around ±9.1% yielding an overall uncertainty in age determination of ±13.0% (or ±255 years).

The good agreement between the known age of the site (1900 ±10 years), while illustrating the subtraction method's potential, also stresses the importance of the water correction in TL dating. The sherds represent practical

TABLE 2 : The Subtraction Technique applied to dating problems

		YOTOCO FERRY		HACILAR		ETRUSCAN BUST
	SHERD :	145a3	145a7	36a1	36a2	81j34
Annual dose-rate (millirads/year)						
Saturation water uptake (% of dry weight)		15.1	11.6	14.4	9.3	10.8
Measured k-value		0.21	0.27	0.087	0.18	0.19
Alpha radiation dose-rate:	dry	152	246	63	120	530
	wet	194	237	54	115	475
Preferred alpha dose-rate (with assumed fractional water uptake quoted)		186	239	56	116	486
		(0.8±0.2)	(0.8±0.2)	(0.8±0.2)	(0.8±0.2)	(0.8±0.2)
Preferred beta dose-rate		86	58	90	193	233
Archaeological dose (rads) from glow-curve analysis						
Fine grain total		390	370	1565	2895	1705
Including a supralinearity correction of		10	0	305	265	385
Inclusion total		188	133	1075	1820	790
Including a supralinearity correction of		44	0	20	0	0
Subtraction age (years) :		1060	1060	8170	8610	1830
		±140	±130	±1100	±1020	±270

extremes of water uptake, yet both yield good dating results when the water correction is fully applied. This suggests that the wall thicknesses between the pores in the pottery fabric are thin compared with an alpha particle's range.

In turn, through equations (1) and (2) the annual environmental dose-rate may be determined that is appropriate to the 'subtraction age' of each sherd and represents a mean value for that archaeological time span. Values of 105 and 64 millirads/year result for the contexts of 90e2 and 90h15, respectively, with errors of approximately ±25% and 40%. For comparison a soil sample, of some 50g weight, was collected from each context for radioactive analysis. Annual dose-rates which represent the present day site conditions were deduced as 124 and 94 millirads/year for the two contexts, again using a water correction of 95% of saturation uptake. Assuming the rest of the data used in the age calculation to be accurate, the difference between the 'subtraction' and 'in situ' environmental levels give an order of magnitude to the long term fluctuations that might have occurred in burial conditions.

Examples of archaeological dating significance

Three particular problems were tackled, where no soil samples were available at the time of TL analysis, to illustrate the involvement of the subtraction technique in fresh archaeological problems (Table 2). In each case the results are correlated to some independent information on dating.

(i) Dating of pottery from Yotoco Ferry, Columbia

Two sherds (145a3, a7) were selected from a group investigated in a broader dating programme of Yotoco style ware[9] as their high dependence upon alpha radiation in their internal dosimetry suggested they would yield good 'subtraction' results (see Table 2). Notably it is the high k-values of the sherds that create this situation as the pottery itself contains comparatively low levels of uranium, thorium and radioactive potassium. Further the low internal beta radiation levels place high emphasis upon the environment in the inclusion dating approach.

For this site a water correction of 80% of saturation is employed in line with some rough guides from archaeological reports. The common TL age obtained of 1060 years (AD 910) agrees reasonably well with conventional radiocarbon dates for the context of AD 1100 ±140 (IVIC-598) and AD 1175 ±65 (GrN-4694).

(ii) Dating of sherds from Hacilar, Turkey

Sherds 36a1, a2 were available from the level I of the early Neolithic site of Hacilar in the Burdur region of Turkey,[8] the earliest phase of which has a mean conventional radiocarbon date of 5090 B.C. ±119. (P.315) 'Subtraction' dates of 8170 years (6200 B.C.) and 8610 years (6640 B.C.) were obtained assuming once more a site water correction of 80% saturation from knowledge that the site is well-drained but has an annual rainfall level similar to many British sites. Error in this assumption would scarcely effect the TL age of sherd 36a2 (see Table 2) as corrections for water uptake and radon retention operate in opposite directions and almost cancel here - the preferred date,even in dry conditions,only moves down to 6130 B.C. For sherd 36a1 this change of assumption would be more drastic, moving the preferred TL age to 5300 B.C.

For comparison two alternatives for dating are available which are in some contradiction. There has been much recent discussion of a long-term deviation of conventional radiocarbon ages from dates obtained by dendrochronology[12] and the precisely-established early Egyptian chronology.[10] However knowledge gleaned from these sources only reach back to around 5300 B.C. at which time conventional radiocarbon ages appear to be some 1000 years too young. From Scandinavian varve chronology for the period of 6000 B.C. to 10500 B.C.[14] conventional radiocarbon dates seem to be correct once more, though lake sediment studies by Stuiver[11] indicate that the correction remains at about 1000 years during this period. The results for Hacilar using TL dating would tend to support the latter conclusion, though from Table 1 it will be seen that the former cannot be completely ruled out having regard to the limits of error of the results.

(iii) Authenticity of an Etruscan Bust

A particularly practical use of the subtraction technique is dating of large terracottas from Museum collections where there is unlikely to be any information whatsoever available on original environment after cleaning and restoration. Such a piece is the Bust of Plate 2. The subtraction age, derived from an analysis of a fragment of the Bust, authenticates its period at AD 140 ±270 in agreement with art historical judgements that claim the piece as Etruscan and dating circa 3rd to 2nd century B.C. While completing the essential work on this Bust, that is to say authenticating it, it is interesting to compare the environmental dose-rate predicted in conjunction with the 'subtraction age', of 203 millirads/year (±30%, approximately), to an alternative estimate assuming the Bust is sufficiently large to yield its own self-dosage, calculated at 217 millirads/year.

Conclusions

It is apparent from the examples given that, if care is taken in choosing which pieces of pottery from a group should be so extensively analyzed (i.e. details of k-value, radioactivity levels and quality of glow curves are carefully weighed up), the subtraction technique has great potential in dating sites where no environmental information is available. Such sites would otherwise be rejected from routine TL analysis.

Acknowledgements

Financial support for this project was given by the Nuffield Foundation. The authors also wish to thank the Metropolitan Museum of Art (New York), the Ashmolean Museum, Dr. W. Bray (of the Institute of Archaeology, London) and Mr. B. Hobley for their cooperation in supplying the pottery samples used in the paper. The assistance of Mr. J.C. Alldred in analysis of dating errors was invaluable and duly appreciated.

References:

1. M.J. Aitken, J.C. Alldred, Archaeometry, 14 (2), in press (1972).

2. M.J. Aitken, M.S. Tite, and S.J. Fleming, Luminescent Dosimetry, 490-501 (1967). (U.S. Atomic Energy Commission, edited by F.H. Attix)

3. M.J. Aitken, M.S. Tite, and S.J. Fleming, Nature 219, 442-444 (1968).

4. M.J. Berger and S.M. Seltzer, Studies in Penetration of Charged Particles in Matter, 205-268 (1964). (Publ. 1133 NAS-NRC, Washington D.C.)

5. R.D. Evans, The Atomic Nucleus, 714 (1955). (McGraw-Hill, New York)

6. S.J. Fleming, Archaeometry, 9, 170-173 (1966).

7. S.J. Fleming, Archaeometry 12 (2), 135-146 (1970).

8. J. Mellaart, Excavations at Hacilar I and II (1970) (Edinburgh).

9. E.H. Sampson, S.J. Fleming, W. Bray, Archaeometry, 14 (1), in press (1972).

10. T. Säve-Soderbergh, I.V. Olsson, Radiocarbon Variations and Absolute Chronology, 35-56 (1970) (Almqvist and Wiksell, Stockholm).

11. M. Stuiver, Radiocarbon Variations and Absolute Chronology, 197-214 (1970) (Almqvist and Wiksell, Stockholm).

12. H.E. Suess, Radiocarbon Variations and Absolute Chronology, 303-312 (1970) (Almqvist and Wiksell, Stockholm).

13. A.B. Tanner, The Natural Radiation Environment, 161-90 (1964) (J.A.S. Adams and W.M. Lowder, eds.).

14. H. Tauber, Radiocarbon Variations and Absolute Chronology, 173-198 (1970) (Almqvist and Wiksell, Stockholm).

15. D.W. Zimmerman, Archaeometry 13 (1), 29-52 (1971).

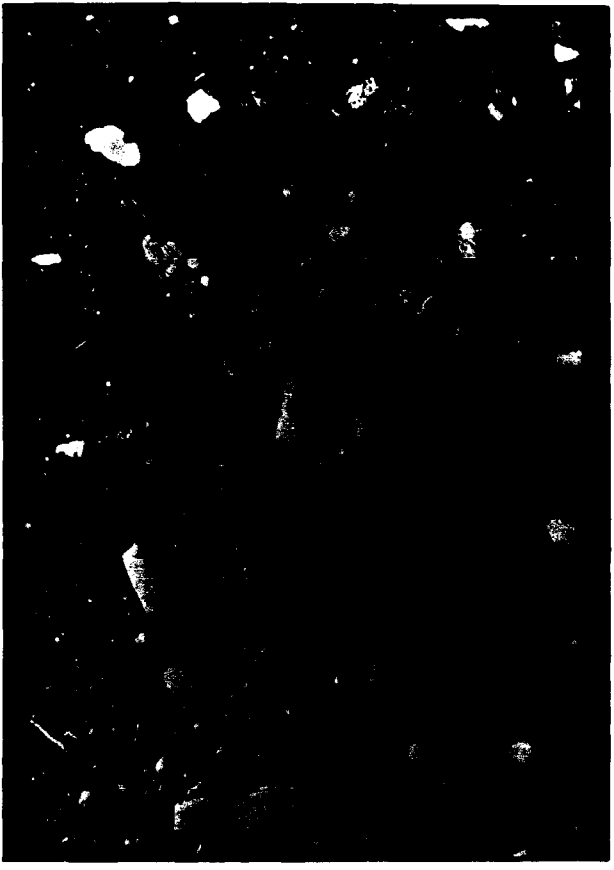

Plate 1 Mineralogical thin section of an Etruscan terracotta For an approximate grain size scale the biotite crystal (B) is 1.5 mm. long.

Plate 2 Etruscan bust of a woman. 16.141. The Metropolitan Museum of Art, Rogers Fund, 1916.

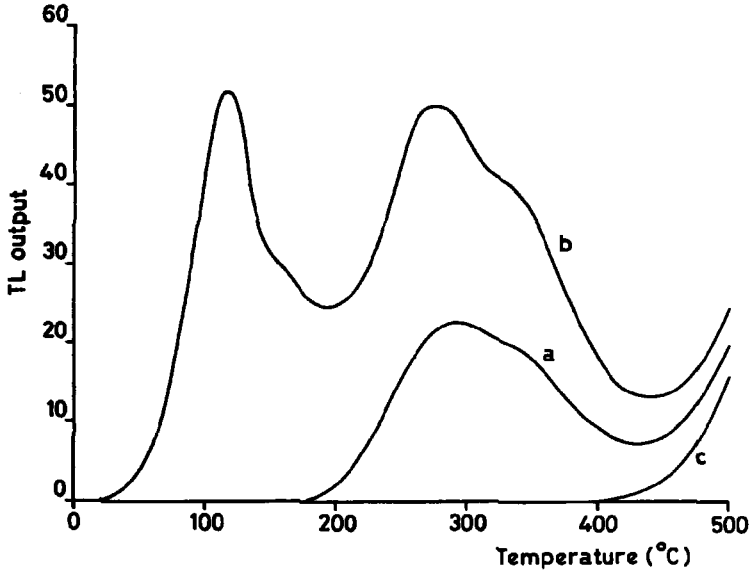

Figure 1 TL glow curves for the fine-grain sample of sherd 90 e 2: a. Naturai TL, b. Natural TL + TL induced by 800 rads of laboratory-applied beta radiation, c. background 'red-hot' glow.

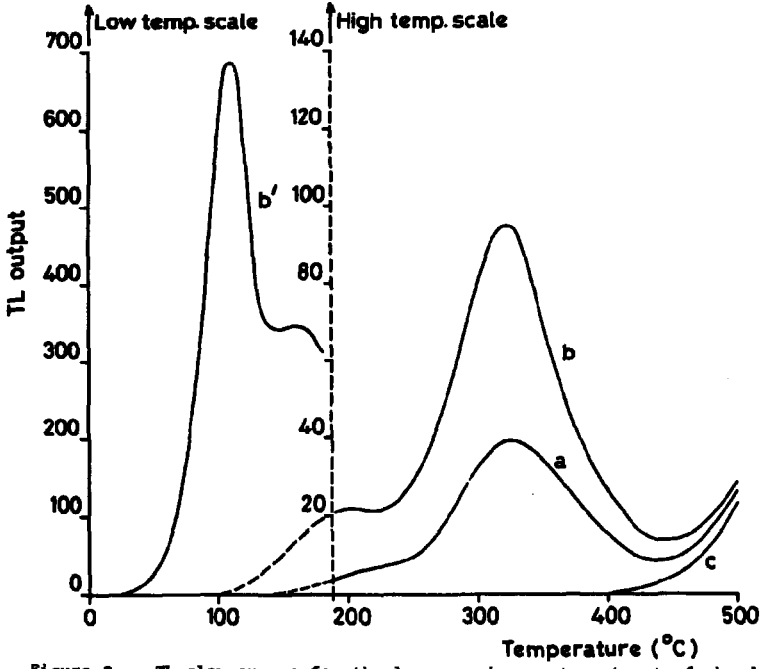

Figure 2 TL glow curves for the large grain quartz extract of sherd 90 e 2: a. Natural TL, b. Natural TL + TL induced by 380 rads of laboratory-applied beta radiation, c. background 'red-hot' glow.

New Techniques of Thermoluminescent Dating of Ancient Pottery: II The Predose Method

by

S.J.Fleming

The Research Laboratory for Archaeology and the History of Art, 6 Keble Road, Oxford.

ABSTRACT

The magnitude of a radiation dose may be measured utilizing the increase it produces in the thermoluminescent sensitivity of quartz in a glow curve peak at 110° C. The sensitivity enhancement is activated by heating the quartz to 500° C after application of the pre-irradiation dose (briefly termed the predose). Little growth of sensitivity is observed for an activation temperature of only 150° C. An enhancement rate of 5% per rad is typical for quartz freshly-annealed from its geological condition at temperatures of between 700 and 1000° C. Such heating conditions would match that experienced by quartz in pottery during the kiln-firing in ancient times. During burial the pottery will suffer a predose from the natural radioactivity of itself and its surroundings that may then be activated by heating to 500° C in the laboratory. The sensitivity of the 110° C peak measured without a 500° C heating represents the original sensitivity of the quartz immediately after the pot's manufacture. Then for a typical annual dose-rate of around 0.25 rads/year during the pottery over 400 years, say, a sensitivity enhancement by a factor of 5 is anticipated. The sensitivity-growth due to the archaeological dose may be calibrated by measuring the additional enhancement created by application of a known laboratory-dose. Knowledge of the annual dose-rate that pottery suffers is obtained from radioactive analysis of itself and its burial media. Combination of this and the predose data yield the age of the sherd.

A test programme of 21 sherds from 10 British sites spanning Mediaeval and Roman times illustrate application of this predose dating method. Criteria

are developed for the suitability, or otherwise, of material to be dated in this way. 14 sherds that satisfied these criteria yielded an accuracy of dating per sherd within 5% of the known archaeological age.

Practical application of the predose dating method include study of (i) a recently-manufactured Etruscan wall-painting on terracotta, (ii) a quartz core from a Degas Bronze dating around 1920 and (iii) authenticity analysis of a Hacilar Figurine where discussion is extended into investigation of whether that piece may have been re-heated in modern times.

Introduction

A change in thermoluminescent (TL) sensitivity induced by application of a heavy radiation dose has become a common observation in phosphors investigated for their usage as medical dosimetry material: most obviously LiF (TLD-100), with its 6-fold sensitivity enhancement after annealing out of a pre-irradiation (called hereafter predose, for brevity) of 10^5 rads, comes to mind.[1] Such changes also occur in the natural mineral, quartz, some features of which were touched upon during the last Luminescence Dosimetry Conference at Gatlinburg, Tennessee.[2] Fig. 1 illustrates a typical quartz glow curve with dominant peaks at 110° C and 375° C and satellite peaks at intermediate temperatures (at 175° C and 230° C). The higher temperature 375° C peak exhibits predose sensitivity changes of a complex nature, increasing non-linearly through an enhancement of less than 10% for a predose of 20 krad to a level of 340 times the sensitivity of undosed material at 1 Megarad. This change has been attributed to defect creation produced by the combined effects of dosage and heating.[3] This contrasts in 'model' to those presently accepted to explain predose phenomena for dosimetry phosphors where a 'centre-interaction' is suggested.[4,11] However the predose characteristics of the 110° C quartz peak are even more distinctive, with enhancement levels of as much as 10% per rad of predose applied for annealed geological quartz prepared in the laboratory for dosimetry purposes[9] and even up 28% per rad of predose in quartz extracted from pottery (see below).

In archaeological dating the contrasting predose responses in the high and low temperature regions of the quartz glow curve have been studied with quite different objectives in view. In the former case the predose effect gave grounds for concern in development of routine pottery dating using extracted quartz (see Fleming[6] for discussion of the so-called inclusion technique) - the occurrance of supralinearity in TL response was anticipated for doses of archaeological significance of up to 10 krad. In the latter case the remarkably high sensitivity changes are put to good use to enable measurement of the archaeological dosage the pottery has experienced during burial following the procedures developed in the predose dating method discussed in this paper.

Radiation-response of the 110° quartz peak

The fundamental properties that control the quartz predose dating method may be outlined through the features of radiation-response listed below as (i) - (iv). The

initial investigations were carried out via the behaviour of a geological quartz annealed at 850° C for 48 hours. The prolonged high temperature treatment no doubt begins its effect on the quartz by activation of the predose enhancement due to the huge geological dose the natural mineral has suffered, but it is believed that the sensitivity the annealed material subsequently exhibits after cooling is unrelated to the previous irradiation. Rather the annealing temperature and rate of cooling probably contribute the variables that modify the annealed quartz's sensitivity through control of concentration and rate of formation of defects in the thermally-disturbed crystal lattice. Any memory of a geological radiation history is expected to have been erased once the quartz has been heated beyond the temperatures of its phase changes at 570° C (the α - ß transition) and at 870° C (through conversion to $ß_2$ - tridymite). Similar arguments are expected to apply to quartz extracted from pottery originally annealed in a similar . shion during kiln-firing by ancient man.

i) The sensitivity enhancement is a result of the combined effect of predose and heating. Heating alone of the type used experimentally here (to 500° C in the course of normal glow curve measurement taken at 20° C /second) causes no sensitivity change in the freshly-annealed quartz (Fig.2).

ii) Similarly radiation alone without heat treatment does not cause a sensitivity change in the 110° C peak. By implication there must exist a thermal characteristic tracing out the sensitivity increase as a function of temperature of heating between room temperature and the 500° C normally used for activation of any specific predose applied. This is exampled in Fig. 3, where the activation temperature is the recorded cut-off point obtained by interrupting the normal 20° C per second heating cycle prematurely. Sensitivity, S, is the recorded peak height in response to a test-dose (which is defined here as a radiation level applied to a magnitude which is virtually negligible in its ability in inducing a predose enhancement in its own right)-of 1 rad in this experimental data. It should be stressed that the thermal characteristic of Fig. 3, while typical of that normally encountered in pottery quartzes, is not unique in shape. Some flexibility of the region where that characteristic is upward-turning has been observed in other laboratory-prepared samples ranging between 275° C and down to around 120° C.

iii) The TL response of the 110° C quartz peak is linear as a function of radiation dose, both before and after application of the predose (Fig. 4). This is important in that it is a necessary criterion of the test-dose to have a practical meaning. For example, from Fig. 4, curve b for predosed material, if a test-dose of greater than 50 rads had been used to generate the enhancement graph (Fig. 2), and the thermal characteristic (Fig. 3), an incorrect relationship to S_o would be derived from the predose phenomenon of the quartz. (On extremely rare occasions supralinearity has been observed[11] and this would be regarded as justification for rejecting a pottery sample from a dating programme.)

iv) The rate of sensitivity enhancement is a linear function of the predose applied. In practice the deviation from linearity that eventually leads to saturation of the predose phenomenon sets in at quite low dose levels of around 200 rads (Fig. 2). The form of this enhancement curve does not depend upon whether the TL traps responsible for the 110° C peak are filled or empty when the thermal activation of the predose is applied. Thus the peak retains a memory of that predose even if the latter has decayed away (a quite rapid process as the 110° C peak has a half-life of only approximately 145 minutes at room temperature).

Possible explanations for the cause of the predose phenomenon are outlined in Appendix A, but in understanding of the use of the effect in dating it is adequate to limit the discussion to phenomenonalogical properties of the quartz at this stage.

Archaeological application.

Certain analogies can be drawn immediately between the laboratory-annealed quartz and the quartzes that one expects to find in ancient pottery fabric. The archaeological dose that the pottery experiences in burial, due to natural radioactivity in the pottery itself and in its surrounding environment, may be equated to some level of S_B (in Fig. 2) that will be induced by heating the quartz in the pottery in present times. The enhancement rate for each individual pottery quartz can be established by application of a predose of known magnitude under laboratory conditions. Fig. 5 illustrates the procedure now developed for evaluation of the archaeological dosage of pottery samples, in this case for a sherd from the Mediaeval site of Nuneaton, in England (sherd 152c8 in Table 1).

The experimental procedure runs as follows:

i) Measurement of S_o, using a test-dose (equal to 1 rad, in this case).

ii) Heating to 500° C, cooling and re-application of a test-dose to measure S_N.

iii) Heating to 500° C again, cooling and reiteration of the sensitivity measurement as S'_N.

iv) Application of a suitable predose to activate a further sensitivity enhancement - the latter is measured, after drainage of the predose to 500° C and cooling, in response to a test-dose, as $S_{N+\beta}$.

The magnitude of S_N and S'_N are expected to be equal to confirm that heating alone causes no sensitivity change while also verifying that the activation process due to the first 500° C heating was completely efficient. This criterion held for all 21 sherds studied in the test programme described here.

The magnitude of the increase, S_N to $S_{N+\beta}$, which has been induced by a known predose level applied in the laboratory, calibrates the sample's enhancement-rate, p_1. The difference between S_o and S_N may then be used to express quantitatively the natural dosage that the pottery has experienced. For the example of 152c8 we have :

$$S_o = 1.2 \text{ light units}$$

$$S_N = 34.3 \text{ light units}$$

$$S_{N+\beta} \text{ (for } \beta = 335 \text{ rads)} = 72.0 \text{ light units}$$

$$\text{with } p_1 = \frac{S_{N+\beta} - S_N}{S_o} \text{ per krad} = 94$$

Natural dosage = 294 rads.

In addition, using another portion of the same quartz extract, a 'direct' $S_{N+\beta}$ of 47.4 light units was measured for a predose of 115 rads applied prior to the heating to 500° C. This is equivalent to a p-value (the enhancement-rate for direct predose) of 96/krad. The close agreement between p_1 and p, as illustrated here, has been developed as a criterion for suitability of a sherd for predose dating (see Appendix B). Similar analysis of the remaining pottery sherds in the test programme is given in Table 1.

The magnitude of p_1 may well vary from portion to portion of quartz extracted from the same pottery sherd for the source of the quartz in the clay fabric is likely to be diverse - beach sand and crushed fragments of older damaged vessels perhaps. The procedure outlined above avoids errors due to this variation by defining the natural dosage through the p_1-value appropriate to each individual quartz portion.

At this stage it suffices to ensure that the predose level does not extend close to or into the region of saturation of the phenomenon in the enhancement curve re-developed above S_N. Limiting of linearity of the predose response is simply studied by checking the constancy of natural dosage estimates obtained (usually termed Equivalent Dose or E.D.) as the predose level is increased using different portions of the quartz extracted.

Within this framework 21 sherds were included in a test-programme involving a group of 10 British sites. The thermoluminescent data obtained from those sherds are given in Table 1 where the ratio S_0/S_N is also recorded to allow discussion of the thermal stability of the phenomenon. The difference between the results presented earlier for quartz freshly-annealed in the laboratory and quartz extracted from pottery is the time elapsed between predose application and thermal activation. In the long term sense stability is defined as the degree to which the sensitivity of the quartz immediately after the pottery firing converts to S_N through thermal activation at ambient ground temperatures i.e. to what degree the S_0 measured today represents the quartz's original sensitivity.

For the sherd 152c8, S_0 is only 3½% of S_N in magnitude excluding any significant thermal activation of the archaeological predose. With any complication of understanding removed, due to the stability question, this sherd might be expected to yield a particularly satisfactory dating result.

TL analysis of the behaviour of the 110° C quartz peak yields only an estimate of the archaeological dosage and to proceed to a date for a sherd it is necessary to gain information of the annual dose-rate the quartz has experienced while embedded in the clay fabric of the pottery. It has frequently been discussed before[6] and is reviewed in Appendix C.

Discussion of results of the dating programme (Table 1, 2)

The dating results here have been divided into two groups distinguished by whether the enhancement-rates p and p_1 differ by more than 10% or not. The 14 sherds for which they do not are then considered to satisfy the criterion for good archaeological dose determination of $p_1 = p$ to within the limits of practical experimentation. It is immediately apparent that those 14 sherds yield good TL predose ages while the remaining 7 sherds are singularly less satisfactory. Consistently, as we expect sherds where $p_1 > p$, to be moving into predose saturation, the poorer dating group contains dominantly older material (only 2 out of the 7 Romano-British sherds passed the p-value test). In closer analysis of the first 14 sherds the predose ages differ from the known age by 4.3%, on average, with a systematic error of close to 3.2% erring on the low side. This is remarkably good and must surely be more accurate than errors in glow curve analysis or radioactivity determinations would predict. However no condition is apparent that is particularly favourable for only the sites studied. While the systematic error may be explained by uncertainty in source calibrations equally it may reflect a tendency for p to be only slightly less than p_1 i.e. deviation from predose linearity towards saturation is imminent.

The sherds in this programme do not offer a severe test of the introduction of correction for residual alpha dosage (see Appendix C) but the two sherds for which there is a significant contribution to the annual dose-rate from that source (157a4, 157a5) the TL predose age closes up on the known archaeological age quite encouragingly.

Among the sherds below the 'demarcation line' the two sherds 151a2 and 152c9 still give predose ages within 10% of the known age while there is only a difference of 12% and 20% respectively between p and p_1. Using p, instead of p_1, to obtain an archaeological dose estimate and then an age the sherds 151a2 and 152a9 would date at 500 and 680 years respectively. The age bracket derived expresses our best knowledge of the TL predose age - even as saturation begins in the initial enhancement curve some reasonable dating accuracy is still possible. The same argument may be applied to the remaining 5 sherds with poorer dates but with much less advantage, consistent with the high deviation of p and p_1.

Among the Romano-British sherds only a tentative suggestion may be made to explain why 2 sherds should give good dates at all - the values of p_1 for sherds 51a4 and 90e2 are far lower than the remainder. Slow enhancement-rate perhaps relates to slow approach to predose saturation. What is not apparent in this group, or indeed in the whole programme, is any evidence that any significant conversion of S_o to S_N has occurred over archaeological periods to yield ages that are too young - Romano-British sherds of this study show no higher S_o/S_N ratios than the younger Mediaeval ware.

Applications of the predose dating method

Archaeologically little has yet been attempted using this new dating approach. Its greatest advantage is the high sensitivity making it ideal for dating truly young material. Three examples here illustrate this.

i) An 'Etruscan' terracotta wall-painting

For many years the art world has been faced with problems of authenticity of ceramics and terracottas and few periods of ancient civilization have been more extensively forged than that of the Etruscans who flourished in Italy around the middle of the first millenium B.C.[3,10] Recent investigations have been made of a new series of material in the form of wall-paintings on terracotta plaques.[7] Such paintings in ancient times were used to decorate Etruscan tombs (see, for example, the Boccanera series in the British Museum and the Campana series in the Louvre, both of which were excavated during the 19th century). Quartz extracted from a fragment of the terracotta shown in Plate 1 yielded TL predose curves as shown in Fig. 6. With a p_1-value of 280/krad it is quite practical to define accurately the terracotta's natural dosage since firing as close to 2 rads only. Radioactive analysis of the clay yielded an annual dose-rate of 0.22 rads/year (assuming that this bulky plaque was responsible for the greater part of its own environmental dosage). The age of 9 years that results places the date of manufacture early in 1962!

ii) A Degas Bronze

It has been a standard technological practice to use a supporting core of sand, clay or silicate powder of some sort to aid bronze casting throughout ancient times. (The early Chinese of the Chou Dynasty during the first millenium B.C. were out-

standing in this respect.) Routine high temperature TL dating is quite practical for this material. Also in much more recent times this method of metal working has continued, notably by Degas around 1920 (Plate 2), using a quartz/feldspar coring powder. Predose analysis of the core material is shown in Fig. 7. The dose the piece has experienced since firing may be estimated at close to 4.8 rads. Now in age determination problems occur in evaluation of the annual dose-rate the bronze has known. Internally the core is extremely low in radioactivity contributing less than 28 millirads/year. We may only assume the environmental conditions contributed around 60 millirads/year and so predict a total dose-rate of 0.1 rads/year. With that assumption the TL age of 48 years is satisfactory, but this piece highlights that the use of predose analysis produces an answer only for the archaeological dose, but shares with routine TL dating techniques a dependence upon knowledge of environment to yield good dates.

iii) A "Hacilar" Figurine

A further problem in authenticity will carry us into discussion of some further refinements and advantageous features of the predose method later. Limiting investigations to the procedures of dating so far described, results of predose analysis of a Figurine in the Hacilar style (Plate 3) are given in Fig. 8, except that here the direct predose (defining p) was used to characterize the piece, for reasons discussed below. Such material should date, in genuine, to the 6th millenium B.C.[8] and originate from Turkey but imitation of excavated ware has been widespread.[1] The Figurine investigated here falls in the latter group with S_N very close to S_o. As the p-value is not very large (around 0.9/krad) only a limit of dosage may be set practically of about 25 rads from natural sources. Radioactive analysis of the clay of the Figurine sets its annual dose-rate of 0.43 rads/year at least limiting its age to the last 60 years.

We must then query whether this judgement on authenticity is in any way naive. Though the analysis above is in agreement with high temperature TL studies there is a possibility to be considered which would negate the results of the latter - reheating of the piece to 300° or more for a prolonged period. Indeed there were rumours to that effect suggesting a drying

procedure, intended to preserve the artefacts, had been used deliberately after extraction of the material from a water-logged archaeological context.[1]

But the heating that would nullify the high temperature TL analysis also activates any predose due to a previous archaeological history. The laboratory-measured 'S_O' would now record the true value of S_N while the original sensitivity before re-heating is apparently lost. Further a tendency towards saturation would be expected for any predose activated appropriate to some 7000 years of dosage (in effect, approximately 3300 rads). The 'direct' laboratory predose used in defining p for this piece anticipates that $S_{N+\beta}$ will scarcely exceed S_N to match a re-heating argument. But in Fig. 8 a p-value results which is sufficient to exclude such a possibility. Even if the original sensitivity of the pottery before re-heating had been minimal, at zero, the growth of 0 to S_N as measured now is predicted to be due to only 1100 rads of natural dosage. At 0.43 rads/year the maximum possible age of the piece is 2550 years. Thus re-heating of the Figurine is satisfactorily excluded.

Response of the 110° C peak under u/v radiation

It is possible to reverse the sensitivity-enhancement due to any predose, by application of heavy u/v dosage, even after it is seemingly 'locked-in' by a 500° C heating. This is illustrated for disc-deposited samples of sherd 152c10 from the test-programme where we know with certainty that the difference between S_O and S_N is due to an archaeological dosage (Fig. 9). Ultra-violet treatment of an unheated sample (which then would have a sensitivity of S_O at the 110° C peak) does not change the sample's sensitivity subsequently. However for a heated sample (which would have a sensitivity, S_N), u/v treatment rapidly erodes away the enhancement until eventually the original sensitivity, S_O, is attained. This 'suppression' is immediately removed by heating to 500° C once more and the sensitivity S_N is recorded once more. (For some sherds u/v radiation itself induces its own predose which would appear superimposed upon this final S_N level.)

It is now appropriate to return to the question of re-heating raised about the Hacilar Figurine above. By analogy with the sherd 152c10 it is anticipated that two levels of sensitivity might be observed for u/v treatment of a sample given no laboratory heating; (i) if the sample has been re-heated prior to reciept in the laboratory, our measured S_O would drop to some extremely

low value of sensitivity representative of its original sensitivity. Certainly we know that u/v irradiation does reverse sensitivity-enhancement for this sample (Fig. 8); (ii) if manufactured in modern times the measured S_o does represent the true original sensitivity of the piece and u/v should fail to alter that sensitivity.

In practice the case (ii) occurs though the purity of argument is slightly upset by a slight growth of the TL level around 110° C. The poor shape definition in the u/v-treated sample suggests many satellite glow curve-peaks have responded to the radiation in a confusing way. Despite this, further support is thus furnished by this u/v investigation to the earlier denouncement of this Figurine as of modern origin.

.....

APPENDIX 'A'

Extensive research into the cause of the predose phenomenon following initial investigations by the author[5] has resulted in a band model that offers a satisfactory explanation. The TL sites postulated are electron traps T_1, T_2 and hole traps L and K (Fig. 11). T_1 is the shallow trap that yields the peak at 110° C during thermal activation of the quartz, by photon emission during de-excitation to L, the luminescence centre. Trap T_2 is presumed to be deep enough not to be emptied by a 500° C heating and K is a luminescence centre which retains charge balance in the crystal and is an important component of the sensitization process. The concentration of traps T_2 is presumed very high, giving it a reservoir quality. Then the rate of filling of T_1 is unaffected by competition effects during irradiation, an argument consistent with the rarity of observation of supralinearity in radiation-response in the 110° C peak. K then also has a high hole trapping capacity. Initial irradiation charges the various centres and subsequent heating through 110° C transfers electrons from T_1 to L in observation of S_o. Further heating up to 500° C thermally activates holes from K to L recharging the latter. As the amount of holes stored in K is proportional to the predose level applied to the level of replenishment of L centres with holes is similarly related.

The quartz is now in a 'predosed' condition so that a test-dose putting electrons into T_1 measures an enhanced luminescence output in subsequent heating. The choice of

L centres available for de-excitation is greatly increased. This model, where heating results in the increase in number of luminescence centres, is supported by observation of (i) increase in radioluminescence (RL), (ii) decrease in thermally-stimulated exoelectron emission (TSEE) for predosed quartz.[11] (These additional experiments rejected an alternative model in which an increased probability of charge capture of the TL traps, T_1, was considered to explain the enhancement.[5] In particular the TSEE signal should have increased with application of a predose.)

The 'quenching' of the predose effect by u/v radiation follows through discharge of the luminescence centres of the predosed material and replenishment of the killer centres, K. A further 500° C heating reverses the discharge and so the predose enhancement is once more observed.

APPENDIX 'B'

Additional investigation has been made of the 110° C quartz peak's sensitivity growth above S_N after the latter has been 'locked-in' by a 500° C heating (Fig. 11). For a direct predose, like that due to the archaeological dosage, activated to anywhere on the linear portion of the enhancement curve, the original growth from S_o is repeated if a fresh enhancement curve is generated using the earlier predose level as origin. The relevant enhancement rates, p and p_1, are equal. Then, using either p or p_1, as calibrating the predose response of the sample, the correct archaeological dose would be predicted from the measured value of S_N.

However, if the point S_N lies in the region of predose saturation of the direct enhancement curve such repetition does not occur. The growth rate falls i.e. $p_2 < p_1$, and an understatement of the archaeological dose results.

In effect this is saying that the enhancement-rate of a sample remains independent of the predose level induced until the complex region of saturation is reached. As a practical example the enhancement-rates at two predose levels were measured for a 1000° C laboratory-annealed quartz with the following results:

i) Initial enhancement-rate, $p = 35 \times S_o$ per krad of predose.

ii) Enhancement-rate after a predose activation for 90 rads applied, $p_1 = 38.5$.

iii) Enhancement rate after a predose activation of 360 rads applied, p_2 = 27.0. At the latter stage the initial enhancement curve, in approach to saturation, has a low growth rate, with a tangential value of about x 3 S_o per krad.

For ancient pottery p_1 can be measured much more accurately than p as the latter is evaluated from what remains of the direct enhancement curve above S_N. Precision levels of ±2% and ±10% seem practically attainable. But much of the need for a very accurate p-value estimate is eased as the decrease of p-value (p_1 to p_2) in moving towards direct predose saturation reduces the hazard of error in archaeological dose determination (Fig. 11). The 10% level quoted has proved adequate in this respect for practical attainment of good predose ages (see Table 1).

APPENDIX 'C'

Certain inhomogeneities in the microstructure of pottery have been identified that define the TL output measured and control the attainment of absolute dates. Though extensively reviewed elsewhere the features are repeated and extended here, relating to the sample preparation appropriate to predose dating :

a) The principal source of the TL from pottery is the crystalline inclusions like quartzes, feldspars and calcite which occur in an extensive range of grain sizes (typically between 1 and 500 microns in diameter). The clay matrix itself emits very little TL.

b) The natural radioactivity of the pottery is carried predominantly by the clay matrix - the crystalline additives are virtually free of any uranium or thorium and the quartzes present contain scarcely any potassium either. The products of internal radioactivity of the pottery are alpha and beta radiation, the former from uranium and thorium only, the latter from uranium, thorium and the radio-isotope of potassium, ^{40}K.

c) The ranges of travel in clay of the natural alpha radiation (on average, 25 microns) and the beta radiation (on average, 1 mm.) distinguish their influence in this quartz dosimetry. While the beta radiation acts as a uniform source of dosage of a large quartz grain, say, 100 microns in diameter, severe attenuation of the alpha radiation dosage occurs in such a quartz grain to the stage where an inner region experiences nothing of that short-range dose component.

d) The natural radioactivity of the soil of the context of pottery burial is the source of a gamma radiation dose for the quartz. Finally there is a small contribution from cosmic radiation amounting to between 14 and 30 millirads/year.

Within the clay, purely on an energy basis, the alpha radiation contribution is overwhelmingly important but its efficiency of production of a predose enhancement, k_p, is low compared to that of beta or gamma radiation. This was investigated by TL analysis of 110° C peak for quartz in pottery samples prepared as a thin deposit (around 5 microns on average) on an aluminium disc following the principles of fine-grain dating.[12] Values of k_p for the 21 sherds in the test programme are given in Table 2. For sherd 157a4, where $k_p = 0.061$ is the largest of the group, a matrix alpha dose-rate of 1.6 rads/year is reduced to 98 millirads/year for fine grains of quartz embedded in that matrix. Additionally for these fine-grains the p_T-value proved to be much smaller than that of large grains of quartz extracted from the same sherd (see Table 2).

The alpha radiation geometry of a large quartz grain then becomes quite complex as the outer regions will be 'contaminated' with elemental impurities introduced by diffusion of ions from the clay during the kiln-firing.[6] This region will exhibit a response similar to that of the fine grains of quartz from the same pot - in the latter case the diffusion process is more likely to have reached inner body of the grains. The p_T-value of the large-grains (Table 1) applies to the inner volume beyond the diffusion front of the impurities. Without knowledge of the depth of diffusion appropriate to each sherd it is impractical to attempt a quantitative estimate of the effective alpha radiation dose a large quartz grain experiences, but a rough calculation is possible. From experience of preparing quartz samples for use in the inclusion method of dating hydrofluoric acid etching from around 20 minutes is enough to remove all the discoloration of the quartz grains that the diffused impurities cause, in the majority of cases. This represents removal of a surface layer about 3.5 microns thick from a 100 micron diameter grain. From theoretical calculations the distribution of alpha dose through the body of the quartz grain is known (Fig. 12).[5] Close to 40% of the alpha dose is taken up outside a penetration depth of 3.5 microns and 60% beyond it. Returning to the example above for sherd 157a4, assuming the k_p value is the same through such a quartz grain and an attenuation factor of close to 0.22 (appropriate to alpha dose dilution for a 100 micron diameter grain)[6] it follows that 8.5 millirads/year affects the outer regions of the crystal and 13 millirads/year affects the more sensitive

inner volume. With the p-values of the outer and inner regions in the ratio of 1:17 only the inner dose will be significant in correction of our annual dose-rates. A similar calculation for the remaining 20 sherds in this test programme yielded levels of correction all of which are appreciably smaller.

Notably an attempt to minimize this alpha dose correction further by etching the quartz in hydrofluoric acid was quite abortive. The chemical treatment seemed to enhance the level of S_N preferentially - in four cases briefly investigated before rejection of such treatment age estimate in error by a factor of 4 to 7 were realized! Further, although the alpha-dose attenuation can be increased by using even larger quartz grains (a factor of 0.11 is applicable at around 200 microns diameter, for example), only in a few cases in the dating programme was this advantage exploited as the majority of the quartz grains extracted from the pottery lie in the smaller size range.

Acknowledgements

This project was supported financially by the Nuffield Foundation. The great cooperation of the archaeologists responsible for the 10 sites studied in this paper is acknowledged as is the generosity of the Metropolitan Museum of Fine Art (New York) in supplying the Degas Bronze core. The technical assistance of many of the samples of Mrs. D. Stoneham and Mrs. E. Whittle is much appreciated.

References:

1) M.J. Aitken, P.R.S. Moorey, P.J. Ucko, Archaeometry, 13 (2), 89-142 (1971).

2) M.J. Aitken, J. Thompson, and S.J. Fleming, Second International Conference on Luminescence Dosimetry, 364-388 (1968) (Available as CONF-680920 from the U.S. National Bureau of Standards.)

3) D. von Bothmer, J.V. Noble, An inquiry into the forgery of the Etruscan terracotta Warriors (1961) (Metropolitan Museum of Art, New York).

4) J.R. Cameron, N. Suntharalingam, G.N. Kenney, Second Internation Conference on Luminescence Dosimetry, 332-340 (1968) (Available as CONF-68P920 from the U.S. National Bureau of Standards).

5) S.J. Fleming, The acquisition of radioluminescence by ancient ceramics (1969) (unpublished D.Phil thesis, Oxford).

6) S.J. Fleming, Archaeometry 12 (2), 135-146 (1970).

7) S.J. Fleming, H. Tucker, J. Riederer, Archaeometry 13 (2), 143-168 (1971).

8) S.J. Fleming, D. Stoneham, This Conference proceedings (1971).

9) S.J. Fleming and J. Thompson, Health Physics 18, 567-568 (1970).

10) O. Kurz, Fakes (1970) (Dover Publications, Inc. New York).

11) J. Thompson, The influence of previous irradiation on thermoluminescent sensitivity (1970) (unpublished D.Phil. thesis, Oxford).

12) D.W. Zimmerman, Archaeometry 13 (1), 29-52 (1971).

TABLE 1 : Results of the quartz predose dating programme.

Sherd reference+	Saturation water uptake (% dry sherd weight)	Annual dose-rate (millirads/year) Beta U,Th	Beta ^{40}K	Environmental (inc. cosmic dose)*	Total (+$\Delta\alpha$)**
136a1	13.2	45	61	40	146(0)
151a3	10.0	65	116	95	280(4)
151a5	15.7	59	129	95	284(1)
141a1	11.0	56	115	55	226(0)
152c2	3.3	74	67	155	299(3)
152c3	8.0	59	163	155	377(0)
152c8	6.5	68	262	155	486(1)
152c10	9.5	62	281	155	499(1)
157a1	13.3	72	71	96	240(1)
157a2	5.6	58	38	96	193(1)
157a4	5.2	58	34	96	200(12)
157a5	4.3	64	167	96	325(8)
51a4	8.3	67	249	97	416(3)
90e2	6.6	53	97	124	279(5)
..	..	..	..	..	..
151a2	11.1	63	129	95	294(7)
152c9	10.9	64	136	155	357(2)
90h15	33.0	53	126	94	273(0)
71a1	14.1	40	103	72	219(2)
71a2	12.0	73	74	72	223(4)
76h11	6.6	49	73	89	214(3)
68e6	10.3	39	110	67	230(4)

+ The British sites studied are: Greenwich Palace (136); Oxford (141); Nuneaton (152); Sandal Castle (157); Wroxeter (51); Baginton (90); Cirencester (71); Gradebridge (76); Dragonby (68).

* Cosmic-ray dose is assumed to be 14 millirads/year appropriate to a burial depth greater than 1 metre.

** Where appropriate an alpha dose is included and recorded in parentheses. The levels used derive from the data of Table 2 with some further corrections if a large grain size was used.

Predose Data:				Age (years)	
S_o/S_N	P_1 (/krad)	P(/krad)	(E.D.) (rads)	TL	Known \rchaeological
0.06	234	232	67	460	470 ± 2
0.14	46	44	131	470	470 ± 25
0.12	57	55	126	445	470 ± 25
0.19	32	33	134	590	645 ± 25
0.22	16	15	206	690	660 ± 10
0.34	8.3	8.6	240	635	660 ± 10
0.04	94	96	295	605	660 ± 10
0.03	102	102	302	605	660 ± 10
0.11	44	45	181	755	710 ± 10
0.25	177	169	128	660	710 ± 10
0.02	295	290	141	705	710 ± 10
0.02	206	198	228	700	710 ± 10
0.29	3.2	3.5	755	1820	1900 ± 10
0.17	5.1	5.3	530	1900	1900 ± 10
..	..	..	..	..	....
0.06	33	29	125	425	470 ± 25
0.04	112	92	216	610	660 ± 10
0.13	75	35	380	1390	1900 ± 10
0.11	33	10	245	1120	1850 ± 30
0.08	49	21	256	1180	1850 ± 30
0.02	285	5	220	1030	1850 ± 30
0.10	35	2	260	1130	1925 ± 25

TABLE 2 : Predose characteristics for disc-deposited pottery.

Sherd reference	p_1-value (fine grain)	k_p	Residual alpha-dose in quartz (millirads / year)*
136a1	1.6	0.033	6
151a3	12.5	0.027	5
151a5	6.0	0.021	4
141a1	6.5	0.006	1
152c2	1.1	0.014	5
152c3	1.2	0.003	1
152c8	14.6	0.010	2
152c10	12.2	0.017	5
157a1	0.6	0.010	2
157a2	13.1	0.007	2
157a4	17.4	0.061	20
157a5	33.5	0.056	12
51a4	0.2	0.017	5
90e2	3.5	0.024	6
151a2	7.0	0.027	11
152c9	17.7	0.022	5
90h15	0.8	0.010	3
71a1	3.5	0.013	3
71a2	8.5	0.020	5
76h11	28.5	0.029	5
68e6	4.2	0.028	5

* This figure is calculated assuming the p_1-value measured for large quartz grains (as in Table 1) and an attenuation factor of 0.2 included for alpha radiation dose in such large grains. As an expression of efficiency to alpha radiation compared with beta radiation in inducing sensitivity enhancement, the k_p-value for fine grains, is assumed to apply through the volume of large quartz grains from the same source.

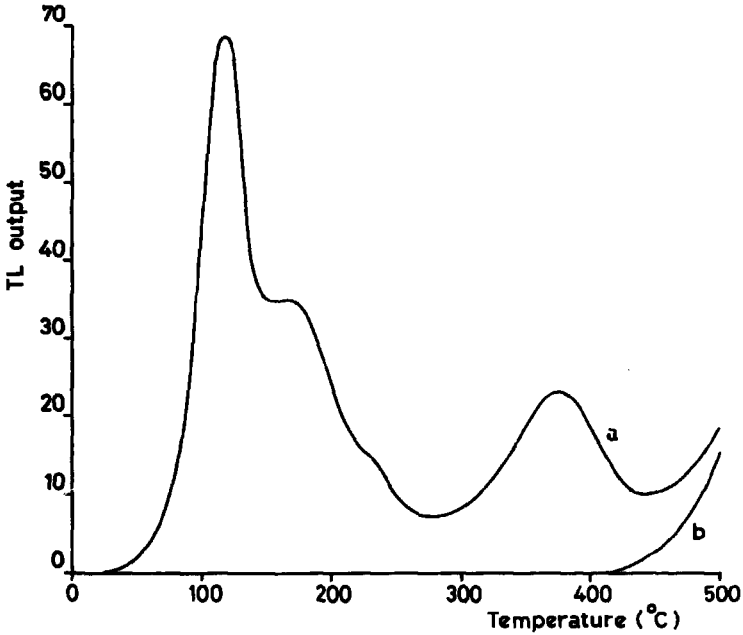

Figure 1 Glow curve for irradiated quartz (curve b is the background 'red-hot' glow).

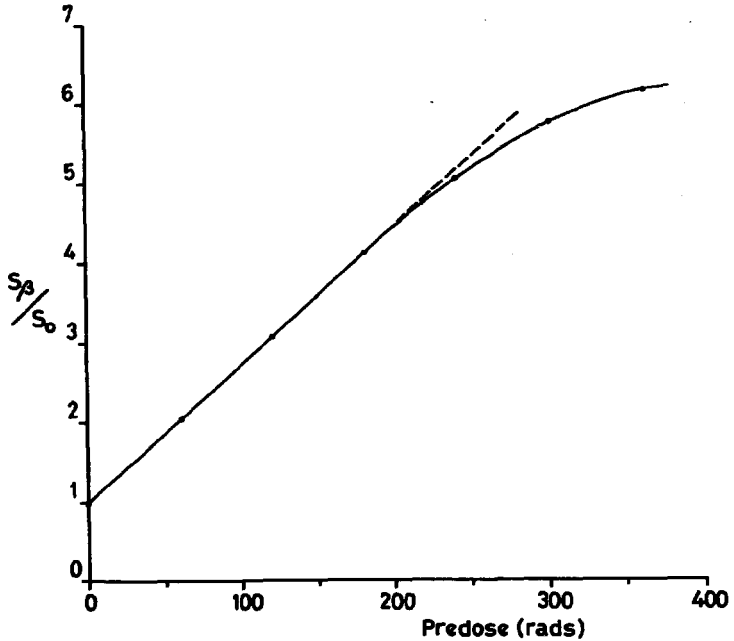

Figure 2 The growth of sensitivity of the 110°C peak in quartz (annealed at 850°C for 48 hours) as a function of predose applied. The predose is activated by a heating to 500°C. Heating alone, without intervening predose, causes no sensitivity change. The test dose used was 1 rad of beta irradiation.

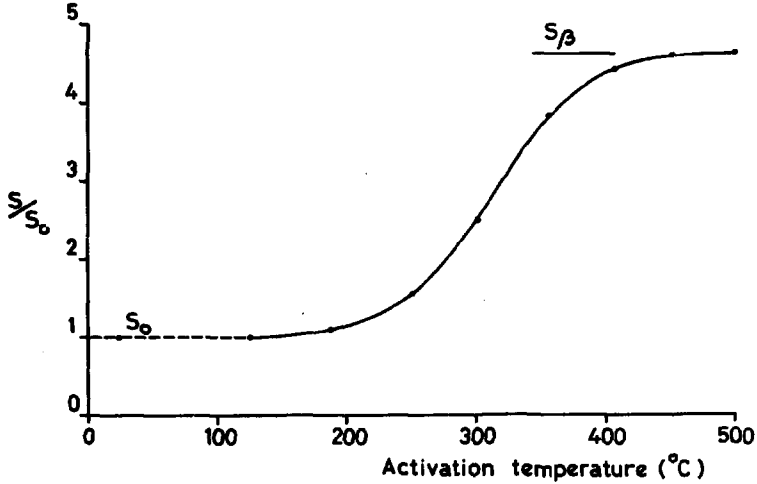

Figure 3 Thermal characteristic for the annealed quartz, plotting the sensitivity activated at a variety of temperatures between 20°C and 500°C, thus spanning the sensitivities S_o to S_β. The predose applied in each case was 220 rads of beta radiation.

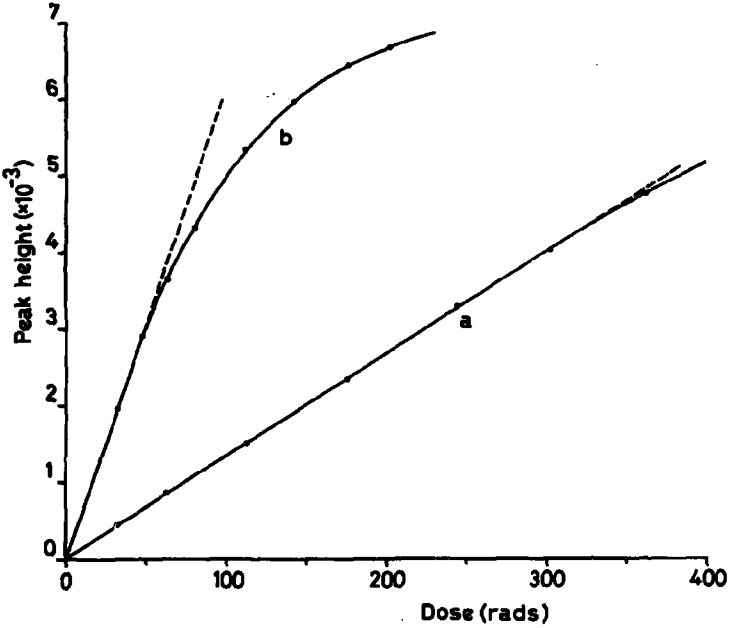

Figure 4 Radiation response of the 110°C peak in quartz for a. freshly-annealed quartz, and b. material sensitized by application of 220 rads of beta radiation subsequently heated to 500°C.

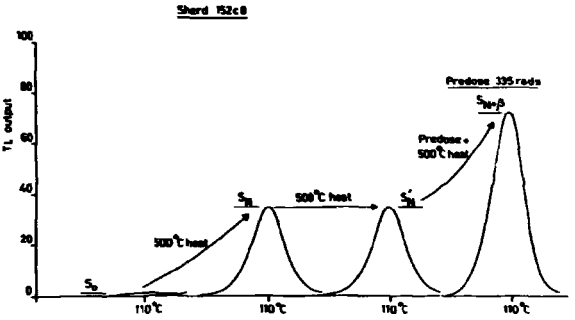

Figure 5 Procedure for measurement of the archaeological dose stored in predose information illustrated here for sherd 152 c 8, from the Mediaeval site of Nuneaton.

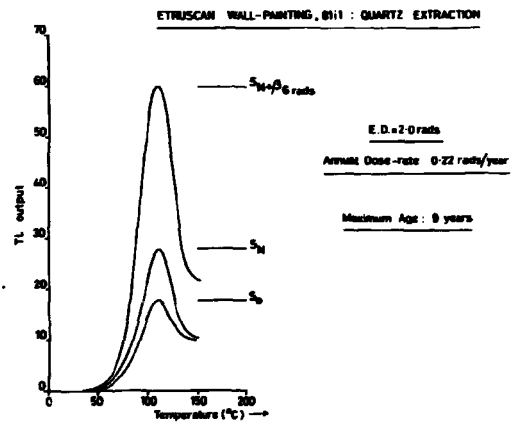

Figure 6 Predose data for an Etruscan wall-painting on terracotta. The sample used was the quartz extracted from a fragment of the clay taken from behind the fountain of the painting (see Plate 1).

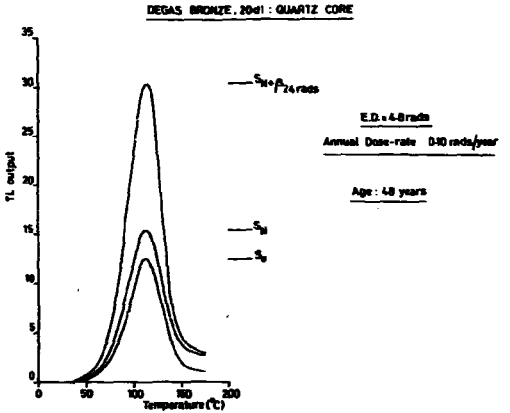

Figure 7 Predose data for the quartz core of a Dégas Bronze dating around 1920 (see Plate 2).

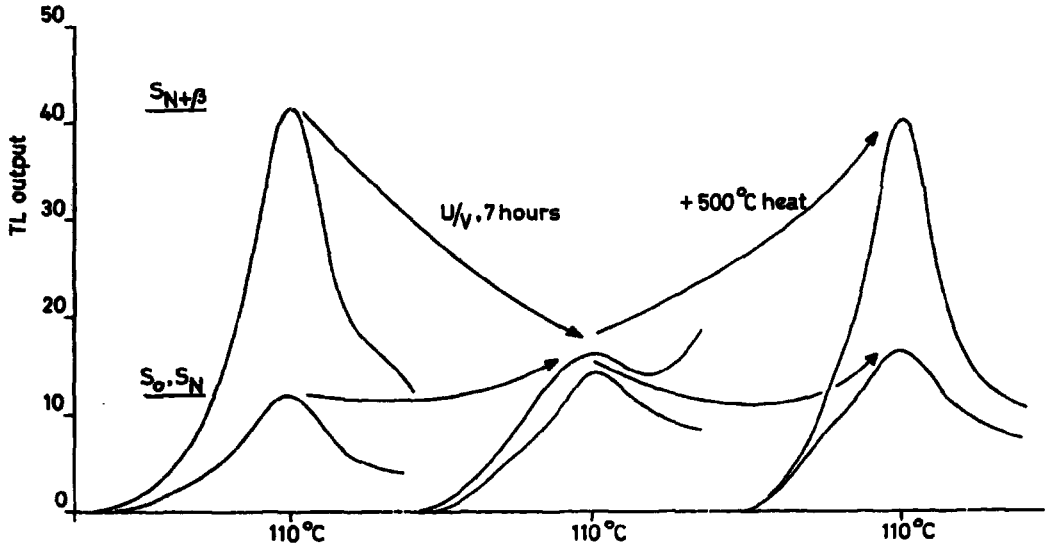

Figure 8 The response of the predose sensitivities, S_o, S_N and $S_{N+\beta}$, for the pottery of the Hacilar Figurine of Plate 3. S_o and S_N are almost identical. $S_{N+\beta}$ was recorded for a predose level of β=2800 rads of beta radiation.

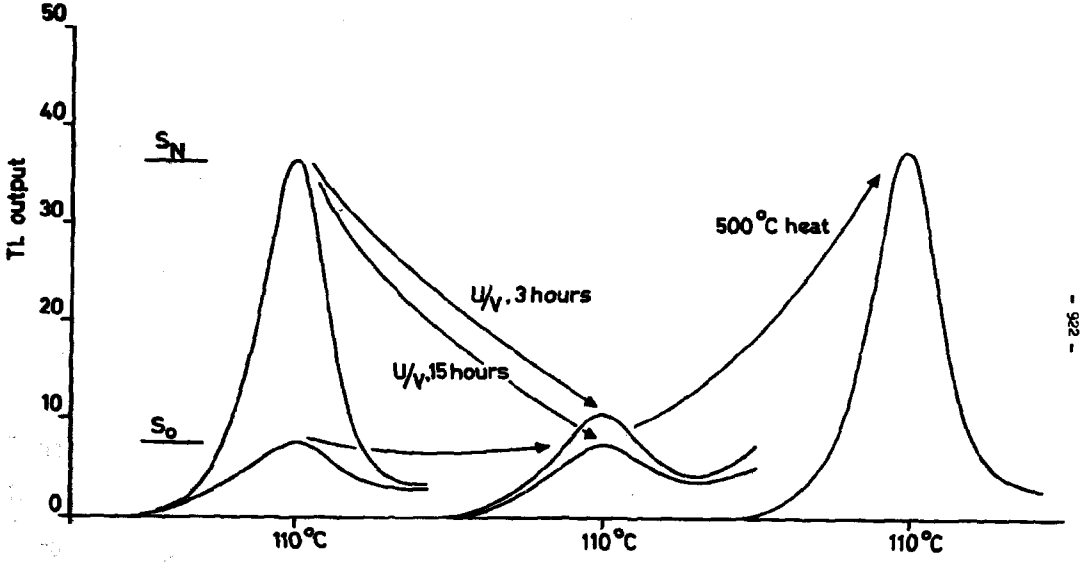

Figure 9 The response of the predose sensitivities, S_o and S_N, of sherd 152 c 10 (Nuneaton). Ultraviolet treatment upon S_N reduces the sample's sensitivity towards S_o by some 85% after three hours and by close to 100% after 15 hours.

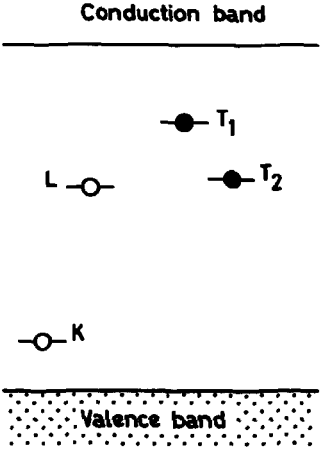

Figure 10 Band model for the explanation of the predose phenomenon.

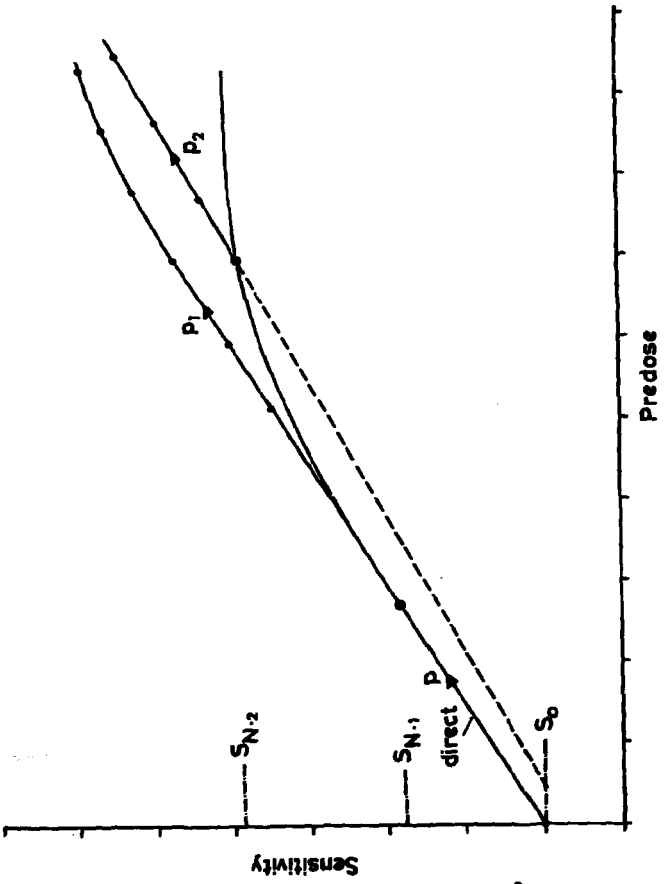

Figure 11 The sensitivity growth observed in the 110°C quartz peak when the enhancement curve is redeveloped after activation of the predose levels corresponding to S_{N-1} (on the linear portion of the 'direct' enhancement curve that starts at S_0) and S_{N-2} (on the saturating portion of the direct enhancement curve). Enhancement ratios p_1 and p_2 are observed where $p_1 = p$ and $p_2 < p$.

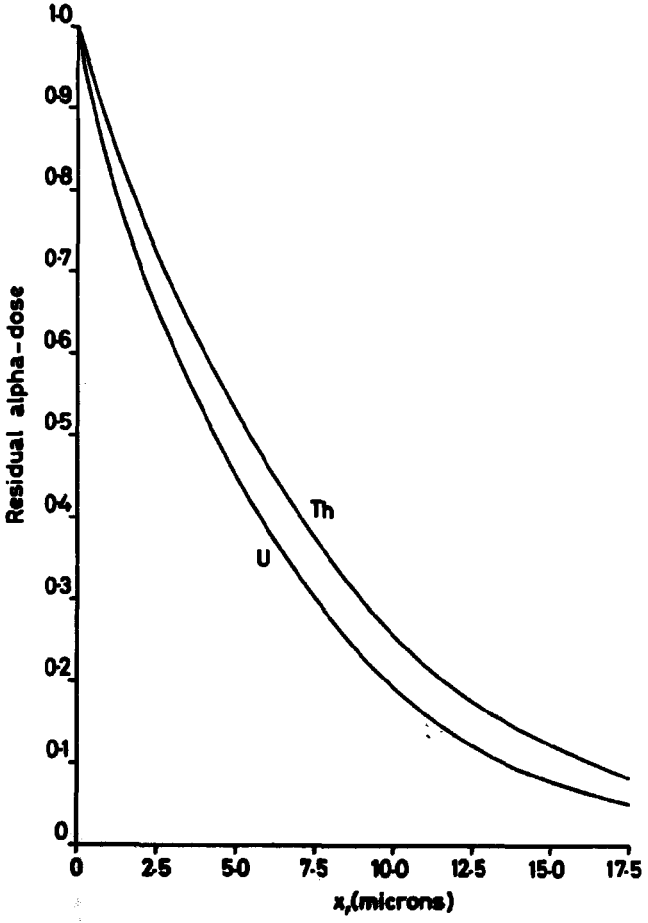

. Figure 12 The residual alpha radiation dose contained within the inner volume of a quartz grain, 100 microns in diameter, beyond a penetration depth, x_p, below the outer surface. The uranium and thorium radioactivity is assumed to be spread uniformly through a clay matrix surrounding the quartz grain.

Plate 1 A wall-painting on terracotta in the Etruscan style depicting the ambush of Troilus by Achilles. The picture is designed to imitate the same scene in a fresco of the Tomb of Bulls in Tarquinia.

Plate 2 Dégas Bronze Seated Woman, 29.100.415. The Metropolitan Museum of Art, Bequest of Mrs. H.O. Havemeyer, 1929. The H.O. Havemeyer Collection.

Plate 3 A Figurine in the Hacilar style.

Becker

Have art fakers already tried to confuse you by irradiating their fakes?

Fleming

Not to my knowledge. It should be stressed that the difference in dosimetry in the fine and large grains in pottery makes such forging difficult. Co-60 gamma dosage of a ceramic would dose all grain sizes equally, a feature distinguishable from the internal response of pottery due to natural radioactive sources.

McDougall

What proportion of the TL is obtained from quartz, and what proportion is from feldspar in the sherds?

Fleming

Quartz seems to be responsible for more than 95% of the TL observed from bulk pottery. Feldspars do have a high TL sensitivity, but in routine dating the crystalline extract is etched in HF-acid; the subsequent TL analysis is therefore limited to quartz.

McDougall

What effect would the presence of flint or chert have on the pre-dose method?

Fleming

As the archaeological dose is determined for each individual portion of crystalline extract for admixtures of quartzes of different natural origins, differences in the sensitivity response in the natural sample are followed by the response to the laboratory predose treatment as well. Thus if the 110°C peaks occur in flint and chert also, they cannot confuse the dating results obtained.

Mejdahl

What precision can you achieve with the subtraction method?

Fleming

Some care in choice of material studied to optimize the features that influence the method makes a $\pm$ 12% accuracy reasonable.

Mejdahl

How far back in time can you go with the predose technique? Can you apply the technique to archaeological samples?

Fleming

To younger archaeological problems, yes. One region where I anticipate it will find extensive use is African archaeology. As indicated in the paper the likelihood of obtaining a predose date decreases with age. My furthest extension so far is a sherd from the Neolithic site of Hacilar, Turkey (approx. 5000 B.C.), but that piece was singular.

PROGRESS IN TL DATING AT RISØ

by

Vagn Mejdahl
Danish Atomic Energy Commission
Research Establishment Risø
Roskilde, Denmark

Abstract

This report outlines our dating technique which is based on the TL emitted by quartz and feldspar inclusions of size 0.3 - 0.5 mm. Beta- and gamma-ray intensities were measured with $CaSO_4$:Mn and $CaSO_4$:Dy respectively.

Results are presented from a dating programme comprising sherds, bricks, burned stones, and burned clay (from kilns) from seventeen excavation sites ranging in age from A.D. 1600 to 4000 B.C.

Introduction

The principles of dating by means of thermoluminescence (TL) have been established during the last decade, mainly through the work of M.J. Aitken and his associates at the Research Laboratory for Archaeology and the History of Art, Oxford[1,2]. The most important progress in recent years has been the development of the "fine-grain" method by D.W. Zimmerman[3] and the "inclusion" method by S.J. Fleming[4]. These methods at present yield absolute ages within 5-10% of the correct value.

During the last few years the Danish Atomic Energy Commission

has supported investigations on TL dating in co-operation with the Danish National Museum and other Danish museums. This report outlines our technique - a version of the inclusion method - and presents results of a dating programme comprising sherds, bricks, burned stones and burned clay from seventeen excavation sites of known age, ranging from A.D. 1600 to 4000 B.C. A report is in preparation[5] which will contain a more detailed description of our technique and a discussion of different sources of error.

Principle of our Dating Method

A clay vessel that is buried in soil will be exposed to cosmic radiation and radiation from radioisotopes, in particular potassium-40 and the uranium and thorium decay series, distributed in the vessel itself and in the surrounding soil. With the assumption that the radiation intensity has been constant, the time elapsed since the firing of the vessel is given by the following simple expression:

$$\text{TL age} = \frac{\text{Accumulated radiation exposure}}{\text{Radiation intensity}}$$

For determination of the accumulated exposure we measured the TL of quartz and feldspar inclusions with a size of 0.3-0.5 mm, and, consequently, neglected the contribution from alpha particles. The environmental radiation was measured with $CaSO_4$:Dy and the radiation from the pottery itself with $CaSO_4$:Mn.

For the two $CaSO_4$ phosphors the peak height of the glow curve was taken as a measure of the exposure; for quartz and feldspar we have a different technique which will be described later; it amounts to integration of part of the glow curve on the high-temperature side of the peak. Calibration of the measurements was carried out with two Co-60 gamma-ray sources.

Our TL-reader was constructed by L. Botter-Jensen and P. Beckmann[6]. The reader incorporates an automatic sample changer which can accomodate twelve metal planchets. Data-logging equipment permits transfer of readings to punched tape for computer processing (fig. 1).

Measurement of Environmental Radiation

The intensity of the environmental radiation at archaeological excavation sites was measured with $CaSO_4$:Dy prepared at our laboratory. The sen-

sitivity of our $CaSO_4$:Dy was the same as that of the phosphor developed by Yamashita et al.[7], but the fading was somewhat larger, about 10% per month at 25°C.

The phosphor was contained in polyethylene bottles, 40 mm in length and with an outer diameter of 9 mm. The bottles were placed with an interval of 10 cm in a steel tube, 1.5-2 m in length and with an inner diameter of 10 mm and a wall thickness of 1.5 mm (fig. 2). At each site three to five steel tubes were hammered into the ground and left for a period of 1-3 months. Included in each tube were a few bottles containing phosphor that had received a known, large exposure; this enabled us to evaluate the effect of fading during the irradiation period.

Results of measurements at about thirty sites have been presented in a previous article[8] which also included a discussion of some sources of error, in particular the energy dependence of response of $CaSO_4$:Dy.

While the intensity of the cosmic radiation (about 30 mR/year at ground level) may be regarded as constant throughout the small area of Denmark, the radiation from the soil varies greatly with soil type. The lowest levels, 30-50 mR/year, occured in the melt-water deposits in West Jutland, whereas considerably higher values, up to 120 mR/year, were found in the moraine deposits in East Jutland and on the eastern islands.

Radiation from Radioisotopes Embedded in the Ceramics

More than two thirds of the radiation dose received by the mineral grains in a sherd is contributed by radiation from radioactive elements in the sherd itself. Our procedure for evaluation of the intensity of this radiation, mainly beta radiation, can be described as follows: The sherds were ground in a mortar and dried in air; then the clay material was put in a polyethylene bag, and a metal planchet to which was cemented a layer of $CaSO_4$:Mn was placed on either side of the bag (fig. 3). Between the phosphor and the bag were several layers of plastic foil to absorb the alpha radiation from the clay. A layer of 30 mg/cm^2 was found to be adequate. During the irradiation, which lasted one week, the bag and its dosimeters were placed in a freezer at -25°C. The exposure was evaluated from calibration with a Co-60 gamma-ray source, and the radiation intensity in the interior of a sherd was taken to be twice the surface intensity.

The technique described has one important limitation: The plastic foil absorbs not only the alpha radiation, but also part of the beta radi-

ation; the layer thickness therefore enters as a parameter to be fixed. The thickness of 30 mg/cm^2 was adjusted so that the TL dates of some selected sherds were correct and was kept constant throughout the present project.

Accumulated Exposure

The total radiation exposure incurred by a sherd since the firing of the vessel from which it originated was determined by means of quartz and feldspar grains with a size of 0.3-0.5 mm. The minerals were separated from the clay by sifting. The grains were washed with diluted HCl and HF, and magnetic grains were removed. 200-mg samples were placed on metal planchets and heated in the reader for about 30 sec. The initial heating rate was approximately 13°C per second, but for continued heating an increasing deviation from linearity occurred; however, the heating cycle could be reproduced with a standard deviation of 1%.

The read-out equipment included a data-logging unit that could register the TL signal at selected time intervals, for instance each second. A read-out cycle consisted of preheating for 10 sec followed by registration of twenty TL-intensity values which were automatically transferred to punched tape.

When the naturally acquired TL (NTL) had been measured, the samples were annealed at 350°C for 30 min and exposed to Co-60 gamma-radiation for calibration. Glow curves for NTL and a calibration exposure of 300 R are shown in figure 4. The twenty TL readings were divided into five groups and for each group the accumulated exposure was calculated. Good agreement was nearly always found between groups 2 and 3, which indicated that the fading from traps corresponding to this part of the glow curve could be neglected. Fading was indicated for group 1 which was generally 20% lower than the two following groups. Group 4 could be included if the signal was sufficiently high; group 5 was not used.

Results of TL Dating

Results obtained during the last two years are presented in table 1 which contains (1) TL ages for individual samples from the same context, (2) mean values for each context, (3) standard deviations of the mean values, and (4) differences between TL age and "archaeological age". The archaeological age is an estimation of absolute age which can be

(a) Estimation from archaeological chronology based on typological and stratigraphical considerations.

(b) Carbon-14 date corrected by means of the dendrochronological calibration curve published by H. Suess[9]. A compilation of carbon-14 dates and corresponding absolute ages has recently been published by H. Tauber[10].

(c) Estimation based on carbon-14 dating of nearby sites containing ceramics of the same type.

The archaeological age is given here as a single number to permit comparison with the TL age; actually it was always stated as an interval of 100-200 years.

The results given in table 1 are not completely comparable because the technique was gradually improved during the period, and new equipment was installed. In addition, some limitations in the material should be noted:

(1) The environmental radiation could not always be measured with sufficient accuracy; in several cases the sites were excavated before the measurement of the radiation.

(2) In order to gain experience a broad range of sites were included, and in some cases it turned out that the archaeological age was not sufficiently well known.

(3) No correction was made for variation in water content of the sherds caused by differences in pore volume.

(4) The beta-dose received by the outer layers of a sherd will be lower than that received by layers in the interior if the surrounding soil has a lower content of radioactive elements than the sherd. This effect was neglected.

(5) Spurious luminescence which could not be removed by flushing with nitrogen occurred in a few cases.

Since in most cases several samples were measured from each archaeological context, the results given in table 1 allow an evaluation of the relative accuracy of our method, expressed as the standard deviation of the average TL age for a context. The distribution of the standard deviations is shown in figure 5 in the form of a histogram. It may be seen that nearly 80% of the standard deviations are below 5%. The larger standard deviations may reflect real differences in age because in most cases the sherds were from

different vessels. For site No. 7, layer PI, 1-6, the first three sherds were from the same vessel; here the largest difference is 60 years, corresponding to about 3%.

While the relative accuracy of a TL date for a context taken as the mean value for a number of samples from the context seems to approch that of a single C-14 date, it is still not clear whether sufficiently absolute accuracy can be achieved. The results in table 1 give a general impression of the absolute accuracy, but only a few of the sites allow a definite test. The best site is probably Fredbjerg (No. 7), where the sherds in layers PG to PL were taken from a square metre surrounding one of the steel probes for measurement of environmental radiation. Several layers could be distinguished, but all sherds were stated to be from the same period: 0 ± 50 years. The average TL age for the twenty-seven sherds was 2106 years ± 50 years (standard deviation) which is about 7% more than the archaeological age, 1970 years. The distribution of all results from the site is shown in figure 6. Statistically, the curve might seem to indicate the presence of two groups of sherds differing in age by 300-400 years, but the measurements were not sufficiently accurate for this interpretation.

Closer agreement was found for the sites Grøntoft, Nørrekær, and Lånum. However, for Grøntoft and Nørrekær an older technique was used in which the determination of accumulated exposure was based on only one TL-intensity measurement for each sample of mineral grains. For Lånum the new technique was used, but the site was not directly C-14 dated; the archaeological age was obtained by adding the Suess correction (650 years) to C-14 dates for sites a few km away which contained ceramics of the same type. Since there can hardly be any doubt that the tombs considered are from the same period, one might be justified in attaching significance to the close agreement between the TL date and the corrected C-14 date.

The results in table 1 and figure 5 indicate that heated stones might be a valuable material for TL dating. One advantage of stones is their greater content of radioactive minerals, which gives a high beta-ray intensity; gamma-radiation from the environment is, therefore, of less importance. The possibility of using heated stones greatly increases the range of TL dating. In Denmark the oldest ceramics found dates from about 4500 B.C. (Ertebølle period), but heated stones (pot boilers) frequently occur in older layers.

Discussion of Individual Sites

The following is a brief discussion of the individual sites listed in table 1. As mentioned above, the results do not allow a general assessment of absolute accuracy, but valuable experience may be gained on various aspects of the method.

No. 1, Torup. A farm that was abandoned around A.D. 1600 because of sand drift. The samples, a granite stone and two bricks, came from the bottom of a baking oven which was made up of flat stones. The top soil (shifting sand) had been removed when the environmental radiation was measured; we therefore used the average (108 mR/year) of the results obtained in the oven and in nearby soil. Insertion of the value obtained for the oven (130 mR/year) would give a lower limit of TL age corresponding to A.D. 1540.

No. 2, Okholm. Layers from the Viking period, A.D. 800-1000. The result for the upper layer is nearly correct, but for the lower layer spurious luminescence caused serious errors. The site is near a marsh area adjacent to the North Sea and has been inundated by the sea. There are indications that the spurious luminescence might be related to sea deposits.

No. 3, Rosenhof (Oldenburg, Germany). Slavic settlement on an island in an inlet from the Baltic Sea. The inlet was drained around A.D. 1930, and the sherds came from extensive layers of waste in the reclaimed land. Also for this site spurious luminescence was a problem.

No. 4, Valdemarsmur. A 2-m thick and 6-7-m high brick wall built about A.D. 1170 as a fortification of the wall Dannevirke (now in Germany). The environmental radiation was not measured in the wall, but in a small laboratory arrangement of the bricks; the value obtained (95 mR/year) is probably too small. Insertion of the highest value (130 mR/year) found in clay-rich soil gives an average TL age of 830 years, corresponding to A.D. 1140. The results indicate that bricks can be used for TL dating, but care must be taken with the measurement of environmental radiation.

No. 5, Dankirke. Settlement for several hundred years in Pre-Roman and Roman Iron Age has yielded strata separated by 50-100 years which were rich in ceramics. The four layers considered here ranged from A.D. 400 to A.D. 100 and provided a unique possibility of testing the relative accuracy of our technique. In figure 7 the TL ages are compared with the corresponding archaeological ages. The figure shows that layers differing in age by 50 years could not be distinguished, but an interval of 100 years (about 5%) could easily be registered. The absolute agreement between TL age and

absolute age is also good, but the significance of this is not certain because we had to insert a value for the environmental radiation that was measured about 500 m away.

No. 6, Dätgen (Germany). Iron Age site. The excavation had been completed and the site covered by a road before the measurement of the environmental radiation; again the radiation therefore had to be measured some distance away.

No. 7, Fredbjerg. Iron Age settlement. Most of the sherds from this site were from an occupation layer close to a steel probe (layers PG to PL). Sherds from layers PM and PN were taken near another probe, but according to the excavation they might be somewhat older than stated in table 1 (se also figure 6).

No. 8, Grøntoft. Settlement from Pre-Roman Iron Age. The environmental radiation was measured only a few metres from the pit where the sherds were taken and is considered to be representative; however, as mentioned earlier, an older technique was used for measurement of the accumulated exposure.

No. 9, Nørrekær. Pre-Roman Iron Age. The sherds were from a small bog which contained a layer of stones; this is probably the reason for the large scatter in individual results. Again the old technique was used for measurement of accumulated exposure, but with this reservation the agreement between average TL age and archaeological age is regarded as significant.

No. 10, Skamlebæk. Extensive occupation layer containing ceramics from the late Bronze Age. Sherds and heated stones were obtained from the immediate surroundings of the steel probes, but, unfortunately, the absolute age of the material was not quite certain.

No. 11, Engedal. Bronze Age period IV. Cremation urns from a small mound. Urn No. 1 had a packing of quartzite which was very low in radioactivity and has therefore acted as a shield towards the radiation from the soil. Except for urn No. 1 the TL age is considerably higher than the archaeological age which is based on typology since no C-14 dates were available. It is at present not clear whether the archaeological chronology for this period is correct or should be increased according to Suess's calibration curve.

No. 12, Birkendegård. An aerial view of this site has revealed a pattern of crop marks that formed traces of three concentric circles, the outer circle with a diameter of 320 m. An archaeological investigation indicated that the marks might have been the foundations of large stones, but

the stones had been removed at some unknown time in the past, and the artifacts found did not allow an estimation of the age of the site. The TL dates were obtained from a few small pieces of ceramics and a number of heated stones from a pit. The average TL date was 1400 B.C.

No. 13, Lånum. A long barrow from the Middle-Neolithic funnel beaker culture (TRB culture), period MNIb. The site has not been carbon-14 dated, but passage graves a few km away containing ceramics of the same type were carbon-14 dated to 2550 B.C. corresponding to an absolute date of about 3200 B.C. The sherds were taken close to one of the steel probes, but the presence of a stone layer caused a rather large variation of results for individual samples. However, the average value is in good agreement with the corrected C-14 date. A TL date obtained from a sample of sand that had been heated in a fire was in satisfactory agreement with that obtained from the sherds.

No. 14, Limhamn (Sweden). The material used for dating was a small sherd and a couple of stones found in a kiln. Since a house had been built on the site, the environmental radiation had to be measured some distance away. The site was not carbon-14 dated, but some of the ceramics found in or near the kiln was stated to be of the pitted-ware type. The TL date obtained from the stones (2436 B.C.), which is probably the most reliable, corresponds to a carbon-14 date of about 2000 B.C.; this is not inconsistent with a late phase of the pitted-ware culture.

No. 15, Lindebjerg. A long barrow of hitherto unknown construction from the Early Neolithic period. The first TL date, 1995 B.C., for burned stones from a fire pit east of the barrow, suggests that the feature does not belong to the primary period of the barrow. Sherds from a superficial layer of mound fill (27) appear to be from a secondary period, but the TL age is considerably less that the archaeological age of the sherds (Early Neolithic). Charcoal found in a primary feature of the barrow (feature C) gave a reading of 3050 B.C. in conventional C-14 years, corresponding to a calibrated date of about 3860 B.C. This was in reasonable agreement with the TL dating of the first sample of sherds from a large pot found in the same feature, 117C (1), but further sherds from the same vessel (117C (2)) gave a much lower mean date, 3064 B.C. Sherds 221 from a primary layer of mound fill gave a TL date of 3693 B.C., which is consistent with the calibrated C-14 date for the charcoal from feature C.

No. 16, Büdelsdorf (Germany). A palisade-fortified Neolithic settlement. Most of the TL results were from clay taken from a kiln. The environ-

mental radiation was measured in soil some distance away, and the value obtained (90 mR/year) might be lower than the level in the kiln because the clay of the kiln had a higher content of radioactive elements than the soil. The average TL date for the site was 3750 B.C. A C-14 date is not yet available, but the archaeological estimation is Middle-Neolithic time, period MNIb. The oldest C-14 date of Danish sites from this period (Vroue) is 2600 B.C. corresponding to a calibrated date of 3250 B.C.[10] Even on an absolute scale, the TL date thus seems to be somewhat too high.

No. 17, Stengade. Early Neolithic house. The site was very rich in ceramics from the funnel beaker period TNB. The two average TL dates are in good agreement and yield a TL date of 3816 B.C. Unfortunately, no material was found for C-14 dating. C-14 dates of sites containing TNB ceramics have been listed by Tauber[10], but tha range is so large (from 3400 B.C. to 4200 B.C. on the calibrated scale) that no conclusion regarding the age of this site can be drawn.

Conclusion

The results presented in this report were obtained from TL dating of sherds, bricks, heated stones, and clay from kilns from seventeen archaeological sites ranging in age from A.D. 1600 til 3800 B.C.

Since in many cases several samples were available from each archaeological context, the results give a clear illustration of the relative accuracy that may be achieved with the TL method. For more than 80% of the contexts the standard deviation of the average TL age for the context was less than 5%; it should thus be possible to use the method for relative dating, for instance of ceramics from sites containing strata or ceramics from different periods occurring in the same context.

The absolute accuracy, taken as the difference between the TL age and the "archaeological" age was in several cases 5% or lower, but, as discussed above, the material does not allow a general evaluation of absolute accuracy. However, the results of the present investigation seem to be sufficiently encouraging to warrant a renewed effort in which the following precautions should be taken:

(1) The known systematic errors should be eliminated.

(2) The measurement of the environmental radiation should be representative; that is, with a few exceptions, only sites under excavation can be accepted.

(3) The sites should be accurately dated by other methods.

Acknowledgements

It is a pleasure to acknowledge the interest and co-operation of the excavation directors and their assistants throughout this project. I am further indebted to Miss L. Damstedt, Mr. L. Kristoffersen, Miss E. Lægård, Mr. F. Pedersen, Mrs. L. Sørensen, Miss U. Rasmussen and Miss L. Vinther Kristensen for skilful assistance during different phases of the project. A grant from the Carlsberg Foundation which permitted the employment of Mr. Kristoffersen and Miss Rasmussen is gratefully acknowledged.

References

1) M.J. Aitken, Phil. Trans. Roy. Soc. Lond. A269, 77-88 (1970).
2) S.J. Fleming, Die Naturwissenschaften 58, 335-338 (1971).
3) D.W. Zimmerman, Archaeometry 13, 29-52 (1971).
4) S.J. Fleming, Archaeometry 12, 133-146 (1970).
5) V. Mejdahl, Risø Report No. 249 (1971) (In preparation).
6) L. Botter-Jensen and P. Beckmann, Proceedings of the Second International Conference on Luminescence Dosimetry, Gatlinburg, (CONF-680920, NBS, Springfield, Virginia) 640-651 (1968).
7) T. Yamashita, N. Nada, H. Onishi, and S. Kitamura, Health Physics 21, 295-300 (1971).
8) V. Mejdahl, Archaeometry 12, 147-159 (1970).
9) H. Suess, In "Radiocarbon Variations and Absolute Chronology" (editor I.U. Olsson). Nobel Symposium 12, 303-309. Almqvist and Wiksell, Stockholm (1970).
10) H. Tauber, Aarbøger for Nordisk Oldkyndighed og Historie 1970, 120-142 (1971). (Summary in English).

Table 1

Results from TL dating of sherds, bricks and stones

Site No.	Site	Layer	TL age (years) Individual sherds from the same context	TL age (yrs) mean value	St. dev. of mean value (%)	TL date	Arch.date	$\Delta A\%$[a]
1	Torup	Oven	461 431 451 650 466	490	8.0	AD 1480	AD 1600	32.4
2	Okholm	RO	844 1100 870	938	8.7	AD 1032	AD 970	- 6.2
		SX	1557 1348	1452	7.2	AD 518	AD 970	45.2
3	Rosenhof (Germany)	Slavic	709 896 874 641 680 889	780	5.5	AD 1190	AD 1050	-15.2
4	Valde-maramur	-	1148 1058 892 857 1009 890 894	960	4.3	AD 1010	AD 1170	20.0
5	Dankirke	E	1605 1560 1490	1552	2.5	AD 418	AD 450	2.1
		F	1557 1460 1499 1586	1526	1.9	AD 444	AD 400	- 2.8
		H7+J8	1636 1661 1655 1693 1652	1659	0.6	AD 311	AD 300	- 0.7
		M	2012 2035 1846 1909	1951	2.4	AD 19	AD 100	4.3
6	Dätgen (Germany)		2072 1784 1750 1808	1850	4.4	AD 120	AD 75	- 2.4
7	Fred-bjerg	Exc. 1969	2183 2197 1902 2462 2339 1852 2362	2190	4.0	220 BC	0 BC	11.2
		PG	2192	2192	-	222 BC	0 BC	11.3
		PH	2534 2409 2123 2056 2366	2298	3.9	328 BC	0 BC	16.6
		PI, 1-6	1945 1918 1977 1780 1721 2184 2037	1937	3.0	AD 33	0 BC	- 1.7
		PI, 7	2057 2094 1880 2453 2045	2106	4.5	136 BC	0 BC	6.9
		PJ	2635 1832 2023 2253 2071	2163	6.3	193 BC	0 BC	9.8
		PK	2102 1977 1871	1984	3.4	14 BC	0 BC	0.7
		PL	2338	2338	-	368 BC	0 BC	18.7
		PM	2097	2097	-	127 BC	0 BC	6.4
		PN	2292 2303 2531 2559	2421	3.0	451 BC	0 BC	22.9
8	Gren-toft	EXV, B	2142 2253 2321	2239	2.3	269 BC	300 BC	- 1.4
9	Nørre-lær	II	2344 2728 2194	2422	6.6	452 BC	450 BC	0.1

Table 1 continued

Site No.	Site	Layer	TL age (years) Individual sherds from the same context	TL age (yrs) mean value	St. dev. of mean value (%)	TL date	Arch.date	$\Delta A\%$[a]
10	Skamlebæk	SK 9	2377 2734 2778 2988	2719	4.7	749 BC	500 BC	10.1
		1 TL, 63	3411 3632 3432 3585 3551 3442	3509	1.1	1539 BC	700 BC	31.4
		2 TL	3358 3081 2188 2185 2954 2995	2794	7.2	824 BC	700 BC	4.6
		1 TL	2935 2756 2997 3220 3113 3157	3031	2.3	1061 BC	700 BC	13.5
		SK 30 TL	3278 2986 3226	3163	2.8	1193 BC	700 BC	18.5
		(2,3,4,5)	2996 3001 1992 2748	2684	8.9	714 BC	700 BC	0.5
11	Engedal	Urn 1	2698 2667	2682	0.6	712 BC	900 BC	- 6.5
		Urn 4	3095	3095	-	1125 BC	800 BC	11.7
		Urn 5	3272	3272	-	1302 BC	900 BC	14.0
		Urn 6	3317 3020 3054	3131	3.0	1161 BC	900 BC	9.1
12	Birkendegård	Stones	3291 3271 3655 3249 2797	3253	4.2	1283 BC	-	-
		Sherds	3439 3563	3501	1.7	1531 BC	-	-
13	Lønna	Sherds	4660 4713 5466 5663 5143	5129	3.9	3159 BC	3200 BC	- 0.8
		Heated sand	5438	5438	-	3468 BC	3200 BC	5.2
14	Lisbæmn	Sherd	4909	4909	-	2939 BC	-	-
		Stones	4376 4392 4402 4452	4406	0.4	2436 BC	-	-
15	Lindebjerg	Stones	3956 3847 4154 3429 4207 4197	3965	3.1	1995 BC	-	-
		27	3564	3564	-	1594 BC	-	-
		39	5121	5121	-	3151 BC	-	-
		117C (1)	5500	5500	-	3530 BC	3860 BC	- 5.7
		117C (2)	5502 4874 5087 4943 4687 5114	5034	2.2	3064 BC	3860 BC	-13.6
		221	5663	5663	-	3693 BC		
16	Büdelsdorf		5521	5521	-	3551 BC	MN1b	
			5868 6015 6771 5102 6007 5573	5889	3.8	3919 BC	MN1b	
			5111 5946 5920 5672 6158	5761	3.1	3791 BC	MN1b	
17	Stengade		5490 5577 5909 6257	5808	3.0	3838 BC	TNB	
			5743 5682 5785 5850	5765	0.6	3795 BC	TNB	

Sherds: No sign. Stones: ----- Bricks:——— Clay from kilns:·····

a) $\Delta A = \frac{\text{TL age-Arch. age}}{\text{Arch. age}}$

Figure 1. Equipment for measurement of TL. Left: Automatic sample changer with a capacity of twelve samples. Centre: Data-logging unit. Right: "Teletype" printer and puncher.

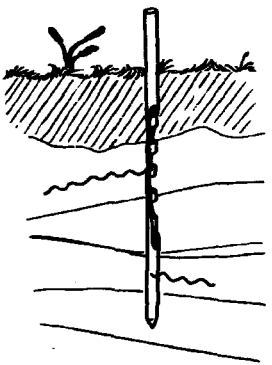

Figure 2. The environmental radiation is measured by placing steel tubes containing bottles with the TL-phosphor $CaSO_4$:Dy at the excavation site for a period of one to three months.

Figure 3. The intensity of beta-radiation originating from radioactive elements embedded in a sherd is measured by means of the phosphor $CaSO_4$:Mn cemented to a metal plate.

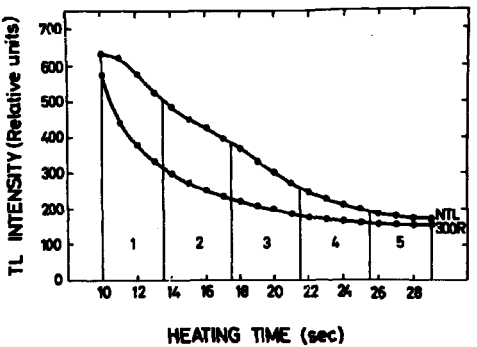

Figure 4. TL intensity as a function of heating time for quartz and feldspar grains extracted from a sherd. NTL is the TL released during the first heating of the sample; "300 R" is the TL induced in the same sample by a Co-60 gamma-ray exposure of 300 R.

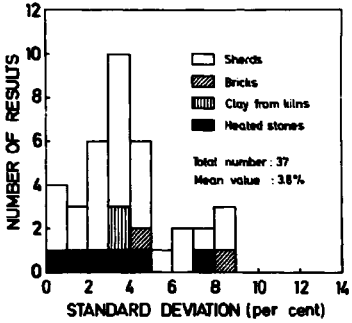

Figure 5. Distribution of the standard deviation of the average TL age for an archaeological context.

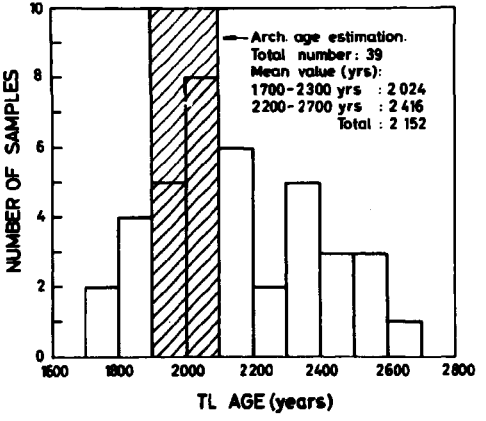

Figure 6. Distribution of TL ages of sherds from the site Fredbjerg.

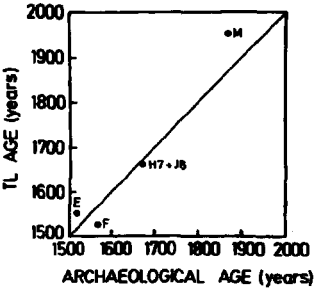

Figure 7. TL age plotted as a function of archaeological age for strata from the site Dankirke.

Higashimura

It seems that on average the TL age obtained is older than the archaeological age. Have you an explanation for this?

Mejdahl

There may be a systematic error in the results because the thickness of the plastic layer that absorbs the alpha radiation during the measurement of radiation from the sherds enters as a parameter.

Niewiadomski

Did you try to investigate the TL of biological fossil materials?

Mejdahl

No, we have not tried to measure the TL of biological materials, but we have sent samples of burned bone from the Bronze Age to Dr. Fremlin at Birmingham. I should like to add in this connection that Dr. Brown informed me that he has measured TSEE of bone with encouraging results.

Some Uncertainties in Thermoluminescence Dating

by

Mark C. Han and Elizabeth K. Ralph

Museum Applied Science Center for Archaeology

The University Museum

University of Pennsylvania

Philadelphia, Pennsylvania

U.S.A.

Abstract

The relative effect of alpha particles versus betas, gammas, and X-rays in producing radiation damage continues to be one of the major uncertainties in the dating of pottery by thermoluminescence (TL). In recent experiments with Po^{210} sources, an attempt has been made to determine the precise range of alphas in clays so that an absolute comparison between the effects could be made. A study of the decay series of U^{238} and Th^{232} has also indicated the necessity of knowing the proportions of these two elements in each sample before any estimation of the total dose from inherent radioactivity can be made. Until more measurements and studies are made and the magnitude of these uncertainties is reduced, we feel that greater reliability is achieved by the so-called "relative" method, that is, by calculating TL dates from a calibration curve based on samples of known age. This procedure circumvents the problem of estimating the total inherent natural radioactivity.

Introduction

In the course of dating pottery by thermoluminescence (TL) here at MASCA (Museum Applied Science Center for Archaeology), University of Pennsylvania, the procedures have been standardized during the past several years. We have determined that from artificial irradiations of X-rays at relatively low dosages (below 3,000 rads), the production of TL is a linear function. After finding that the Artificial-TL induced by X-rays in pottery is linear and is similar to that produced by beta and gamma irradiations at low doses, we have thus proceeded to use a standard X-ray dose as the means of determining the susceptibility of each given pottery sample. This is done after the TL induced by the natural process from its internal radioactivity has been determined. We have assumed that the major part of the inherent dose is proportional to the rate of alpha disintegration which is readily measurable with ZnS scintillation counters. This assumption leads us, however, to the important problem of the relative effectiveness of alpha particles in producing radiation damage.

Alpha Experiments

In the decay series of U^{238} and of Th^{232}, alpha disintegrations are much more abundant than betas or other particles. However, alphas are less effective in producing radiation damage and consequently, thermoluminescence (TL). In recent experiments we have attempted to evaluate the relative effectiveness of alphas, betas and gammas versus X-rays.

A calibrated Po^{210} source in the form of a circular disc 2 cm in diameter was obtained from the National Bureau of Standards. (The disintegrations from Po^{210} consist of 100% alphas). Since the half-life of Po^{210} is relatively short (138.4 days) all subsequent calculations were corrected for the decay of the source. To convert alpha disintegrations per unit of time to rads per hour for comparison with X-ray and other doses, it was necessary to determine the range of alphas in our samples of powdered pottery and the densities of the samples.

For the range determination, a piece of mylar film 0.0254 mm thick was placed over the ZnS screen of one of our regular alpha counters[1]. The effect of this film and the overall efficiency of detection were measured. Then, one by one, increasing thicknesses of powdered pottery were placed between the mylar film and the Po^{210} source. The decrease in the counting rate with increasing thickness of pottery is plotted in Figure 1. This plot shows that the range is about 22 μ (microns).

With this information and the measurements of the densities of these samples of powdered pottery, it was then possible to compare the doses of various thicknesses of pottery from different sources. In order to do this, it was necessary to prepare samples of varying thicknesses, some very thin, which could be heated subsequently for the TL measurements. This sounds easy, but we soon discovered that thicknesses of less than 30μ could not be prepared by standard petrographical techniques due to the fragility of the pottery and the necessity of transferring it from glass plates prior to heating. Fortunately, we found a high temperature resin (PR 990 Resin, El Monte Chem. Co. of Pasadena, Calif.) that solved the problem. With this we were able to mount uniform coating of pottery on aluminum foil ranging in thickness from 7 μ to 110μ. Series were prepared with two types of pottery.

These were irradiated with the calibrated Po^{210} source obtained from the NBS. From the series of different thicknesses, it was found again that the average effective range of alphas in both types of pottery with different susceptibilities was 22μ.

The next step was to irradiate samples of one selected thickness with the Po^{210} source for different lengths of time, and to compare the TL from these exposures with the TL from the X-ray, gamma, and beta doses. (Subsequent rechecks with X-rays and irradiation of a few samples with alphas without prior exposure to X-rays, etc. indicated that none of these doses had changed the susceptibility of these samples to radiation damage). By means of the previously determined precise value for the range of alphas, the alpha doses could then be converted to rads (units of radiation) for this comparison. (See Appendix). (The doses for the X-rays, etc. were measured with an ionization chamber). The results are shown in Figures 2, 3, 4 and 5.

From these results we find that alpha particles are 10% as efficient in producing TL while betas are 16% and gammas are 20% compared with X-rays.

However, to apply this information to the natural TL dose, one is led back to the difficulty of estimating the proportion of alphas in the total inherent and adjacent external radioactivity. Since the decay chains of U^{238} and Th^{232} differ, one needs to know the ratio of these two -- the major radioactive elements as well as the K^{40} content and the contribution from external gamma radiation. Chemical methods of measuring U^{238} and Th^{232} in these small quantities are too imprecise to be of much use. The rates of alpha decay are too slow and the energy distributions too similar to be differentiated by radioactive means.

TL Dating of Egyptian Faience

Preliminary experiments with three objects indicate that ancient Egyptian faience does exhibit the phenomenon of thermoluminescence (TL), that is, the artifacts give off light when heated. X-ray irradiation of these same objects shows also that faience is susceptible to radiation damage in a manner similar to pottery. However, faience, since it consists mostly of quartz, does not contain traces of uranium and thorium. This fact was confirmed in tests with our alpha counters -- there were no alpha disintegrations. Therefore, the natural TL of faience must be due to other causes -- namely:

1. K^{40} inherent in the faience.

2. Irradiation from natural radioactivities within and surrounding the tombs or other burial sites.

3. Cosmic ray exposure.

The first can be determined by analysing (by flame photometry) the total potassium content of each object, and calculating the dose from the known ratio of K^{40} to total K. The second and third can be determined by placing dosimeters (small vials of $CaSO_4$ doped with dysprosium or other suitable phosphors) in the tombs from which the faience artifacts have been excavated. After six months to a year have elapsed, the dosimeters can be

brought back to the laboratory and the TL that they have accumulated will give a relative measure of the external radiation dose (items 2 and 3) that the objects have received.

This project appeals to us in that it involves some new techniques, and as far as we know, has never been done before. Also, it may be the ideal technique for dating or comparing the relative dates of the Egyptian dynasties. The main reason is that abundant samples of faience representative of these periods are available and expendable. We anticipate that the technique will be successful for relative dating and might, possibly, furnish absolute dating as well if enough corollary experiments are performed. Dosimeters have been arranged to be installed in the following Egyptian tombs:

a) Tomb no. 34 (Tuthmosis III) in Valley of Kings.

b) Tomb no. 35 (Amenhotep II) in Valley of Kings.

c) Tomb no. 35 (of Bekenhons) at Dra-Abu-el'Naga.

d) Tomb no. 269 at Dra-Abu-el'Naga.

e) Tanis Royal Tomb III (Psusennes I)

Another reason is the need for precise relative dating of the Egyptian dynasties. Now that more is known about the problems of C^{14} dating[2,3,4] from the dating of the dendrochronologically-dated bristlecone pines[5], we realize that correction factors must be applied to C^{14} dates. For the period of the First Egyptian Dynasty, about 3000 B.C., this correction is of the order 700 years. In addition to the now determined long-cycle deviation in C^{14} dates, there may also have been wiggles in the atmospheric C^{14} inventory with periods of 100 to 400 years. Until more is known about these, C^{14} dating should not be relied upon for very precise comparisons of contiguous Egyptian dynasties.

Acknowledgement

We should like to thank Dr. N. Suntharalingam of Jefferson Medical Center for his helpful discussions and advice, and for the irradiation of samples with beta and gamma sources. Funds for this study were provided by the National Science Foundation (GS-2716).

References

1. E. K. Ralph, and M. C. Han, Thermoluminescence of Geological Materials. ed. D. J. McDougall, 376-387 (Academic Press Inc., New York, 1968).

2. H. N. Michael, and E. K. Ralph. Radiocarbon Variation and Absolute Chronology. ed. I. U. Olsson, 109-120 (John Wiley and Sons, Inc., New York, 1970).

3. H. E. Suess, ibid., 303-311.

4. P. E. Damon, ibid., 571-593.

5. C. W. Ferguson, ibid., 237-259.

Appendix

In order to calculate the dosage from the alpha irradiation, we need to know the effective amount of the pottery sample which was exposed to the calibrated Po^{210} source. The calculations are as follows:

Volume (V) of pottery used in measurement

$V = A \times T$ where A = area
$= \pi r^2 \times T$ T = thickness = 22 μ
$= 3.142\ cm^2 \times 2.2 \times 10^{-3}\ cm$ and r = radius = 1 cm.
$= 6.912 \times 10^{-3}\ cm^3$

Mass of pottery = $V \times \rho$ where ρ = density = 3.20 g/cm^3
$= 6.912 \times 10^{-3}\ cm^3 \times 3.20 \frac{gm}{cm^3}$
$= 2.21 \times 10^{-2}\ gm$

The energy (E) of alphas from the Po^{210} source is:

$E = 5.305$ mev/α
or $E = 5.305$ mev/$\alpha \times 1.602 \times 10^{-6} \frac{ergs}{mev}$
$= 8.50 \times 10^{-6}$ ergs/α

and per gram of pottery: $E = \frac{8.50 \times 10^{-6}\ ergs/\alpha}{2.21 \times 10^{-2}\ gm}$

$= 3.85 \times 10^{-4}$ ergs/gm-α

In terms of rads (1 rad = 100 ergs/gm) we obtain:

$E = 3.85 \times 10^{-6}$ rads/α

which is the effective dose received by these two experimental samples of pottery per alpha disintegration.

Thus, we can calculate the dosage received over varying lengths of time as shown below in Table 1, and as illustrated in Fig. 4.

Table 1

Alpha dosage in rads; calculated from: Effective energy absorbed per alpha x average alpha dis/sec during irradiation x length of exposure time to source. In the fourth column the A-TL induced by the corresponding doses is listed.

Length of Exposure time in hours	Average alpha dis/sec during exposure time	Calculated alpha dosage in rads	A-TL Induced
Sample P-T-74			
24	1255	416	0.270×10^{-8} A
48	1215	806	0.600
48	1246	827	0.613
72	1054	1050	0.670
72	1231	1226	0.744
96	1122	1490	1.020
120	1275	2116	1.273
144	1150	2290	1.470
168	1188	2760	1.650
192	1020	2708	1.680
216	968	2892	1.840
216	1086	3244	2.220
Sample P-T-190			
24	1855	616	0.131×10^{-8} A
48	1917	1272	0.263
72	2010	2001	0.430
117	1884	3048	0.628
144	1310	2609	0.540
168	1354	3146	0.693
192	1601	4251	0.843
240	1412	4686	0.930
283	1792	7013	1.344
408	1507	8503	1.680

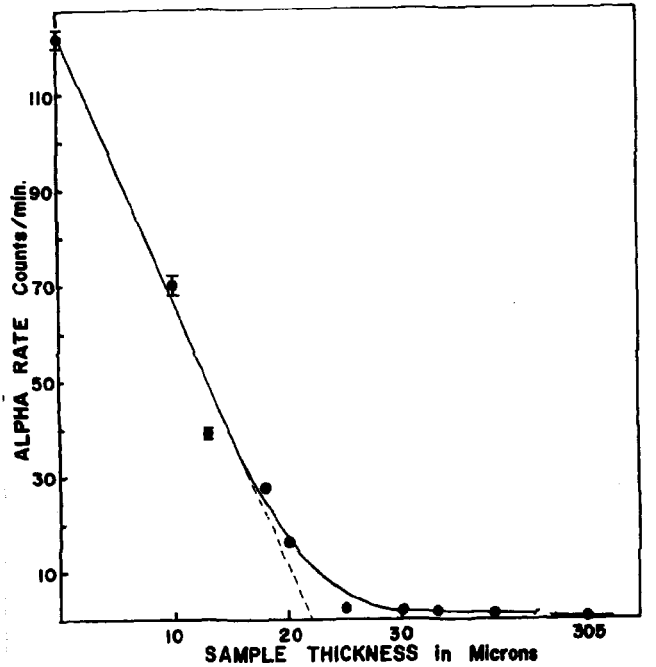

Figure 1: The decrease of alpha counting rates from the Po^{210} source with increasing sample thickness which were placed in succession between the source and the screen.

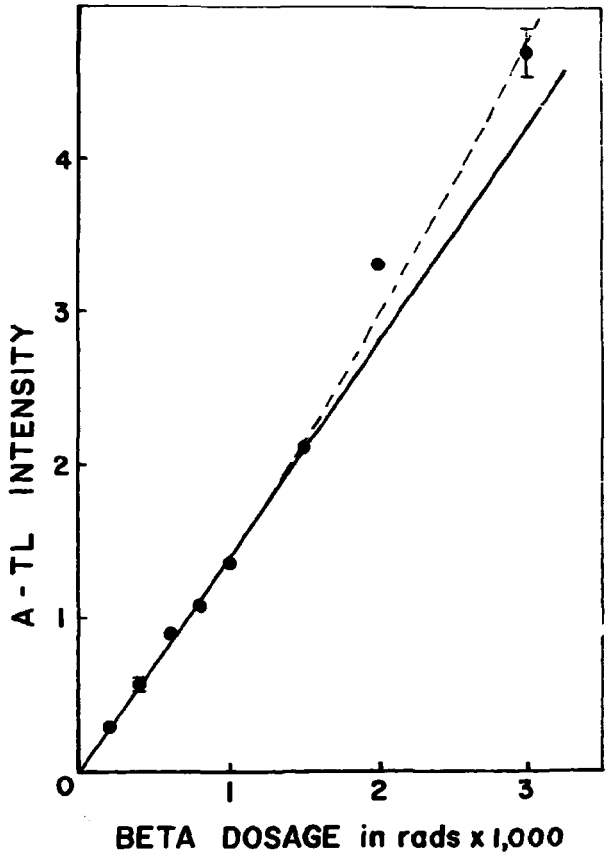

Figure 2: A-TL (artificial thermoluminescent) intensity induced from increasing doses of beta radiation up to 3,000 rads.

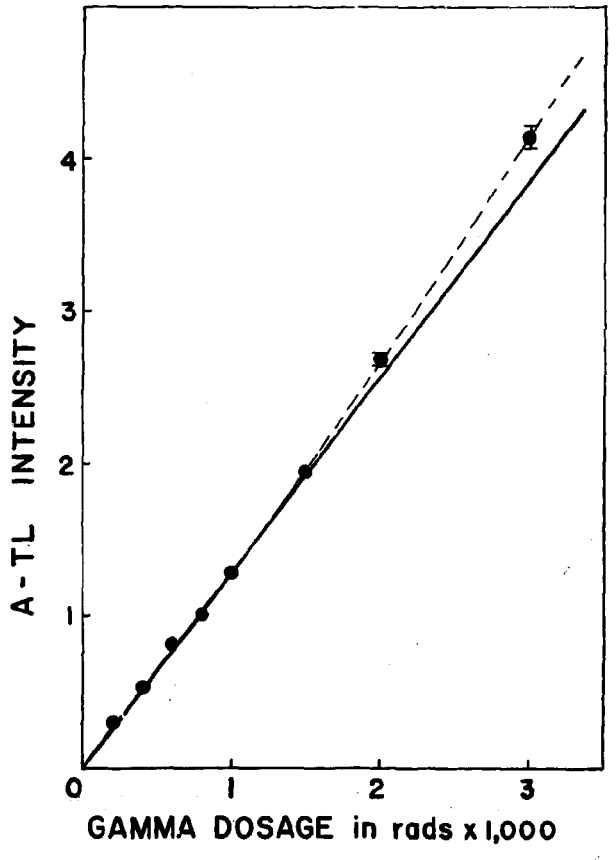

Figure 3: A-TL intensity induced from increasing doses of gamma radiation up to 3,000 rads.

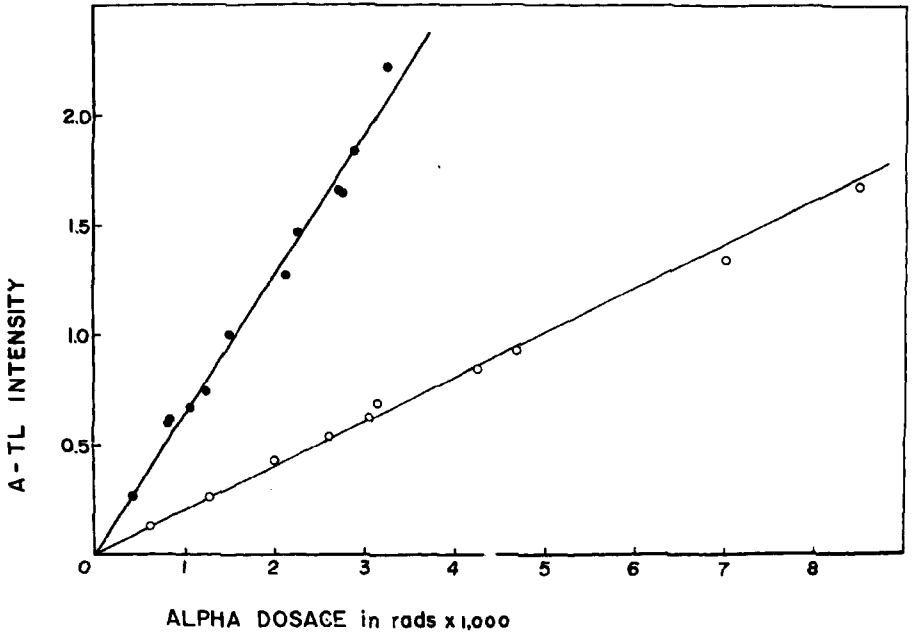

Figure 4: A-TL intensity induced from increasing doses of alpha radiation for two samples having different susceptibilities up to 3,500 and 8,500 rads respectively.

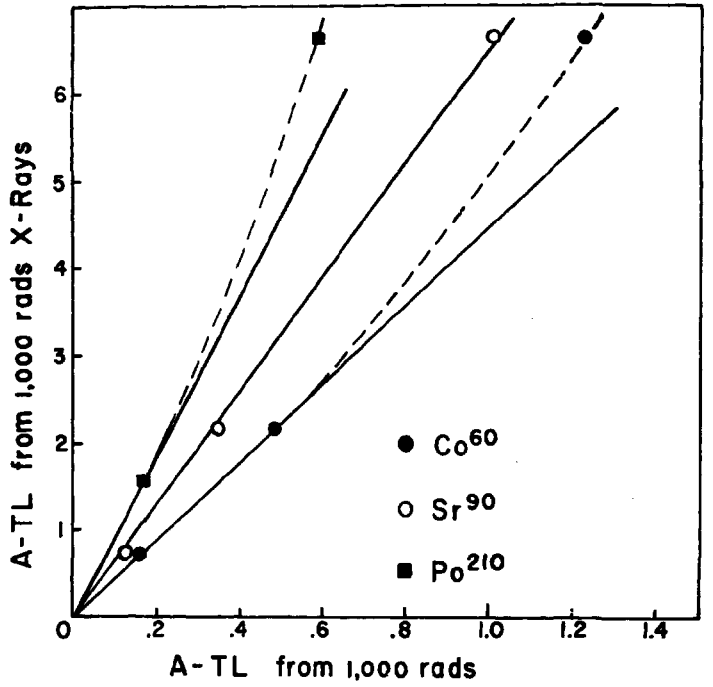

Figure 5: The susceptibility of samples (as indicated by their A-TL) to alpha, beta and gamma radiation compared with X-ray dosages of 1,000 rads.

Spurny

Which dating method is up till now the better, TLD or C-14? As far as I know, C-14 dating differs systematically from dendrochronological age; is the same the case with the TLD method?

Han

There is no doubt that the C-14 method is better. However, the problem in C-14 dating does not occur in the TL method, and it is our hope that TL can be used as an independent approach to the establishment of the chronology for the past and can be used to complement the well-established C-14 method.

Tauber, H. (C-14 laboratory, Danish National Museum)

C-14 dates deviate from dendrochronology for material older than 500 B.C. this is due to a higher production of C-14 in the upper atmosphere, caused by a lowering of the earth's magnetic dipole moment, and does not effect TL dating, except perhaps for a very slight change in environmental dose. In this respect TL dating has an advantage over radiocarbon dating. However, when calibrated by dendrochronology C-14 dating is still the most accurate method for dating the prehistory both as to relative and absolute accuracy.

Third International Conference on Luminescence Dosimetry

Risö, Denmark, October 11 to 14, 1971

Environmental and Personnel Dosimetry in Tropical Countries[1]

Klaus Becker[2], Rosa Hong-Wei Lu and Pao-Shan Weng
National Tsing Hua University
Hsinchu, Taiwan, Rep. of China

ABSTRACT

Personnel dosimetry and long-term measurements of background radiation usually cannot be carried out with satisfactory precision under tropical climate conditions with photographic films. This is mainly due to accelerated fading at frequently high humidity and/or temperature, which can be reduced or avoided by the use of properly selected solid-state detectors.

In addition to extensive field tests at 23-32°C and 75-95% relative humidity with track and ordinary photographic films and various TLD detectors in Taiwan, laboratory fading experiments have been carried out in the 25 to 150°C temperature range with LiF:Mg,Ti, $CaSO_4$:Dy, $CaSO_4$:Tm, CaF_2:Mn and CaF_2:Dy TLD materials. It is concluded that $CaSO_4$:Tm and $CaSO_4$:Dy powders, which combine high sensitivity and stability, are most suitable for TLD background radiation measurements with a precision of about ± 0.2 to 0.5 mR, while encapsulated LiF:Mg,Ti or BeO:Na could be used in personnel dosimetry. Ceramic BeO:Si is most promising for environmental or personnel TSEE dosimetry.

---

[1]Research sponsored by the International Atomic Energy Agency (the views expressed in this paper are those of the authors).

[2]On leave of absence from Health Physics Division, Oak Ridge National Laboratory, Oak Ridge, Tennessee, operated by the U.S. Atomic Energy Commission under contract with the Union Carbide Corporation.

1. Performance of Dosimeter Films

It is by now a well-established and well-known fact that nuclear track emulsions cannot be used for fast neutron personnel dosimetry in large areas of the world because of the rapid fading which occurs at higher humidities (Fig. 1 shows, as an example, that more than 60% fading occurred within two days in field tests in a tropical climate). It is not so widely recognized that the less pronounced fading in the normal x-ray and gamma monitoring films (Fig. 2) still amounts to between 60 and 90% within four weeks, no matter whether the film had been sealed in an additional polyethylene foil or not (actually, most foils only delay the penetration of humidity by a few days).

It should be noted that the climatic conditions under which those tests were carried out in May and June 1971 in Taiwan represent by no means the worst which are encountered in large parts of the Americas, Africa and Asia. It is evident that film dosimeters lead under tropical condition to even more grossly misleading results than in moderate climate zones and that their use should be discontinued as soon as possible. It is equally evident that no measurement of the natural radiation background with films can be successful under those circumstances.

2. Fading of TLD Phosphors

Obviously one of several possible alternatives for the film is TLD, and the long-term stability of several detectors has been determined in laboratory and field tests. A Teledyne/Isotopes 7710 reader was used. A potential source of error in long-term studies turned out to be a drift in the instrument sensitivity which could not be improved by the use of a voltage

stabilizer (Fig. 3). The light source readings within one month may differ by as much as 25% and day-to-day fluctuations can amount to about 8%. Calibration curves obtained at different dates are compared in Fig. 4. Of course, corrections had to be made for such fluctuations, for instance by storing an exposed reference sample in a lead container in the deep freezer.

In our experiments, we used three relatively new commercial materials, namely $CaSO_4$:Tm (Matsushita Co., Osaka), $CaSO_4$:Dy and CaF_2:Dy (both made by Harshaw Co., Cleveland, Ohio), in comparison with the well-known phosphors ^{7}LiF:Mg,Ti (Teledyne/Isotopes Inc.) and CaF_2:Mn (Harshaw). For most experiments, aliquots of ~25 mg each of the powders as dispensed by the Conrad Vibrator have been used. Optimum heater current was established as a compromise between the highest signal to background ratio, and as complete as possible annealing of the signal. The reading of all phosphors was highly linear in the dose range of interest (~10^{-4} to 10^2 rad of gamma radiation). At doses above ~100 mrad, a standard deviation of not more than ~2% could be obtained by an experienced operator. There have been, however, a few cases of exceptionally high readings. To avoid errors, each data point given in the graphs and tables represents the average of two to five individual readings.

Relative sensitivities of the different materials, as measured with our reader, are listed in Table I. The lowest dose which could be measured with reasonable accuracy is ~0.1 mR of gamma radiation with $CaSO_4$:Dy, LiF:Mg,Ti had to be annealed for reuse by the generally recommended, time-consuming and complicated procedure. It is a great advantage of the other detector materials that they only require a few minutes of heating to about

450°C, and that variations in the annealing conditions do not affect the sensitivity of the material. All materials can be reused many times.

CaF_2:Dy exhibits by far the most fading of the phosphors compared (Fig. 5). At room temperature (27 ± 3°C), 20% fading occurred within two days relative to the reading a few minutes after exposure, and 50% fading in less than one month. At higher temperatures, the fading rate is, of course, accelerated: At 60°C, 50% fading occurs in less than 10 hours. Even if stored below freezing temperature, 12% fading was found during one month. This clearly limits the use of this material in long-term studies.

CaF_2:Mn, on the other hand, was found to be exceedingly stable. At 120°C, only about 20% fading occurred within three weeks, and no clear evidence of fading has been found at temperatures below 100°C in several weeks. However, the reproducibility of dose readings was rather poor, probably because the TLD 7100 reader is not designed for use at the high reading temperatures required.

LiF:Mg,Ti (Fig. 6) is sufficiently stable for most applications. During one month at ambient temperature, less than 10% fading is observed, and at 60 to 80°C, a still tolerable 20% fading would require about 100 hours. At 100°C, however, the fading becomes rather rapid. In field tests, only a few percent fading have been observed in one month.

In $CaSO_4$:Tm and $CaSO_4$:Dy, no fading could be found at room or slightly elevated temperatures (Figs. 7 and 8). Also, no fading has been detected in either material within one month in field tests. Assuming somewhat simplified kinetics for the isothermal annealing of TL, one arrives at the relation between fading rate and ambient temperature given in Fig. 9.

According to the extrapolation, many years at 30 to 35°C would be required to produce 20% fading in these materials. They are, therefore, suitable for area monitoring, personnel monitoring in the absence of low-energy photon radiation, reactor experiments at slightly elevated temperatures, and for intercomparison studies of radiation sources by mail.

3. Area Monitoring

For area background radiation monitoring in Taiwan, polyethylene vials containing 100 to 200 mg of the phosphor powders were first sealed in polyethylene bags and then wrapped in black paper as a protection against water and light. Bamboo sticks, about 7 cm in diameter and 130 cm long (Fig. 10), were used for storing the detectors in a well-protected space about 1 m above the ground. The air had free access to the storage volume above a knot in the bamboo through several ventilation holes, and the detectors were protected by a styrofoam layer 4 cm thick and a screwed-on metal "roof" carrying warning signs. Two experiments of about four weeks each have been carried out. Irradiated detectors have been stored together with the freshly annealed ones for checking the fading rate.

One of the goals of the study was the measurement of the background radiation level at the construction site of a 500 MW(e) nuclear power station in Chin-Shan. It is located near the northern tip of Taiwan in a narrow valley opening to the sea (Fig. 11). In a second valley, separated from the reactor valley by a steep ridge, administration and housing facilities are being built. Measurement stations have been distributed in this area, attempting to get representative results. In addition, stations have been placed in a rice field outside a new resettlement village for the former

inhabitants of the valleys, outside the research reactor building, and in the professor's living compound on the National Tsing Hua University campus, about 800 m from the reactor, and, in another experiment, also in various locations at the site of the new Institute of Nuclear Energy Research, where a 40 MW research reactor is presently being built. Doses between 8.5 and 22 mR/month were found at various locations and times.

Some typical results of the first measurement (April/May 71) are summarized in Table II. The dose of stations 1 to 10 in the first experiment (9.5 ± 1 mR/month) was about one third lower than in the second experiment (13 ± 1 mR/month). This can in part be attributed to the fact that the detectors in the second experiment have been stored for a few days prior to evaluation in a laboratory close to the NTHU reactor, which was shown in the same experiment to have twice the normal background radiation level. There appears, however, to remain a real difference of about 20% between the two consecutive months.

The good agreement between the readings of different detectors at the same stations should be noted. Due to the low sensitivity of LiF and the fading of CaF_2:Dy, their readings turned out to be less reliable than the $CaSO_4$:Tm and $CaSO_4$:Dy results. The good agreement between the results of LiF, with its fairly photon energy-independent response characteristics, and the other highly energy-dependent detectors indicates a low (if any) contribution of low-energy photons to the total dose under the conditions of these measurements. Energy dependent detectors can, therefore, be used in area monitoring without need for energy compensation filters.

Obviously, the storage time requirements in area monitoring are not so much limited by the sensitivity of the materials, as by the time interval

during which the detectors are not "on duty", namely between annealing and distribution, and between collection and reading. Those intervals should be made as short as possible in relation to the actual monitoring time. Four weeks seem to be a reasonable minimum exposure time.

Due to the lack of a good TSEE reader, no TSEE detectors could be used in this study. Based on the results of laboratory studies at ORNL,[1,2] however, it is safe to assume that ceramic BeO:Si detectors (Brush Thermalox 995), after optimized pretreatment consisting of one hour of heating at 1400°C and overnight storage in liquid water, would be superior even to the best TLD detectors for area monitoring:

1. With a sensitivity of up to 10^4 counts/mrad/cm^2 when evaluated in a gas-flow proportional counter, and a very low background reading, doses as low as 10^{-5} rad are detectable; and
2. with a main emission peak of ~325°C and no low-temperature TSEE peaks present, no detectable fading occurs even at temperatures exceeding 100°C.

On the other hand, lack of simple commercial TSEE instruments may complicate the use of such detectors in areas with limited facilities and highly trained specialists.

4. Personnel Monitoring

In addition to the fading, other factors such as frequently inferior quality of inexpensive or self-made equipment, its rapid deterioration due to lack of air-conditioning and proper maintenance, administrative difficulties in ordering spare-parts or other needed materials, inadequate calibration facilities, insufficiently trained and underpaid evaluation

personnel, etc. often affect film badge services in developing tropical countries much more than their counterparts in moderate zones. This contributes to an even more impressive lack of reliability of the results than the one which has frequently been reported for film badge services in Europe and the USA. According to a recent survey,[3] out of a total of ~200,000 monitored persons which were included in the survey, 70,000 are already using solid-state detectors in their personnel dosimeters, and more institutions with an additional 40,000 radiation workers plan to adopt them in the near future. Obviously, such a switch to solid-state detectors is particularly urgent in tropical countries, and often also particularly easy because a newly established service can avoid large investments in film processing equipment, densitometers and complicated multi-filter badges.

The decision which of various methods should be adopted, and at what time, is more an administrative than a technical one and has to be made on the basis of local conditions. Two options are:

1. The most conservative approach would be to start by adding a solid-state dosimeter to the existing film badge. For example, LiF:Mg,Ti capillaries or Teflon disks, or BeO:Na capillaries (Matsushita) could be placed in the open-window area of the badge between gamma and track film. Care has, of course, to be taken to anneal all detectors after each monitoring period at the same time to avoid variations in sensitivity or background in case of the use of LiF/Teflon disks.

2. A more "radical" approach would be to abolish at once the film badge completely and replace it with some type of plastic I.D. or credit card, into which one or two detectors are incorporated (similar to the one recently introduced at NRL in Washington).[4] In larger institutes, the cards can be collected and the detectors read on a weekend and the annealed dosimeters redistributed the following Monday. In a mailing system for exchange, two sets of detectors would be required.

To minimize costs, the most common system of a uniform one-month monitoring period could be modified: One relatively small "high-risk" group of people more likely to receive substantial radiation doses should be monitored monthly, and the dosimeters of the larger "low risk" group can be read only once a year.

Table I. Gamma Radiation Response of TLD Phosphors

Phosphor	Relat. Sensit. (LiF = 1)	Background (mR γ-equivalent)
LiF:Mg,Ti	1	∿2
CaF_2:Mn	4.3	∿2
CaF_2:Dy	30.5	∿1
$CaSO_4$:Tm	38	∿0.2
$CaSO_4$:Dy	31	∿0.1

Table II. Results of Area Monitoring Experiment I

(Dose mR/month)

Station No.	$CaSO_4$:Tm	CaF_2:Dy	LiF:Mg,Ti
1	11.5	11.0	11.0
2	9.5	9.5	10.5
3	9.5	9.5	9.5
4	9.5	8.5	9.0
5	8.5	9.5	7.5
6	9.0	11.0	10.5
7	8.5	9.0	7.5
8	10.0	---	8.0

References

1. K. Becker, K. W. Crase, J. S. Cheka and R. B. Gammage, Proceed. IAEA Symp. New Rad. Detectors, Vienna 1970.

2. K. W. Crase, R. B. Gammage and K. Becker, ORNL-TM, in press.

3. F. H. Attix, Health Phys., to be published.

4. F. H. Attix, Health Phys., in press.

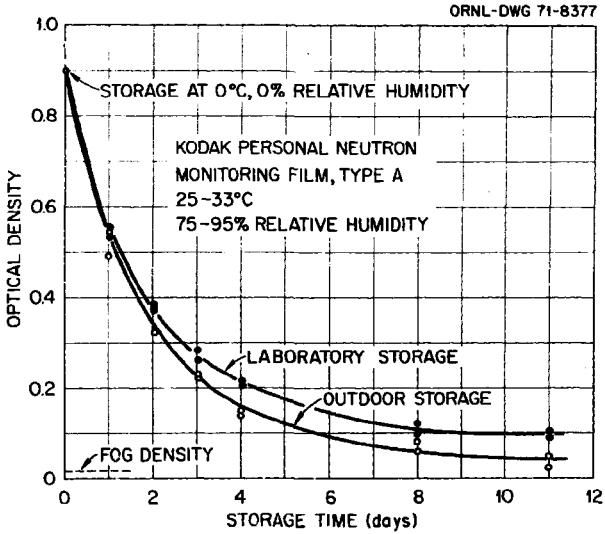

1. Optical density of Kodak Personal Neutron Monitoring Film, Type A, as a function of storage time of gamma-exposed film in a protected space outdoors, and in a laboratory in Taiwan.

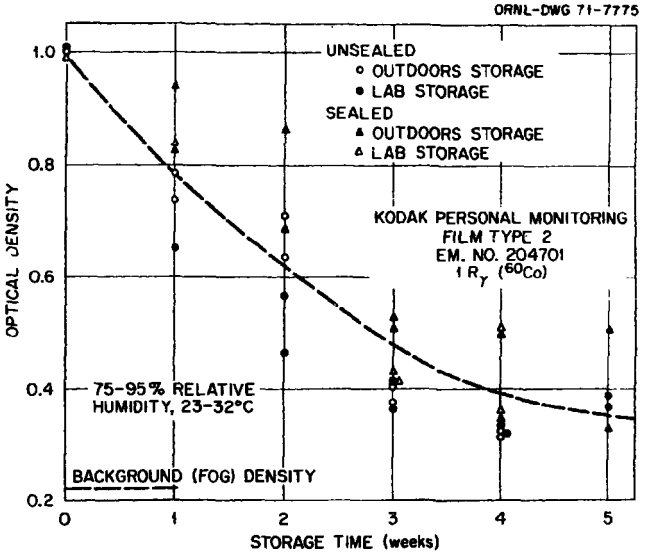

2. Optical density of gamma-irradiated Kodak Personal Monitoring Film, Type 2, sealed in polyethylene bags and unsealed, as a function of storage time between exposure and processing. Storage in unmodified climate inside and outside of a laboratory building in Taiwan.

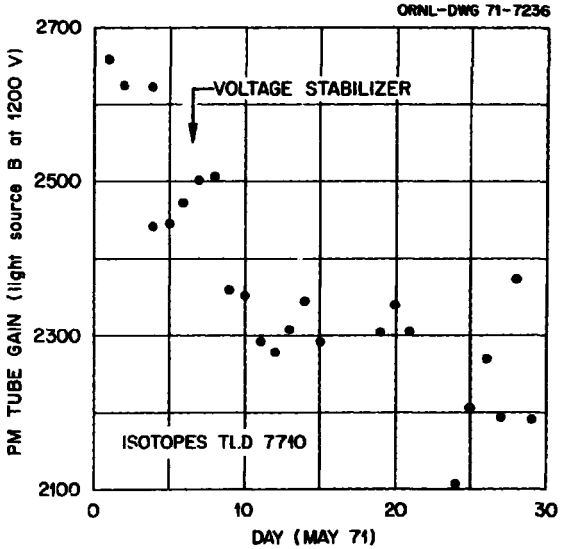

3. Photomultiplier tube gain of a Teledyne/Isotopes TLD 7710 Reader as a function of time in May 71, before and after the use of a voltage stabilizer.

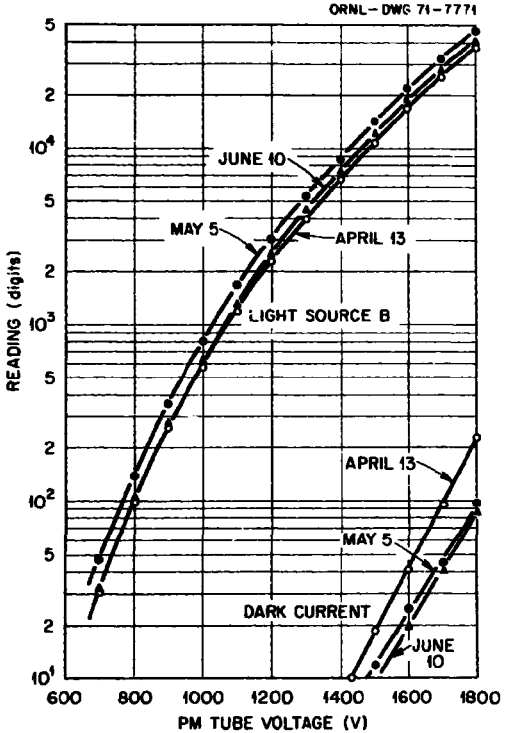

4. Reading of a radioactive light source, and dark current of photomultiplier in TLD 7710 Reader, as a function of PM tube voltage at various times.

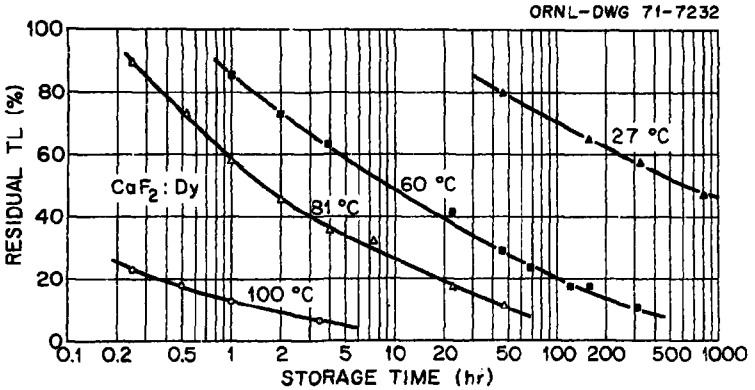

5. Fading of TL in γ-exposed CaF_2:Dy as a function of time at different storage temperatures.

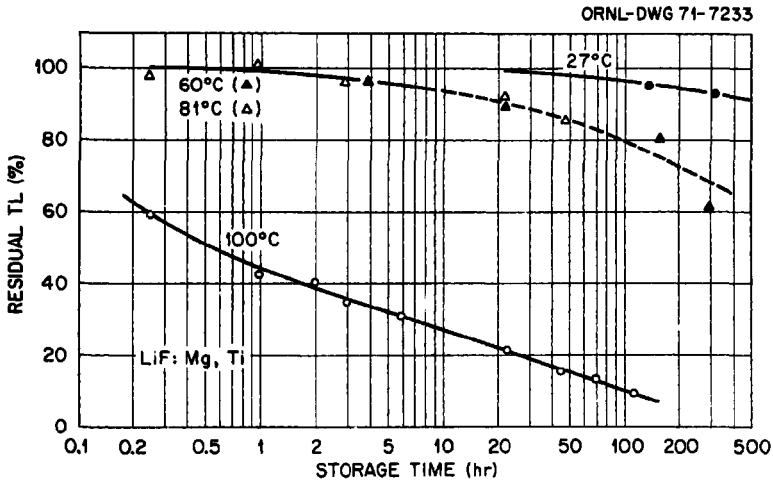

6. Fading of TL in γ-exposed LiF:Mg,Ti (LiF-7) at different storage temperatures.

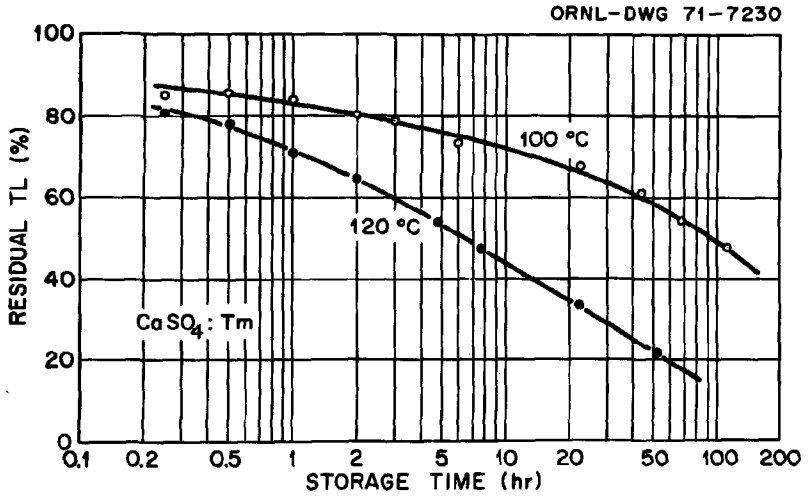

7. Fading of TL in γ-exposed $CaSO_4$:Tm at different storage temperatures.

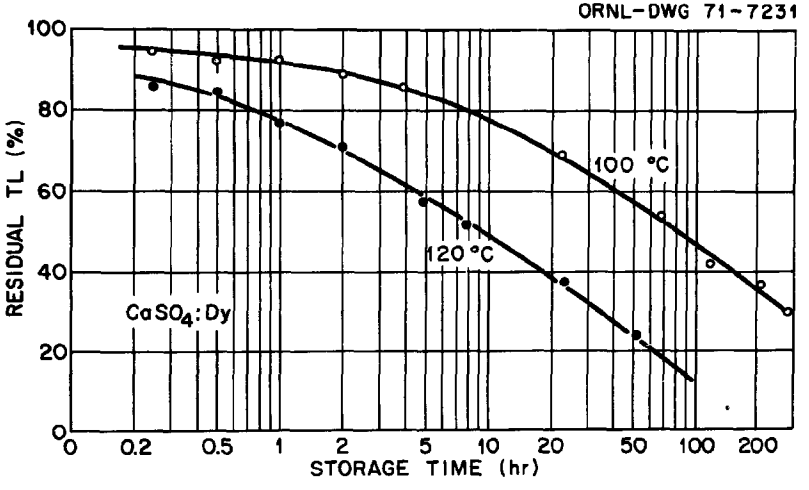

8. Fading of TL in γ-exposed $CaSO_4$:Dy at different storage temperatures.

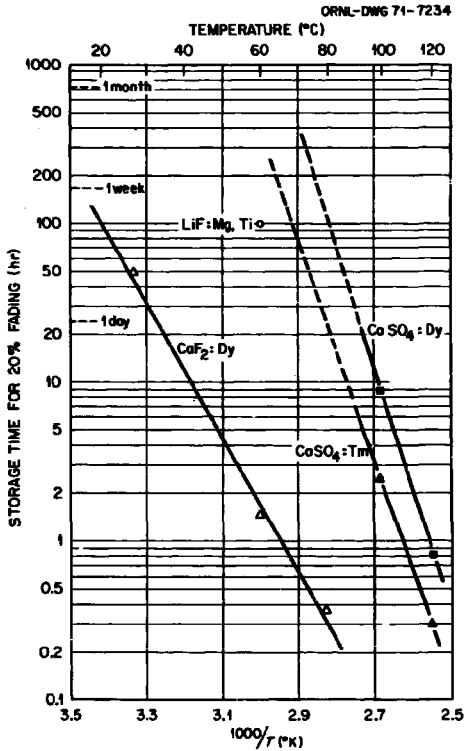

9. Storage time required to induce 20% fading in various phosphors, as a function of storage temperature.

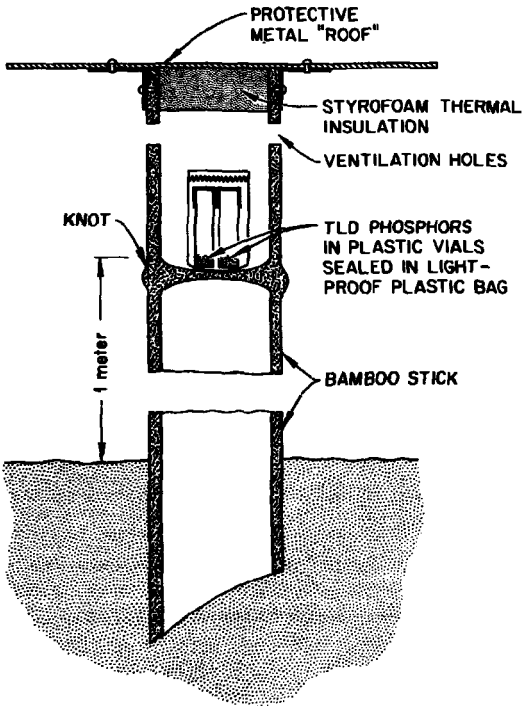

10. Bamboo sticks used for storage of TLD phosphors in environmental studies.

ORNL-DWG 71-8376

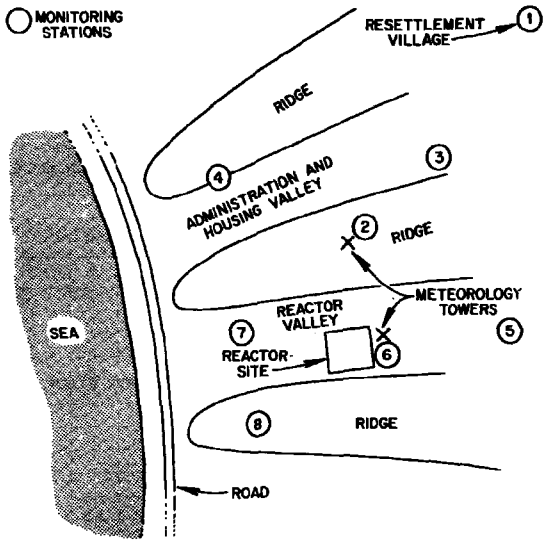

Site of Chin-Shan 500 MW(e) Power Reactor.

11. Sketch of monitoring station locations around Chin-Shan power reactor site.

Sunta

You showed in your slides a very large degree of fading in most phosphors; yet the results of exposure for one month in the environment are similar for different phosphors. You also seem to obtain correctly a normal background with all phosphors. How did you do your measurements?

Becker

With the exception of CaF_2:Dy, no substantial fading was observed within a month at ambient temperature and, consequently, no correction was required. In the case of CaF_2:Dy, irradiated samples have been stored together with the freshly annealed materials and corrections made for the fading.

Sunta

Our experience has shown that the CaF_2:Dy glow curve changes very considerably with dose, and different glow peaks do not rise linearly with exposure. How did you measure exposures with this phosphor?

Becker

As we worked only at very low dose levels, no non-linearity was observed.

Attix

I should like to comment that studies by Dr. A. Lucas at Harshaw Chemical Co., now underway, are indicating that radioactive light standards presently available are very poor with respect to stability as a function of temperature change. One hopes that improved light standards can be developed for TLD readers as a result of these studies.

Webb

The Teledyne Isotopes light source is a mixture of C-14 with a commercial blue-emitting Sylvania scintillator. Would you say that there is generally no low-energy component in environmental radiation, and that dosimeters with a poor energy response such as $CaSO_4$:Dy can be used without shielding?

Becker

According to our results, there is no low-energy component, but this may be due to the shielding effect of the bamboo stick. Sohei Kondo in Kyoto recently made some measurements which seem to indicate the presence of a small, very soft component.

Natural Radiation Background Dose Measurements With CaF_2:Dy TLD*

by

D. E. Jones, C. L. Lindeken, and R. E. McMillen
Lawrence Livermore Laboratory, University of California
Livermore, California 94550

Abstract

Four quarterly and one monthly integrated environmental dose measurements were made with CaF_2:Dy TLD's in approximately 100 homes of LLL employees and at selected out-of-doors locations. Another project is a nearly uniform geographic sampling of background dose in the 50 United States. These data are particularly interesting since they represent simultaneous integrated measurements with uniform geometry. The quarterly data also represent the average seasonal dose rates for specific locations in the Livermore Area. At the median exposure (9.6 mR) from the quarterly home data, the individual values have a standard deviation of ±5%. This report summarizes these data and emphasizes the technique and methods for overcoming phosphor limitations.

This technique for natural background dose measurement is reliable and relatively inexpensive. The major accuracy limitation is proper recognition and handling of potential nonrandom errors. These include factors such as fading and energy dependence. The phosphor response to cosmic radiation is under study as a potential source of error in TLD environmental measurements. This study was started when our results were compared with the data from other techniques. The comparison was inconclusive in elucidating the response. Preliminary results are shown for response to cosmic radiation and high energy protons and alpha particles.

*Work performed under the auspices of the U.S. Atomic Energy Commission.

Introduction

A growing interest in low level radiation dosimetry suggests evaluation of the TLD technique because the relatively low cost and simplicity of TLD measurements can lead to better characterization of environmental radiation. This paper summarizes the results of a local study and a national environmental radiation survey, the method used for dosimetry, and discusses the precision and accuracy of the results.

The Lawrence Livermore Laboratory (LLL) is engaged in an environmental evaluation program that includes measurements of environmental radiation exposure rates and their variations in the vicinity of Livermore, California. In this program, a few TLD's were first placed at monitoring stations in the Livermore Valley where periodic instrumental measurements were also being taken. The results encouraged us to use LLL TLD packets to study radiation levels in the homes of about 100 employees. This study included a preliminary month-long measurement and four contiguous quarterly ones.

This study was of special interest since employees normally spend more total time at home than at work and they take their TLD packets home. As most employees receive little or no occupational exposure, these data will help us to assign the natural background contribution for determination of the occupational exposure.

A second experiment was designed to measure the natural background radiation throughout the 50 United States. A nearly uniform geographical distribution was obtained by the selection of 120 weather stations. TLD packets were mailed to these stations and mounted in standardized instrument shelters, thus ensuring similar exposure geometries.* The data therefore represent directly comparable, integrated three-month exposures for 120 stations.

EXPERIMENTAL PROCEDURE

Detectors

The data of this report were obtained with CaF_2:Dy TLD chips 1/8 in. × 1/8 in. × 0.040 in. These detectors were chosen for their uniform response and excellent sensitivity. They also have very low self-dose, because the extended time at high temperature during crystal growth volatilizes any

*These instrument shelters are constructed of wood, with louvered sides, are 30-in. wide, 20-in. deep and 32-in. high, and the base stands 4 ft above the ground.

natural potassium present in the starting material. The response of the TLD's used in these studies has a standard deviation of 1.6% for doses near one rad.

Packaging

The TLD's were packaged in the standard LLL dosimetry packet.[1] In most of our low dose studies, the TLD packet contains two CaF_2 TLD's and one LiF TLD. The LiF data have been used only for control purposes and have not been analyzed extensively. Because no filters were used to flatten the CaF_2 energy response, corrections were required for the phosphor over-response at lower photon energies (below 100 keV). However, this packaging simplifies handling and will allow use of our automatic dosimeter reader.[1]

Fading Correction

The presence of low temperature traps in the CaF_2:Dy causes appreciable fading as shown in Fig. 1. We did not apply a fading correction; instead, the TLD's were all stored in a 3-in. thick lead shield (pig)* at least 24 hours before reading, and calibration exposures were performed at the mid-point of the exposure time. This procedure introduces a small error since the fading is not linear; however, the fading after 24 hours was about 20% and some error in this fraction is of little significance. From an operational standpoint, this method of correcting for fading greatly simplifies handling.

Calibration

Calibration exposures were performed at the LLL Hazards Control Calibration Facility.[2] Several sources are available, and three have been used for our low level measurements—a 7 Ci ^{241}Am source, a 30 mCi ^{137}Cs source, and a 3 mCi ^{60}Co source. Intercalibration is good, and we have obtained satisfactory data from all of them.

We did find a major source of error (~4%) in the calibration exposures. This was attributed to timing inaccuracies and to positioning errors due to lack of a standard fixture for holding the TLD's and the sources. This source of error has subsequently been reduced.

*This pig was also lined with cadmium and copper to reduce secondary x rays.

Energy Dependence

Currently, the greatest uncertainty in our environmental measurements concerns the TLD response to high energy cosmic radiation. A cursory analysis indicated the response was satisfactory, however, an analysis with more data showed the response light output per rad was probably low. For example, comparison with the data of Wollenburg, et al.[3] (terrestrial radiation only) showed our dose rates to be about 16% higher, undoubtedly due to cosmic response. This percentage does not reflect the full cosmic dose and implies either reduced response or improper correction for the energy dependance of the TLD's to terrestrial radiations.

To learn more about the response to high energy particulate radiation, exposures with Lawrence Berkeley Laboratory accelerators are underway. A related experiment is exposure to cosmic radiation in lead shields at different altitudes and with varying thicknesses of lead. Data to date are shown in Tables 1 and 2.

The data of Table 1 were taken from 7-in. diameter spherical lead shields lined with tin and copper. The TLD's were placed in a central cavity of 1-1/8 in. diameter and 1-1/8 in. long. Exposure durations were 18 days.

For Table 2 the proton and alpha particle fluence values were measured by 3/8-in. square by 1/8-in. thick polystyrene blocks. These blocks were placed directly behind a mosaic of nine TLD's one-TLD thick. The beam was not uniform so the exposures to individual TLD's ranged from the low to high values (in effective ^{60}Co rads) shown in the table.

The phosphor energy-dependence over the "normal" x- and gamma-ray energies must be considered when environmental radiation is measured. This is because scattering causes the radiation energy-distribution to be nearly independent of source strength,[4] with a broad peak at about 70-80 keV. Because the CaF_2 TLD's deviate markedly from air (or tissue) equivalence in energy absorption for these low energies, a correction must be applied to any unfiltered TLD reading.

Natural background gamma spectral measurements were made at several locations in the Livermore Valley with a 3 × 3 in. NaI(Tl) detector. Based on previous surveys, the sites selected represented relatively high, low, and intermediate background levels. In addition, we obtained background spectra inside private homes. An example, typical of the spectra observed, is shown in Fig. 2.

In all cases we observed the Compton continuum peak at about 80 keV. Although the counting rates varied according to location, the relative distribution of energy within the spectrum remained remarkably constant.

These observations are in agreement with the results of a previous one-year study of natural gamma background in the energy region from 10 to 100 keV, in which we found the energy distribution to be constant to within about ±5%.[4] This apparent uniformity in energy distribution of natural terrestrial gamma background spectra makes it possible to calculate an energy-weighted millirad/milliroentgen response factor for CaF_2 to this radiation.

At selected energy intervals the respective intensities were converted to equivalent milliroentgen values.[4] These exposure rates were summed over the energy range from 20 keV to 1.5 MeV. For each energy interval, the fractional contribution each made to the total was calculated. Then each fractional milliroentgen value was multiplied by the corresponding millirad/milliroentgen response of CaF_2 at that energy. Finally, these values were summed to obtain the equivalent milliroentgen value. It should be noted that our conversion factor is based on the energy response of CaF_2—not CaF_2:Dy (TLD-200). Recently we obtained experimentally determined energy response data for TLD-200.[5] While the presence of dysprosium increases the response below 100 keV, as expected, recalculation of this factor over the same energy range (20 keV to 1.5 MeV) using the TLD-200 data increases this factor by only about 2%. The value used in this report is 1.47 mrad per mR of natural radiation exposure.

Control Dosimeters

Proper dose measurement at these low environmental levels requires careful handling of control dosimeters (controls). These controls should either receive negligible exposure or be stored in a location with a known low exposure rate. The controls were therefore stored in the pig to minimize the background exposure to control and calibration TLD's. Some controls were given the same handling when out of the pig as the calibration TLD's, with the exception of the calibration exposure itself, thus ensuring that no exposures occurred from unkown sources. In the national survey, distribution of TLD's was accomplished through ordinary postal service. Control dosimeters accompanied the detectors sent to five typical weather stations and were immediately returned. A similar process was followed on the return mailing. These 10 controls supplied data for the range of transit-exposures to be expected for the survey.

Storage Pig Dose Rate

The dose rate (in effective CaF_2 millirad per day) in the pig was determined by analyzing data from six separate exposure periods throughout most of a year. To calculate this dose rate several assumptions were made. These were that 1) TLD response was linear, 2) nonradiation response from such things as PMT dark current, thermal glow and nonradiation-induced TL reached a saturation or constant level, 3) radiation self-dose was negligible, and 4) that fading was properly corrected by the timing of the calibration exposures. With these assumptions, the dose rate was determined as follows.

The overall TLD and reader system response, LR, was determined for each data set by applying the method of successive differences to the calibration and control readings using Equation (1).

$$TB(I) \cdot LR(I) + D(S) \cdot LR(I) = TLO(S) \qquad (1)$$

where,

TB = total background (dose equivalent),
D = dose from calibration exposure (CaF_2 mrads),
LR = system response (counts per mrad),
TLO = total light output from the sample readings (counts),
I = 1 to 8, index of data sets, and
S = index of calibration and control samples within a data set.

The typical response, LR, was found to have a standard deviation of about 4%. This error was primarily due to calibration exposure errors as discussed above.

Using the response figure for each data set, each set was evaluated to find a total dose equivalent background, TB. For this step, the data were weighted according to the ratio of control light-output to sample light-output.

The six total background values were then evaluated by the method of successive differences to determine the pig dose rate, R, and nonradiation background, b, in effective CaF_2 mrads using Equation (2).

$$b + R \cdot T(I) = TB(I) \qquad (2)$$

where,

b = nonradiation background (mrad equivalent),
R = pig dose rate in mrad per day (equivalent), and
T = storage time in pig in days.

Errors were propagated throughout the calculation to determine the statistical reliability of the results.

RESULTS AND DISCUSSION

The complete results of the home study and the national survey have been, or are being, published elsewhere.[6,7] This paper is concerned mainly with the technique, so only a summary of these data is given. Figures 3 and 4 show the dose distribution and the seasonal ratios for the home study. All data were normalized to 93 days for comparison purposes. Table 3 shows the data from scattered geographic stations of the national survey.

The cosmic ray component of the total environmental radiation exposure rate was calculated from the relationship between cosmic radiation and elevation reported by Lowder and Beck.[8] Their data applies to 50°N geomagnetic latitude; accordingly corrections were made for departure from this reference latitude at each station.[8]

The background dose rate in the storage pig was found to be 0.046 ± 0.003 mrad (equivalent CaF_2) per day. The system nonradiation response was 0.32 ± 0.09 mrad (equivalent). This latter value is expected to vary from one data set to the next, since operator adjustments to the reader system may directly change it independently of the reader sensitivity. Thus, there is *no a priori* reason for it to have a specific value, especially for data covering a year-long interval. The important point is that the low dose rate in the pig and its relatively low uncertainty allows good precision for environmental dose measurements. For example, a median quarterly home exposure of 9.6 mR has a statistical uncertainty of about ±5%. This estimate does not consider that two TLD's were used for each point instead of one. Currently the important uncertainties are those related to nonrandom errors.

At present we are mostly concerned with the response to penetrating cosmic radiation. This response appeared to be reduced relative to "normal" gamma radiation as shown by the agreement between our data and that of others. For example, the agreement with the Berkeley scintillation counter implies a reduced response for cosmic rays. Since cosmic contribution to the total natural background dose should be about 50% of the total dose for the San Francisco Bay Area, the TLD may be underestimating this component by roughly 70%. This is certainly less than an ideal situation. Furthermore, looking at the national survey data, if we assume the cosmic response is negligible, correct the TLD reading for terrestrial response, and add the calculated cosmic contribution, the data compares favorably with that from other sources. For example, the median projected annual dose from terrestrial radiation was 46 mrads, which agrees with the 50 mrad "average" for the United States.[9] The median projected dose from the cosmic

component was 27 mrad, which again is in good agreement with the 29 mrad previously determined for middle latitudes at sea level.[9] However, as we expected, the preliminary data of Table 1 show the cosmic response is not negligible. The ratios in the table approximate the 0.7 hard-to-total flux and ionization ratio noted by Lowder and Beck.[6] Thus, the simple analysis for assigning the exposure values (R) of Figs. 4 and 5 is inappropriate. This study of analysis techniques and energy response is continuing in order to determine the best technique and to evaluate the need for a filter to flatten the response.

It should be noted that CaF_2:Dy could behave differently in response to energetic particles than the better characterized CaF_2:Mn due to the marked difference in impurity doping.

Once the energy response is established, the cosmic contribution can be estimated sufficiently well for most purposes. Then relative and absolute measurements can be performed with minimal effort and expense when compared to previous techniques. Since readings can be made with automated equipment such as the LLL Automatic Dosimeter Reader,[1] we have shown the feasibility of very large scale studies of natural background radiation (or other sources) on modest budgets.

ACKNOWLEDGMENTS

We wish to thank the many persons responsible for helping with various portions of these studies. Special thanks go to J. V. Boggs and R. Banneck for their considerable effort in providing known exposures to many sources; to Lloyd Stephens, A. R. Smith, and J. McCaslin for assistance with the high energy irradiations and their characterization; to E. D. Taylor for fabrication of many special pieces of apparatus; to C. R. Veith for help with computer data reduction; to K. E. Peterson for assistance in arranging for the national survey; and to the personnel of the National Oceanic and Atmospheric Administration for their cooperation in the national survey.

REFERENCES

1. "LRL TLD Badge for Personnel Monitoring," D. E. Jones, K. F. Petrock, E. G. Shapiro, and B. G. Samardzich, submitted to Nuclear Instruments and Methods, Lawrence Livermore Laboratory Rept. UCRL-73084 (1971).
2. "Calibration and Standards Facility Operational Status," Boggs, J. V., Hazards Control Progress Report No. 38, Lawrence Livermore Laboratory Rept. UCRL-50007-70-1 (1970).
3. "Natural and Fallout Radioactivity in the San Francisco Bay Area," Wollenberg, H. A., Patterson, H. W., Smith, A. R., and Stephens, L. D., Health Physics 17, (1969) p. 313.
4. "Estimating Natural Terrestrial Background in the 17- and 60-keV Regions From the Compton Continuum Peak," Lawrence Livermore Laboratory, Rept. UCRL-72927, (1971).
5. "Energy Dependence of LRL Personnel Dosimeters," Boggs, J. V., Hazards Control Progress Report No. 38, Lawrence Livermore Laboratory Rept. UCRL-50007-71-1 (1971).
6. "Natural Terrestrial Background Variations Between Residences," Lindeken, C. L., Jones, D. E., and McMillen, R. E., presented at Health Physics Society 16th Annual Meeting, New York, New York, July 12-16, 1971, Lawrence Livermore Laboratory Rept. UCRL-72964 (1971).
7. Geographical Variations of the Environmental Radiation Background Within the United States, Lindeken, C. L., Peterson, K. R., Jones, D. E., and McMillen, R. E., to be published.
8. Lowder, W. M., and Beck, H. L., J. Geophys. Res. 71 (1966) p.4661.
9. "Report of the United Nations Scientific Committee on the Effects of Atomic Radiation," Official Records, Twenty-First Session Supplement No. 14 (A/6314), (1966) p. 15.

Table 1. TLD readings (in effective CaF_2 mrads based on ^{60}Co) for 18-day exposures in spherical lead shields.

Location	Calculated cosmic air dose (mrad)[a]	TLD (mrad)[b]	Ratio TLD/calc.	Shield
Livermore	1.38	0.96 ± 0.03	0.71	Spherical
Mt. Diablo	1.82	1.24 ± 0.04	0.68	Spherical
Mt. Hamilton	1.89	1.19 ± 0.03	0.63	Spherical
Livermore	1.16 ± 0.03			1/2-in. lead cylinder[c]
Livermore	1.04 ± 0.04			1-in. lead cylinder[c]
Livermore	0.95 ± 0.03			2-in. lead cylinder[c]

[a] Calculation is described in text.

[b] Average of nine readings.

[c] Top half of shield replaced by 7-in. lead cylinders of the thickness indicated.

Table 3. TLD response for four exposures at 184-in. Cyclotron.

Phosphor	Source	Lowest dose[a]	Highest dose[a]	Fluence[b]	Response[c] (rads[a]/particle)
CaF_2:Dy	735-MeV protons	197	425	9.57×10^8	2.99×10^{-7}
Li^7F	735-MeV protons	39.8	309	3.83×10^9	3.30×10^{-7}
CaF_2:Dy	930-MeV alpha	280	326	1.28×10^9	2.10×10^{-8}
Li^7F	930-MeV alpha	283	339	1.35×10^9	2.10×10^{-8}

[a] Effective rads (CaF_2 or LiF) based on ^{60}Co calibration.

[b] The number of particles that passed through the 3/8-in. square polystyrene blocks.

[c] Assuming linearity of response from lowest dose to highest dose for each exposure.

Table 3. Environmental radiation background levels from March 1—June 1, 1971 survey.

Station	Geomagnetic latitude (deg N)	Elevation (ft)	TLD reading[a] (μrad/hr)	Corrected cosmic radiation[b] (μR/hr)
Miami, Florida	37.0	10	4.6	3.3
Caribou, Maine	58.3	630	7.8	4.0
Memphis, Tennessee	45.6	280	5.1	3.6
Colorado Springs, Colo.	48.7	6170	16.3	6.7
Anchorage, Alaska	60.9	80	5.6	3.5
Keowakapu Beach, Maui, Hawaii	20.8	20	3.2	3.0

[a] Effective CaF_2 rads.

[b] Calculation is described in text.

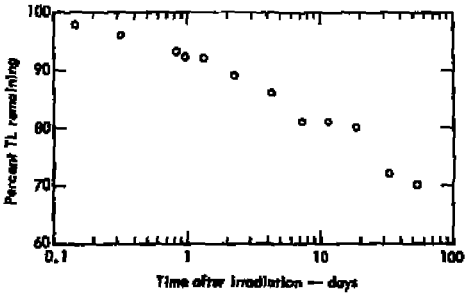

Fig. 1. CaF_2:Dy fading (integrated TL).

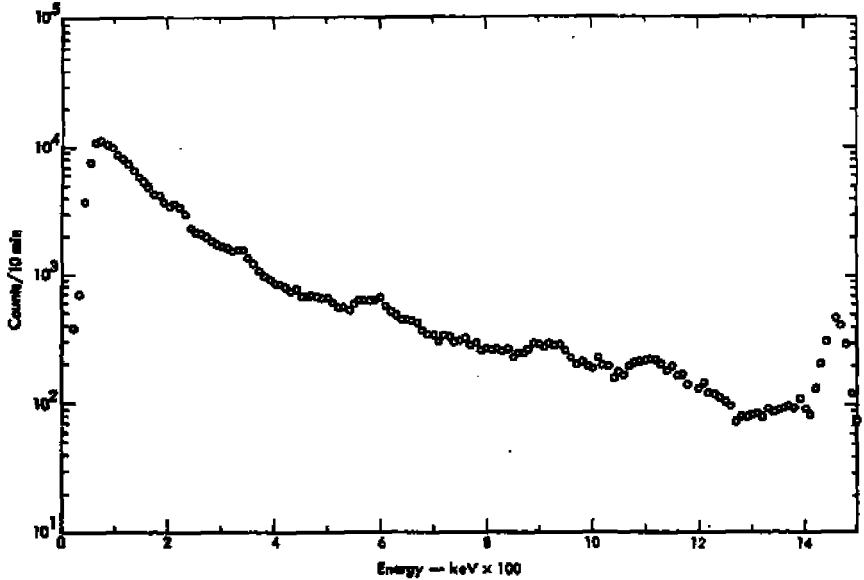

Fig. 2. Natural background spectrum vs energy for the 3 × 3-in. NaI detector—Livermore Valley, August 1970.

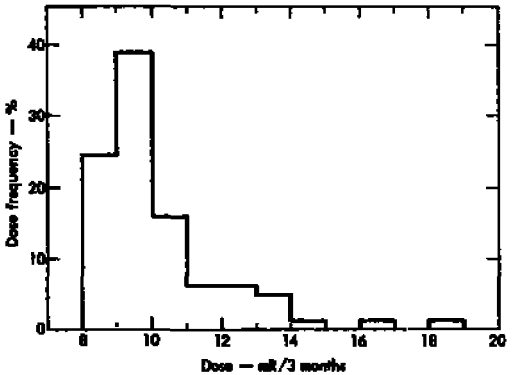

Fig. 3. Natural background distribution within 82 Hazards Control homes observed over 3-month period—June 23 to Sept. 23, 1970 (summer months). Median = 9.6 mR.

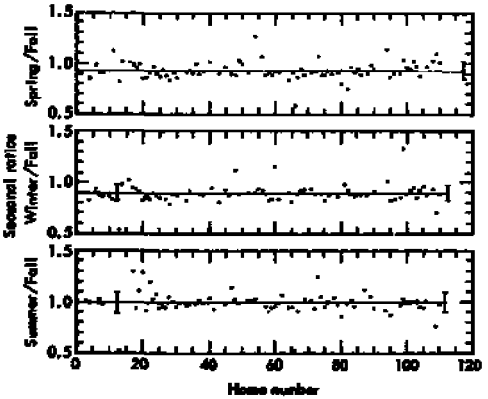

Fig. 4. Seasonal exposure ratios from TLD readings in employees' homes. Top curve is Spring 1971 to Fall 1970 ratio. Center curve is Winter 1970-71 to Fall 1970 ratio. Bottom curve is Summer 1970 to Fall 1970 ratio. Solid line is the average ratio and the error bars represent the standard deviation of a single reading.

Suntharalingam

It is very encouraging that you have demonstrated that TLD systems can be used for environmental monitoring also in developed countries like the United States and not just for underdeveloped countries. Was the high precision you were able to achieve due to your special "hot nitrogen jet" reader?

Jones, D.K.

In part, the answer is yes. For routine measurements we find these readers to give the best signal-to-noise relationship. The reading head and electronics for the reader of this study are essentially identical to our automated personnel dosimeter reader. The other part of the high precision is due to the high sensitivity and reproducibility of the CaF_2:Dy chips. We have found this phosphor to be linear down to at least 1 mrad in our reader. We have not attempted to check linearity below this level, although much lower doses are measurable in our system.

Fleming

Have you studied the levels of self-radioactivity of your CaF_2:Dy?

Jones

We have not analysed the TLD's. We do know that they are prepared from large crystals that are grown from a melt. This procedure requires long times at temperatures in the range of the CaF_2 melting temperature and should result in most of the usual potassium impurities volatilising away. Morgan Cox of Harshaw has stated the potassium content to be less than 1 ppm.

Fleming

What temperature of phosphor annealing achieves potassium volatilisation?

Jones

I would not anticipate much improvement by annealing since the boiling point of KF is about 1500°C and the melting point of CaF_2 is under 1400°C. The long

times at elevated temperature and perhaps some purification during crystal growth are the factors I consider important when comparing with a procedure such as phosphor preparation by precipitation.

Impurities and Thermoluminescence in Lithium Fluoride

by

M.J. Bosnitr, D.B. Rees-Evans, and S.C. Ellis

Division of Radiation Science, National Physical Laboratory, Teddington, England

Abstract

Single crystals of lithium fluoride have been grown with additions of magnesium and titanium. The distribution of these impurities along the crystal has been studied and correlated with the radiothermoluminescence (TL) and optical absorption properties. The addition of magnesium alone yields material with a main glow peak near 200°C, the TL sensitivity depending greatly on the purity of the lithium fluoride used. Whereas the magnesium is found to be uniformly distributed along the growth axis of the crystal, the TL sensitivity is not constant. This variation of sensitivity initially parallels the distribution of titanium when it is present in addition to magnesium. At the higher titanium levels studied concentration-quenching of TL is observed. The intensity of an optical absorption band near 200 nm in the unirradiated crystal is found to be proportional to titanium content, but the radiation induced absorption is unrelated to titanium. These results are considered to provide strong evidence that titanium functions as the luminescence centre in TL lithium fluoride.

Introduction

The constitution and preparation of the well known thermoluminescent phosphors TLD-100 and TLD-700 was made known in 1967[1]. Impurities magnesium Mg, titanium Ti, and aluminium Al are added to lithium fluoride during a crystal growth procedure. Most investigations of the thermoluminescence process in LiF have been carried out on these commercial products. Since irradiation of these materials in single crystal form produces colour centres (principally at 310 nm and 380 nm) clearly related to the presence of the main impurity magnesium, the thermoluminescence process has been discussed to date mainly in terms of the trapping centres associated with Mg. Thus following the optical bleaching experiments of Mayhugh et al,[2] the centres absorbing at 310 nm and 380 nm are identified as trapped-electron centres. Jackson and Harris[3] related the emptying of the 310 nm traps to glow peaks 4 (195°C) and 5 (210°C), and the 380 nm traps to glow peaks 2 (115°C) and 3 (160°C). Following the thermal release of electrons from these traps recombination and photon emission occurs, similar emission spectra applying to each glow peak[4].

The full details of the photon emission process have not been described but a scheme has recently been proposed by Mayhugh[5] following work which identified a hole trap near the absorption edge in the vacuum ultra-violet at 113 nm. Electron-hole recombination is proposed at the site responsible for

an absorption band near 200 nm in the unirradiated crystal. An important role has previously been assigned to this centre by Zimmerman and Jones[6] who also showed that the intensity of the band increased with the titanium content of the crystal.

The aim of our work has been to produce a range of LiF crystals containing Mg, Al, and Ti either alone or in combination and over a range of concentration thus providing well-characterised material for further study. Correlations between impurity concentration, intensity of thermoluminescence, and optical absorption properties, have shed more light on the relative importance and role of the secondary impurities.

Experimental

LiF crystals have been grown by the Stockbarger technique in an argon atmosphere as previously described[7]. Their dimensions and the method of sectioning are shown in figure 1. Twelve 5 mm discs are obtained and six alternate discs, either I to VI or I' to VI' polished for spectrophotometric examination. The top 0.8 cm is discarded and the remaining discs and tip crushed and sieved. Variation of the thermoluminescence sensitivity along the growth axis of a crystal was studied by separate examination of each section. Before examination of the powder samples an initial anneal of 24 hours at 400°C was standard procedure, this period being required to develop the full thermoluminescence sensitivity[7]. The crystals were sectioned in this manner as impurities are expected to be distributed according to Pfann's expression[8] given in figure 1. Finally the average bulk dose-response curve for a crystal was determined after mixing the six crushed discs with the crushed tip. Chemical analyses were performed on the fine powder left after sieving the crushed sections.

The details of the read-out procedure were as previously described[7] using a linear heating rate of $1^{\circ}C\ sec^{-1}$. Glow curves were obtained by plotting light output against temperature. In addition the area under the glow curve between preset temperature limits, usually set to include peaks 4 and 5, was obtained as a measure of thermoluminescence output.

Results and Discussion

Addition of magnesium alone. Three main types of 'pure' LiF have been used as starting material, the first two having been grown as single crystals as a final purification stage. They are referred to as (a) air-grown, (b) vacuum-grown, using (a) as starting material, and (c) zone-refined. All are now available from BDH Chemicals Ltd, Poole, England. A crystal grown from any of these materials with 80 ppm Mg added (200 ppm MgF_2), resulted in a product showing a main glow peak close to 200°C and smaller subsidiary peaks. The level of sensitivity was greatly dependent on the starting material. No advantage could be detected in adding a greater quantity of magnesium.

These crystals show a very non-uniform distribution of thermoluminescence along the crystal as shown in figure 2, however chemical analysis of Mg distribution showed that it was close to uniform. Typical results have been published[7]. The analyses were too scattered for the distribution expression to be applied but $k = 1$ was indicated. Elsewhere[9] k has been given as 0.7 to 0.8. These results therefore indicate the presence of an unknown impurity favourable to thermoluminescence in each starting material. On crystal growth this impurity is distributed so that the maximum concentration is near the tip of the crystal is $k > 1$.

Dose response curves for the mixed sections of these crystals are shown in figure 3. The upper curve is close to that obtained for TLD-700.

Addition of secondary impurities. When aluminium (as $Li_3 AlF_6$) or europium (as EuF_3) has been added in addition to magnesium no increase in the thermoluminescence sensitivity of any product has been found. Neither was the distribution of thermoluminescence sensitivity within a crystal affected. The effect of adding titanium (as $Li_2 Ti F_6$) is indicated in the glow curves of figure 4. For low Ti additions a large increase in sensitivity results in products based on vacuum-grown LiF, but the distribution of thermoluminescence within the crystal is unchanged. The similarity between the first set of glow curves in figure 4 and the upper set in figure 2 (zone-refined LiF plus Mg alone) suggests that each crystal contains a similar concentration of Ti. When the average Ti addition is increased to 15 ppm a reversed sensitivity distribution is observed for peaks 4 and 5 as shown in the second set of glow-curves in figure 4. Crystals with intermediate concentrations of Ti were also grown.

Sections from three crystals with Ti additions in the range 6 to 15 ppm were analysed by X-ray fluorescence and the results indicated a distinct concentration gradient in each, the highest level being at the crystal tip. By applying Pfann's relation it was possible to deduce the value of the distribution coefficient k as 1.7 ± 0.1. In addition the Ti content of vacuum-grown LiF was set at 3.5 ± 1 ppm.

With knowledge of the distribution coefficient it is possible to relate any property of a crystal section to Ti content, either measured or calculated. Thus the relationship between the height of glow peak 5 and Ti concentration is given in figure 5 for portions of four different crystals dosed to 10 rads. Figure 5 is a typical luminescence quenching plot in which luminescence efficiency first increases as the concentration of activator is increased, then reaches a maximum and starts to decrease. Johnson and Williams[10] have developed a theory for the concentration quenching of luminescence which fits the behaviour of a number of phosphors determined experimentally. Medlin has produced similar curves for thermoluminescent systems[11].

The dose-response characteristics of mixed sections of crystals of different added Ti content are shown in figure 6 in which thermoluminescence output per rad is plotted as a function of absorbed dose. The degree of supralinearity is evidently dependent on Ti content. The behaviour of a specimen with 15 ppm Ti added is close to that of TLD-700 as expected. (TLD-700, in addition to Mg and Al, contains 55 ppm $Li_2 Ti F_6$, equivalent to 15 ppm Ti). Zone refined or air-grown LiF to which Mg alone is added follow the behaviour of the 1.5 ppm Ti addition curve in figure 6. The similarity of dose response behaviour and thermoluminescence distribution within a crystal for these preparations, to that of a crystal based on vacuum grown LiF plus magnesium and 1.5 ppm Ti again indicates the same total Ti content in each. This may therefore be set at 5 ppm is 3.5 ppm Ti initial content of Ti in vacuum-grown LiF plus 1.5 ppm addition.

Optical Absorption

The absorption spectra of unirradiated polished crystal sections 3 to 4 mm thick, were measured at wavelengths above 180 nm in an Optica CF4 spectrophotometer. No marked absorption near 200 nm occurred in crystals based on vacuum-grown LiF with no Ti addition. An absorption band developed in this region on the addition of Ti and for a set of discs from one crystal

the intensity of absorption near 200 nm followed the known Ti distribution as shown in figure 7. Crystals based on zone-refined or air-grown LiF, and assumed to contain 5 ppm Ti on the basis of their thermoluminescence characteristics did not show the marked trend in absorption intensity shown in the first set of absorption spectra in figure 7. The absorption constant maxima tended to cluster together and not to exceed 1.5 cm^{-1} in value. Similar behaviour was found in a crystal to which 1.5 ppm Ti had been added in the form of TiO_2 although the thermoluminescence behaviour was as predicted. On this basis it is suggested that the Ti impurity in zone-refined or air-grown LiF is in an 'oxygenated' condition with somewhat modified absorption properties.

For crystals based on addition of Ti in the form of $Li_2 TiF_6$, the individual Ti content of each section has been calculated enabling the relationship between this content and the absorption intensity near 200 nm to be plotted as in figure 8.

The growth of the 310 nm absorption with radiation dose has been examined for a number of crystal sections of differing Ti content and typical results published elsewhere[7]. In general the extent of this absorption was little affected by the Ti content in contrast to the thermoluminescence behaviour of powdered sections. These results indicate that titanium is involved in the final photon-emission step in the thermoluminescence process.

Conclusion

Based on the work on the addition of titanium as a secondary activator to LiF : Mg it has been necessary to conclude that certain forms of 'pure' LiF, specifically the air-grown and zone-refined types used here, initially contain approximately 5 ppm Ti. It has been shown that Ti concentrates in the solid phase during crystal growth. The lower concentration of Ti in vacuum-grown LiF must therefore arise in the selection of material from the air-grown crystal used as starting material.

Zimmerman and Jones[6] first suggested that Ti was intimately involved in the photon emission process in LiF. This was on the basis of the similarity between the 200 nm absorption and photoluminescence excitation spectra, and between the photoluminescence emission spectrum and thermoluminescence emission spectrum near 200°C. Mayhugh[5] proposed a band-gap scheme in which thermally freed holes are trapped at the activator responsible for 200 nm absorption, and then combine with electrons which tunnel from nearby F-centres. Our main evidence for Ti as a photon-emission centre is presented in figure 5 which has the typical form of a concentration-quenching curve for thermoluminescence as a function of Ti activator concentration. In addition it has been shown[7] that the radiation-induced absorption spectra were unrelated to Ti content, whereas thermoluminescence intensity depends strongly on this.

The relationship between Ti content and intensity of the absorption band at 200 nm has been established (figure 8), but materials deduced to contain 5 ppm Ti initial impurity may not show the expected extent of absorption. Claffy[12] contested the proposal of Christy et al.[13] that the '196 nm' impurity centre formed a recombination centre in LiF on the grounds that some samples showing high 200° thermoluminescence did not have large absorption in this region. A possible explanation of this in terms of 'oxygenated titanium' has been offered here.

The optimum level of Ti as an activator in LiF : Mg is extremely low at ~8 ppm (figure 5). It is therefore feasible that other elements which

appear to act as activators in this system may do so due to the accidental inclusion of titanium with the relatively high concentration of element added.

The properties of thermoluminescent LiF powder are the average of the properties of crystallites of differing activator concentration. This relates to glow curve characteristics and dose-response behaviour. The interpretation of the supralinear dose-response behaviour shown in figure 6 is therefore made additionally complicated.

References

1. Patent Specification No. 1059518, The Patent Office, London (1967).
2. M.H. MAYHUGH, R.W. CHRISTY, and H.M. JOHNSON, J. appl. Phys., 41, 2968-2976 (1970).
3. J.H. JACKSON and A.M. HARRIS, J. Phys. C: Solid St. Phys., 3, 1967-1977 (1970).
4. A.M. HARRIS and J.H. JACKSON, J. Phys. D: Appl. Phys., 3, 624-627 (1970).
5. M.R. MAYHUGH, J. Appl. Phys., 41, 4776-4782 (1970).
6. D.W. ZIMMERMAN and D.E. JONES, Appl. Phys. Lett, 10, 82-84 (1967).
7. M.J. ROSSITER, D.B. REES-EVANS, and S.C. ELLIS, J. Phys. D: Appl. Phys., 3, 1816-1823 (1970).
8. W.G. PFANN, Trans. Am. Inst. Mining Met Engrs., 194, 747-753 (1952).
9. A.J. SIMON, E.G. HOBB, and R.E. THOMA, Oak Ridge National Laboratory, ORNL-3658 (1965).
10. P.D. JOHNSON and F.C. WILLIAMS, J. chem. Phys., 18, 1477-1483 (1950).
11. W.L. MEHLIN, J. chem. Phys., 30, 451-458 (1959).
12. E.W. CLAFFY, Phys. St. Solidi, 22, 71-76 (1967).
13. R.W. CHRISTY, H.M. JOHNSON, and H.H. WILLIAMS, J. appl. Phys., 38, 2099-2106 (1967).

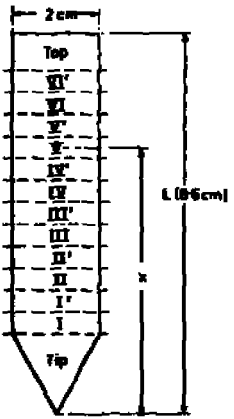

C_0 = average concentration of impurity in crystal

C_x = concentration of impurity x cm from tip

k = distribution coefficient of impurity

$$C_x = kC_0\left(1-\frac{x}{l}\right)^{k-1}$$

Figure 1. Method of sectioning crystals.

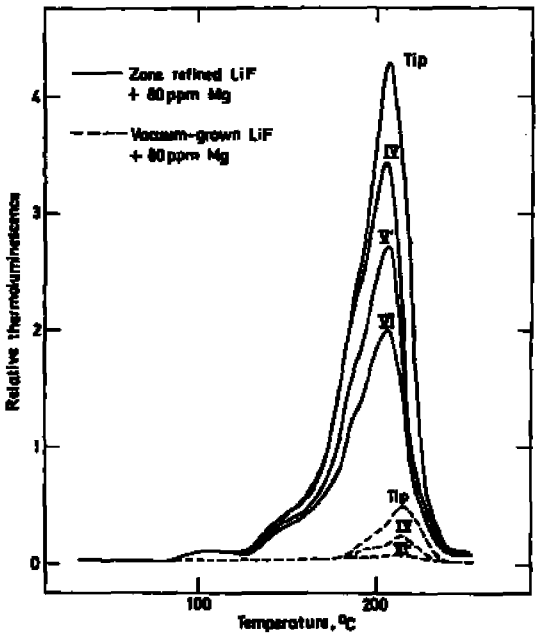

Figure 2. Glow curves from sections of crystals with Mg alone added. Dose 1 k rads.

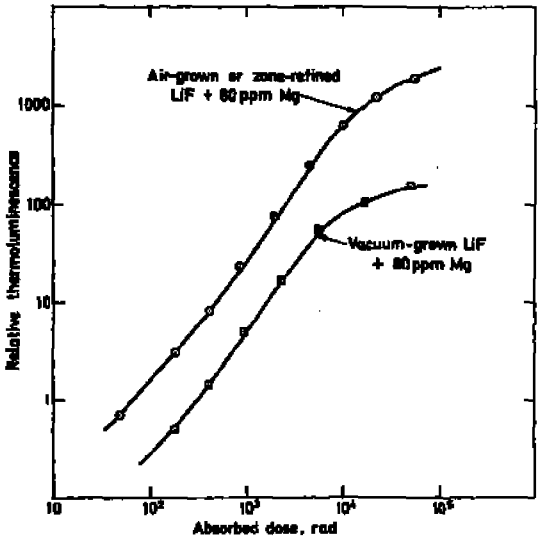

Figure 3. Dose-response curves for mixed sections of crystals with magnesium alone added.

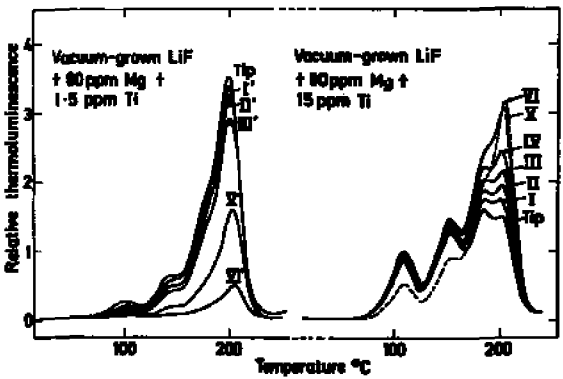

Figure 4. Glow-curves of sections from crystals with added magnesium and titanium. Dose 10 rads.

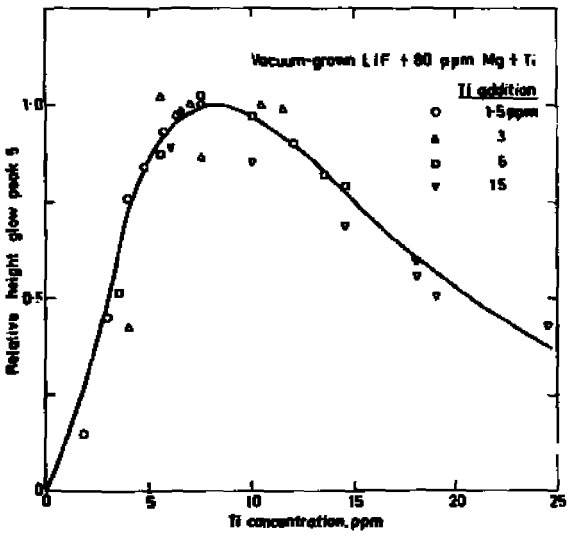

Figure 5. Normalised height of glow peak 5 in glow curves of sections from crystals with magnesium and titanium added. Dose 10 rads.

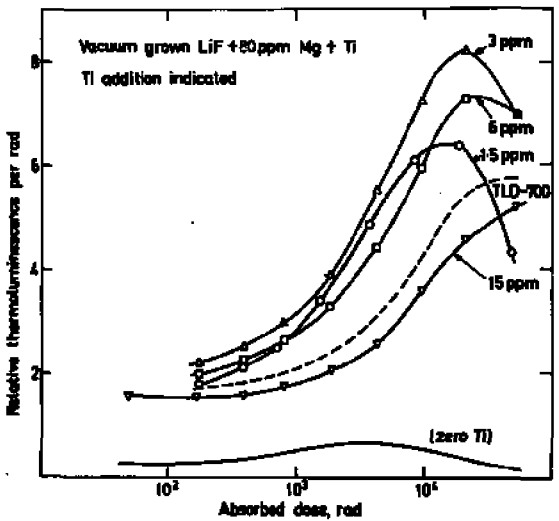

Figure 6. Comparative dose-response curves of mixed sections from crystals with magnesium and titanium added.

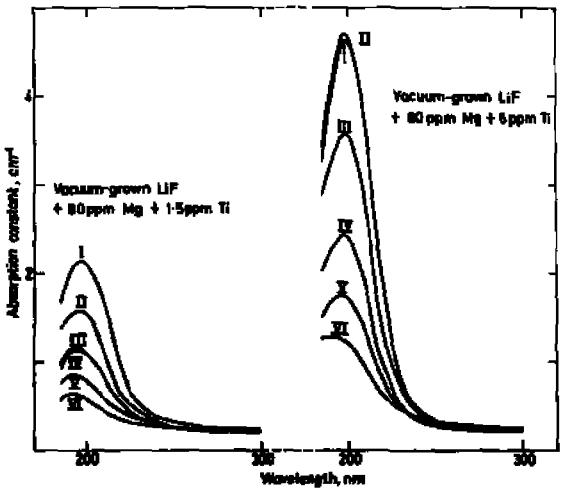

Figure 7. Absorption spectra of unirradiated polished sections from crystals with magnesium and titanium added.

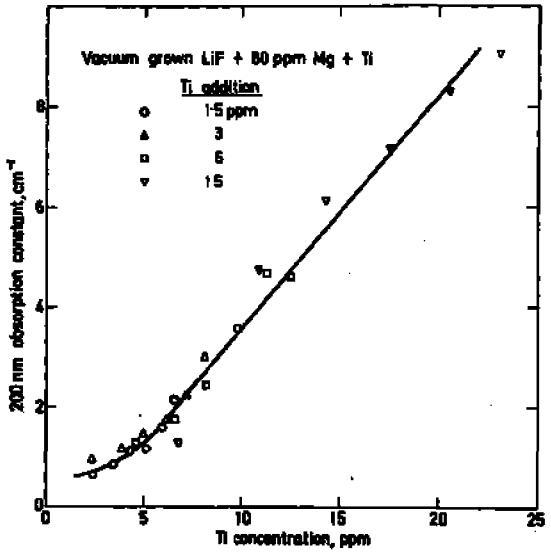

Figure 8. 200 nm absorption constant versus titanium concentration for sections from four crystals with magnesium and titanium added.

The Measurement of Dose from a Plane Alpha Source

by

J. R. Harvey and S. Townsend

Central Electricity Generating Board,
Berkeley Nuclear Laboratories,
Berkeley,
Gloucestershire,
U.K.

Abstract

In order to check theoretical predictions of the dose to the basal layer of the epidermis from alpha active material near the skin surface, finely ground thermoluminescent lithium fluoride was used to measure the microstructure of dose from a plane source of alpha radiation.

Since it is difficult to fabricate very thin layers of LiF a difference method was employed in which dose was assessed from measurements made behind various thicknesses of melinex foil. The LiF was calibrated by irradiation with alpha particles in vacuum.

The results throw light on the variation of sensitivity of LiF with LET, the correctness of the present estimates of the range of alpha particles in solids, and the theoretical model used for predicting alpha dose.

Introduction

Recent accurate measurements[1] have shown that the epidermal cells which are regarded as critical in radiation protection lie closer to the surface of the skin than previously supposed. This new evidence indicates that at a number of body sites in a significant fraction of people these cells lie at a depth of 30 microns or less. This contrasts with the previously accepted "minimal" depth of 70 microns. One important consequence of these measurements is the recognition that alpha particles originating outside the

body, from any skin contamination, can irradiate the critical cells. Theoretical dosimetry[2] has indicated that dose rates from low levels of skin contamination can be significant. The theory was based on a simplified model of the variation of specific ionization along an alpha track and involved the use of an estimate of the range of alpha particles in tissue about which there is still uncertainty[3]. In view of these uncertainties, measurements with thermoluminescent LiF were undertaken in an attempt to ensure that the theoretical predictions were not widely different from the measured dose rates in a tissue-like substance adjacent to a plane source of alpha radiation.

Equipment

The thermoluminescent material was fine-grained LiF derived from crushed TLD 100^4. This material, which has a mean grain diameter of 2.3μm was developed by workers at Leeds University to measure dose in small cavities in bone[5] and was used in the present investigation because it could be fabricated into thin, plane, compacted layers. For read-out 5 mg. quantities were spread evenly over the heater tray and heated with constant tray current and ambient nitrogen flush in a Conrad 5100. Readings were taken with a fundamentally unaltered Conrad light integrating system. Photo-multiplier current was plotted as a function of time to give the glow curves.

For irradiation, the LiF was compacted into layers in cylindrical perspex pots by means of an accurately constructed flat faced cylinder. The dimensions are shown in Fig. 1. Four pots were constructed with various base thicknesses within the range 0.98 to 3.7 mg.cm^{-2}. The average weight per unit area of the melinex sheet used for each base was derived by area and weight measurements and its regularity confirmed by point measurements using a micrometer. For gamma calibration layers of LiF of thickness 50 mg.cm^{-2} were exposed behind 3 mm of perspex to uncollimated radiation from a standard ^{226}Ra source.

The alpha radiation was derived from a commercially available spectrometry source constructed from a 25 mm diameter steel disc with a 7 mm diameter central area electroplated with a very thin layer of ^{241}Am.

Alpha spectra were taken with a 16 mm diameter silicon surface barrier detector coupled to commercial amplifiers and a 100 channel pulse height analyser.

Experimental Procedures

The compacted LiF layers behind the various thicknesses of melinex were exposed at 4 cm from the alpha source in a vacuum of 10^{-2} torr and also in close contact with the source under normal atmospheric pressure. Each irradiation consisted of at least ten identical exposures each involving 5 mg. of LiF. The LiF from similar experiments was aggregated in a container, thoroughly mixed by shaking, left for several days for tribo-effects to diminish and then read out.

The alpha spectrometry system was calibrated with a three nuclide source containing ^{239}Pu, ^{241}Am, ^{244}Cm similar in construction to the one described above, and with 1.47 MeV alpha particles produced by thermal neutron interaction with a foil consisting of ^{10}B coated at an average thickness of $0.2 \mu g.cm^{-2}$ on a steel base. A background subtraction was necessary to derive the alpha spectrum from the ^{10}B (n, α)^{7}Li reaction. The peak produced by this reaction was broadened because of self-absorption in the boron foil and its upper edge was taken to correspond to the unattenuated alpha particle energy.

As a further check on the system it was shown that there was no change in the spectrum when the angle of incidence of ^{241}Am alpha particles was varied between 0^{o} and 45^{o} thus confirming the absence of a significant absorbing layer on the surface of the detector.

The alpha spectra (Fig. 4) were taken with detector and source under a vacuum of at least 10^{-2} torr and with various thicknesses of melinex adjacent to the surface barrier detector which was 4 cm from the ^{241}Am source.

Results and Discussion

1. Glow Curves

The glow curves, Fig. 2, which were derived with a fast heating rate and a peak temperature of over $300^{o}C$, show the full extent of broadening and the subsidiary high energy peak which is characteristic of glow curves produced by high LET radiation. The curves in Fig. 3 were produced at the lower rate heating cycle used for normal dosimetry in which the heating current terminates ten seconds after the cycle is initiated. The area under the curves in Fig. 3 represents the integrated light output measured by the reading system. Each of the plotted curves in Figs. 2 & 3 is the mean of three glow curves taken from material given the same dose.

2. Gamma Calibration of LiF

300 mg of LiF were exposed at 5 cm from a standard radium source. The absorbed dose in LiF was calculated using the "f" factor for LiF[6] based on a mass energy absorption coefficient calculated on the basis of the electron density of LiF and data given by ICRU[6]. On the basis of exposures made in a similar container made out of cleaved LiF crystal a 3% correction was made for the fact that the build-up material was perspex rather than LiF.

3. Alpha Calibration of LiF

The spectra produced by the calibration sources and by ^{241}Am alpha particles which had traversed various thicknesses of melinex are shown in Fig. 4. These data were used to define the sensitivity of the thermo-luminescent LiF to alpha radiation of various energies. The energy absorbed in the surface barrier detector from alpha particles which had traversed various thicknesses of melinex was calculated by summing the product of energy and number of alpha particles in each energy group. Since there is little backscattering of alpha particles this was taken to be same as the energy absorbed in the LiF layers exposed behind the same thicknesses of melinex. The depth of the LiF layer exceeded the alpha particle range in all cases. The average dose to the LiF was calculated from the absorbed energy and the weight of the LiF layers. These dose rates are shown in Table 1 together with the dose rates as measured with gamma-calibrated LiF. The ratio of the two gives the relative light output produced by a given absorbed dose of alpha and gamma radiation, and is shown as a function of mean alpha particle energy in Fig. 5 where it is contrasted with some other published data. The differences between the results quoted by various authors could well be due in part to the various forms of LiF used.

Table 1

Derivation of the Sensitivity of LiF to Alpha Radiation

Melinex Thickness $mg.cm^{-2}$	Mean energy of alpha particles entering the LiF, MeV	Dose rate calculated from alpha spectra, rads in LiF/hr	Dose rate indicated by gamma-calibrated LiF, rads in LiF/hr	Dose indicated by gamma-calibrated LiF / alpha dose (± one standard deviation)
0.98	4.48	0.481	0.113	0.234 ± .01
1.88	3.46	0.309	0.088	0.285 ± .01
2.86	2.85	0.293	0.061	0.209 ± .01
3.76	1.68	0.173	0.023	0.130 ± .02

4. Measurement of Dose from a Plane Alpha Source

The measurements of the variation of dose rate with distance from a plane source of alpha particles were made with a constant thickness of LiF (13 mg.cm^{-2}) behind various thicknesses of melinex (0.98 - 3.7 mg.cm^{-2}) and the dose structure derived by a difference method. It is shown in the Appendix that the average dose, $\bar{D}_{mel}$ in a melinex layer of thickness ΔY is given by:-

$$\bar{D}_{mel} = \frac{\Delta\bar{D}_{LiF}\rho_{LiF}X}{\Delta Y \rho_{mel}} \quad \text{rads in melinex} \qquad \ldots(1)$$

where;

$\Delta\bar{D}_{LiF}$: the decrease in average LiF dose rate produced by increasing melinex thickness by ΔY; rads in LiF

X : the thickness of the LiF layer

ρ_{LiF}, ρ_{mel} : the densities of LiF and melinex

The dose rates measured behind various thicknesses of melinex are tabulated in Table 2 and the average doses in the various melinex layers are derived. The thermoluminescence efficiency for each exposure was calculated by weighting efficiency at a given alpha energy (Fig. 5) by the proportion of the total dose due to alpha particles entering the LiF at that energy and is given in Table 2. The stages in the derivation of the dose rates are given in Table 2.

Table 2

Measurements of Dose Rate made in Contact with the Alpha Source

Melinex thickness mg.cm^{-2}	Dose rate indicated by gamma-calibrated LiF, rads in LiF/hr	Alpha sensitivity relative to gamma sensitivity	Alpha dose rate, rads in LiF/hr	% Dose rate difference, rads in LiF per hr.	Dose rate (from eq.1) rads in melinex per hr.
0.98	17.66	0.22	78.8	46.6	473
1.88	7.16	0.22	32.2	18.7	243
2.86	2.44	0.18	13.5	7.2	106
3.76	0.58	0.09†	6.3		

† Based on extrapolation of data in Fig. 5 below 1.8 MeV

5. Theoretical dosimetry

The experimental results are plotted together with theoretical

predictions in Fig. 6. The formula for the dose rate at various distances from a plane alpha source which is derived elsewhere[2] is:

$$D = \frac{NE}{40X}\left\{2a \ln\frac{X}{x} + 3b\left(1 - \frac{x^2}{X^2}\right)\right\} \quad x \leq X \qquad \ldots(2)$$

where:

D	: dose rate	MeV $g^{-1}sec^{-1}$
N	: source strength	$cm^{-2}sec^{-1}$
ρ	: density of medium	$g\ cm^{-3}$
X	: 0.96 x extrapolated range	cm
a,b	: constants[2]	
x	: perpendicular distance from the source	cm
E	: energy of the alpha particles	MeV

The constants a and b and the extrapolated range were derived from a specific ionisation curve calculated on the basis of stopping cross-sections given by Walsh[3] and the unit monomer formula for melinex ($C_{10}H_8O_4$). The agreement between theory and experiment is good although the measurements suggest a somewhat lower dose towards the end of the alpha range and a higher dose near the surface than does the theory. This may be due to the fact that the alpha particle range used in the theoretical dosimetry is greater than the true range. The value used may be in error by as much as 15%.

Conclusions

The experiments have illustrated that the principal problems of measuring alpha dose with thermoluminescent materials arise because the short range of alpha particles necessitate the use of small quantities of phosphor in accurately defined geometries and because the sensitivity of phosphors vary with alpha particle energy. In the present measurements we used a difference method which eliminated the need to fabricate very thin layers of LiF. The variation of sensitivity with alpha energy did not produce serious difficulties because the irradiation geometry allowed a relatively simple calculation of the effective alpha energy. In more complex geometries accurate interpretation could be difficult. The experimental results were in reasonable agreement with theory and gave confidence in a theoretical model used to predict skin dose from alpha contamination.

Acknowledgements

This paper is published by permission of the Central Electricity Generating Board.

Appendix

Evaluation of Dose in Melinex by a Difference Method

Consider a layer of LiF of thickness X subjected to dose D_{LiF} varying as a function of x and reaching zero at $x_{max.} < X$. The energy absorbed per unit area in the LiF layer:

$$E_{LiF} = \int_0^X D_{LiF}\, \rho_{LiF}\, dx$$

where:-

ρ_{LiF} : density of LiF

The dose averaged over the thickness of the LiF layer is given by

$$\bar{D}_{LiF} = \int_0^X \frac{D_{LiF} dx}{X}$$

Hence from 1 and 2

$$E_{LiF} = \bar{D}_{LiF} \rho_{LiF}\, X$$

The dose structure is produced by radiation which has traversed a melinex sheet of thickness Y. If the thickness is increased by ΔY the energy lost to the LiF must be absorbed in the additional melinex (ΔE_{mel}).

i.e. $\Delta E_{LiF} = \Delta \bar{D}_{LiF}\, \rho_{LiF}\, X = \Delta E_{mel}$

It follows that the average dose to the melinex layer is:

$$\bar{D}_{mel} = \frac{\Delta \bar{D}_{LiF}\, \rho_{LiF}\, X}{\rho_{mel}\, \Delta Y}$$

References

1. Mrs.J. T. Whitton, U.K., C.E.G.B. Report RD/B/N1934, (1971).
2. J. R. Harvey, To be published in "Health Physics", (1971).
3. P. J. Walsh, Health Physics, 19, 312, (1970).
4. G. D. Zanelli, Phys. Med. Biol., 13, No.3, 393, (1968).
5. G. D. Zanelli, F. W. Spiers, Second International Conference on Luminescence Dosimetry, Conf. - 680920, p.920, (1968).
6. I.C.R.U. Physical Aspects of Irradiation NBS Handbook 85, (1964).
7. C. L. Wingate, E. Tochilin, E. Goldstein, Proceedings of the First International Conference on Luminescence Dosimetry, Stanford, USAEC conf. - 650637, p.421, (1967).
8. R. C. Woodley, W. H. Johnson, Proceedings of the First International Conference on Luminescence Dosimetry, Stanford, USAEC conf. - 650637, p.502, (1967).
9. M. J. Aitken, M. S. Tite, S. J. Fleming, Proceedings of the First International Conference on Luminescence Dosimetry, Stanford, USAEC conf. - 650637, p.490, (1967).
10. A. C. Lucas, C. Reinholt, Proceedings of the Second International Conference on Luminescence Dosimetry, Gatlinburg, USAEC conf. - 680920, p.456, (1968).

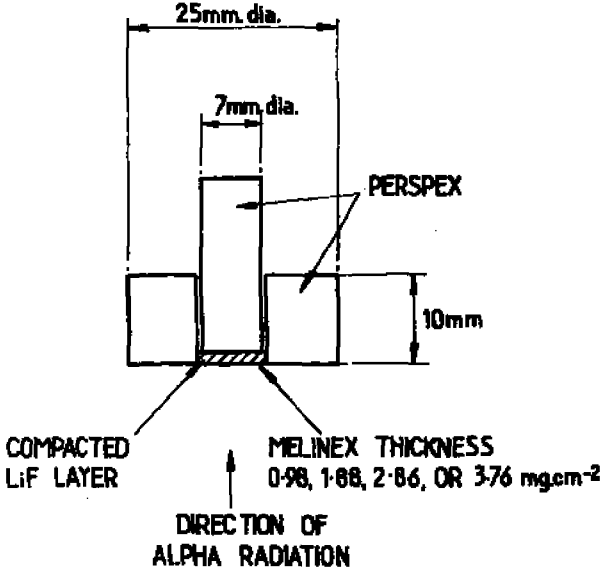

Fig. 1 Alpha irradiation assembly

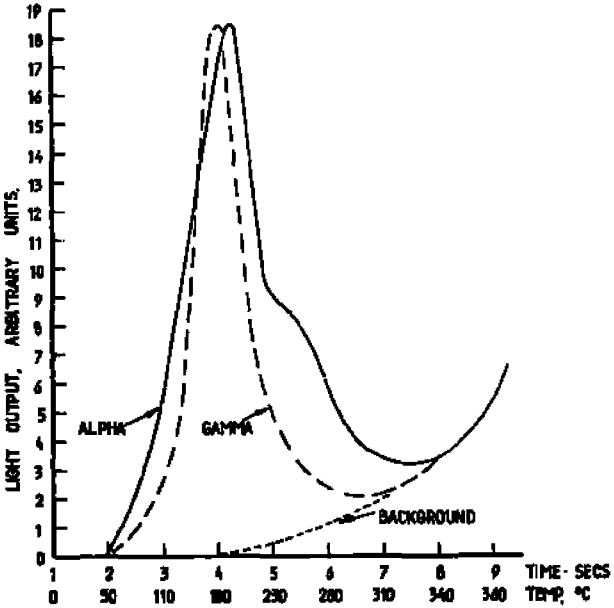

Fig. 2 Glow curves: fast heating rate

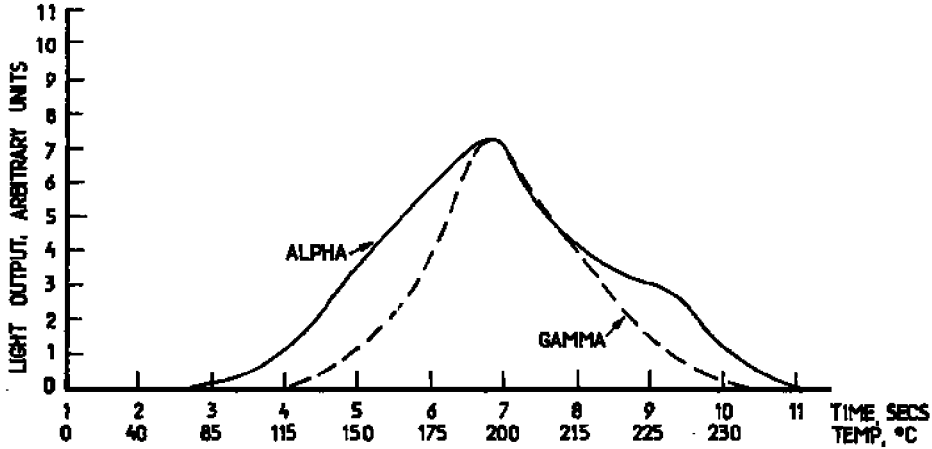

Fig. 3 Glow curves: slow heating rate

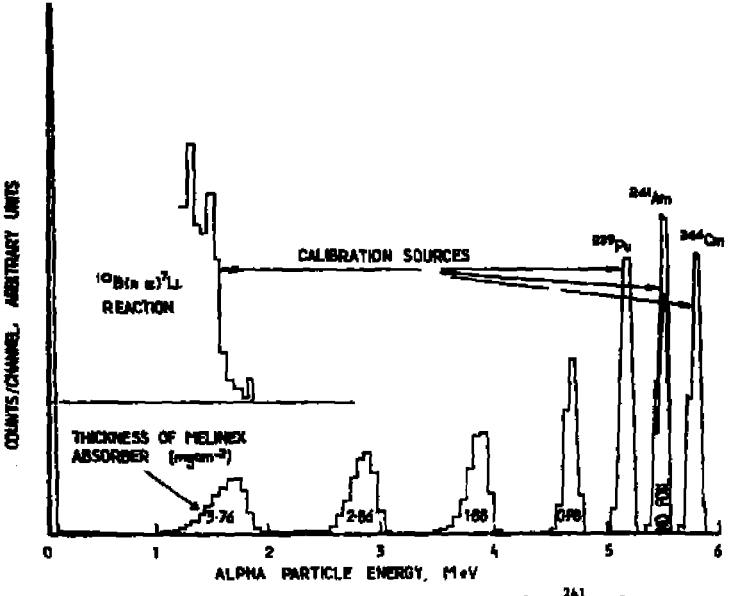

Fig. 4 Alpha spectra from calibration sources and from ^{241}Am alpha particles which had penetrated various thicknesses of melinex

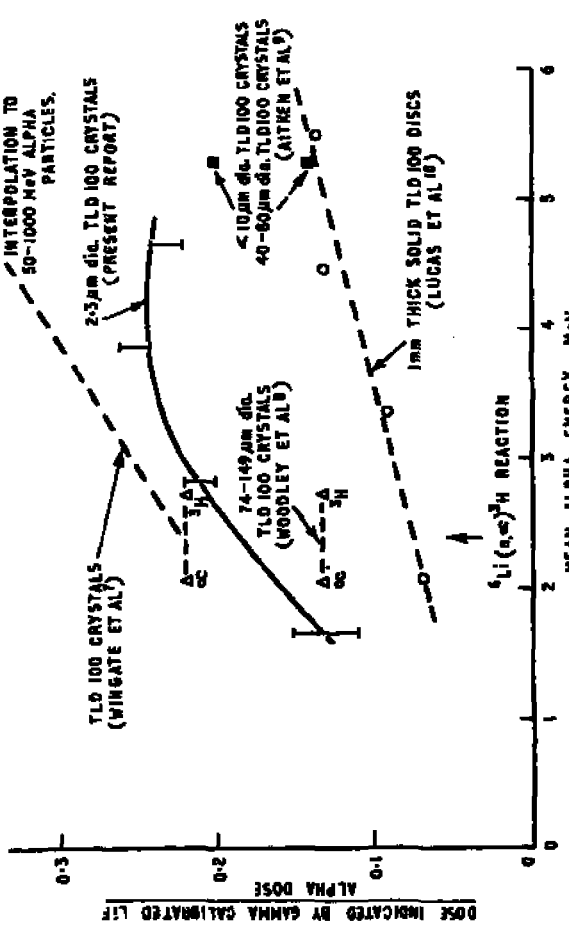

Fig. 5 The sensitivity of LiF to alpha dose relative to the sensitivity to gamma dose

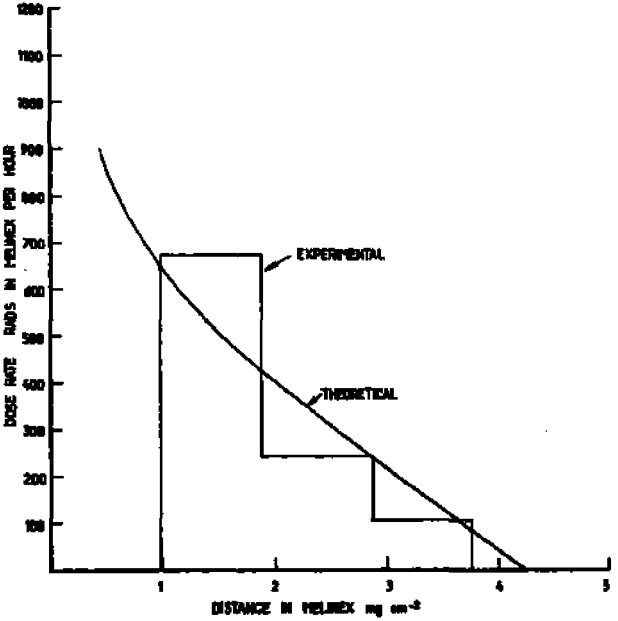

Fig. 6 Dose rate adjacent to a plane ^{241}Am alpha source

Rotondi

Am-241 emits also X-rays, have you evaluated an eventual contribution to the measured dose?

Harvey

Yes, the contribution, even in the worst case, is negligible.

Thermoluminescent Research of Protons and Alpha-Particles with LiF (TLD - 700)

by B. Jähnert
Hahn-Meitner-Institut für Kernforschung GmbH
Abteilung Strahlenphysik
Berlin-West, Germany

Abstract

The thermoluminescent dosimeters, which consists of LiF (TLD - 700 powder), were irradiated with alpha-particles in the energy range of 1.7 up to 3.7 MeV and with protons in the energy range of 2.4 up to 13.3 MeV.

The readout of the irradiated dosimeters was performed by thermal stimulation. The heating rate was 35°C/sec. To reduce zero effect a nitrogen atmosphere was used.

For each kind of irradiation the glow-curve and the integral thermoluminescent response was compared with ^{60}Co-gamma irradiations. The beginning of supralinearity was observed for alpha irradiation at $2 \cdot 10^3$ rad, for gamma irradiation it was at 500 rad.

The thermoluminescent response is dependent on the LET of the radiation. The response was normalized to that for ^{60}Co-gamma-rays. For protons the TL response was found to be 87 % for 13.3 MeV and goes down to 58 % for 3.7 MeV protons. For alpha particles in the energy range of 1.7 up to 3.7 MeV the average response was 16 %.

To fit the experimental data a mathematical attempt was made which describes the processes during irradiation and readout.

TL-dosimeters

The TL-dosimeters consisted of LiF powder (TLD - 700 : 99.99 % ^{7}Li, 0.01 % ^{6}Li), which was obtained from Harshaw Inc. The LiF mass for γ-irradiation was 150 mg, for α-irradiation 250 mg, and for proton-irradiation it varied from 150 up to 1200 mg. Before each irradiation the electron traps were thermally annealed by a standard heating cycle of 1 hr at 400°C and 24 hrs at 80°C[1].

Irradiation of the dosimeters

The α-irradiation of the LiF-samples was performed with a ^{210}Po-source, which was mounted in a low-pressure chamber. The energy of the α-particles could be changed by varying the pressure of the chamber. For the α-irradiations four energies were chosen: 1.7; 2.4; 3.3; 3.7 MeV. The α-energy was measured with a Si-detector. The thickness of the α-irradiated LiF-layer was 40 mg/cm^2, so that α-particles are totally absorbed in the LiF. The mean α-dose in LiF was varied from $5 \cdot 10^2$ rad up to 10^5 rad.

The proton-irradiations were carried out with a Van-de-Graaf Generator. To get protons in the MeV-range the nuclear reaction $^2_1$H ($^3_2$He, $^1_1$H) $^4_2$He was used. The proton energy was changed by Al-absorption foils of suitable thickness, which were placed between the target and the LiF. For irradiation the proton-energies were 2.4; 5.7; 7.2; 13.3 MeV, which were measured with a Si-detector. Corresponding to proton-energy the thickness of the p-irradiated LiF-layer was varied from 64 up to 380 mg/cm^2, so that the protons were totally absorbed in the LiF. The mean proton dose in LiF was in the range from 3 up to 34 rad.

As reference radiation for comparing the TL-sensitivity and the effect of supralinearity γ-radiation from a ^{60}Co-source was used. The γ-dose in LiF was in the range from 20 up to 80 rad.

TL-readout

After each irradiation the LiF-powder was well stirred. The TL-measurements were made with samples of 43 mg with a thickness of 38 mg/cm^2, so that selfabsorption of the emitted light in the LiF was negligible [2,3]. The integral TL-intensity was measured with a CON-RAD readout-instrument (model 4100). Simultaneously with the integral TL-intensity, the glow-curve was plotted. During the heating cycle of 10 sec the LiF-sample was heated at a constant rate of $(35 \pm 1)^{\circ}$C/sec.

Results and Discussion

With the experimental data it is possible to find out the TL-sensitivity. In fig. 1 it is shown the relative TL-sensitivity for 3.7 MeV α-particles and ^{60}Co-γ-rays[4], as function of the absorbed dose in LiF. Each curve is normalized to the observed sensitivity of the corresponding type of radiation in the low-dose range. The relative γ-sensitivity increases strongly above about 10^3 rad and reaches a maximum value of about 4 at a dose of $4 \cdot 10^5$ rad. Compared with γ-rays the variation of the α-sensitivity with dose is much smaler and no maximum is observed up to doses of 10^5 rad. The relative α-sensitivity increases slowly above about 10^3 rad and reaches a value of 1.3 at 10^5 rad.

In fig. 2 the dependence of the TL-yield in the low-dose region from the average LET of the particles in LiF is shown. In this figure the measured TL-yield was normalized to the TL-yield for γ-irradiation ($\eta = 1$ for γ-rays). Below an LET of about 5 keV/μm in LiF the TL-yield is rather independent of the LET and equal to that for γ-rays. This is also confirmed by measurements with electrons and TLD - 700 [5,6]. Above 5 keV/μm the TL-yield decreases monotonical with increasing LET. The slope of the curve can be approximated by an exponential function. The relative TL-yield for 13.3 MeV protons, which have an LET of 21 keV/μm, was measured to be 0.85 ± 4 %; it decreases down to 0.56 ± 4 % for 2.4 MeV protons with an LET of 57 keV/μm in LiF. For the α-particles

with a mean energy from 1.7 up to 3.7 MeV, the average relative TL-yield was 0.165 ± 4 %. The LET for the used α-rays lays in the range form 305 up to 340 keV/μm.

The decrease of TL-yield with increasing linear energy transfer L can be explained by a saturation effect during the filling of the traps when the LiF is irradiated with high-ionized particles. In the temperature region from 200 up to 300°C hole-capture seems to be the major process for thermoluminescence with LiF[7]. Therefore it is only interesting to regard the concentration of the holes. The concentration n(t) of holes per cm^2 in the valence-band at time t after passage of a particle is given by the relation:

$$(1) \qquad \frac{dn}{dt} = -\left[\lambda + w_i N_i(t)\right] n(t)$$

In this equation λ is the probability for immediate electron hole recombination and w_i is the probality for hole-capture in a trap of type i, normalised to the concentration $N_i(t)$ of unoccupied traps of type i. The TL-yield is defined as the quotient of the freed luminescence-energy divided by the incident energy taken to the crystal during the irradiation

$$(2) \qquad \eta_i^{\mathrm{TL}}(n_0) = \frac{k N_i}{k_0 n_0}$$

In this equation k is the luminescence-energy per occupied trap; k_0 is the mean energy for producing one hole; n_0 is the initial concentration of holes per cm^3 in the valence band corresponding to the LET of the ionising particles. $N_i(t)$ is the concentration per cm^3 of the occupied traps:

$$(3) \qquad N_i(t) = N_{oi}\left[1 - e^{-\frac{w_i n_0}{\lambda}\left(1 - e^{-\lambda t}\right)}\right]$$

N_{oi} is the initial concentration per cm^3 of unoccupied traps of type i. From equation (2) and (3) it is possible to calculate the TL-yield normalised to the TL-yield obtained with γ-radiation. The final equation for the relative TL-yield is shown in the following relation:

$$(4) \qquad \eta(L) = \sum_i a_i \frac{1 - e^{-p_i L}}{p_i L}$$

with $p_i = w_i / \lambda k_o Q$ and $\sum_i a_i = 1$. Q is the effective cross section of one ion-column. To get equation (4) it was summing up over all types of trap. a_i is a factor, which shows how much each type of trap contribute to the TL-yield.

In figure 2 the trap parameters a_i and p_i are fitted to the experimental data with α-irradiation. The dotted line was calculated for $i = 1$, that means one type of trap. The closed line results for two types of traps ($i = 2$). In the regarded LET-region the dotted line seems to be the better fit, but with this theory of one type of trap it is not possible to explain the increasing of the high-temperature peak in the glow-curve with increasing LET(For proton irradiation the part of the high-temperature peak relative to the whole TL-intensity was about 8 % for α-irradiation it was about 30 %). Experimental data with high ionizing particles[8] also indicate that the slope of the curve must be continued for high LET values in a way which resemble the theory of two types of traps. Therefore the theory for two types of traps will probably be more suitable to explain the experimental results.

References

(1) J.R.Cameron, D.J.Zimmerman, G.Kenney, R.Buch, R.Bland
Health Physics 10, 25 (1964)

(2) N.Stolterfoht, W.Jacobi
Strahlentherapie 134, 536 (1967)

(3) G.A.R.Andrea
CONF - 650637, 435 (1967)

(4) N.Stolterfoht
Thesis, Fr. Univ., Berlin (1967)

(5) A.P.Pinkerton, J.G.Holt, J.S.Laughlin
Physics in Medicine an Biology 11, 129 (1966)

(6) E.H.Crosby, P.H.Almond, R.J.Shalek
Physics in Medicine and Biology 11, 131 (1966)

(7) C.C.Klick, E.W.Claffy, S.J.Gorbics, F.H.Attix, J.H.Schulman, J.G.Allard
Journal of Applied Physics 38, 3867 (sept. 1967)

(8) E.Tochilin, N.Goldstein
CONF - 680920, 424 (1968)

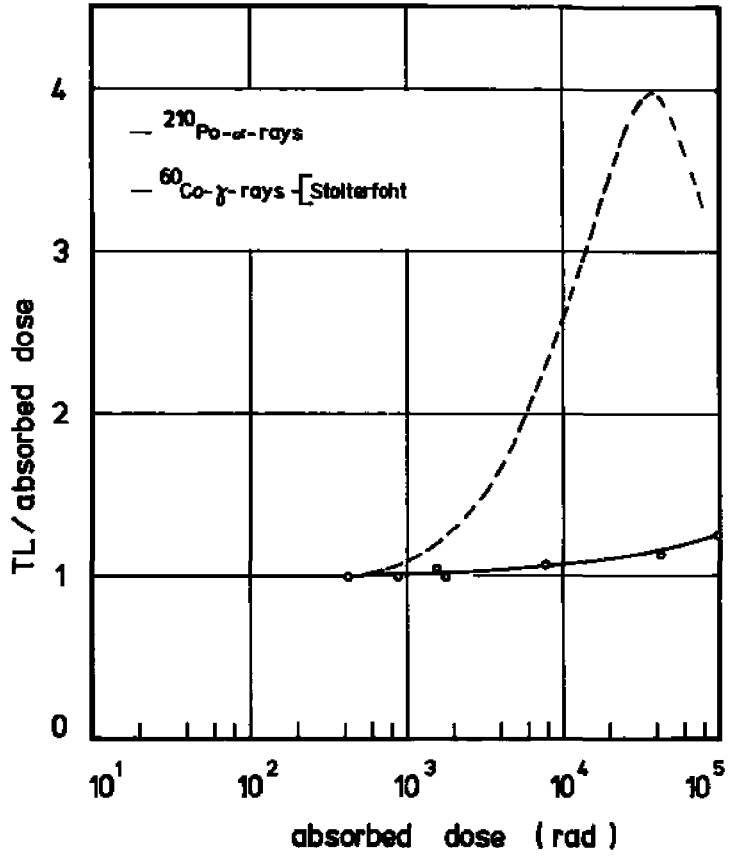

Fig. 1

Relative TL-sensitivity as a function of the absorbed dose in LiF

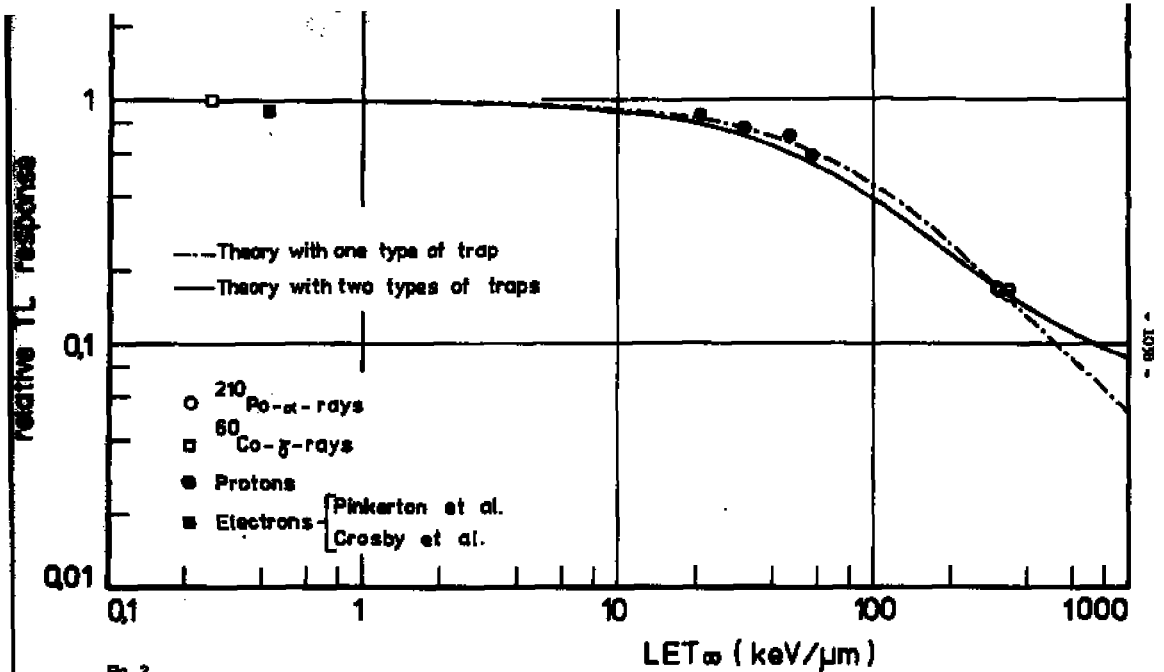

Fig. 2

Relative TL-yield as a function of the average stopping-power (LET∞) for LiF

Becker

As we all know, most solid-state dosimeters have the unpleasant property of decreasing sensitivity with increasing LET, and we have several nice theories to explain why this is so. There are, however, a few reports indicating that in some cases such as BeO (Tochilin) and ZnS (Kuznin) sensitivity increases with LET. Have you noticed such effects in other materials, and could you offer an explanation?

Hemmert

No, we only worked with LiF.

Aitken

Work carried out by Zimmerman while at Oxford indicated that the low effectiveness of alpha particles in inducing TL could be adequately explained in terms of saturation of the TL traps within the high ionisation density of the alpha track. He found, for instance, that phosphors which saturated early in their gamma-induced TL growth-with-dose curves also had a low effectiveness for alpha particles. This could be an alternative explanation for the results you report.

Carlsson, C.

If there is saturation of filled traps along the alpha particle tracks, there should be no supralinearity. Surprisingly there is. This must be due to interference between the delta rays from different alpha tracks.

Hemmert

Yes, that might be an explanation. The increase of sensitivity with dose for our measured alpha irradiation is low, it goes from 1 up to 1.3, but there is a supralinearity.

THERMAL NEUTRON DOSIMETRY BY PHOSPHOR ACTIVATION

M.R. Maybugh, S. Watanabe, and R. Muccillo
Instituto de Energia Atomica, Cx. Postal 11049, Sao Paulo, SP, Brazil

ABSTRACT

Three common thermoluminescent phosphors, $CaSO_4$:Dy, CaF_2:Dy, and CaF_2: natural, have been examined to determine the feasibility of their application in thermal neutron dosimetry. Basically, the phosphor is exposed to thermal neutrons (and other radiations) causing activation of nuclei in the phosphor. Next, the phosphor is stored to undergo self-irradiation from the internal radioactive nuclei, in this case all beta emitters. Later one reads the thermoluminescence induced by the beta emission during storage. This reading depends on the original neutron exposure, and could thus provide a dosimetry system. The phosphors contain suitable isotopes ^{44}Ca or ^{164}Dy (and ^{34}S). Limits for the lowest detectable fluence were determined by extrapolating results from high fluence measurements. Using the decay of ^{165}Dy (2.3 h half-life) the lowest detectable fluence is estimated to be 5×10^{7} n/cm^2. Using ^{45}Ca decay (165 d half-life), this limit is raised to about 5×10^{10} n/cm^2. Methods for improvement are discussed.

INTRODUCTION

Detecting thermal neutrons in mixed radiation fields necessarily relies on the neutron's nuclear interaction with the detector. The useable nuclear interactions might be roughly divided between those which happen rapidly, therefore leaving their mark during irradiation, and those of simple activation wherein the product is detected after irradiation. An example of the rapid type is the $^{6}LiF/^{7}LiF$ thermoluminescent system which detects[1] the neutron by the energy deposited from the (n,α) reaction in ^{6}Li. The ^{7}LiF is used to measure and correct for the energy deposited by the other radiations. Metal foils provide an example of detection by simple activation. In this case the neutrons produce radioactive nuclei in the foil, and these are later detected upon their disintegration, usually by beta counting. This technique requires no correction for effects of other radiations.

A thermoluminescent system based on simple activation, like foils, has been studied earlier at this laboratory[2,3]. Natural CaF_2 was exposed to thermal neutrons in a mixed field, the neutrons causing activation of ^{44}Ca to ^{45}Ca and the other radiations inducing thermoluminescence (TL). Next, the samples were annealed to eliminate the TL induced during irradiation, and then they were stored to undergo self-irradiation as betas are emitted from the radioactive ^{45}Ca. Finally, the TL was read after a suitable storage time. This final TL reading is related to the number of disintegrations occuring during storage which in turn depends on the original neutron fluence. Like foils, the signal is independent of the other radiations in the mixed field provided that the crystal does not suffer permanent radiation damage. An advantage over foils is that integration of the decay betas occurs outside the detecting apparatus.

Herein we further examine the feasibility of using phosphor activation as a thermal neutron dosimeter. Our purpose is to establish the lower limits for the detectable fluence with CaF_2,natural, and to extend the study to $CaSO_4$,Dy and CaF_2,Dy. The ^{164}Dy in the latter two phosphors might provide a thermal neutron dosimeter useful in accident situations.

EXPERIMENTAL

The CaF_2 was collected from a mine located in Santa Catarina State, Brazil and was ground and sieved through 80 onto 200 mesh Tyler screens for use. This powder can be very sensitive to light so that a 10 second exposure to incandescent room light could be detected. Since work under darkroom conditions was not convenient, the samples were annealed in air for 45 min at 570°C whereupon the light induced TL was just detectable after a 10 min exposure to room light. Sensitivity to gamma-rays is also reduced by the annealing treatment. Several batches of about 2 grams each were prepared and two were selected for further study on the basis of their similar response to gammas. Light was normally avoided except for subdued room light during the reading process.

The CaF_2:Dy (TLD-200) and $CaSO_4$:Dy samples were purchased from Harshaw Chemical, the former stated to be 80 to 200 Tyler, and the latter found to pass 80 mesh and not 200 mesh. The CaF_2:Dy was annealed at the highest reading temperature before use, nominally 400°C. The $CaSO_4$:Dy powder was initially annealed 90 min at 700°C, then at 400°C for reuse[4].

Gamma irradiation was at two meters from a 40 Ci ^{137}Cs source, and mixed field irradiations occured at a pneumatically served station alongside the core of IEAR-1, the swimming pool reactor located at this Institute. The neutron flux at this station is about 2×10^{12} n/cm^2-sec as determined by gold foil activation measurements. Samples were exposed in cylindrical polyethylene capsules having a 1 mm wall and 3 mm inside diameter.

Glow curves were recorded as photocurrent against time on two Harshaw model 2000 systems, both with the phototubes at room temperature. The relative sensitivity of the two machines was compared by reading identically treated LiF dosimeters in both instruments. All measurements in this work were made by dispensing a fixed volume of powder. The corresponding masses are CaF_2:Dy, 20.1 mg; $CaSO_4$:Dy, 18.9 mg; and CaF_2:natural, 20.7 mg, with the total fluctuation at about ± 0.3 mg. Although the Harshaw readers do heat the sensing thermocouple linearly, a particular peaks' position is not reproducible unless the reading cycle is rigidly controlled: time of initiation, time of termination, and time of drawer open and close. Since these conditions were not met for our measurements, relative peak positions between different glow curves are only approximate. The heating run's

temperature was determined for a typical cycle by spotwelding a thermocouple to an old pan and registering the temperature against time. This temperature curve is not strictly linear as reflected by the slight nonlinearity in the temperature scale of Fig. 1.

RESULTS AND DISCUSSION

a) Gamma-Ray Irradiation.

The TL induced by a one R gamma exposure is shown in Fig. 1 for equal volumes of CaF_2:Dy (dot-dashed line), $CaSO_4$:Dy (dashed line), and CaF_2:natural (solid line). The shapes of the glow curves are similar to those observed by others[4,5,6]. For CaF_2:Dy and $CaSO_4$:Dy the height of the highest peak was used as a measure of the TL. For convenience, the three peaks in CaF_2:natural were labled 1, 2, and 3 in ascending temperature order, and normally changes in both peaks 2 and 3 were followed, again using the peak height. On this basis CaF_2:Dy gives about 30% more TL than the same volume of $CaSO_4$:Dy, as shown in Fig. 1. The response of CaF_2:natural is about ten times smaller; hence, its glow curve has been increased a factor of two in the figure. The response of CaF_2:natural might be increased if the high temperature annealing were in H_2 and not air[7].

b) Beta-Ray Irradiation from Internal ^{45}Ca (and ^{35}S).

When calcium compounds are exposed to thermal neutrons, some of the ^{44}Ca (σ = 1.16, natural abundance = 2.06%) is activated to ^{45}Ca a beta emitter with a 165 d half-life. To observe our phosphors' response to this internal activity, we irradiated a sample of each for 1 min in HEAD-1. Several days later, phosphor was placed in the reading pan and heated one minute at the maximum temperature, nominally 400°C. (The photo tube was inactivated during this heating, otherwise the high light levels spoil the subsequent low level readings). The samples could then be read at various intervals to determine the response as a function of the self-irradiation time. This technique has the advantage that spurious luminescence is largely eliminated since the powder is not handled between readings.

The responsesof the three phosphors are shown as a function of the self irradiation time in Fig. 2. In contrast to gamma irradiation,

$CaSO_4$:Dy gives about 5 times more TL than either CaF_2:Dy or CaF_2:natural (peak 3). The shapes of the glow curves are largely unchanged from those shown in Fig. 1, although peak 2 in CaF_2:natural is relatively smaller compared with peak 3, as indicated in Fig. 2. Some of the response in $CaSO_4$:Dy can be attributed to ^{35}S (88 d half-life) created during irradiation from ^{34}S (σ = 200 mb, natural abundance = 4.22%). Assuming that the TL is proportional to the total decay energy times the number of disintegrations, one finds that the ^{35}S contribution in $CaSO_4$:Dy would be about 70% that of ^{45}Ca during the first 10 days. Therefore, considering only the ^{45}Ca decay, $CaSO_4$:Dy is about 3 times more sensitive than the other two phosphors. (We suppose throughout that interactions with fast neutrons are negligible). The greatly increased relative response of CaF_2:natural may correlate with an increased sensitivity to light. (See below). The linear response is expected in all cases since the times are short compared with the half-lives.

Any application of these materials to high fluence dosimetry requires knowing the response as a function of irradiation time (i.e. fluence). The linear response in Fig. 2 leads us to expect a linear behavior with number of disintegrations and hence with neutron exposure as well. Since samples exposed to high fluence can not be reused, verification of the response concentrated on CaF_2:natural because it is not expensive. In a typical experiment, samples of CaF_2:natural were irradiated for 0.5, 1, 2, 4, and 6 min in HEAR-1, and then after several days they were annealed at 400°C, stored in capsules, later read, annealed again, stored for a different time, read, and so forth. In Fig. 3 the heights of peaks 2 and 3 are shown as a function of the original irradiation time, for readings taken after 16 h storage. The response is linear for peak 2, as expected, and peak 3 also appears to respond linearly though there is more fluctuation. The high exposure inherent in the irradiation increases the light sensitivity of CaF_2:natural the order of 10 times. This increase does not depend strongly on radiation time 0.5 to 6 min, and probably corresponds to the filling of deep traps originally emptied by annealing. Filling such deep traps could cause the increased relative sensitivity of CaF_2:natural to internal beta[6].

In any case, the increased light sensitivity can not account for the poor reproducibility generally encountered in these experiments. (Figure 3 is the best run). Typically two out of five capsules, either with ascending or identical irradiations, would display unexpl-

able response despite similar handling of all samples. Sometimes peak 3 would be at about the expected level, but peak 2 much higher than expected, and sometimes both peaks would be higher than expected. Similar problems were not encountered with CaF_2:Dy and $CaSO_4$:Dy, but these were not used extensively.

Despite these problems, we can establish a limit for the lowest detectable fluence by making the linear extrapolations implied in Fig. 2 and 3. For $CaSO_4$:Dy the signal after 0.5 h and 1 min irradiation (Fig. 2) is about 9 times larger than the smallest detectable one. Since the fluence in this case is about 1.2×10^{14} n/cm^2 we conclude that for 0.5 h storage the lowest detectable fluence would be about 1.3×10^{13} n/cm^2. To detect lower fluences the storage time must be increased, although this recourse also has limits. For these long half-life decays the fundamental limit is that the internal activity must induce TL at a rate comparable to that due to background radiation and natural internal activity. Typically, this background is equivalent to the order of 0.5 mR per day, and we rather arbitrarily define the detection limit as 20% above the background, or the equivalent of 0.1 mR per day. The growth observed for $CaSO_4$:Dy in Fig. 2 is the gamma equivalent of about 6.8 mR/h. Reducing this rate to 0.1 mR per day implies a reduction of the detectable fluence to about 4×10^{10} n/cm^2 (40 rem). For CaF_2:Dy the value would be about 2.5×10^{11} n/cm^2 (5 times less TL per neutron, 30% higher sensitivity to background). These estimates are only valid if the sensitivity to background remains unchanged after the neutron exposure. Since the relative sensitivities change this may not be the case. The CaF_2:natural can be supposed to change sensitivity, as evidenced by changing light response.

In any case the lowest detectable fluence of 4×10^{10} n/cm^2 (about 40 rem) for $CaSO_4$:Dy can be considered as an order of magnitude boundary for use of ^{44}Ca (and ^{34}S) activation as a dosimeter. Isotope enrichment could provide an improvement by a factor of about 45, and storage in low background environments could also improve sensitivity. Employing this system at high fluence may be useful since other TL systems saturate. Exposing TLD-100, 600, and 700 1 min in JEAR-1 gives glow curves clearly in the saturation region, although the curves shape might still give the absorbed dose.[8] To reach the low fluence region useful for personnel dosimetry, a method must be found to obtain more TL per disintegration, or the system must rely on a different isotope.

c) Beta-Ray Irradiation from Internal ^{165}Dy.

Like ^{44}Ca, ^{164}Dy (σ = 2600 b, natural abundance = 28.2%) can produce TL after activation to ^{165}Dy, the latter a beta emitter with a 2.32 h half-life. To observe TL due to decay of this isotope, a recently irradiated sample was placed on the reading pan and read every half-hour, without moving the sample. Figure 4 shows the decay in the induced TL as a function of time elapsed since a 1 min irradiation in IEAN-1. Each point for CaF_2:Dy is multiplied by 10 to eliminate overlap of the two curves. The decay clearly follows the 2.32 h half-life for ^{165}Dy which is indicated by the solid lines. In the final stages both samples leave the exponential decay as longer half-life isotopes begin to influence the response. For $CaSO_4$:Dy the experimental points are initially slightly above the ^{165}Dy decay line, indicating that another short half-life impurity may be present. Extrapolating to the irradiation time, and comparing with the ^{45}Ca results shown in Fig. 2, we can conclude that in the first 0.5 h the ^{165}Dy decay produces at least 7×10^3 more TL than ^{45}Ca. In one day the ^{165}Dy decay would produce approximately 1×10^3 more TL than ^{45}Ca. This would lower the limit for the detectable fluence to about 4×10^7 n/cm^2 (40 mrem) for either $CaSO_4$:Dy or CaF_2:Dy (30% higher), again supposing that the sensitivity to background radiation is not changed. Also, we have supposed that there is no time delay between irradiation and the start of storage. In practice this could only be realized by irradiating at high temperature to eliminate the intermediate anneal. Finally, since this case is not just a comparison of background and self-irradiation rates, the phosphor must be sensitive enough to detect the 0.1 mR supposed as the daily detection limit.

Several improvements on the ^{164}Dy system are possible. A factor of about 3 could be obtained by isotope enrichment. More important, the Dy concentration might be increased, or the system might be changed to a mixture of some Dy compound and a TL phosphor. Significant interaction would be expected between the two powders since the maximum beta range is about 2.1 mm (in $CaSO_4$)[9]. (Similar interaction from ^{45}Ca betas is small, as we have observed, because the maximum range in $CaSO_4$ is about 0.15 mm). A mixture of Dy_2O_3 and ^7LiF, for example, would have the advantage of being removable, even after exposure to high fluences.

REFERENCES

1) J.R. Cameron, D. Zimmerman, G. Kenney, R. Buch, R. Bland, and R. Grant, Health Phys. 10, 25 (1964).

2) R. Muccillo and S. Watanabe, Presented to the Health Physics Society Meeting, Chicago, 1970.

3) R. Muccillo, Masters Thesis, Universidade de Sao Paulo, Sao Paulo, Brasil (1970) (unpublished).

4) T. Yamashita, N. Nada, H. Onishi and S. Kitamura, Proc. Int. Conf. Luminescence Dosimetry, 2nd, Gatlinburg, Tennessee, September 1968.

5) W. Binder and J.R. Cameron, Health Phys. 17, 613 (1969).

6) E. Okuno and S. Watanabe, These proceedings.

7) M.J. Aitken, Same proceedings as Ref. 4.

8) F.S.W. Hwang, J. Phys. D 4, 598 (1971).

9) Kobetich and Katz, Phys. Rev. 170, 170 (1968).

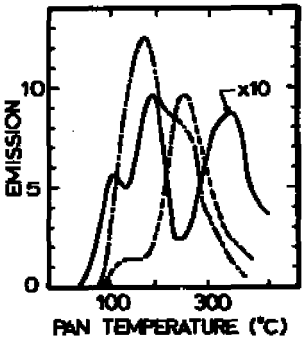

Fig. 1 The TL induced by a 1 R exposure to ^{137}Cs gamma. Dot-dashed line, CaF_2:Dy. Dashed line, $CaSO_4$:Dy. Solid line, CaF_2:natural.

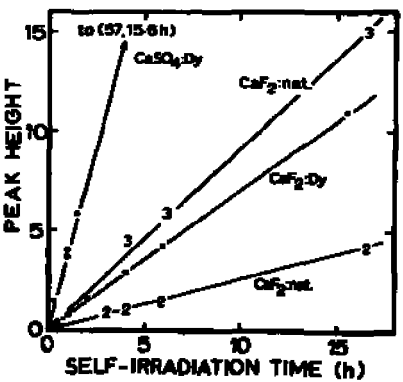

Fig. 2 The growth of the TL as a function of the self-irradiation time, for a 1 minute irradiation.

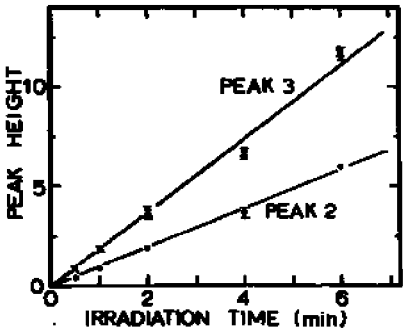

Fig. 3 The TL as a function of the original irradiation time for a 16 h storage time. (This data is not typical - see text).

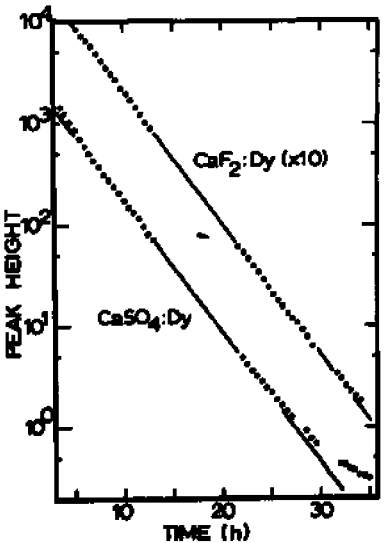

Fig. 4 The TL induced in a 0.5 h self-irradiation as a function of time since the original irradiation. The solid lines represent decay with a 2.32 h half-life.

Aitken

We have found with natural fluorite (BEUE) that by carrying out the annealing in nitrogen instead of air it is possible to remove the light sensitivity without attenuating the radiation sensitivity.

Determination of the Sensitivity of the CaF_2:Mn Thermoluminescent Dosimeter to Neutrons

by

M.Prokić

Boris Kidrič, Institute of Nuclear Sciences Vinča, Belgrade, Yugoslavia

Abstract

In a mixed (n+γ) radiation field, intensive neutron radiation may cause difficulties in assessment of the gamma dose. In this work sensitivity of the CaF_2:Mn thermoluminescent gamma dosimeter to fast, fission, intermediate and thermal neutrons was studied. The magnitudes of the mentioned sensitivities were determined by first collision dose calculation in CaF_2:Mn. The relative thermoluminescent response as a function of LET for neutrons of different energies enables determination of the CaF_2:Mn thermoluminescent sensitivity to neutrons in terms of equivalent ^{60}Co R per 10^{10} n/cm^2.

Experimental check of the calculated sensitivity values was performed irradiating hot pressed CaF_2:Mn powder (TLD-08,IJS) in different types of neutron fluxes.

Introduction

The aim of the work described here was to study the sensitivity of CaF_2:Mn to thermal, intermediate and fast neutrons.

In a (n+γ) mixed field it is often important in the TL dosimetry of gamma radiation to know the error introduced by the presence of neutrons. The sensitivity was determined both by calculation and by experiment.

In our case calculations were based on the elementary composition of the dosimeter and on the mechanisms of interactions of neutrons with the CaF_2:Mn.

The neutron sensitivity is primarily a function of neutron energy and it is necessary to know the relative thermoluminescent response of CaF_2:Mn because of its inefficiency for high LET particles.

We described the procedure of the calculation performed as well as the experimental methods and presented the results obtained for the TLD-08,IJS type of CaF_2:Mn thermoluminescent dosimeter.

Calculated Neutron Sensitivity

For the same absorbed energy, dosimeter reading is different for the different type of radiation and is a function of its energy. It means that in a given material absorbed doses from the same fluences of different energy spectra will the different.

When an energy is absorbed by matter, in this case CaF_2:Mn, it goes into lattice excitation and electron-hole pairs production. The charged particle traversing matter, loses energy at a rate which depends on both the nature of the particle and its energy.

Murray and Mayer[1] assumed that the liberated electrons can suffer two events, either recombining with a hole in the wake of the incident particle or being trapped at an unspecified site in lattice. For a high LET radiation, the density of electrons along a track is higher and there will be more of electrons available for filling the traps. If we plot the relative light response of TLD per unit absorbed dose for particles of different

LET, (taking ^{60}Co gamma ray response as unity)we observe decreasing of TLD response with increasing LET. A similar decrease in luminescence efficiency with LET has been observed for other solid-state detectors, as the alkali halides and silver phosphate glass dosimeters.

As was proposed by Birks[2], the primary effect which causes the decrease in light response is influenced by electron-hole recombination and is a function of ionization density,which increases with a rate of energy loss. The secondary effect influenced by the concentration of locally available activators, involves the energy transfer at activator sites in TLD. These two effects reduce the efficiency of response to high LET particles.

First Collision Dose

If the range of the secondaries is short compared with the attenuation length of the primary radiation, the absorbed dose at the point of radiation equilibrium is approximately equal to the first collision dose.

If we know the relative TL response and the value of the absorbed dose in the dosimeter, it is possible to calculate the neutron sensitivity for the given thermoluminescent dosimeter. The first collision dose $D_f(E)$ per neutron per square centimeter at energy E is defined by ICRP[3] and is given by

$$D_f(E) = \sum_j N_i \sigma_{ij}(E) \varepsilon_{ij}(E), \qquad (1)$$

where N_i is the number of atomic particles of type i that can react with a neutron radiation and produce charged particles. If the reaction is of type j, the cross section for the process is $\sigma_{ij}(E)$ and the average kinetic energy imparted to the charged particles is $\varepsilon_{ij}(E)$.

Thermal Neutrons - The atomic composition of CaF_2:Mn leads to conclusion that the only possible interaction of thermal neutrons is radiative capture. Thermal neutrons affect CaF_2:Mn primarily through the radioactivity they induce in fluorine and manganese

which decay emitting beta and gamma rays with mean beta energies $\bar{\epsilon}_{\beta} = 2.65$ MeV and 0.86 MeV, respectively.

The $^{19}F(n,\gamma)^{20}F$ reaction (48.2 per cent of ^{19}F in CaF_2:Mn) has very small activation cross section of 9.8 mbarns for thermal radiative capture so that, even that there is relatively large number of fluorine atoms in the dosimeter, the absorbed dose from ^{20}F β-rays will be relatively small.

^{55}Mn (3 per cent of ^{55}Mn in CaF_2:Mn) has a rather large activation cross section of 13.3 barns for thermal neutrons. Thus, the thermal neutron absorbed dose at CaF_2:Mn is primarily determined by the concentration of manganese, which was also confirmed by Fuite[4].

Calcium isotopes, ^{44}Ca, ^{46}Ca and ^{48}Ca have low per cent of isotope abundances, hence the thermal neutron absorbed dose which gives β -rays activation, can be neglected.

The number of thermal neutrons necessary to produce 1 rad in CaF_2:Mn was determined by using equation (1). The effect of the capture γ- rays is negligible compared with that of the β - rays, as was shown by Randolph[5].

Because of the small difference of linear energy transfer (LET) values between ^{56}Mn β- rays and the mean energy of secondary electrons produced by ^{60}Co γ- rays, the relative response for thermal neutrons is expected to be very close to unity. We calculated that the thermal neutron sensitivity was 0.77 equivalent ^{60}Co R per 10^{10} n/cm^2.

Intermediate neutrons - Intermediate energy neutrons are in the region $0.5\ eV \leq E_n \leq 0.01$ MeV. The spectrum of these neutrons is often approximated by a 1/E distribution. The absorption and activation cross sections generally vary inversely proportional to the neutron velocity (1/v).

The reactions taking place in the intermediate energy range are usually radiative capture and elastic collision. Recoiling atoms arising from nuclear collisions with neutrons of these energies, do not have sufficient energy to ionize matter and their effect on the dosimeter is negligible.

^{55}Mn and ^{19}F can be activated by the resonance absorption of intermediate neutrons. For ^{55}Mn this type of absorption occurs at a number of different neutron energies, but predominantly at 337 eV; for ^{19}F resonance absorptions occur at the energies higher than the upper energy range limit of 0.01 MeV. In the intermediate energy range the 1/v contribution to the resonance integral cross section for ^{19}F is about 4.5 mbarns; thus the contribution from β activation induced in CaF_2:Mn from ^{20}F, can be neglected.

The first collision dose absorbed in CaF_2:Mn from intermediate neutrons was determined by using equation (2) which represents the average absorbed dose in the dosimeter.

$$D = 1.602 \times 10^{-8} \sum_{i=2} F_i \, \Phi_i \, I_{act_i} \qquad (2)$$

where the quantity $I_{act} = \int_{0,5eV}^{\infty} \sigma(E) \frac{dE}{E}$ is called resonance integral cross section. For ^{55}Mn it is taken a value of 14 barns, given by Aliev et al[6].

The calculated average neutron sensitivity for the intermediate neutrons amounts 0.80 equivalent ^{60}Co R per 10^{10} n/cm^2.

Fast neutrons - According to widely accepted division of the neutron energy spectra, fast neutrons fall in the energy region 0.01 - 10 MeV. In this work we carried out the analysis up to 14 MeV neutrons.

Since the most important interaction of fast neutrons with matter is elastic scattering, in the upper part of this energy range, inelastic scattering and reactions account for an appreciable part of the total cross section.

In CaF_2:Mn fast neutrons mainly produce heavy ion recoils (Ca and F ions) by elastic collisions which lose their energy through ionization and excitation of the lattice ions. The principle nuclear reactions which take part with fast neutrons are (n,p) and (n,α) in calcium and fluorine nuclei. Since the recoils

and ejected charged particles are completely stopped in a thickness of CaI_2:Mn which is thin by comparison with the mean free path of neutrons first collision dose was calculated using the following equations:

1. Isotropic elastic collisions

$$D(E) = 1.602 \times 10^{-8}\ En \sum_i N_i \sigma_i 2M_i/(M_i + 1)^2 \qquad (3)$$

2. Isotropic inelastic collisions

$$D(E) = 1.602 \times 10^{-8}\ En \sum_i N_i \sigma_i 2M_i/(M_i + 1)^2/1-(M_i+1)E^*/2M_iEn/(4)$$

3. Reactions which produce charged particles

$$D(E) = 1.602 \times 10^{-8}\ En \sum_i N_i \sigma_i 2M_i/(M_i + 1)^2/1-(M_i+1)Q/2M_iEn/\ (5)$$

where En is the neutron energy in MeV, N_i is the number of atoms per gram of the i^{th} species, M_i is the mass in a.m.u. of the i^{th} species, E^* is the excitation energy and Q is the Q value for the reaction. The scattering was assumed to be isotropic in the centre-of-mass system, as it is shown by Davy et al[7].

Assuming that the calcium and fluorine recoils account for most of the energy transferred by fast neutron interactions, and using Snyder's[8] results we could make a rough estimate that the average initial LET for these recoils was higher than 200 keV/μ . Figure 1, taken from Attix et al[9] shows similar curves for LiF given by Wingate et al[10] and silver phosphate glass dosimeter given by Tochilin et al[11]. It can be seen that for high LET radiation, there are no pronounced differences in relative response for various luminescent dosimeters. Hence, for fast neutron recoils for CaF_2:Mn, we could take that the relative response is mostly 0.15 of that of a 1-MeV electron (minimum LET).

Figure 2 shows the dose values obtained in our calculations in CaF_2:Mn for various energy fast neutrons. We also calculated the fast neutron sensitivity of CaF_2:Mn in function of neutron energy and the results are displayed in Figure 3.

Fission neutrons - Within the energy range from 0.1 to 10 MeV, which includes practically all fission neutrons, the fission spectrum for the reactor RA at Vinča can be represented by mathematical expression, given by Mirić et al[12]

$$\phi(E_n) = 9.733 \times e^{-2.75 E_n} E_n^{1/2} \qquad (1)$$

where $\phi(E_n)$ is the number of fission neutrons per unit energy normalized to one fission neutron.

The average sensitivity to fission neutrons for CaF_2:Mn, can be obtained from the calculated values for the sensitivity to fast neutrons and the mathematical expression for fission neutron spectrum; it amounts 0.55 equivalent ^{60}Co R per 10^{10} n/cm^2.

The reason for such a low sensitivity is that most of fission neutrons have energies between 0.1 and 3 MeV, and only a small per cent have energies higher than 5 MeV.

Experimental Methods and Results

Experimental verification of the calculated sensitivity was performed by irradiation hot pressed CaF_2:Mn powder (the characteristics of which are given by Uran[13]:TLD-08,IJS, Yugoslavia) in different types of neutron fluxes (thermal, intermediate and 14 MeV neutrons). Simultaneously, the relative termoluminescent responses per unit absorbed energy in CaF_2:Mn were experimentally determined.

The samples exposed to thermal and intermediate neutrons were encased in Plexiglas containers of 3 mm wall thickness. This encasing was done to approximate secondary electron equilibrium. In each container there were about ten samples.

Thermal neutrons - TLD-08 (200 mg weight) were exposed at the thermal column of the RA Reactor at Vinča. The thermal neutron fluxes were measured by gold foil activation (the cadmium ratio was less than one per cent). Associated gamma ray exposure was determined with a small G-M (18529) counter.

Exposed to a mixed (n+γ) field the dosimeter will indicate the integral dose, a larger part of which is due to γ radiation and a smaller part will be due to thermal neutrons. In order to remove any thermal neutron contamination from the measured gamma dose, we encased the TLD samples in a neutron

absorbes. As a thermal neutron shield material, borax was used. Figure 4 shows the absorption of thermal neutron vs. borax thickness.

We obtained the value of (1.05±0.08) equivalent ^{60}Co R per 10^{10} n/cm^2 for thermal neutron sensitivity of CaF_2:Mn (TLD-08).

Intermediate neutrons - As a source of the intermediate neutrons was used the horizontal channel (HK-E) of the reactor RA at Vinča. The accurate determination of the intermediate neutron sensitivity was difficult since the intermediate neutron flux was accompained with the three times lower fission flux and about three times higher thermal neutron flux, as well as intensive γ radiation. Since the fission neutron sensitivity of CaF_2:Mn is low, we neglect its contribution to the dosimeter reading. On the other hand, the thermal neutron and γ radiation contribution on the TL reading, had to be taken into account.

The effect of thermal neutrons on the dosimeters cannot be eliminated by borax shielding, because the present fluxes of fission and intermediate neutrons, would be thermalized by elastic collisions in borax, and the dosimeter reading could be even increased.

The result obtained for intermediate neutron sensitivity was (1.10±0.16) equivalent ^{60}Co R per 10^{10} n/cm^2.

14 MeV Neutrons - TLD-08 samples were exposed to mono-energetic 14-MeV neutrons produced by ^{3}H(d,n)^{4}He reaction available in 1.4MV accelerator at Vinča. The exposed samples were not encased in Plexiglas containers, for the fast neutron sensitivity would be increased by the recoil protons from a high content of hydrogen in Plexiglas.

The neutron flux was determined by measuring the activity of ^{114m}In and ^{32}P released from the reactions ^{115}In(n,2n)^{114m}In and ^{32}S(n,p)^{32}P, respectively. Gamma contamination which was negligible was measured by Kodak-RK film detectors. The value obtained from these exposure data for 14 MeV neutron sensitivity was (2.30±0.03) equivalent ^{60}Co R per 10^{10} n/cm^2.

Discussion and Conclusions

Table 1. Neutron sensitivities of CaF_2:Mn(TLD-08) expressed in equivalent ^{60}Co R per 10^{10} n/cm^2

Neutrons	Sensitivity R per 10^{10} n/cm^2		Relative TL response
	Calculated values	Measured values	
Thermal	0.77	1.05±0.08	1.19±0.08
Intermediate	0.80	1.10±0.16	1.20±0.16
Fission	0.55	-	-
14 - MeV	3.54	2.30±0.03	0.13±0.03

In Table 1 are shown the measured and calculated results for neutron sensitivities of CaF_2:Mn (TLD-08). We found the experimental results for TLD-08 which are in reasonable agreement with the calculated values for an "ideal" thermoluminescent CaF_2:Mn dosimeter. Namely, if we know that the neutron flux measurements as well as γ dose values were performed with an error greater than 10 per cent, the agreement is good. We also must take into consideration the reading errors for the dosimeter.

On the other hand, the disagreement can be due to the uncertainties of the cross section data especially for inelastic scattering and nuclear reactions of fast neutrons with the CaF_2:Mn.

Also, it will be noted that the higher values for the experimentally determined intermediate neutron sensitivity, as well as the higher measuring error, were presumably due to proton recoils from elastic collisions of fission neutrons in the Plexiglas containers. We suppose that in the case of thermal (for the samples exposed without borax absorbers) and intermediate neutron sensitivities, somewhat higher dosimeter readings was due to the contribution from the activity of samples on

each other. Namely, after irradiation at the thermal coloumn and at GK-E, the activity of samples was relatively high.

The upper discussion is related to somewhat higher values for thermal and intermediate neutron relative responses per rad in CaF_2:Mn.

The sesitivity of CaF_2:Mn (TLD-08) for fast neutron energies up to 14 MeV is low but strongly dapendent on energy. Its low neutron sensitivity make it possible to use it as a γ dosimeter in mixed neutron-gamma fields. This dosimeter is especially convenient for measurements of γ doses at the nuclear reactor beams where the most per cent of neutrons have energies between 0,1 and 3 MeV.

Correction factors for CaF_2:Mn (TLD-08) used in mixed beam dosimetry can be calculated only from a known incident neutron spectrum.

References

1. R.B.Murray, A.Meyer, Phys.Rev. 122, 815 (1961).
2. J.B.Birks, I.E.E.E. Trans.Nucl. Sci. 11 (3):4 (1964).
3. NBS Handb. 75 (1961).
4. K.J.Puite, Health Phys. 20, 437 (1971)
5. M.L.Randolph, Rad.Res 7, 47 (1957).
6. Spravochnik Yadernofizicheskie Konstanty dlya Neitronnogo Aktivacionnogo Analiza, (Edited by A.I.Aliev et al), Atomizdat Moskva (1969).
7. D.R.Davy, B.G.O' Brien, Health Phys. 17, 471 (1969).
8. W.S.Snyder, Biological Effects of Neutron and Proton Irradiations. IAEA, Vienna (1964).
9. Radiation Dosimetry, Second Edition, (Edited by F.H.Attix and E.Tochilin), Volume III, Academic Press (1969).
10. C.L.Wingate, E.Tochilin, et al, Proc.Int.Conf.Luminescence Dosimetry, Stanford (1965).
11. E.Tochilin, J.T.Lyman, et al, Rad.Res.19, 200 (1963).
12. I.Mirić, P.Mirić et al, Second Congress ICRP, Brighton (1970).
13. D.O.Uran, Symposium on New Developments in Physical and Biological Radiation Detectors, IAEA, Vienna (1970).

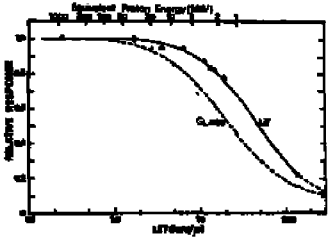

FIG. RELATIVE RESPONSE OF A LiF THERMOLUMINESCENT DOSIMETER AND SILVER PHOSPHATE GLASS vs. THE LET OF CHARGED PARTICLES

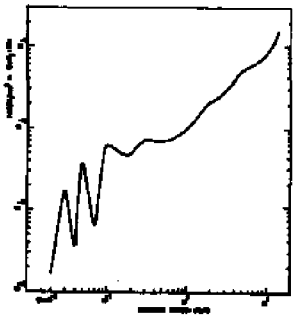

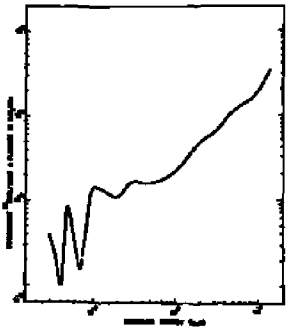

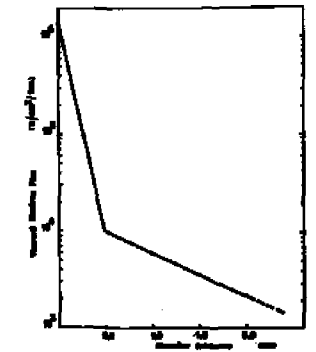

Title: Triplet Exciton Annihilation Fluorescence Changes Induced by Fast Neutron Radiation Damage in Anthracene

by

D. Pearson, P. R. Moran, J. H. Cameron*

Physics Department and Department of Radiology

University of Wisconsin, Madison, Wisconsin

Abstract

The triplet exciton annihilation fluorescence (delayed fluorescence) of anthracene crystals is known to be sensitive to radiation damage. Our investigations are primarily related to annihilation fluorescence changes induced by fast neutron irradiation. The three factors that determine the fluorescence behavior are the optical production efficiency of the triplet excitons, the bimolecular annihilation coefficient, γ, and the fluorescence unimolecular decay rate, β. Using flashlamp excitation we find that β is directly proportional to the absorbed dose R: $\beta(R) = \beta_0 + \alpha R$. The proportionality constant, α, was determined for 14 MeV neutrons, 2.5 MeV neutrons, 30 keV effective x-rays and 662 keV γ-rays. Typically β_0 is about 100 sec^{-1}, and both β_0 and α vary somewhat with sample batch of the anthracene. We will discuss how these sample quality dependences limit the reliable sensitivity to about 10 rad for measuring the annihilation fluorescence changes at room temperature. We have also measured total steady state blue fluorescence yield, F_0, for controlled red light excitation. At low excitation light levels, we find the fluorescence decreases with radiation dose according to the form $[F_0(0)/F_0(R)]^{1/2} - 1 = (\alpha/\beta_0)R \ll 1$. From this behavior we conclude that only the decay constant β is strongly affected by the radiation damage. At room temperature the observed damage effects appear to be stable with fading rates certainly less than 1% per month.

Introduction

Anthracene has long been used as a scintillator for fast neutron detection via proton recoil[1]. The scintillations one detects are the prompt blue fluorescence of the singlet excitons. Radiation damage effects have been observed by many investigators at doses of the order of 10^5 to 10^6 rads[2]. Anthracene also exhibits a delayed blue fluorescence from the bimolecular annihilation of mobile triplet excitons[3]. The lifetime of the triplet exciton and hence the decay rate of the delayed fluorescence is known to be a very sensitive measure of sample purity[4]. Weiss and co-workers[5] observed a linear increase in the triplet decay rate as a function of γ-ray dose for doses of the order of 10^2 to 10^3 rads. We wish to report similar findings for fast neutron exposures.

Theory

A simplified energy level diagram for anthracene is shown in figure 1. The state of interest is the first excited triplet state at 1.8 eV. It can be populated either from the first excited singlet state by an intersystem crossing or directly from the ground state by a weak red absorption. It is a mobile state with a diffusion constant of the order 10^{-4} cm^2 sec^{-1}. Its principle decay modes are a monomolecular, non-radiative decay to the ground state with rate constant β, and a bimolecular annihilation of neighboring triplets giving rise to an excited singlet which promptly fluoresces. This bimolecular process causes the observed delayed blue fluorescence and dominates the decay rate at high triplet concentrations. At low triplet concentrations the decay rate is dominated by the monomolecular process although one still samples the triplet population by observing the fluorescence from the bimolecular mechanism.

Our experiment is to populate the triplet state directly with red light and observe changes in the delayed blue fluorescence as a function of fast neutron exposure. The kinetic equations for the excitons involved are shown, somewhat simplified in figure 2 along with their solutions for the particular cases of weak steady red light excitation and free decay from some initial population. In this figure T is the triplet concentration, α the absorption coeff., Ir the intensity of red light, β the monomolecular decay constant, γ_T the triplet bimolecular annihilation coefficient, S the singlet population with decay constant k, F_d is the blue delayed fluorescence intensity. One expects that the radiation damage might affect the optical absorption coefficient or the bimolecular annihilation coefficient γ, or the monomolecular decay rate β. Weiss was able to explain his results assuming that X-irradiation produced a change only in the monomolecular decay rate β. We find similar behavior for fast neutron irradiation. The appropriate equations are shown in figure 3.

Experiments

A schematic drawing of our apparatus is shown in figure 4. With flashlamp excitation we measure the triplet decay constant from the slope of the logarithm of the photomultiplier current which is displayed on the scope. We can follow the monomolecular decay for about two decades of fluorescence intensity. We measure the blue fluorescence intensity under steady red illumination from the projection lamp at an intensity such that $\beta >> \gamma T$. The sample holder allows the photocube to see only a uniformly illuminated region near the center of the crystal. The samples are removed for exposure and remounting and repositioning samples is a major source of error in the measured values.

Our samples are disks 0.5 inch diameter by 2 mm thick which were cleaved from cylindrical crystals purchased from Harshaw Chemical Company (no longer available). The optical quality varies with sample and does the decay constant β, the latter being around 100 sec^{-1}.

Our neutron source is a 200 keV deuterium accelerator which uses the D-T reaction, $^{3}H(d,n)^{4}He$, to produce 14 keV neutrons, and the D-D reaction, $^{2}H(d,n)^{3}He$ to produce 2.5 keV neutrons. The neutron fluences were measured copper activation for the 14 keV neutrons and sulfur activation for the 2.5 keV neutrons. These fluence measurements are believed to be within 50% of the true value.

From published values of Kerma[6] the neutron fluence for 100 ergs/gm was calculated for 14 keV and 2.5 MeV neutrons. These are shown in table 1 along with the number of recoil protons produced. For our sample size the Kerma was taken to equal the absorbed dose.

Results

Some of the results of our measurement are shown in figures 5 through 10. Figures 5 and 6 show the change in the decay constant β and the fluorescence intensity F_0 with 14 MeV neutron dose. Figures 7 and 8 (for comparison) show the same for 30 keV x-rays (x cal 52) and Cs γ -rays (662 keV)(x cal 54). Figures 9 and 10 show the same for 2.5 MeV neutrons. Table 2 summarizes the results. The agreement with Weiss's model is quite good.

Discussion

It is also gratifying to see the constant "a" varying proportional to the number of recoiling protons. This must be checked at other neutron energies.

As a dosimeter the anthracene exciton system has several good features. It is a solid state integrating system with non-destructive readout--a readout which can in principle be very fast--a few hundred milliseconds to measure β. The observed effect is a bulk property and samples can in principle be made very small. Fading at room temperature was never observed and is certainly less than 1% per month, and γ contamination is not severe. However the limitations are rather formidable: The readout is essentially a subtractive technique--measuring a small difference between two large numbers. Measurement of β to one percent would allow one to detect 10 rads of 14 MeV neutrons or 1 rad of 2.5 MeV neutrons with about 50% confidence. The crystals are reasonable fragile and plastic deformation causes triplet quenching[7].

---

* This work was supported in part through USAEC contract AT(11-1)-1105.

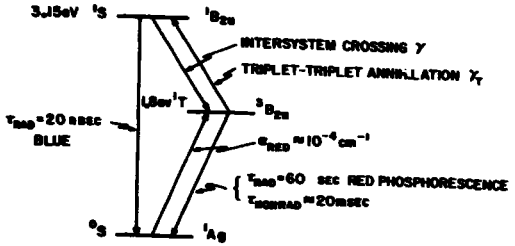

Figure 1. Simplified energy level diagram for the anthracene exciton system.

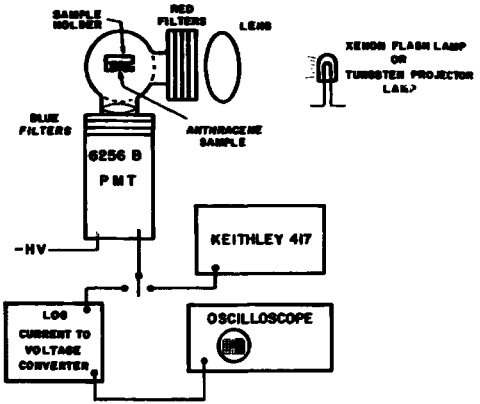

Figure 2. Schematic diagram of the experimental apparatus.

$$\frac{dT}{dt} = \alpha I_r - \beta T - \gamma_T T^2$$

$$\frac{dS}{dt} = \frac{1}{2}\gamma_T T^2 - k S$$

$$F_r = K S$$

$$F_r = K \frac{\gamma_T}{2} \frac{a^2}{\beta^2} I_r^2 \quad \text{STEADY STATE}$$

$$F_r(t) = F_r(0)\, e^{-2\beta t} \quad \text{FREE DECAY}$$

Figure 3. Simplified kinetic equations for the excitons in anthracene. T is the triplet consentration. α is the triplet optical absorption coefficient, I_r is the intensity of the incident red light, β is the monomolecular decay constant, γ_+ is the triplet-triplet annihilation coefficient, S is the singlet consentration, k is the singlet decay constant, F_r is the intensity of the delayed fluorescence and K is a constant involving light collection efficiency. The steady state and free decay solutions are valid for low triplet concentrations such that $\beta >> \gamma_+ T$.

$$\beta = \beta_o + a R$$

$$\left[F_r(0) / F_r(R)\right]^{\frac{1}{2}} = 1 + \frac{a}{\beta_o} R$$

Figure 4. Equations for the decay constant β and fluorescence intensity F_r as a function of absorbed dose R. These were derived using Weiss's model of triplet quenchers and the assumption of small triplet population: $\beta >> \gamma T$.

NEUTRON ENERGY	n/cm^2 FOR ONE RAD	NUMBER OF RECOILING PROTONS FOR ONE RAD
2.5 MeV	4.7×10^8 n/cm^2	5.5×10^7 p/cm^3
14 MeV	2×10^8 n/cm^2	6×10^6 p/cm^3

Table 1. Neutron fluences for Kerma of 100 ergs/gm to anthracene calculated from the Kerma tables of R. L. Bach and R. S. Caswell, Rad. Research, 35, 1 (1968)

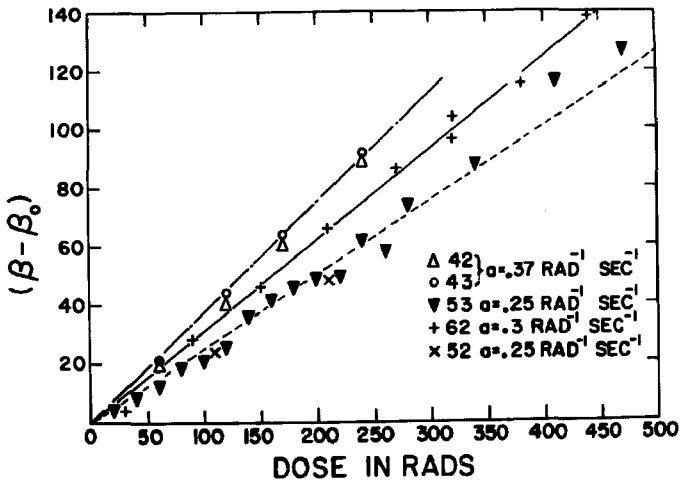

Figure 5. Change in triplet decay constant as a function of 14 MeV neutron dose. The lines satisfy the equation $\beta - \beta_o = \alpha R$ where R is the dose for the values of the constant α shown.

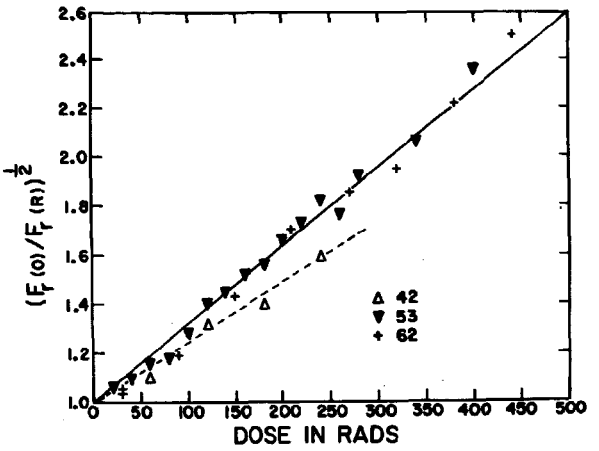

Figure 6. Change in blue fluorescence intensity under steady red illumination as a function of 14 MeV neutron dose.

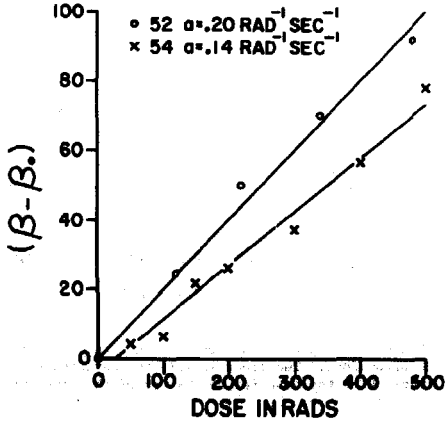

Figure 7. Change in triplet decay constant as a function of γ-ray dose. Crystal 52 was exposed to 30 keV effective x-rays. Crystal 54 was exposed to 662 keV γ-rays from ^{137}Cs. The lines fit the equation $\beta - \beta_0 = \alpha D$ for the values of α shown.

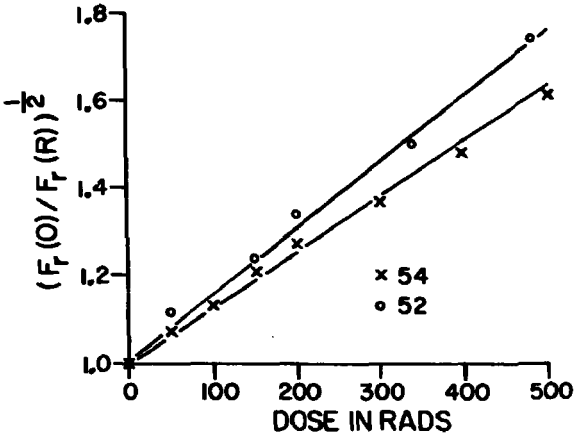

Figure 8. Change in the blue fluorescence intensity under steady red illumination as a function of γ-ray dose. Crystal 52 was exposed to 30 keV effective x-rays. Crystal 54 was exposed to 662 keV γ-rays from ^{137}Cs.

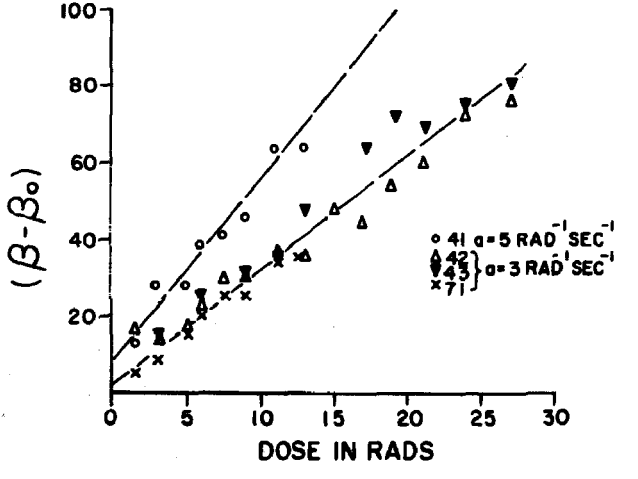

Figure 9. Change in triplet decay constant as a function of 2.5 MeV neutron dose. The lines satisfy the equation $\beta - \beta_0 = a\Phi$ for the values of a shown.

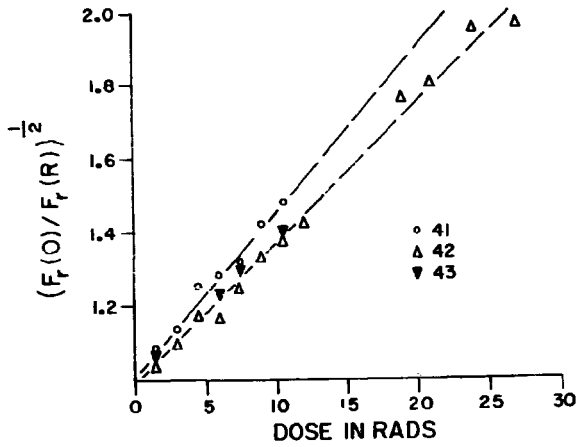

Figure 10. Change in blue fluorescence intensity under steady red light illumination as a function of 2.5 MeV neutron dose.

NEUTRON ENERGY	SAMPLE	η RAD^{-1} SEC^{-1}	β_o SEC^{-1}	α/β_o	SLOPE OF $\left[\frac{Fr(0)}{Fr(R)}\right]^{\frac{1}{2}}$
2.5	41	5	110	4.5×10^{-2}	4.5×10^{-2}
MeV	42	3	96	3.1×10^{-2}	3.8×10^{-2}
	43	3	100	3×10^{-2}	3.8×10^{-2}
14	42	0.37	135	2.7×10^{-3}	2.4×10^{-3}
MeV	53	0.25	88	2.8×10^{-3}	3.2×10^{-3}
	62	0.3	100	3×10^{-3}	3.2×10^{-3}
^{137}Cs	54	0.14	109	1.3×10^{-3}	1.27×10^{-3}
30keV X-RAYS	52	0.2	95	1.9×10^{-3}	1.55×10^{-3}

Table 2. Summary of results.

Moran

A clarification of Table 2 might be useful: the column labelled "a/β_o" is determined by a direct flash-lamp measurement of β vs. dose, and the final column is determined by measuring fluorescence yield under steady-state red light excitation.

Spurny

Which is your final decision, is this method hopeful for fast-neutron detection or not? For accident dosimetry it seems to be promising, is that right?

Moran

Yes; I believe it is promising for both accident and therapy levels. The method of measuring lifetimes is relatively very insensitive; however, if the triplet lifetime decrease is caused by an optical radiative process induced by neutrons, then measuring the resulting increase in red phosphorescence will be orders of magnitude more sensitive than the essentially subtractive lifetime methods. I think the method might be promising even at the personnel dosimetry level. However, the material one would eventually use should probably not be anthracene because of the severe sample preparation and stability problems involved.

Becker

Are the irradiated anthracene samples re-useable?

Moran

No, there is no annealing possible, and no fading occurs.

Becker

Have you tried higher polyphenyls?

Moran

No.

Mixed Neutron-Gamma Dosimetry

by

S.K. Dua*, R. Boulenger**, L. Ghoos** and E. Mertens***

ABSTRACT

Studies on the measurement of mixed neutron-gamma doses have been made using CaF_2:Mn discs, $CaSO_4$:Mn, LiF-6 and LiF-7 microrods from ISOTOPES/CONRAD and TLD-100 and TLD-700 microrods from Harshaw Chemical Company. The dosimeters were irradiated at thermal neutron fluences varying from 10^7 to 10^{14}n cm^{-2}. The cadmium ratios at the points of irradiation were more than 100. The gamma doses were measured by shielding the dosimeters with ^{6}Li or ^{10}B. The thermal neutron response of a given dosimeter depends on the abundance of the thermal neutron sensitive element in it. LiF-6 dosimeters which are suitable for the measurement of low thermal neutron fluences showed a decrease in response at high fluences of about 10^{12}n cm^{-2}. They also showed memory effects at thermal neutron fluences of about 10^{10}n cm^{-2}. Change in colour of LiF-6 and TLD-100 was also observed at about 10^{13}n cm^{-2}.

By partly covering the planchet of the commercial TLD reader higher temperatures required for neutron dosimetry could be reached without increasing the background contribution from the planchet. This paper also presents glow curves from samples irradiated with ^{60}Co and neutron-gamma radiations.

Introduction

The estimation of gamma ray field in the presence of thermal neutrons is complicated by the fact that most detectors respond to both types of radiation. The response to thermal neutrons depends on the abundance of neutron sensitive element in the phosphor. In the present study we

---

* On A.G.C.D., Belgium Scholarship to Dosimetry Section, S.C.K./C.E.N. Mol, Belgium from Health Physics Division, Bhabha Atomic Research Centre, Trombay, Bombay-85, India

** Contrôle-Radioprotection, Brussels, Belgium

***Dosimetry Section, S.C.K./C.E.N. Mol, Belgium

have evaluated the neutron and gamma response of some commercially* available phosphors : CaF_2:Mn, $CaSO_4$:Mn, LiF-6, LiF-7, TLD-100 and TLD-700. These phosphors may be combined to measure mixed neutron-gamma fields in various ratios. Also the influence of neutron irradiation history of LiF-6 dosimeters has been studied.

Materials and Method

General

Thermoluminescent phosphors are often to be used in mixed neutron-gamma fields in order to evaluate the gamma component of the irradiation field[1-10]. Table 1 summarizes some characteristics of the dosimeters used in the present study.

Table 1

SOME CHARACTERISTICS OF DOSIMETERS

Phosphor	Shape	Dimensions	Main thermal neutron sensitive element	Thermal neutron cross section (barns)	Percentage abundance of neutron sensitive element**
CaF_2:Mn	disc	6mm Ø x 0.13mm thick	Mn	13.2	unknown
$CaSO_4$:Mn	rod	1mm Ø x 10mm long	Mn	13.2	unknown
LiF-6	rod	1mm Ø x 6mm long	^6Li	945	95.6
LiF-7	rod	1mm Ø x 6mm long	^6Li	945	0.007
TLD-100	rod	1mm Ø x 6mm long	^6Li	945	7.5
TLD-700	rod	1mm Ø x 6mm long	^6Li	945	0.007

**values specified by the manufacturers

Owing to the extremely high cross section of ^6Li, LiF-6 is mainly intended for thermal neutron dosimetry. Should saturation of LiF-6 arise at high neutron fluences, TLD-100 seems adequate to replace LiF-6 in a very convinient way. In principle, TLD-700 and LiF-7 may be exposed to measure the gamma component of dose which normally accompanies thermal

---

* CaF_2:Mn, $CaSO_4$:Mn, LiF-6, LiF-7 from ISOTOPES/CON-RAD in teflon matrix. TLD-100, TLD-700 from Harshaw Chemical Company in extruded form.

neutrons. Since CaF_2:Mn and $CaSO_4$:Mn contain small amount of neutron sensitive manganese, they can also be used to measure gamma radiation in a mixed field.

Annealing

All the dosimeters were annealed before use. Table 2 gives the annealing procedure adopted for this study.

Table 2

ANNEALING PROCEDURE FOR DOSIMETERS

Type of dosimeter	Time and temperature of annealing
CaF_2:Mn	5 hours at 300°C
$CaSO_4$:Mn	30 minutes at 300°C
LiF-6 and LiF-7	24 hours at 300°C followed by 24 hours at 80°C
TLD-100 and TLD-700	1 hour at 400°C followed by 2 hours at 100°C

Readout method

The thermoluminescence output of the dosimeters was obtained by integrating the anode current from the PM tube using a storage capacitor. The instrument used was the ISOTOPES/CON-RAD TLD reader, which has a fast but approximately linear heating rate. Nitrogen gas was flushed at the rate of 8 cubic feet/hr during measurements. The heater current was chosen such that the second reading obtained after two minutes was less than 2% of the first. Table 3 contains the heater currents,as indicated on the reader, which were used for the various dosimeters.

At very high gamma and neutron doses a higher heater current, as given in the Table 3, was used. Its use increased thermal radiation from the supporting planchet. However, when the planchet was partly covered with a polyimide resin, commercially available under the name of Vespel*, this radiation could be minimised. Thermal radiation values for undosed LiF-7 and TLD-700 microrods at various heater currents are shown in Table 4 and are compared with the readings obtained when the

---

* Vespel Precision Parts, Plastic Department, E.I. DuPont de Nemours and Co (INC) Wilmington, Delaware 19898, U.S.A.

planchet is partly covered with Vespel. Vespel plates were always used for all the readings with microrods.

Table 3

HEATER CURRENTS

Type of dosimeter	Heater current
CaF_2:Mn	0.60 amp
$CaSO_4$:Mn	0.24 amp
LiF-6	0.28 amp At very high doses 0.32 amp
LiF-7	"
TLD-100	"
TLD-700	"

Table 4

INFLUENCE OF VESPEL ON THE THERMAL RADIATION FROM PLANCHET

Heater current	Photomultiplier voltage 1000 volts			
	Undosed dosimeter type LiF-7		Undosed dosimeter type TLD-700	
	Average reading in digits*		Average reading in digits**	
	Without Vespel	With Vespel	Without Vespel	With Vespel
0.24 amp	41.4	3.1	28.7	1.1
0.26 amp	136.7	6.0	111.7	2.0
0.28 amp	1112.8	11.8	773.6	4.0
0.30 amp	4125	24.3	2457	14.0
0.32 amp	15543	29.0	12239	30.0

* For LiF-7 1 digit = 65 mR, ** For TLD-700 1 digit = 18.7 mR

Exposure Conditions

Calibration with ^{60}Co

For irradiations with ^{60}Co the dosimeters were mounted on a perspex plate with a thickness of 4 mm. The thickness of perspex infront of the dosimeters was varied from 0 to 10 mm. Plots of integrated light output from the dosimeters Vs. thickness showed that the minimum thickness of perspex required for charged particle equilibrium was 3 mm. This thickness was always used for irradiation and calibration with ^{60}Co.

All the measurements of irradiated samples were done atleast 48 hours after irradiation to allow the decay of the low temperature peak. Since $CaSO_4$:Mn has a high rate of fading, its decay was studied (Fig.1) Since $CaSO_4$:Mn is sensitive to light, all the irradiations were done in lightproof containers.

Irradiations in BR1 reactor

For exposing the dosimeters to mixed neutron-gamma doses, they were mounted in spherical containers of perspex and irradiations were done in a natural uranium graphite moderated reactor (BR1). Two positions - self service and X-29 - were used. The neutron fluxes at these positions are 3.83×10^8 and $0.98 \times 10^{11} n\ cm^{-2}\ sec^{-1}$ respectively for 1 MW reactor power. The fluxes were measured by the activation of Al 1% Au foils. The cadmium ratios at these positions are more than 100. Reactor powers ranging from 1 kW to 1 MW and irradiations times varying from 30 seconds to 1200 seconds were used to get the desired integrated fluxes of 10^7 to $10^{14} n\ cm^{-2}$. Gamma doses were estimated by filling the annular space between the perspex spheres with ^{10}B or ^{6}Li powder to shield against thermal neutrons.

Glow Curves

Figs. 2a, 2b, 2c and 2d show glow curves obtained from various phosphors irradiated in ^{60}Co and neutron-gamma fields. Change in shape of the glow curves from lithium fluoride phosphors can be noted at high neutron doses. TLD-100 shows a second peak at 480 R of ^{60}Co radiation while only one at 320 R. The ratio of the second to the first one increases with neutron dose in TLD-100. G. Busuoli et al.[11] have measured neutron and gamma doses of a mixed field by using the ratio of the areas under the two peaks in TLD-100

Results and Discussion

Fig. 3 gives the equivalent ^{60}Co reading in roentgens for the various types of dosimeters as a function of neutron fluence.

The values of the gamma response for the different types of dosimeters are all within 10%. The curve for gamma response presents a discontinuity at a neutron fluence of $10^{12} n\ cm^{-2}$, as different irradiation positions with different gamma-neutron ratios were used above and below this value.

CaF_2:Mn and $CaSO_4$:Mn dosimeters when irradiated in mixed neutron-gamma fields showed the outputs equal to those which were obtained with

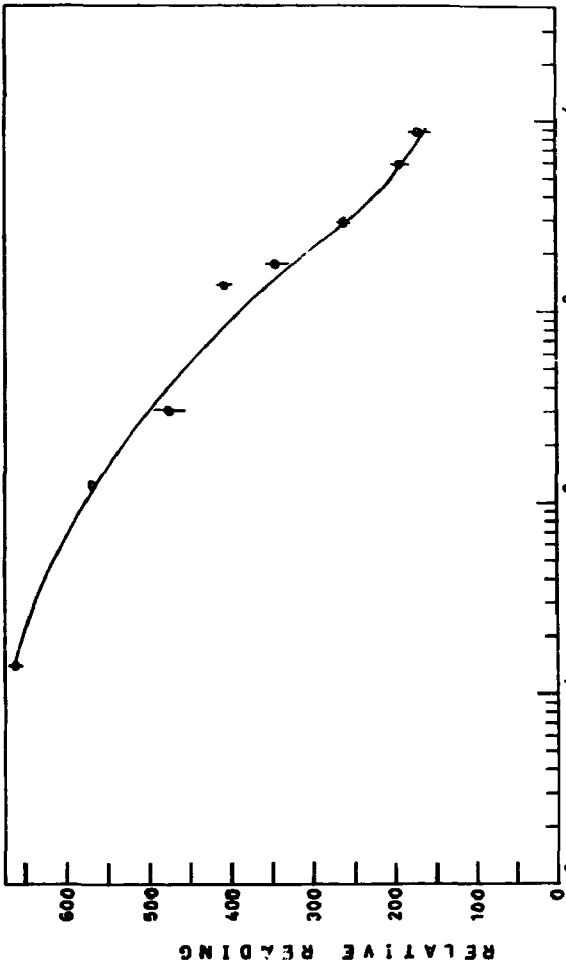

Fig.1 Decay of $CaSO_4$:Mn Microrods Stored at room Temperature

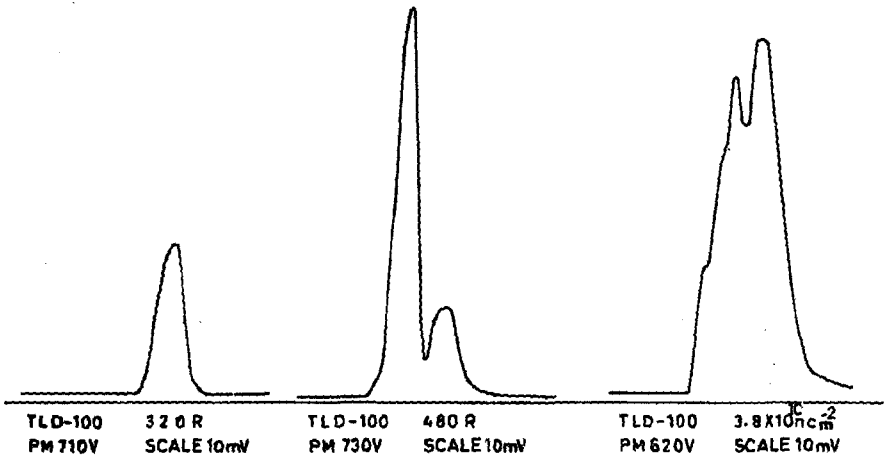

Fig. 2a Glow Curves

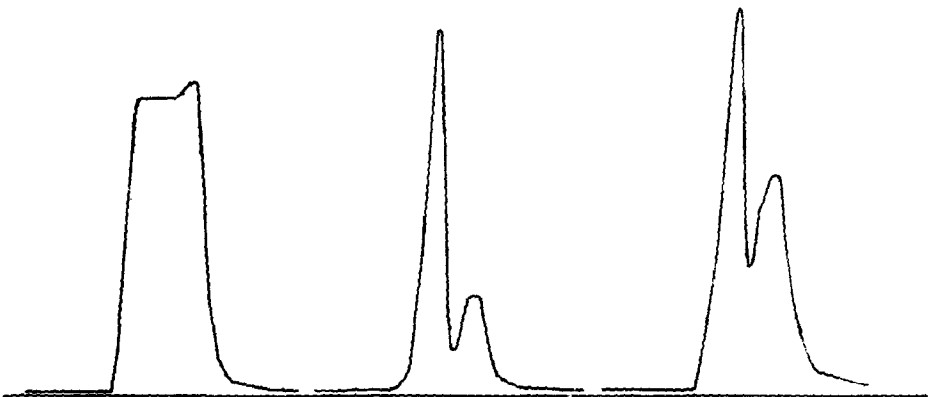

Fig. 2b Glow Curves

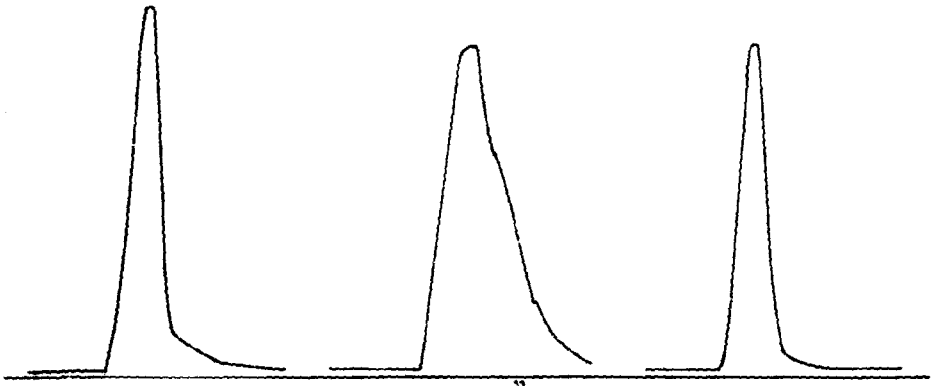

Fig. 2c Glow Curves

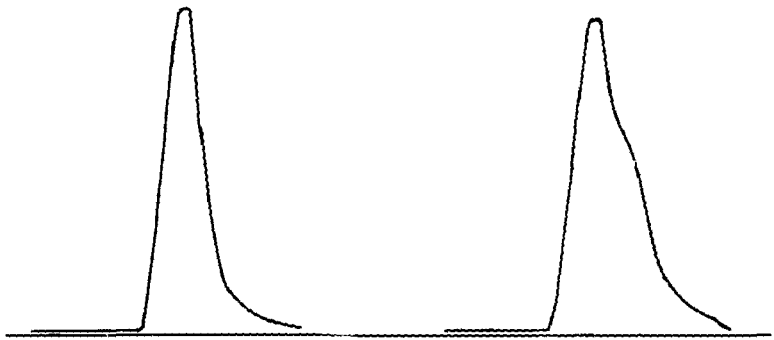

Fig. 2d Glow Curves

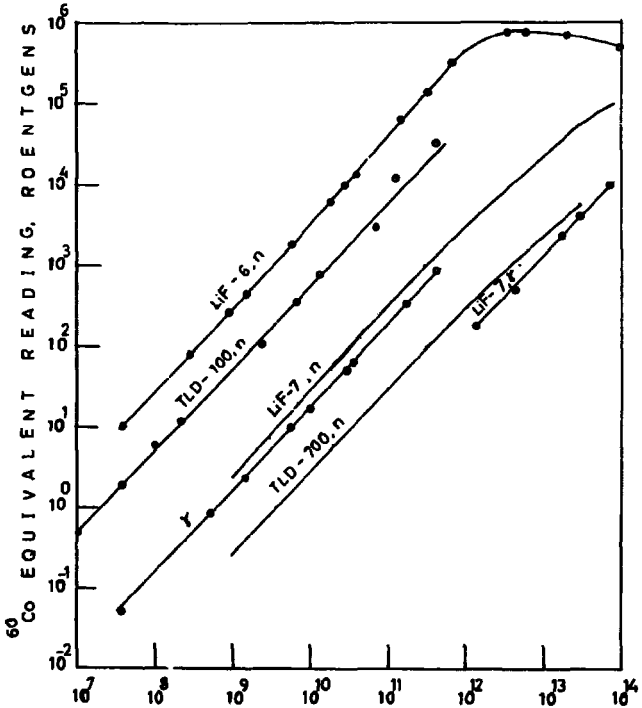

Fig.3 Thermal Neutron Response, n, of Some Phosphors and γ-ray Levels

other phosphors when shielded against thermal neutrons. Further, no change in output was observed whether CaF_2:Mn and $CaSO_4$:Mn dosimeters were irradiated bare or shielded with ^6Li powder. One may conclude from these observations that these dosimeters have negligible response to thermal neutrons.

The response of LiF-6, TLD-100, LiF-7 and TLD-700 to a fluence of thermal neutrons equal to 10^9n cm^{-2} is respectively about 265, 49, 2.3 and 0.25 times the response to 1 R of ^{60}Co gamma radiation. Although the manufacturers claim a low concentration (0.007%) of ^6Li in LiF-7 and TLD-700, the enhanced response of LiF-7 and TLD-700 suggests higher concentrations of ^6Li in these phosphors. We note the difference in response of LiF-7 and TLD-700. Similar observations have been reported by other experimenters also.[1-3]

From Fig. 3 we see that the response of LiF-6 is linear up to a thermal neutron fluence of 2 x 10^9n cm^{-2}. Above this value it becomes supralinear up to the value of 7 x 10^{11}n cm^{-2} where it starts to flatten off until its response decreases for thermal neutron fluences above 10^{13}n cm-2. At such high doses LiF-6 and TLD-100 change their colours to greenish yellow. In their experiments Marrone et al. have observed fall in response in TLD-100 at 3 x 10^4 R of ^{60}Co radiation.

Memory Effects in LiF-6

For this study LiF-6 microrods were exposed to various neutron fluences and subsequently annealed. Microrods which had no previous neutron irradiation were also annealed simultaneously. All the reannealed dosimeters were then given a further dose of gamma rays or thermal neutrons.

The results are summarized in Table 5. It is seen that the dosimeters which had been previously exposed to low neutron fluences of about 10^9n cm^{-2} showed no change in sensitivity whereas the dosimeters with 10^{10} or higher initial doses showed a significant increase in sensitivity.

Further experiments with undosed annealed dosimeters at low neutron and gamma doses (3.83 x 10^8n cm^{-2} and 80.7 R respectively) showed that the sensitivity of LiF-6 dosimeters does not change whether thermal neutron preceeds gamma irradiation or vice versa and that the neutron and gamma doses are additive.

The results in Table 5 further support the experimental response of LiF-6 shown in Fig. 3. Indeed the response is linear at low neutron doses (about 10^9n cm^{-2}) and it becomes supralinear at higher doses. The decrease in response at about 10^{12}n cm^{-2} indicates the damage to the crystal.

Table 5

MEMORY EFFECTS IN LiF-6

Initial neutron fluence, n cm^{-2}	Additional gamma or neutron dose	Sensitivity relative to no initial neutron dose
3.83×10^{7}	gamma 82.46 R	1.00
1.15×10^{8}	"	1.00
1.67×10^{9}	"	1.02
3.83×10^{10}	"	1.08
3.83×10^{11}	"	2.15
3.93×10^{12}	"	1.75
1.96×10^{13}	"	1.16
2.88×10^{8}	neutron 3.83×10^{8} n cm^{-2}	1.00
9.59×10^{8}	"	1.00
6.13×10^{9}	"	1.00
3.07×10^{10}	"	1.08
1.61×10^{11}	"	1.22

Conclusions

The use of Vespel plates appreciably reduces thermal radiation from the supporting planchet and higher temperatures required for neutron dosimetry can be reached.

LiF-6 shows high sensitivity to thermal neutrons. Since LiF-6 exhibits supralinear behavior and since it presents memory effects at high neutron fluences, its use is not prefered for measuring thermal neutrons above 10^{10}n cm^{-2}. At higher fluences the use of TLD-100 and at still higher fluences the use of LiF-7 must be envisaged. TLD-700 and even more LiF-7, has a response to thermal neutrons higher than we can expect from the concentrations specified by the manufacturers. The sensitivity of CaF_2:Mn and $CaSO_4$:Mn to thermal neutrons barely exceeds the experimental error. These dosimeters may be combined to measure mixed neutron-gamma fields in various ratios. Eventually shielding of the dosimeters with ^6Li or ^{10}B material must be provided.

Acknowledgements

The authors express their sincere thanks to M/s G. Legrain, J. Thije, A. Renoy, N. Maene and H. Bervoets of BR1 reactor for irradiation and measurement of neutron fluxes in the reactor. Thanks are also due to Mrs. R. Geukens for her secretarial help.

References

1. R.F. Bayer, Proc. 2nd Int. Conf. Luminescence Dosimetry, 1968, CONF-680920, pp. 543 - 551 (1968)
2. E.W. Mason, Phys. Med. Biol., 15, 79 - 90 (1970)
3. A.R Reddy, K. Ayyangar and G.L. Brownell, Radiat. Res., 40, 552 - 562 (1969)
4. J.R. Cameron, D. Zimmerman, G. Kenney, R. Buch, R. Bland and R. Grant, Health Phys., 10, 25 - 29 (1964)
5. C.W.R. Endres and T.F. Kocher , Proc. 2nd Int. Conf. Luminescence Dosimetry, 1968, CONF-680920. pp. 486 - 500 (1968)
6. K.J. Puite, Health Phys., 17, 661 - 667 (1969)
7. K.J. Puite, Health Phys.,20, 437 - 442 (1971)
8. R.E. Simpson, Proc. Int. Conf. Luminescence Dosimetry, 1965, CONF-650637, pp. 444 - 456 (1967)
9. J. Kastner, B.G. Oltman and P. Tedeschi, Health Phys., 12, 1125 - 1128, (1966)

10. L. Wingate, E. Tochilin and N. Goldstein, Proc. Int. Conf. Luminescence Dosimetry, 1965, CONF-650637, pp. 421 - 434 (1967)

11. G. Bussuoli, A. Cavallini, A. Fassò and O. Rimondi, Phys. Med. Biol. 15, 673 - 681 (1970)

12. M.J. Marrone and F.H. Attix, Health Phys., 10, 431 - 436 (1964)

Energy Response of Certain Thermoluminescent Dosimeters and Their Application to the Dose Measurements

by

H.K. Pendurkar*, R. Boulenger**, L. Ghoos**,
W. Nicasi*** and E. Mertens***

ABSTRACT

The energy dependence of some commercially available thermoluminescent LiF, $Li_2B_4O_7$:Mn and CaF_2:Mn dosimeters was investigated over X- and γ-ray energy range from 8 keV to 1.25 MeV with a particular interest in the low energy region below 50 keV. The radiation sources included monochromatic fluorescent radiations form different target materials, heavily filtered X-ray beams from 10 kV to 280 kV exciting potentials and γ-ray energies from ^{137}Cs, ^{226}Ra and ^{60}Co sources. The dosimeters used were in the form of microrods, extruded ribbons and discs. The experimental response is compared with calculated energy response of these dosimeters. The determination of mean energy below 50 keV was done by using scintillation spectrometry method.

The response of LiF-Teflon discs and LiF extruded ribbons to beta rays was also investigated using beta ray emitters (e.g. ^{185}W, ^{204}Tl, ^{89}Sr, ^{90}Sr-^{90}Y and ^{106}Rh) in the energy range 0.43 to 3.54 Emax MeV.

The application of LiF-Teflon disc dosimeters in the estimation of dose to finger tips while handling radioactive material in laboratory work was studied. The use of $Li_2B_4O_7$:Mn-Teflon microrods in the determination of exposure was also examined.

Introduction

Among the technical characteristics of thermoluminescent dosimeters the energy dependence deserves first consideration in any practical dosimetry system. The light output of a sample of thermoluminescent dosimeters is a function of energy absorbed. The absorbed energy depends upon its mass energy absorption coefficients at different photon energies. In this way the energy dependence is determined by the value of the effective atomic number ($\bar{Z}$) of the dosimeter in comparison with tissue or air.

---

* On A.G.C.D., Belgium Scholarship to Dosimetry Section, S.C.K./C.E.N. Mol, Belgium from Directorate of Radiation Protection, Bhabha Atomic Research Centre, Trombay, Bombay-85, India

** Contrôle-Radioprotection, Brussels, Belgium

*** Dosimetry Section, S.C.K./C.E.N. Mol, Belgium

This paper presents the experimental energy response of solid thermoluminescent dosimeters available commercially in the form of microrods, discs and extruded ribbons to different photon energies from 8 keV to 1250 keV. These dosimeters are manufactured with 100% phosphor content[1] or embedded in Teflon matrix[2].

The relative response of two types of LiF-Teflon discs and xtruded ribbons to beta radiations of energy from 0.43 MeV max to 3.54 MeV max is also presented.

The applications of some of these dosimeters are discussed.

Photon Energy Response

Material

The dosimeters used for this study along with the details given by the manufacturers are shown in table 1.

Table 1

SOLID TL DOSIMETERS

Material	Manufacturer	Physical form	Dimensions	Phosphor Content
1) LiF TLD-100	Harshaw	Microrod	1mm ø x 6mm	10 mg
2) LiF TLD-700	"	"	"	"
3) LiF TLD-100	"	Extruded Ribbon	3mm x 3mm x 0.87mm	25 mg
4) LiF TLD-700	"	"	"	"
5)*D-LiF-7-033	Isotopes/ Conrad	Disc	13mm ø 0.13mm thick	10 mg
6)*D-LiF-7-08	"	"	13mm ø 0.4mm thick	30 mg
7)*CaF_2:Mn	"	"	6mm ø 0.4mm thick	6 mg
8)*LiF-7	"	Microrod	1mm ø x 6mm	0.4 mg
9)*$Li_2B_4O_7$:Mn	"	"	"	"

* In Teflon matrix

Annealing

The dosimeters except the extruded ribbons and CaF_2:Mn-Teflon discs were taken from new batches. The annealing procedures were carried out in two separate ovens, one maintains the temperature at 300°-400°C as per requirements and the other at 80°-100°C. The temperature is regulated to $\pm$ 1°C by electronically controlled circuit.

The temperature gradient is very small inside the ovens. Special aluminium blocks having grooves to accomodate individual dosimeters were used to ensure uniform temperature to each dosimeter in the group. An intermittent check of temperature in the ovens is done by using a calibrated thermocouple millivoltmeter arrangement. The Harshaw dosimeters were annealed before use at 400°C for 1 hour, cooled to room temperature and then heated to 100°C for 2 hours. Conrad LiF-Teflon discs and LiF-Teflon microrods were annealed at 300°C for 24 hours followed by 80°C for 24 hours. Precise 80°C treatment is important as variation of 1°C would cause 5% change in sensitivity as quoted by Webb[3]. The importance of correct annealing procedures has been examined by Zimmerman[4] et al. The $Li_2B_4O_7$:Mn-Teflon microrods and CaF_2:Mn-Teflon discs were annealed at 300°C for 5 hours.

Sources of radiation

Monochromatic X-rays were used in the energy region from 8 to 25 keV (energies generally used for diffraction studies and contact therapy). Above 25 keV the exposure rates were too low to obtain useful exposures. The monochromatic X-rays were generated by interposing different target materials in the primary beam of 50 kV X-ray generator. A specially designed fluorescent chamber similar to the one described by Villforth[5] et al. was used. The monochromaticity of the emergent secondary beam was tested by using a scintillation spectrometer previously calibrated for known energies of Y-ray sources. Table 2 shows the X-ray exciting potentials, secondary targets and effective energies of secondary radiations obtained with monochromator. It was not considered necessary to use secondary filters.

Table 2

MONOCHROMATIC X-RAYS

X-ray tube pote-tial kVp	Secondary Target (metal sheet)	Effective X-ray Energy keV
30	Zn	8.7
30	Mo	17.6
50	Cd	23.2
50	Sn	25.3

Filtered X-rays ware used from 8 keV to 235 keV effective energies obtained from two X-ray machines. Between 8 to 42 keV mean energy was determined by the use of scintillation spectrometer and compared with the effective energies obtained by HVL method. From 62 to 235 keV the effective energy was determined by HVL method and showed good agreement with the published data by Drexler and Gosgrau[6] using spectrometric

method. Table 3 shows the details of these measurements for corresponding tube potentials and filtrations.

Table 3

FILTERED X-RAYS

X-ray machine type and Inherent filtration	Operating Potential kVp	Added Filtration mm	H.V.L. mm	Effective Energy keV	Mean energy by spectrometric method keV
Philips 50 kVp contact therapy 0.03mm Al equi. inherent filtration	10	0.05 Al	0.053 Al	7.9	8.1
	10	0.5 Al	0.095 Al	9.6	9.8
	15	1 Al	0.27 Al	14	14.3
	20	2 Al	0.54 Al	17.5	19
	30	2 Al	0.92 Al	21	24
	30	2Al + 0.1 Cu	1.3 Al	23	26.5
	50	4Al + 0.2 Cu	3.25 Al	32	36
	50	4Al + 0.6 Cu	5.1 Al	39	42
G.E. Maxitron 300 kVp 4.75mm Be inherent filtration	80	2 Cu + 1 Al	0.54 Cu	62	66*
	100	5 Cu	1.2 Cu	82	82*
	120	1 Sn + 5 Cu	1.74 Cu	100	103*
	200	1 Pb + 3 Sn + 2 Cu	4.1 Cu	160	170*
	280	3 Sn + 4 Pb	6.2 Cu	235	-

* Values reported by Drexler and Grossrau (ref.6)

Monochromatic and filtered X-ray exposures in the range 8 to 35 keV were measured by 2.5 R Victoreen Condenser R-meter chamber type 377 (wall thickness 7mg/cm^2). This chamber was compared against Victoreen 250 R skin equivalent condenser chamber type 651 calibrated at "Rijksinstituut voor de Volksgezondheid", Utrecht, The Netherlands. Exposures from 42 keV to 235 keV were measured by 2.5 R Victoreen Condenser R-meter chamber type 633 (wall thickness 220 mg/cm^2) which

was calibrated at "Physikalisch-Technische Bundesanstalt", Braunschweig, Germany.

In addition to the monochromatic X-rays and filtered X-rays, the calibrated Y-ray sources of ^{137}Cs (660 keV), ^{226}Ra (840 keV av.) and ^{60}Co (1250 keV) were used. Gamma ray output was calculated for particular exposure time, source strength, half life of the source at a measured distance on calibration table which is designed for scatter free conditions. The outputs so calculated are checked from time to time by calibrated Victoreen condenser R-meter chamber type 552 (wall thickness 450 mg/cm^2) as same irradiation facility is being routinely used for calibration of personnel monitoring films of Dosimetry section. The exposure rates at various positions from source are $\pm$ 5% accurate. The source strengths have accuracy of $\pm$ 2%.

Irradiations Procedure

In all cases, the different dosimeters in a group of 5 were enclosed in thin (3.5 mg/cm^2) black polyethylene. They were mounted on a paper support in a plane array normal to the X-ray beam and as far away as possible from large scattering objects to approach free air exposure conditions. The uniformity of the X-ray beam in both cases i.e. the primary beam and secondary beam obtained from monochromator was tested by an industrial type radiographic film. In case of Y-ray exposures from ^{137}Cs, ^{226}Ra and ^{60}Co, the dosimeters were exposed behind 3 mm of perspex to obtain electronic equillibrium. The dosimeters Sr. No 1 to 7 (table 1) were exposed to approximately 1 R exposure and both remaining types were exposed to nearly 10 R exposures in view of the smaller phosphor content in them.

Reading Method

All the dosimeters were read on ISOTOPES/CONRAD type 7100 integrating reader after allowing 48 hours time lapse following each irradiation. This reader incorporates S-11 photomultiplier tube having max sensitivity at 4200 Å. A heat absorbing glass filter is used on the face of the P.M. tube. This photomultiplier is suitable for emission spectrum of LiF. The emission spectra of $Li_2B_4O_7$:Mn and CaF_2:Mn are 6050 Å and 5000 Å respectively for which the sensitivity of this photomultiplier is very low. It was not found practicable to change this photomultiplier to the suitable S-20 type for the measurements of $Li_2B_4O_7$:Mn and CaF_2:Mn material as the reader is routinely used for LiF dosimeters of Dosimetry section. The high voltage applied to the photomultiplier tube was allowed to stabilise for at least 30 minutes before start of measurements. A nitrogen gas flush of 8 cu.ft/hr was used for cooling the front face of photomultiplier and to reduce non radiation induced signals[7]. Special heating elements were used for reading microrods, discs and ribbons. While reading microrods an insulating wafer of Vespal (heat insulating resin product of DuPont) was used to cover the heater plate except the area of two metal bars holding the rod. This arrangement is useful to avoid the signal due to thermal radiations from heater. A similar arrangement was used by Christensen[8] with 5 mil. kaptan film. The discs were read on a special heater plate having a perforated metal screen fastened to the edge of nichrome heating plate in order to ensure good thermal contact of disc against heater plate. The disc is pushed under the screen before readout. The extruded ribbons were read on a heater plate having a small dip at the centre.

For reading 6mm dia CaF_2:Mn-Teflon discs a Vespal plate with 9mm dia hole was used over the heater plate. Initial calibration of respective batches of dosimeters was done for known exposures of ^{60}Co radiation. The performance of reader was intermittently checked by the β-ray excited phosphor source giving constant light output. The optimum adjustment of heater current was decided by the method of second reading for few samples of dosimeters. The suitability of this method for integrating TLD has been examined by Webb[9]. Different heating currents were chosen depending upon the main glow peak temperature of dosimeter. All the readings were corrected for background reading obtained from unexposed samples from the same batch of dosimeters.

Results

The experimental energy response curves for all types of dosimeters studied are shown in Fig. 1 to 5. The response is normalised to the response of ^{60}Co radiation.

Observed response for Harshaw LiF TLD-100 and TLD-700 dosimeters is shown in Fig. 1. The calculated response is plotted by taking the ratios of mass energy absorption coefficients of LiF to air at different photon energies. The data of mass energy absorption coefficients for LiF, $Li_2B_4O_7$ and CaF_2 is obtained from tabulations done by Joffre[10]. The experimental response of TLD-100 and TLD-700 dosimeters is found to be similar. Due to difference in geometry of microrods and ribbons effect of self absorption was found below 10 keV. Peak sensitivity of 48% to that of ^{60}Co occurs between 25 and 28 keV. Isotopic effects responsible for small difference in sensitivity between TLD-100 and TLD-700 as reported by Attix[11] were not observed probably due to uncertainties in determination of standard exposure and accuracy of reader instrument. The experimental response of LiF-Teflon microrods is shown in Fig. 2. At 8 keV the sensitivity is 0.58 times of that of ^{60}Co and reaches a max value of 1.52 at 24 keV. Beyond 200 keV energy independence is observed. The response of LiF-Teflon 0.4mm and 0.13 mm discs is shown in Fig. 3. The difference in sensitivity below 10 keV is due to self absorption effect. In case of both the types of dosimeters the max sensitivity occurs at 24 keV. The results are 50% higher than for ^{60}Co. Endres [12] et al. have reported 55% increase in sensitivity at 40 keV for LiF-Teflon discs of 0.4 mm thickness. Marshall and Docherty[13] have also reported 55% increase in sensitivity at 30 keV for 8.9 mg/cm^2 LiF-Teflon discs. The energy independent behaviour was observed beyond 200 keV for all the types of LiF dosimeters we studied. From 80 to 200 keV the departure from unity response is max by only 5%.

Fig. 4 shows the response for CaF_2:Mn-Teflon discs. The observed peak sensitivity lies at 25 keV and is 11 times that of ^{60}Co. However, the calculated response for CaF_2 shows about 14 times max sensitivity. The difference between observed and calculated values may be due to the presence of Teflon in disc as the mass energy absorption coefficients of CaF_2 and Teflon differ considerably in the photoelectric region.

The experimental and calculated energy response curves of $Li_2B_4O_7$:Mn Teflon microrods are shown in Fig. 5. The presence of Teflon matrix appears to influence the sensitivity as we already noticed in the previous case of CaF_2:Mn. The max sensitivity is found around 32 keV and it is 15% higher than that measured for ^{60}Co.

It can be seen from above results that in the case of LiF material

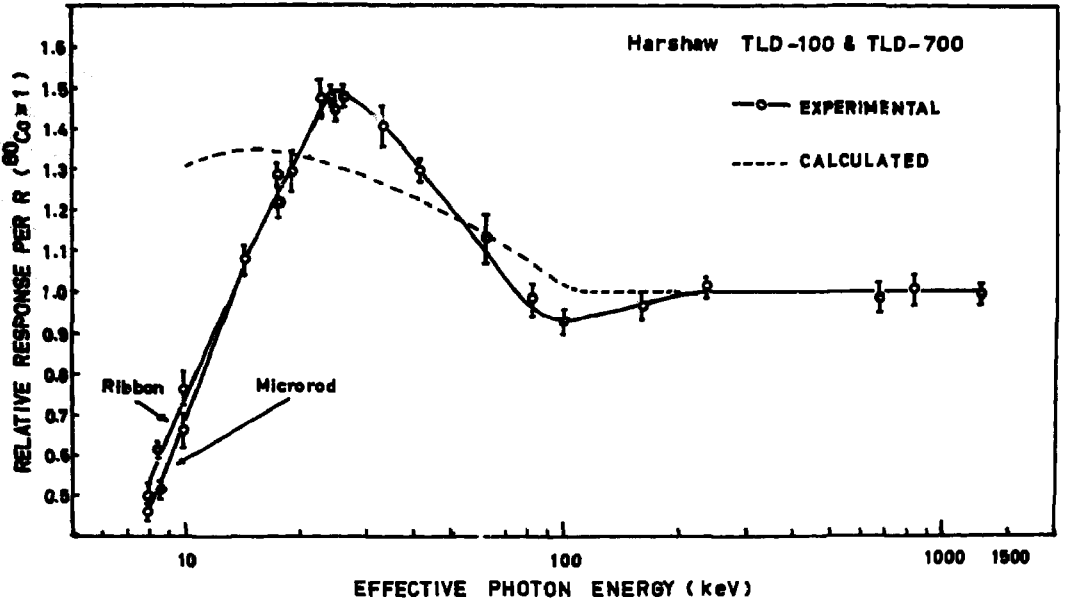

Fig. 1. Photon energy response of Harshaw TLD-100 and TLD-700 dosimeters.

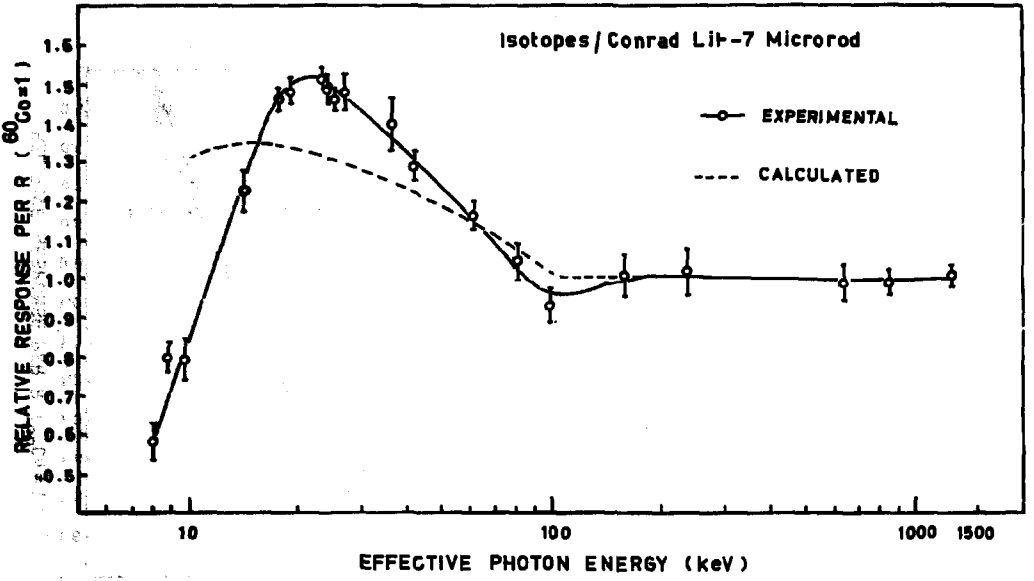

Fig. 2. Photon energy response of Isotopes/Conradm LiF-7 microrod.

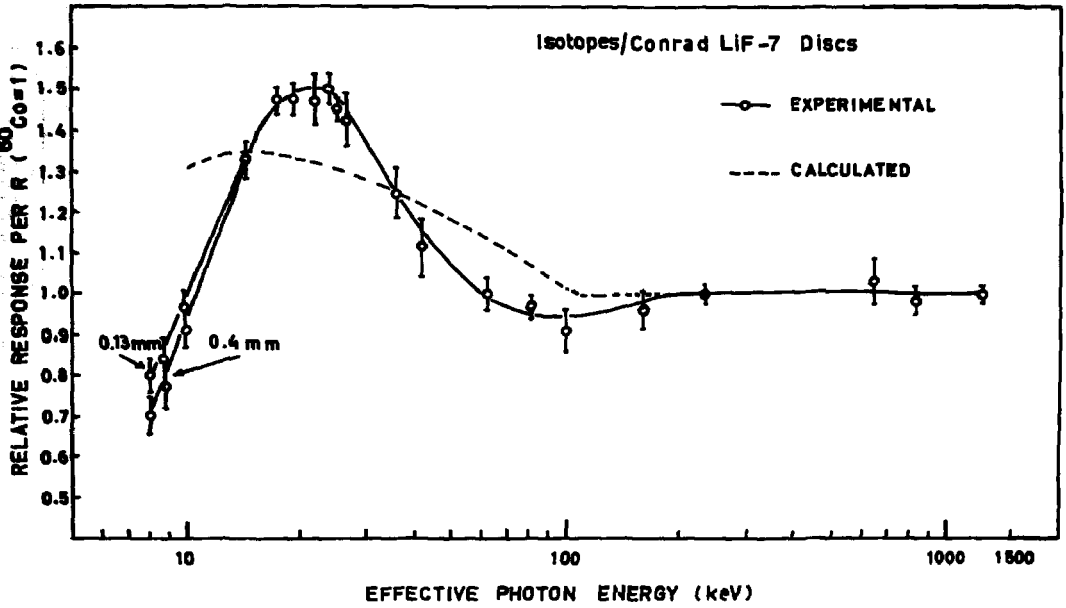

Fig. 3. Photon energy response of Isotopes/Conrad LiF-7 discs.

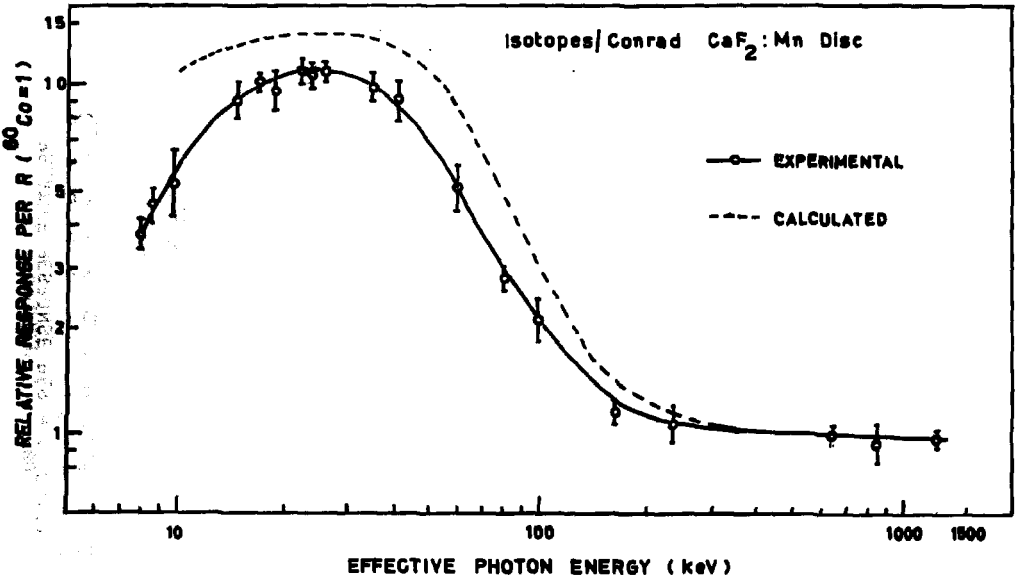

Fig. 4. Photon energy response of Isotopes/Conrad CaF_2:Mn discs.

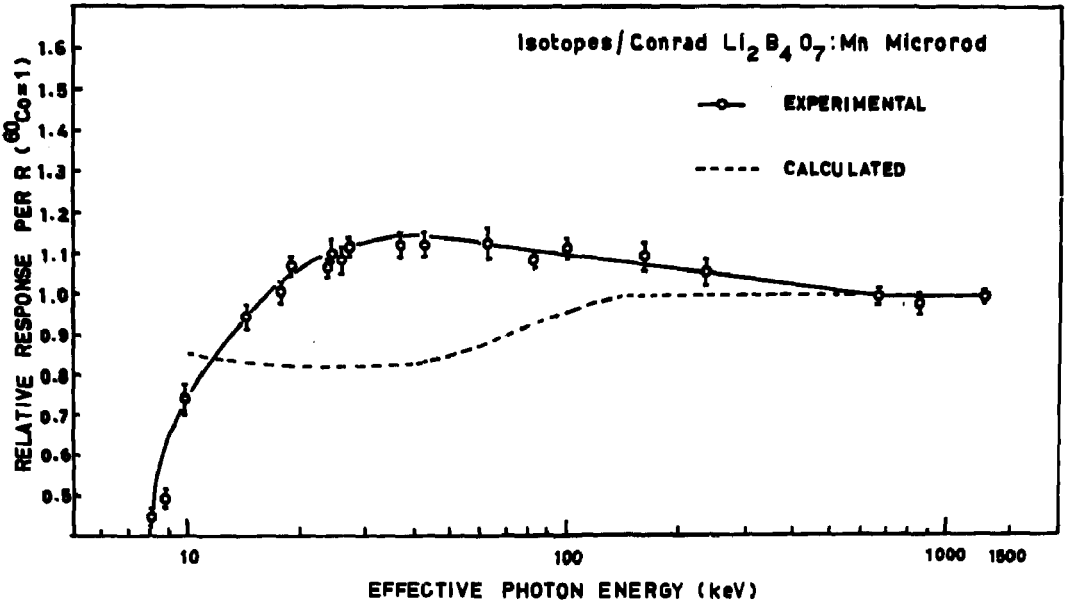

Fig. 5. Photon energy response of Isotopes/Conrad LiB_4O_7:Mn microrod.

the experimental response is more than the calculated one. This may be due to various impurities of high Z materials compared to LiF which account for large photoelectric cross section. A similar inference has been drawn by Jayachandran[14] after chemical analysis of LiF TLD-100. Tochilin[15] et al. however, have accounted this as an LET effect. The presence of Teflon also accounts for the departure of experimental response from the calculated values. This effect is more pronounced in case of $Li_2B_4O_7$:Mn-Teflon and CaF_2:Mn-Teflon dosimeters. Hence, the results obtained by the experimental observations can only serve as a proper guide for dosimetric applications.

Beta ray response

Material

In view of the different thickness, the LiF-Teflon discs (0.13 mm and 0.4 mm thick) and TLD-100 extruded ribbons (3mm x 3mm x 0.87mm) were used for this study. The suitable annealing procedures were performed as stated previously.

Sources of radiation

The beta ray sources used were thin dried liquid sources in a circular cup of 8 mm dia and 1 mm deep on a 50 mm dia 2 mm thick perspex holder. Only the ^{106}Rh source was covered with 10 mg/cm^2 of plastic. The dose rate was calculated for ^{185}W source using formula given by Loevinger[16]. For ^{204}Tl, ^{89}Sr, ^{90}Sr-^{90}Y and ^{106}Rh the dose rates were taken from calculations tabulated by Cross[17]. The description of sources and calculated dose rates are shown in table 4.

The dosimeters were irradiated in 3.5 mg/cm^2 polyethylene bags as well as bare condition. The dosimeters were read with necessary precautions as described earlier.

Table 4

BETA SOURCES

Source	E max MeV	E average MeV	Distance cm	Dose rate rads/hr
^{185}W	0.43	0.1367	10	5.92
^{204}Tl	0.766	0.252	10	4.45
^{89}Sr	1.463	0.55	10	3.6
^{90}Sr-^{90}Y	0.546 2.27	0.2 0.9	10	8.1
^{106}Rh	3.54	1.4867	10	3.05

Results

The results of beta ray response are shown in Fig.6 for three different types of dosimeters studied. Their relative responses normalizing at 3.54 MeV are given. When used as a detector for beta radiation, it is important to remember that there exists a rapid dose gradient through the thickness of dosimetric material. This demands a very thin detector to register efficiently even low energy beta radiations as can be seen from the curves in Fig.6. The effect of 3.5 mg/cm^2 polyethylene enclosure is also noticed. Hence to measure surface doses due to beta radiation the 0.13 mm disc dosimeter is the suitable one among the three types studied. The basal layer of epidermis is at a depth of 7 to 15 mg/cm^2 and hence a dosimeter of 27 mg/cm^2 (0.13 mm thick) with an enclosure of 3.5 mg/cm^2 will indicate the average dose between 3.5 to 30.5 mg/cm^2 depth i.e. at about 15 mg/cm^2 depth. So using 0.13 mm thick dosimeter gives a fairly good estimate of dose to the basal layer.

Some applications of solid TL dosimeters

i. Determination of exposure with $Li_2B_4O_7$:Mn-Teflon microrods

The experimental response characteristic (Fig.5) obtained with $Li_2B_4O_7$: Mn-Teflon microrod suggests the use of this material for exposure measurements in the energy renge from 15 keV to 1.25 MeV. The exposure measurement of any unknown energy between this region can be determined with a max error of + 15%. Above 100 keV the error introduced is only 10% which is acceptable in many dosimetric applications. This dosimeter can be used for measuring the output of X-ray machines and Y-ray sources, table top exposures in fluoroscopy etc. The upper limit of exposures may be restricted to 1000 R where the supralinearity effects are observed.[18] The smaller phosphor content of 0.4 mg in the dosimeter results in low sensitivity, however, integral measurements over a long time can be done. With Isotopes/Conrad type 7100 reader the background was of the order of 1.5 R equivalent. So the exposures of around 5 R can be measured easily. We feel that with the use of proper photomultiplier (S-20 response) this value may be reduced to 2 R.

ii. Field application of disc dosimeter

A case of radiation injury to thumb and index finger of a technician was reported from a laboratory while handling ^{76}As beta source. In order to measure max dose to the finger tips, an exact restoring condition of the incident was established by using reactor produced sample of ^{76}As source in quartz vial. The quartz vial was having 0.75 mm wall thickness and 4 mm outer diameter containing 100 mg of As_2O_3. The vial was irradiated at a neutron flux of 10^{14} n/cm^2/sec for 6 hours. The dosimeters used were LiF-Teflon discs of 13 mm dia having 0.13 and 0.4 mm thickness. In order to investigate the homogeneity of the source in the vial small dosimeter strips (1mm x 10mm) cut out of 0.13 mm disc were also used. A perspex tube phantom was constructed having 5.6 mm internal diameter and 10 mm wall thickness to simulate human finger. Dosimeters were kept between source vial and perspex phantom completely surrounding the source vial. The irradiations were carried out after 186 hours time lapse leaving the source from reactor, as it was in the

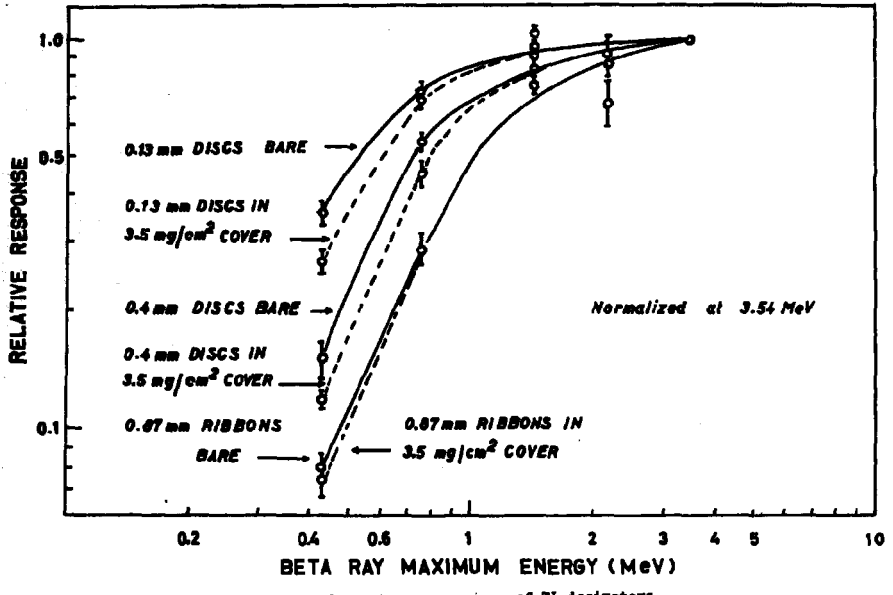

Fig. 6. Beta ray response of TL dosimeters.

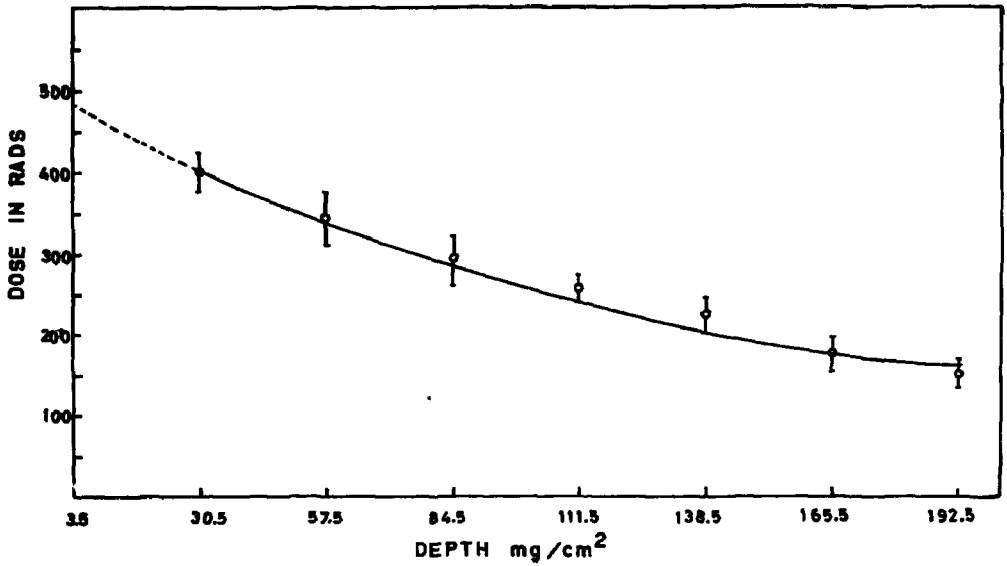

Fig. 7. Dose measurements with LiF-Teflon disc dosimeters.

original incident. Stacks of 4 and 7 discs were used to give information of depth dose distribution. The results obtained are shown in Fig. 7. The strip dosimeters, however very small in size gave very reproducible results at the doses which were around 400 rads. They were read on heater plates normally used for disc dosimeters.

Conclusions

It is necessary to consider experimental energy response of different TL dosimeters before using them in dosimetric applications. The increased response in the energy region below 100 keV is partly due to the presence of matrix material and various impurities. A teflon embedded lithium borate microrod constitutes a proper means of exposure measurements of unknown photon energy. However, as the inherent sensitivity of LiF is higher than that of $Li_2B_4O_7$:Mn, for personnel monitoring uses LiF supersedes. For beta ray dosimetry the thickness of dosimeter is important and it should not be more than 30 mg/cm^2, if a proper estimate of skin dose is to be made below 1 MeV max energy. The thin disc dosimeter is very suitable for assessment of finger dose while handling radioactive material.

Acknowledgements

The authors gratefully acknowledge the assistance of Mr. E. Mattelin for providing X-ray irradiation facility and Mr. R. Jacquemin for preparation of beta sources. They also wish to thank Mr. A. Bakker for assistance in workshop requirements and Mrs. R. Geukens for typing the manuscript. The co-operation of other members of Dosimetry section is also acknowledged.

REFERENCES

1. F. Morgan Cox, Proc. 2nd Int. Conf. Luminescence Dosimetry, CONF-680920, 1968, pp. 60 - 77

2. B.E. Bjarngard and D. Jones, Solid State Dosimetry, Proc. Nato Summer School, Brussels 1967, Edited by S. Amelinckx, pp. 585 - 634

3. G.A.M. Webb, RD/B/N-693 (1966)

4. D.W. Zimmerman, C.R. Rhyner and J.R. Cameron, Health Physics 12, 525 - 531 (1966)

5. J.C. Villforth, R.D. Birkhoff and H.H. Hubbel (Jr), ORNL-2529 (1958)

6. G. Drexler and M. Grossrau, 1st European Congress on Radioprotection, Menton Oct. 1966, Session D3, No. 26

7. K.E. Perry, Nuclear Engineering, 11, 875 - 877 (1966)

8. P. Christensen, Proc. 2nd Int. Conf. Luminescence Dosimetry CONF-680920, 1968, pp. 90 - 117

9. G.A.M. Webb, J. Sc. Instr., 44, 481 - 483 (1967)

10. H. Joffre and L. Pages, Report CEA-R-3655 (1968)

11. F.H. Attix, Phys. Med. Biol., 14, 147 - 148 (1969)

12. G.W.R. Endres, R.L. Kathren and L.F. Kocher, Health Physics 18, 665 - 672 (1970)

13. M. Marshall and J. Docherty, AERE R-6500 (1970)

14. C.A. Jayachandran, Phys. Med. Biol. 15, 325 - 334 (1970)

15. E. Tochilin, N. Goldstein and J.T. Lyman, Proc. 2nd Int. Conf. Luminescence Dosimetry, CONF-680920, 1968, pp. 424 - 437

16. R. Loevinger, E.M. Japha and G.L. Brownell, Radiation Dosimetry, Chapter 16, Academic Press, New York, 1956

17. W.G. Cross, AECL-2793 (1967)

18. Isotopes/Conrad, Thermoluminescence Dosimetry System, Dosimeter manual, B5 (1968)

Attix

I am surprised that the experimental energy-dependence curves fall below the theory in the 100 keV region. Could this possibly be due to a lack of charged-particle equilibrium? What material did you enclose the dosimeters in during the X-irradiation, and how thick was it?

Ghoos

X-ray irradiations were performed by exposing the dosimeters in free air. They were enclosed in a polyethylene bag with a thickness of 3.5 mg/cm^2, and they were mounted on a very thin paper support. Trying to interprete the fall in response in this energy region as a lack of charged-particle equilibrium, during irradiation we put in front of the dosimeters different thicknesses of perspex sheets from 0.5 mm up to 2 mm. These sheets gave only an absorption effect, so we do not feel that lack of charged-particle equilibrium is the reason.

Becker

Did you consider the activators in the calculated photon energy dependence of the detectors?

Ghoos

No.

Becker

Therefore, most of the difference between your theoretical and the measured values can obviously be explained by the effect of the high-Z activators.

Tm-and-Dy-activated $CaSO_4$ Phosphors for UV Dosimetry

*K.S.V. Nambi and T. Higashimura

Research Reactor Institute,

Kyoto University,

Kumatori-cho, Sennan-gun, Osaka,

JAPAN.

Abstract

A simple and sensitive method of measuring integrated UV irradiances using the thermoluminescent properties of Tm-and-Dy activated $CaSO_4$ phosphors, is presented in this paper. The two phosphors behave almost identically and results are presented for a typical case of $CaSO_4$: Tm. A high temperature peak (at~450 C) is created by heavy gamma-irradiation of the phosphor and then annealed in such a way that this remains as residual thermoluminescence (RTL) in the sample. Such a phosphor when exposed to UV light (especially 253.6 nm photons) and subsequently heated, produces the usual dosimetric peak at~200°C with a slight depletion in the RTL. The creation of this dosimetric peak has been found to be linearly proportional (on a log-log plot) to the UV irradiances in the range of about 1 $\mu W \cdot sec \cdot cm^{-2}$ to 1000 $\mu W \cdot sec \cdot cm^{-2}$ at 253.6 nm and is independent of dose rate. Other important dosimetric characteristics such as photon energy dependence, reusability of the phosphors etc. are also discussed.

---

* Permanent address : Health Physics Division, Bhabha Atomic Research Centre, Bombay - 85 AS, India.

Introduction

The first attempt to detect ultraviolet using thermoluminescent properties of the detector was made by Lyman[1] who measured the transparency of air between 1100-1300 A using a $CaSO_4$: Mn TL detector. Subsequently Tousey et al[2] used the same TL phosphor for measurements of solar extreme ultraviolet rays from rockets. In these studies measurements were made in the wavelength bands 1050-1230 and 1230-1340 A beyond which the phosphor was not sensitive.

Ultraviolet irradiation especially with 253.6 nm photons is being increasingly employed in medicine and industry for bactericidal actions such as disinfecting clothings, packages, enclosures etc. Measurement of UV irradiance is a periodic necessity in such applications and a method has already been reported[3] for UV dosimetry using the TL properties of fluorites. This paper describes yet another simple and sensitive method of measuring integrated UV irradiances using the thermoluminescent properties of Tm-and-Dy-activated $CaSO_4$ phosphors, which are perhaps the most sensitive (yet possessing very little fading) TL phosphors commercially available today.

Experimental set up

To record detailed glow curves, a linear heating rate of 30 C/min was employed using a temperature programmer and for each reading 5 mg of the phosphor powder used.

For routine dosimetry however, about 15 mg of powder was spread over a kanthal metal strip through which a steady current of 30 A was passed and the glow curves were recorded in about 45 sec.

In both the cases, the termination of heating was around 550° C and the TL light emitted was recorded by EMI 9514 s photomultiplier coupled to a dc amplifier and recorder.

TL Properties of the Phosphors

Work has been done[5] with the phosphors commercially available from Matsushita Central Research Laboratories, Osaka, Japan. These have been

claimed[4] to possess highest sensitivity with essentially a single glow peak around 200°C for application in radiation dosimetry. However these phosphors, for gamma doses $\geq 10^6$ rads, give glow curves (when heated at a linear rate of 25°C/min) exhibiting peaks at about 70°C, 105°C, 190°C, 350°C and 450°C (see fig. 1a). If these phosphors after such heavy irradiations were heated only upto about 350°C (as is usually done in routine radiation dosimetry) so that the peak at $\sim$ 450°C remains residual (fig. 1a) and then exposed to UV light, the residual peak is somewhat bleached and peaks are created at about 70°C, 105°C, 190°C and 250°C (fig. 1c). The peak at 190°C, which is usually employed in radiation dosimetry work, is still the strongest even after such an UV exposure and this is made use of in UV dosimetry.

UV Sensitivity of the Phosphors

Batches of the TL phosphor were exposed to a range of Co-60 gamma doses from about 10^3R to about 10^8R and were all annealed at 400°C for half an hour, thus retaining almost the entire peak at 450°C while erasing all the earlier TL peaks in the sample. All these predosed and partly erased samples were given the same UV exposure at a fixed distance from a 15 Watts Philips Germicidal Lamp whose emission consisted mainly of 253.6 nm photons. Then each sample was flashed to read out the heights of the newly created TL dosimetric peak at $\sim$ 200°C and the depleted residual peak at $\sim$ 450°C. Fig. 2 shows a plot of UV produced TLD peak vs the predose while Fig. 3 shows a plot of the UV produced TLD peak vs the Residual TL peak at 450°C before UV irradiation. It is quite clear from these results that

i) the sensitivity is maximum for a phosphor predosed at $\sim 5 \times 10^7$R of Co-60 gamma rays

and ii) the UV sensitivity is directly proportional to the residual TL peak at 450°C.

Calibration

A bulk of the phosphor is given a gamma dose of 5×10^7R and then annealed at 400°C for $\frac{1}{2}$ hour. Small quantities are drawn from this master

sample and given various known UV exposures at the same distance from a Philips Germicidal Lamp and the TL is read out. The peak height at 200°C is plotted against the exposure period which can also be given in terms of integrated UV irradiance* in $\mu W \cdot sec \cdot cm^{-2}$ (*This was estimated by comparing the lamp's output at the same distance with that from a standard Tungsten filament lamp at $\lambda \approx 253.6$ nm). Fig. 4 gives such a typical plot wherein the height of the residual TL at 450 C is also plotted to show its simultaneous bleaching alongside the creation of the dosimetric peak. These results show that

i) calibration is linear in the range of about 1 $\mu W \cdot sec \cdot cm^{-2}$ to 1000 $\mu W \cdot sec \cdot cm^{-2}$ during which the bleaching of RTL is rather little ;

and ii) Saturation sets in beyond 1000 $\mu W \cdot sec \cdot cm^{-2}$ and at such UV irradiances, the RTL is decreased considerably.

Dose Rate Independence

This is checked by exposing the predosed and partly erased phosphors at various distances from the UV lamp for a fixed period and reading out the TL each time. The TL peak obtained at $\sim$ 200°C was normalised each time for unit integrated UV irradiance incident on the phosphor and this is plotted against the dose rate (UV intensity in $\mu W \cdot cm^{-2}$). Fig. 5 presents such a plot which shows clearly that such a dosimetry phosphor is having complete dose rate independence at least in the two decade ranges examined in our study.

Precautions

1) These phosphors do exhibit photon energy dependence (fig. 6) and as such care should be taken to do the calibration exactly for the same spectral quality as would be involved in any application.

2) As the UV sensitivity is dependent on RTL and the RTL is depleted after each UV exposure, it is necessary to have a fresh calibration for every reuse. However if the UV exposures involved are very low wherein the RTL depletion could be almost negligible, the phosphors can be reused without

any recalibration provided care is taken to terminate the heating around 300°C during any TL read out.

References

1. T. Lyman, Phys. Rev. 48, 149 (1935)

2. R. Tousey et al, Phys. Rev. 83, 792 (1951)

3. C.M. Sunta, S.P. Kathuria and K.S.V. Nambi, Paper presented in National Symposium on Radiation Physics held at Bhabha Atomic Research Centre, Bombay, 1970.

4. T. Yamashita, N. Nada, H. Onishi and S. Kitamura, Proc. 2nd Int. Conf. Luminescence Dosimetry, Clearinghouse for Federal Scientific and Technical Information, Spingfield, Virginia (1968).

5. K.S.V. Nambi and T. Higashimura, J. Nucl. Sci. Technol. 7, 51 (1970).

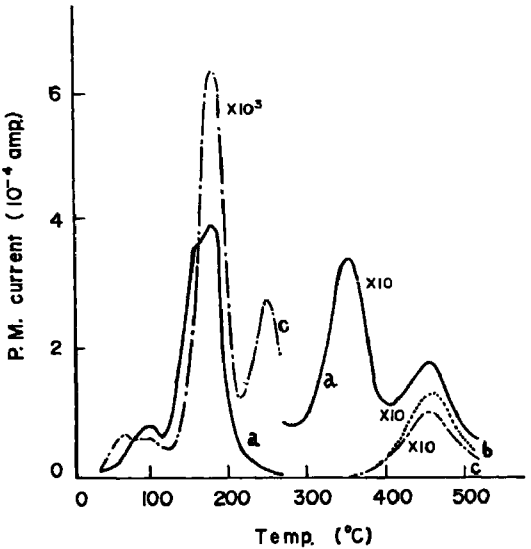

Fig. 1. TL glow curves of $CaSO_4$: Tm

a) after 5.6 x 10^7R of ^{60}Co gamma irradiation. (Temperature during irradiation was not controlled and hence the TL peak I has faded)

b) after annealing at 400 C for 1/2 hour.

c) after UV irradiation with 253.6 nm photons.

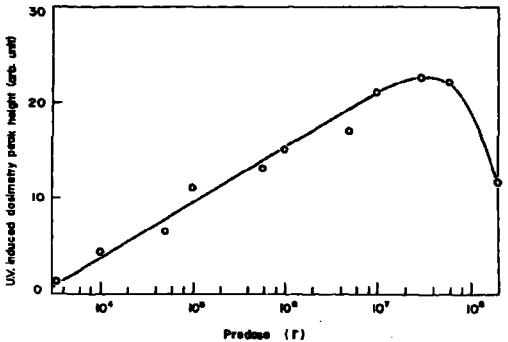

Fig. 2. UV sensitivity as a function of predose for $CaSO_4$: Tm phosphor. A fixed UV exposure is given for each sample. (after giving the predose and annealing at 400°C for 1/2 hour)

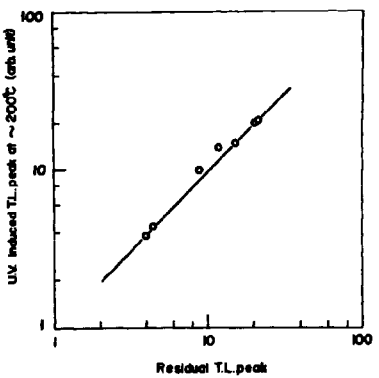

Fig. 3. UV sensitivity as a function of residual peak at 450°C for $CaSO_4$: Tm phosphor. (A fixed UV exposure is given to each sample)

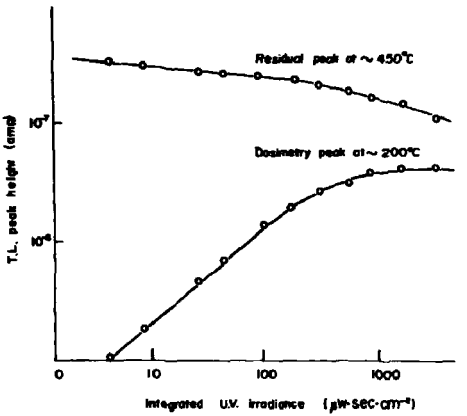

Fig. 4. UV response curve for $CaSO_4$: Tm TLD

UV source : 15 W PHILIPS germicidal lamp at a distance of 50 cms.

Irradiation wavelength 253.6 nm.

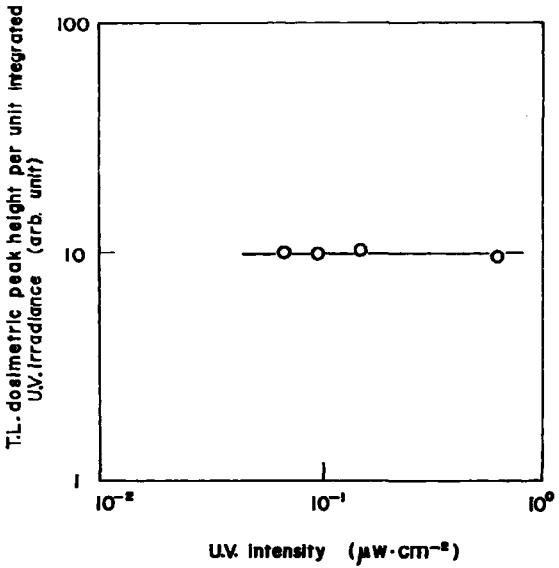

Fig. 5. Dose rate independence of $CaSO_4$: Tm TLD for UV exposures at λ = 253.6 nm.

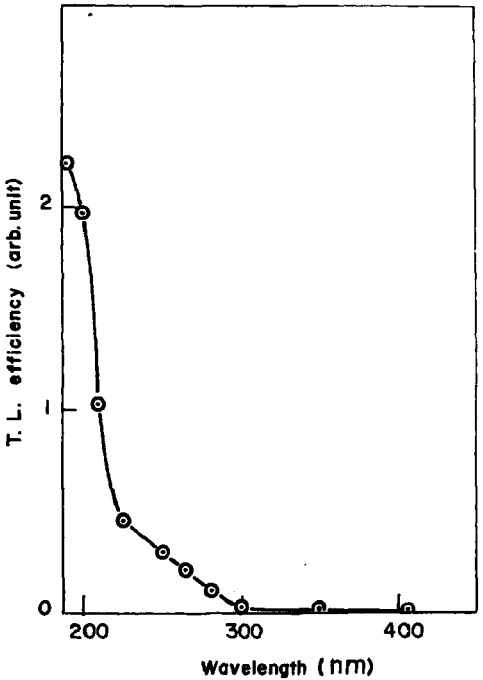

Fig. 6. Photon energy dependence curve for optically excited TL in $CaSO_4$: Tm (The phosphor was heavily irradiated and then annealed at 400°C for 1/2 hour before subjecting to optical excitation)

Transferred Thermoluminescence in CaF_2:nat as a Dosimeter of Biomedically Interesting Ultraviolet Radiation

Edwin C. McCullough, Gary D. Fullerton
and John R. Cameron
Department of Radiology
University of Wisconsin
Madison, Wisconsin 53706, U. S. A.

Ultraviolet (uv) radiation is an important factor in a wide variety of biological phenomena and medical situations. For example, there is sufficient clinical and epidemiological evidence that in the unprotected skin chronic exposure to solar uv produces not only premature aging (senile elastosis) but can be responsible for the induction of skin cancer. Also, there has been an increased interest in solar uv as the aggravant in a wide variety of drug-induced and spontaneous light-sensitive diseases of the skin. For the study and/or management of these situations it is of interest to have available quantitative information about terrestrial uv.

Amongst dermatologists and skin photobiologists, there is considerable interest in having a dosimeter of uv radiation in the sunburn range (i.e. $\lambda < 320$ nm). In particular, a uv dosimeter whose spectral sensitivity approximates the erythemal (sunburn) response of human skin would provide a measure of the erythemally effective energy present at the time of measurement. A primary objective of the research reported here was to develop a uv dosimeter whose spectral response approximates the erythema action spectrum of human skin.

The use of TL phosphors for uv dosimetry is desirable for a number of reasons. The phosphors are small in size making them suitable for *in vivo* studies (e.g. skin transmission) and personnel dosimetry. In addition, they require no electronics at the site of measurement and

operate unattended. The existence of commercial TL equipment, already available at most medical centers, is conducive to a situation of uniformity between laboratories.

Investigations on the use of transferred TL in CaF_2:nat as a dosimeter of erythemally effective uv were carried out under both daylight and artificial illumination. The CaF_2:nat phosphor was obtained by removing the glass envelope from a M.B.L.E. PNP 233 dosimeter. The glass envelopes of the dosimeters were removed to permit the uv to reach the phosphor. In addition to using the M.B.L.E. dosimeters we have carried out identical tests on crystals of CaF_2:nat cleaved from a large piece of fluorite. For any of the measured characteristics, we have observed no difference between the cleaved crystals and the M.B.L.E. dosimeters.

For a phosphor annealed to 700°C and subsequently exposed to uv, no TL signal is recorded upon heating. However, if the phosphor is given an exposure to γ-radiation (we used 4 kR ^{137}Cs γ-radiation), then heated to 400°C for 10 minutes, a subsequent exposure to uv will yield TL glow peaks with temperatures below 400°C. The amount of TL transferred to these peaks are related to the total energy of the uv and its wavelength, as well as the population of the high temperature (> 400°C) traps (i.e. the original γ-radiation exposure minus electrons previously transferred out by earlier uv exposures).

In a dosimeter which had been exposed to 4 kR ^{137}Cs γ-radiation and annealed to 400°C, an exposure to 1 minimal erythema dose of 300 nm radiation (12 mJ-cm^{-2}) transfers TL equivalent to the TL which would be observed after a virgin dosimeter is exposed to 42 R of ^{137}Cs γ-radiation.

The CaF_2:nat phosphor was found to be most sensitive at 300 nm with a reduced sensitivity at longer wavelengths. Because of the non-negligible sensitivity above 320 nm we have adopted a scheme in which we subtract transferred TL readings made with from those made without a 2 mm thick Schott WG-320 sharp cut off filter covering the phosphor. The spectral sensitivity corresponding to subtracted readings is a reasonable approximation of the erythemal response of human skin. The CaF_2:nat phosphor was found to be sensitive to ambient light, indicating the dosimeters should be stored in light tight containers.

Both the traps corresponding to higher temperature (> 400°C) glow peaks and the uv induced transfer TL have been found to be stable against degradation at room temperature. Exposure times greater than 5 minutes in the midday, mid-September sun in Madison, Wisconsin produced a non-linear response in the transferred TL as a result of bleaching of transfer TL peaks. This effect was shown to be eliminated by the reduction of dosimeter uv exposure through the use of neutral density filters.

For the measurement of large uv exposures, the applicability of a higher temperature trap sampling technique was investigated. In this technique, the high temperature trap populations are assessed by a short uv exposure just prior to and immediately after a large uv exposure. It was found that the upper trap did not empty according to the expected exponential decrease. However, a usable relationship between total uv exposure and short test uv exposure TL has been derived.

Using CaF_2:nat phosphors, measurements of terrestrial solar uv have been carried out. These have been compared to computed estimates based on atmospheric constituent data. The comparison of measured TL currents and minimal erythema times will be discussed with regard to future applications of CaF_2:nat as a thermoluminescent dosimeter of erythemally effective terrestrial solar uv.

Storage Stability of TL and TSEE from Six Dosimetry Phosphors*

by

A.E. Nash, V.H. Ritz, and F.H. Attix

Naval Research Laboratory
Washington, D.C. 20390
U.S.A.

*This work was supported by the Division of Biology and Medicine of the U.S. Atomic Energy Commission.

Storage Stability of TL and TSEE from Six Dosimetry Phosphors*

by

A.E. Nash, V.H. Ritz, and F.H. Attix

Naval Research Laboratory
Washington, D.C. 20390
U.S.A.

Abstract

The thermally-stimulated exoelectron emission (TSEE) and thermoluminescence (TL) signals resulting from β-irradiation have been simultaneously measured for each of six dosimetry phosphors: LiF(TLD-100), CaF_2:Mn, CaF_2(fluorite), $Li_2B_4O_7$:Mn, and $CaSO_4$:Mn (all in powder form) and BeO-998 sintered discs. The samples were initially annealed for 1 hr at 400°C (600°C for BeO), then either dosed and read out promptly, or dosed and read out after storage, or stored and then dosed and read out. Storage was done in the dark at room temperature in either dry air or argon, for 1 week or 1 month. Some additional samples were stored in air at 100% humidity.

Results are presented and discussed. In general TL signals show greater time stability than TSEE. BeO seems to offer the most advantages as a TSEE dosimeter of the materials studied.

*This work was supported by the Division of Biology and Medicine of the U.S. Atomic Energy Commission.

Introduction

In an earlier report[1] one of us described a methane-flow proportional counter for use in measuring thermally-stimulated exoelectron emission (TSEE), and which could be easily converted into a thermoluminescence (TL) reader.* This apparatus allowed a phosphor sample (typically 10 mg of powdered phosphor) to be measured, first in one mode and then the other, to compare the TL and TSEE "glow" curves, i.e., light intensity vs temperature for the TL, or electron count-rate vs temperature for the TSEE. Several dosimetry phosphors were studied in this way, but the results were regarded as being only provisional, pending further study of the counter characteristics. The apparent height of the counter pulses resulting from the exoelectron emission had been unexpectedly found to be a direct function of the TSEE "glow-peak" temperature[1], and the cause of this was not known at that time.

Later at NRL Ritz and Attix[5-7] assembled a new TL-TSEE apparatus that was an improvement over the original design, especially in allowing the simultaneous measurement of both outputs during a single heating run, thus eliminating the possibility that sample-to-sample or run-to-run variations in the TL or TSEE output or the heating rate might invalidate the intercomparison. The new proportional counter is shown in Fig. 1. This design is similar in most respects to the original one[1], except that:

(a) a small quartz window has been added in the top to allow either simultaneous measurement of the TL signal as the exoelectrons are counted, or optical stimulation of exoelectron (or photoelectron) emission,

---

* The earlier apparatus was constructed at the United Kingdom Atomic Energy Research Establishment while F.H. Attix was on sabbatical leave with the Health Physics and Medical Division. Since he returned to NRL in 1969, the original instrument has been employed by Joan Thompson[2], and later by L.D. Brown[3-4] who has studied the effects of further modifications in design.

(b) the chamber top is hemispherical instead of cylindrical as in the earlier version,

(c) the spring-type electrical contact at the side of the sample cup is heavily gold-plated and mounted on a stand-off insulator (not shown in Fig. 1) so that the current cannot take a parallel path through the lip of the graphite sample dish, leading to possible counting noise and variability in heating rate, as noted by Brown[5], and

(d) the methane-gas inlet was positioned to sweep gas through the space between the loop and the sample, as suggested but not tried in reference 1, to break up convection currents rising from the sample.

This latter phenomenon was identified by Ritz and Attix[7] as the cause of the reported dependence of TSEE pulse height on glow-peak temperature[1]. Observing the pulse-height distributions from LiF(TLD-100) with a 100-channel analyzer, they found that the differences from one glow-peak to another were nearly eliminated when the methane flow-rate was increased from the $\approx 3 cm^3/min$ employed by Attix to $\approx 100 cm^3/min$, which was evidently enough to break up and sweep away the hot gas column, thus preventing the gas gain from being increased by the rise in gas temperature at the loop. Moreover it was found that the pulse-height distributions, which appeared as straight lines of negative slope on a plot of log (counts/channel) vs peak height, all steepened by factors ranging from 3.7 (for 150°C glow peak) to 4.3 (for 330°C peak), indicating a general decrease in gas gain over the whole temperature range of interest. This was surprising because the water cooling in both the original and present chamber designs does not allow the chamber walls to warm up significantly, but evidently the gas near the loop does so even when the sample temperature is raised to only 150°C.

Present Operating Parameters

To compensate for this decrease in gas gain at the higher methane flow rate of $100 cm^3/min$, it was necessary to increase the gain by other means. Increasing the loop potential alone was found to cause excessive pulse distortion in the pre-amplifier when the ^{14}C β-ray calibration source was inserted for counting. The operating parameters finally chosen for the present work were: +4300V loop potential obtained from a

Hamner N-4050 supply; X 1 gain setting on the Ortec 109PC pre-amplifier; X 1 input attenuation and approximately maximum gain setting of the Ortec 410 linear amplifer, with 1μsec pulse-shaping time constants; and Ortec 406A single-channel analyzer with pulse-height threshold set at 0.08 volts. The output was fed simultaneously to an Ortec 441 linear ratemeter and an Ortec 703 overflow register.

The TL signal was detected by an EMI 6094S photomultiplier tube operated at -950V, positioned to view the sample through the quartz window. A Corning 4303 blue-green filter attenuated the heat signal relative to that of the TL light. The PM tube was operated in a Jarrell-Ash 83-055PM cooled housing, which was not essential but lowered the dark current to a totally negligible level. The PM tube output current was amplified by a Keithley 410 μμ-ammeter, and total charge was summed by an Elcor A308C integrator.

The thermocouple amplifier and linear heating control consisted of a Keithley 155 null-detector microvoltmeter which sensed the imbalance between the control thermocouple potential and a linear time-ramp voltage signal from a Hewlett-Packard 17108A time-base generator. The output of the Keithley null detector was fed into a Brown Electronik recorder, with a Variac adjustable autotransformer mechanically coupled to its pen drive. In this way the autotransformer adjusted the power to the sample heater to maintain a constant time-rate of temperature rise during the heating for TL and TSEE readout. The normal heating rate employed was about 3.3°C/sec, but other rates of 0.6 and 6.8°C/sec were also used to test for heating-rate dependence in certain cases to be described later.

The surface temperature of the graphite sample-cup shown in Fig. 1 was measured in an auxiliary experiment in which the loop assembly was removed and a 0.008-cm diameter chromel-alumel thermocouple was cemented to the center of the cup. The temperature there was found to lag roughly 10°C behind that indicated by the control thermocouple under normal operating conditions with 100cm^3/min of methane flow and at 3.3°C/sec heating rate, in the temperature range 50°-400°C. The glow curves presented in this paper will be plotted as a function of the graphite surface temperature, labeled "pan temperature."

The Present Experiment

The purposes of the present experiment were threefold:

(a) To measure the TSEE and TL responses obtained simultaneously for several useful TL dosimetry phosphors, and to compare their TSEE vs TL "glow" curves,

(b) To make a preliminary survey of the dependence of TSEE and TL response on storage time, the irradiation being given either before or after the storage period, thus indicating charge leakage or changes in sensitivity, respectively, and

(c) To try to observe the influence of gases on surface traps by storing the samples in dry air or argon. (Later, water-saturated air was tried for three of the phosphors).

The materials selected for study were LiF(TLD-100)[a], CaF_2:Mn[b], natural fluorite[c], $Li_2B_4O_7$:Mn[d], $CaSO_4$:Mn[b], and BeO-998[e]. The latter was in the form of sintered pellets 1 cm in diameter X 1 mm in thickness. The $CaSO_4$:Mn was a very fine powder, passing a 400-mesh screen. The other four materials had grain sizes mainly in the 100-200 mesh range. All samples except BeO weighed approximately 10 mg, leveled in individual graphite sample cups which they occupied continuously for the duration of the experiment. The cups were handled carefully to avoid disturbing the phosphor. All storage was done in the dark at ≈22°C, and radiation exposure, readout, and other procedures were carried out in subdued light to avoid inducing or altering TL or TSEE signals.

All samples were virgin material, but an initial annealing for 1 hour at 400°C in air was administered to eliminate any spurious TSEE or TL signal due to grinding, sintering, etc. In the case of the BeO, 400°C was found to be inadequate to

---

[a] Harshaw Chemical Co., Solon, Ohio, U.S.A.

[b] Prepared by R.J. Ginther, NRL.

[c] Provided by C. Brooke, Manufacture Belge de Lampes et de Materiel Electronique S/A, Bruxelles, Belgium.

[d] Prepared by R.D. Kirk, NRL

[e] Brush Beryllium Co., Elmore, Ohio, U.S.A.

eliminate a high-temperature TSEE peak, and 600°C for 1 hour was successfully substituted. Upon removal from the oven, all samples were placed in a desiccator pre-filled with either dry air or argon, and allowed to cool rapidly to room temperature in that environment as more gas was flowed through. It was thought that the gas in question thus would be adsorbed on the phosphor surface, and have its maximum influence on surface traps, if any were present.

Twenty four samples of each phosphor were prepared. After annealing, half of these were placed in the air-filled desiccator and the other half in dry argon. After cooling, samples of each phosphor were removed from the desiccators on the same day they were annealed. These were either β-irradiated or not (in the case of controls) and promptly read out in the TL-TSEE modes simultaneously. Other samples of each phosphor were removed from the desiccators, β-irradiated, and promptly returned to storage there for 1 week or 1 month. Still other samples were stored in the undosed condition for 1 week or 1 month before removal, β-irradiation, and immediate readout. Undosed controls accompanied all dosed samples, including the 1-week or 1-month-storage cases.

In a subsequent experiment closely resembling the first in other respects, the three phosphors LiF(TLD-100), $CaSO_4$:Mn, and BeO-998 were cooled and stored for 1 week in an air-filled desiccator at ≈100% relative humidity and room temperature.

The β-irradiations were carried out with a 7-mCi source of (^{90}Sr-^{90}Y), with the ^{90}Sr β-rays (≈0.5 MeV max.) removed by an aluminum filter. The irradiation fixture was calibrated in terms of tissue dose through TL measurements with 10-mg samples of LiF(TLD-100), comparing with a known ^{60}Co γ-ray source. Three sample distances were so calibrated, approximating β-ray dose rates of ≈10, 1.0, and 0.1 rad/min. The doses administered to each sample were adjusted in trial runs to provide a measurable signal in the TSEE readout mode, and the PM tube voltage was then adjusted to accommodate the TL signal and amplify it to a conveniently measurable output current.

Dry-Gas Results and Discussion

The TL and TSEE glow curves obtained for the six phosphors are shown in Figs. 2-7. For each phosphor the "A" figure refers to case where the β-ray exposure was made before storage, and "B" is for β-irradiation after storage and immediately before readout.

No significant differences between samples stored in dry air or Ar were observed; thus the curves in Figs. 2-7 represent both gases. This was to be expected for the TL data, since thermoluminescence is known to originate inside the phosphor crystals rather than at the surface. However it has been generally supposed that some of the TSEE glow peaks might result from the release of electrons from surface traps, and that such traps could reasonably be expected to be influenced in some way by adsorption of gas molecules on the crystal surface. The present experiment revealed no such influence. This does not disprove the existence of TSEE surface traps, but does suggest that such traps, if present, are indigenous to the crystal-surface discontinuity, rather than being related to the adsorbed gas layer. More will be said about this later, in connection with Figs. 2A-2B.

No attempt was made in the present experiment to substitute another gas for the methane flowing through the chamber, except for verifying that ultra-high-purity methane gave the same counter operating characteristics as the Matheson C.P. grade gas usually employed. However a direct comparison of TSEE glow curves for identical LiF(TLD-100) - graphite samples prepared by Becker and hand-carried to NRL revealed no difference in glow-curve shape between Oak Ridge National Laboratory and NRL results, except for some difference in temperature scale factor. The counter used by Becker in this intercomparison was of the G-M type, employing 99.05% He + 0.95% isobutane as the flow gas. This finding also supports the general conclusion that ambient gases do not influence the TSEE process significantly, whether during storage or readout.

In this connection it is worth noting that in no case did we observe a significant TSEE or TL signal due to storage alone, without irradiation. The TL measuring apparatus did not have adequate sensitivity to detect weak triboluminescence signals

if they were present, besides which the absence of oxygen from the methane counting gas would be expected to quench such spurious light signals.

We will not attempt here to discuss and analyze all the complexities of the curves presented in Figs. 2-7. Instead, a few interesting features will be pointed out and some general observations made.

First, in LiF (Figs. 2A-2B) it will be seen that pronounced TSEE peaks exist at ≈100°C, 175°C, 200°C, and 295°C. Allowing for some differences in temperature scale Becker et al.[8] have seen these same peaks, but the center two were relatively less well-defined and were tentatively attributed by those authors to production and detection of photons in their counter. The present results rule out that conclusion since the TL and TSEE curves do not follow one another, either as a function of temperature or storage time. It will be seen that the 175 and 200° TSEE peaks tend to be enhanced by storage either in the dosed or (to a lesser extent) the undosed condition. Moreover we have observed that mixing the LiF with 50% graphite powder as usually done by Becker et al. enhances the 295°C TSEE peak relative to the others. This combined with prompt readout of samples probably accounts for the relative unimportance of the 175°C and 200°C peaks in Becker's results[8].

Gordan and Scharmann[9] studied TSEE emission from pure LiF single crystals cleaved, irradiated, and heated for TSEE counting while continuously located in a high vacuum. They did not observe the 175°C or 200°C glow peaks, since those peaks seem to require the presence of Mg doping, as in LiF(TLD-100). However they observed the two other TSEE peaks shown in Figs. 2A-2B. By graded annealing procedures, alternating with optical density measurements, they identified the higher-temperature peak as being related to the F-center, *i.e.*, electrons at F centers are released into the conduction band and migrate to the crystal surface to be released. They could not relate the ~100 TSEE peak to an absorption band. Moreover when the crystal surface was etched away by HF after x-irradiation, that peak disappeared. Gordan and Scharmann therefore identified it as a surface trap. As noted earlier, we find that this peak is nevertheless insen-

sitive as to whether the phosphor is stored in dry argon or dry air.

In comparing TL and TSEE glow-peak temperatures in Figs. 2-7 one finds few instances of correspondence. Only the 200°C peak in LiF(TLD-100) and the 100°C peak in $CaSO_4$:Mn show close temperature correlation between TL and TSEE. The ≈225°C peak in fluorite, the ≈90°C peak in $Li_2B_4O_7$:Mn, and the ≈255°C peak in BeO-998 all occur in the TSEE mode 5-10°C below the TL mode. It is possible that this approximate correspondence in temperature indicates that both phenomena spring from a single type of trap, but further verification would be needed, such as a similarity in the time variations of the TL and TSEE peaks.

In fact the data in Figs. 2-7 show little such evidence. The peak amplitudes are usually observed to change more strongly for TSEE than for TL, whether the samples were stored in the dosed or the undosed condition. For example the 200°C TSEE peak in LiF(TLD-100) nearly triples during one month's storage in the dosed state, while the corresponding TL peak decreases slightly (see Fig. 2A). For the undosed case (Fig. 2B), the TSEE peak increase is 45%, the TL peak essentially nil*. The 225°C TSEE glow peak in fluorite shows instability during a month's storage, either dosed or undosed, while the TL peak remains constant (see Figs. 4A-4B). The 90°C TL and TSEE peaks both fade away completely in dosed lithium borate stored for one month (Fig. 5A), but in the undosed material the TL is constant while the TSEE decreases by 20% (Fig. 5B). The 100°C peak in dosed calcium sulfate likewise fades completely in a month in both readout modes (see Fig. 6A), but the undosed material exhibits stable TL while the TSEE rises 15%, as can be seen in Fig. 6B. Finally, the ≈255°C peak in dosed BeO-998 shows stability during one month of storage, while the TSEE peak drops by 15% (Fig. 7A); in the undosed case the TL is again stable while the TSEE drops 15% and then rises again, as shown in Fig. 7B. In general

*This is not always the case. Where the lower-temperature TL peaks are relatively more pronounced than in the present samples, the 200° peak may increase to some extent, due to migration and aggregation of simple trapping centers into more complex ones, as discussed by Booth et al.[10]

these data lend little support to the proposition that the TL and TSEE modes of readout provide two "windows" for viewing the same thermal un-trapping events, even for those cases where there is reasonably close temperature coincidence between the two types of glow peaks. This subject will be touched upon again in the Conclusions.

It is evident from inspection of the glow curves in Figs. 2-7 that the individual TSEE peaks generally vary with time more strongly than do the TL peaks, whether the dose is administered beforehand or later. The time variability of the total TSEE counts from the same samples is summarized in Figs. 8-13. The time variability shown by these data is likewise quite large, with only the BeO (Fig. 13) exhibiting sufficient stability to recommend its further consideration for dosimetry applications. It should be recognized that the stability of the sensitivity during storage before the dose is received is just as important as the stability after dosing, in typical personnel-monitoring operations for example. Yet most studies of new dosimeters include the latter and not the former. The initial annealing procedure used is probably an important parameter in determining the subsequent stability of TSEE, but we have made no attempt to optimize this in the present investigation.

A convenient estimate of the relative sensitivity of TSEE response per rad may be obtained by dividing the total-count numbers in parentheses in Figs. 2-7 by the β-ray doses given. Table I contains a summary of these dose-sensitivity data. It is immediately evident that, although all six of these phosphors are known to be sensitive TL dosimeters having comparable light outputs per unit dose within roughly an order of magnitude[11-12], they are not all comparably efficient with respect to TSEE. Three of the phosphors (CaF_2:Mn, fluorite, and $Li_2B_4O_7$:Mn) are very weak in TSEE response compared to the other three. Of the latter, BeO-998 and $CaSO_4$:Mn are two orders of magnitude more sensitive than LiF(TLD-100). One should keep in mind, however, that TSEE response per unit dose is usually found to be a decreasing function of the dose level, especially where the phosphor sample is not made conductive by admixture of graphite or other means. This may tend to exaggerate the sensitivity differences shown in Table I to some extent, but not enough to alter the general pattern of sensitivities shown there.

One curious feature of the TSEE glow curves in Figs. 2-7 deserves mentioning, although its significance (if any) is unknown: In the 20°C-390°C temperature range, each of the phosphors, with the exception of BeO-998, displays four TSEE peaks. In $CaSO_4$:Mn only two of the peaks are shown in Figs. 6A-6B, but at tenfold greater doses (≈10 rad) two other peaks appear, at 65°C and 265°C. BeO-998 does not yield more than the single TSEE peak shown in Figs. 7A-7B within this temperature range, even for doses as great as 100 rad.

In the course of studying the TSEE response of BeO-998, it was found that the total TSEE counts depended strongly upon the heating rate employed. Increasing the heating rate decreased the output, as shown in Fig. 14. Neither of the other two sensitive TSEE materials ($CaSO_4$:Mn and LiF(TLD-100) exhibited this effect (see Fig. 14), nor did it appear in brief checks of the other three phosphors. The most obvious explanation of this behavior would seem to be that the surface of the BeO disc is too well-insulated from electrical ground, and that exoelectrons leave that surface in a positively charged condition which retards further TSEE. The faster the heating rate, the less opportunity there is for other electrons to be conducted from ground to the BeO upper surface. However one would expect this effect to become more pronounced with increasing dose, but it does not, as shown in Fig. 14. We tried suppressing this heating-rate dependence by evaporating a conducting gold layer on the BeO disc, making sure that this layer was electrically grounded during readout. The gold film did not affect the heating-rate dependence, for average thicknesses up to the point where the TSEE was stopped by the complete coverage of the disc's surface with gold.

These findings cast considerable doubt on the dismissal of the heating-rate dependence in BeO-998 as simply another manifestation of poor electrical conductivity with sample, which is also believed to give rise in some cases to non-linearity of response vs dose. It will be seen from Fig. 14 that in the present BeO-998 discs the response was found to be approximately proportional to dose. In view of the potential usefulness of BeO discs in TSEE dosimetry applications, further studies should be undertaken to explain and perhaps eliminate this effect.

High-Humidity Storage Results

Samples of the high-sensitivity TSEE materials LiF(TLD-100), $CaSO_4$:Mn, and BeO-998 were subjected to a subsequent and abbreviated experiment which duplicated the conditions of the dry-gas storage study, except that

(a) Only air was used as a storage gas,

(b) A dish of water and a sponge were placed in the glass storage vessel to produce near-saturation humidity conditions, and

(c) The study was limited to TSEE and a 1-week storage period only.

The results are given in Figs. 15-17. Figures 15A, 16A, and 17A are for the prompt readout cases, in which samples were cooled to room temperature in the humid air after removal from the annealing oven, then promptly irradiated and the TSEE measured. The resulting TSEE glow curves are shown compared with the corresponding dry-gas curve. Figures 15B, 16B, and 17B give the same data for the case where the samples were stored for one week in wet air after dosing; Figs. 15C, 16C, and 17C show like results for the case where the dose was given immediately after the 1-week storage, just before readout.

These results show that the cooling down and storage of these samples in water-saturated air has a marked influence on the TSEE amplitude. This contrasts sharply with the finding that different dry gases (air vs argon) had practically identical effects (probably nil) on the TSEE. One might expect the adsorbed moisture released in the counter during sample heating to have some influence on counting characteristics, but it is evident from comparing curves in Figs. 15-17 that the size and direction of the TSEE peak amplitude change is variable from peak to peak, material to material, and between storage conditions as well. Thus one can rule out moisture-induced counting bias as the sole controlling influence, although it may contribute to the observed effects.

One interesting feature of the curves in Figs. 15B and 16B is the accelerated fading of the 100°C peak in wet air as opposed to dry. This may be an indication that this peak is due to a surface trap in $CaSO_4$:Mn as well as in LiF[9], but the

argument is weakened by the effect the moist air has on most of the other peaks as well.

The BeO is unusual among these materials in showing essentially the same reduction in TSEE (≈23%) due to moisture whether read out promptly or stored with or without dose. The act of cooling down the sample in the moist air seems to be the controlling factor in that case.

Conclusions

1. There is no significant difference between the γ-ray-induced TSEE signals from samples cooled down and stored in dry air vs dry argon. This means that if surface traps are present, they are apparently unaffected by ambient dry gases.

2. Cooling down or storing samples of LiF(TLD-100), $CaSO_4$:Mn and BeO-998 in wet air caused the amplitudes of individual TSEE peaks to change in nearly every case. (The other phosphors were not tested in this way.) This could be simply interpreted as an indication that most of the TSEE peaks are due to surface traps, but one should not ignore the possible influence of moisture on the surface work function, and on the counter characteristics.

3. In general the TSEE outputs showed greater dependence on dry-gas storage time than did the TL signals, whether the dose was administered before or after storage.

4. BeO-998 and $CaSO_4$:Mn gave the strongest TSEE, two orders of magnitude greater than LiF(TLD-100), and three to four orders of magnitude greater than $Li_2B_4O_7$:Mn, CaF_2:Mn, and natural fluorite. These latter three materials may be dismissed from further consideration as useful TSEE dosimeters.

5. BeO-998 discs have the dosimetry advantages of very high radiation sensitivity, a simple TSEE glow peak exhibiting relatively less storage-time dependence than the other phosphors, minimal effect due to moisture in ambient air, and good handling convenience. However they exhibit a strong dependence of TSEE output on heating rate, which should be investigated further. Becker and his co-workers[14-18] have studied BeO-998 and a similar material designated BeO-995 which differs mainly in having some 27 times as much silicon (2150 ppm instead of 81). Since they found the BeO-995 to be superior in TSEE sensitivity due to the Si content, their work has dealt mainly with that

material. Our findings with BeO-998 do not necessarily imply similar characteristics in BeO-995, either in regard to time instability or heating-rate dependence. Moreover the higher-temperature annealing procedures employed by Becker are sufficiently different from the present procedures to render direct comparisons in dosimetry performance tenuous.

6. In general the TSEE glow peaks in all the phosphors tested occur at different temperatures than the TL peaks. In the five instances where TL and TSEE peaks show reasonable temperature correspondence (within ≈10°C), they display little similarity in their time stability.

7. The almost complete lack of coincidence between TL and TSEE behavior in these phosphors suggests that the untrapping mechanisms responsible for these phenomena may be naturally separated in some simple and general way. It is possible that in most cases TL is the result of the thermal release of holes which then recombine with electrons held at luminescence centers, while TSEE is usually the result of the release of electrons into the conduction band with their subsequent escape or ejection from the crystal. Alternatively it could be postulated that TL is related to volume traps while TSEE results from electrons released from surface traps. While these models are attractive in their simplicity, it is obvious that our results do not prove either one, and that the actual processes involved may be more complex.

Table I

TSEE Total Counts per Tissue Rad

Phosphor	Dose	Prompt	1 Week		1 Month	
			Dosed Before*	Dosed After†	Dosed Before*	Dosed After†
LiF(TLD-100)	62 rad	2,800	3,200	4,100	3,300	3,500
CaF_2:Mn	1240	37	74	64	56	25
CaF_2 (fluorite)	1240	30	24	33	17	51
$Li_2B_4O_7$:Mn	620	270	160	290	69	260
$CaSO_4$:Mn	1.17	180,000	170,000	180,000	210,000	300,000
BeO-998	2.34	430,000	400,000	370,000	350,000	440,000

*Derived from parenthetical data in Figs. 2A-7A.

†Derived from parenthetical data in Figs. 2B-7B.

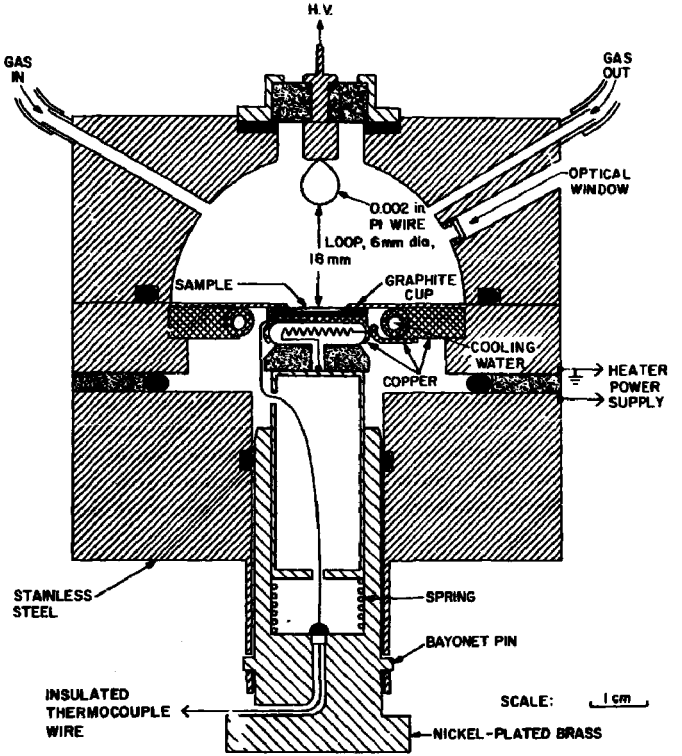

EE PROPORTIONAL COUNTER

1. New model proportional counter for TSEE, with quartz window added for simultaneous measurement of TL emission or optical stimulation of samples Samples are typically 10 mg of powdered phosphor in the graphite cup, firmly pressed against the central hole in the chamber floor by the spring-loaded telescoping sample holder. See references 1 and 7 for more details.

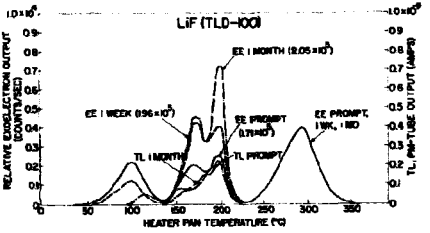

2A. Exoelectron emission and thermoluminescence of LiF(TLD-100). 10 mg sample of virgin powder in a graphite planchet. Annealed in air for 1 hr at 400°C, then removed and placed in dry air or dry argon to cool rapidly to room temperature. β-irradiated at once to 62 rad, then the TL and TSEE signals were read out simultaneously at a heating rate of 3.3°C/sec, either promptly or after storage for 1 week or 1 month in the dark in dry air or dry argon. No significant differences between air or argon storage were observed, hence the curves represent both results. Data in parentheses give the total TSEE counts occurring during the entire period of heating to 390°C.

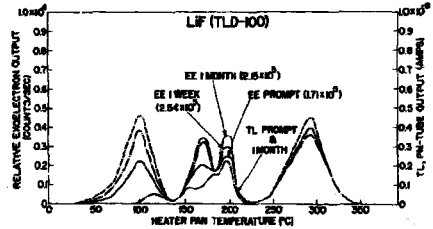

2B. Same as for Fig. 2A, except that the β irradiations were delivered immediately before the readout was performed, either promptly after cooling from the 400° annealing, or 1 week or 1 month later.

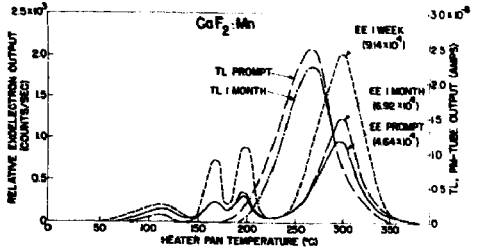

3A. Same as for Fig. 2A, except that the phosphor powder is CaF_2:Mn, and the dose 1240 rads.

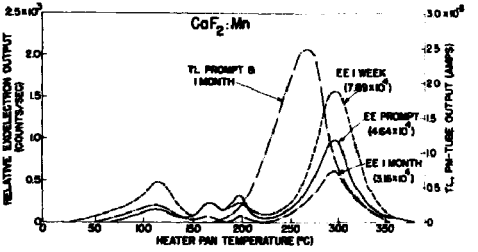

3B. Same as for Fig. 2B, except that the phosphor powder is CaF_2:Mn, and the dose 1240 rads.

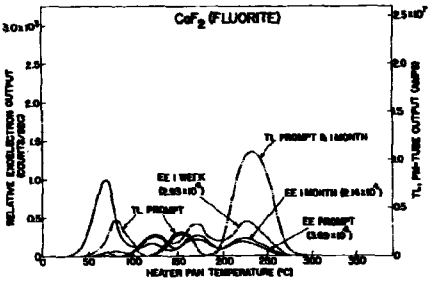

4A. Same as for Fig. 2A, except that the phosphor powder is CaF_2 (natural fluorite) and the dose 1240 rads.

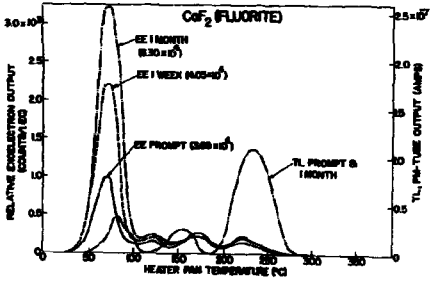

4B. Same as for Fig. 2B, except that the phosphor powder is CaF_2 (natural fluorite) and the dose 1240 rads.

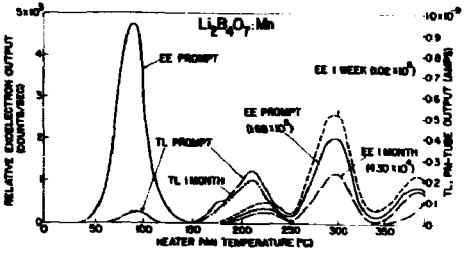

5A. Same as for Fig. 2A, except that the phosphor powder is $Li_2B_4O_7$:Mn and the dose 620 rad.

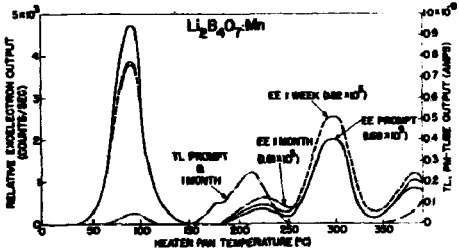

5B. Same as for Fig. 2B, except that the phosphor powder is $Li_2B_4O_7$:Mn and the dose 620 rad.

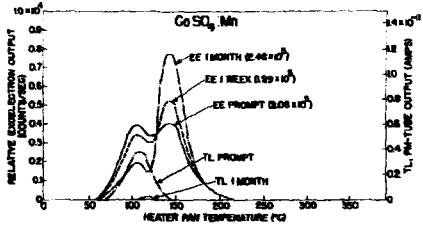

6A. Same as for Fig. 2A, except that the phosphor powder is $CaSO_4$:Mn *and the dose* 1.17 rad. Two other minor TSEE peaks are found to appear at 65°C and 265°C at much higher doses (≈ 10-100 rad).

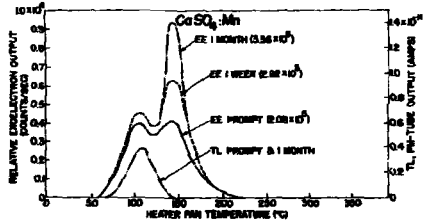

6B. Same as for Fig. 2B, except that the phosphor powder is $CaSO_4$:Mn and the dose 1.17 rad. Two other minor TSEE peaks are found to appear at 65°C and 265°C at much higher doses (≈ 10-100 rad).

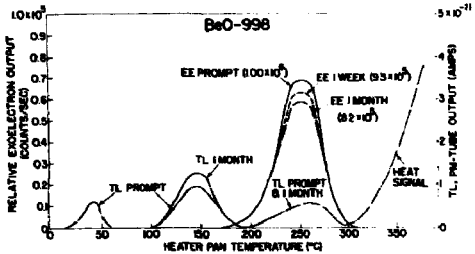

7A. Same as for Fig. 2A, except that the phosphor is BeO-998 in the form of sintered discs, the annealing temperature was 600°C, and the dose 2.34 rad.

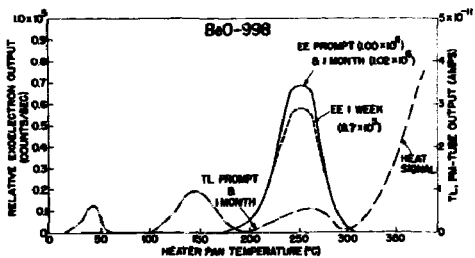

7B. Same as for Fig. 2B, except that the phosphor is BeO-998 in the form of sintered discs, the annealing temperature was 600°C, and the dose 2.34 rad.

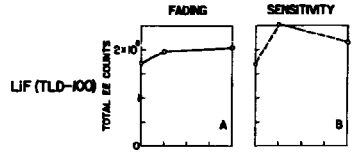

8A. Time variation of total TSEE counts in LiF(TLD-100), dosed before storage. Data taken from Fig. 2A.

8B. Time variation of total TSEE counts in LiF(TLD-100), dosed after storage. Data taken from Fig. 2B.

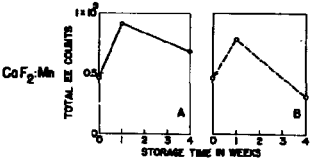

9A. Same as Fig. 8A, but for CaF_2:Mn, based on Fig. 3A.

9B. Same as Fig. 8B, but for CaF_2:Mn, based on Fig. 3B.

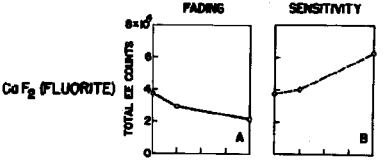

10A. Same as Fig. 8A, but for fluorite, based on Fig. 4A.

10B. Same as Fig. 8B, but for fluorite, based on Fig. 4B.

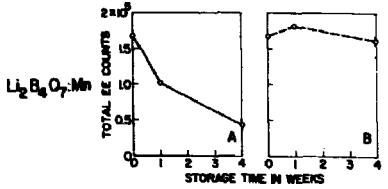

11A. Same as Fig. 8A, but for $Li_2B_4O_7$:Mn, based on Fig. 5A.
11B. Same as Fig. 8B, but for $Li_2B_4O_7$:Mn, based on Fig. 5B.

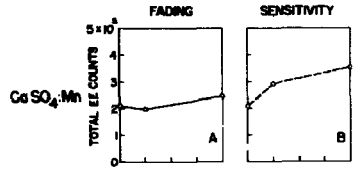

12A. Same as Fig. 8A, but for $CaSO_4$:Mn, based on Fig. 6A.
12B. Same as Fig. 8B, but for $CaSO_4$:Mn, based on Fig. 6B.

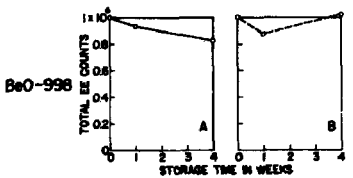

13A. Same as Fig. 8A, but for BeO-998, based on Fig. 7A.
13B. Same as Fig. 8B, but for BeO-998, based on Fig. 7B.

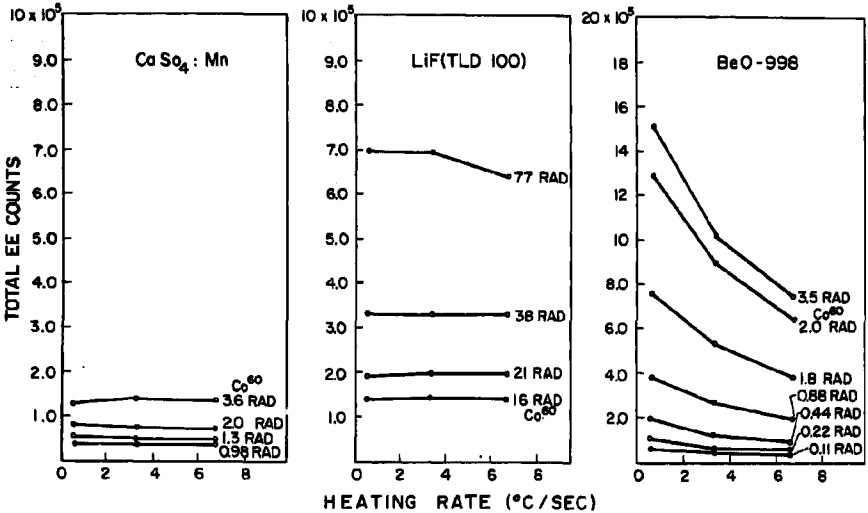

14. Total TSEE counts as a function of heating rate, at various ^{60}Co γ-ray dose levels in $CaSO_4$:Mn, LiF(TLD-100), and BeO-998.

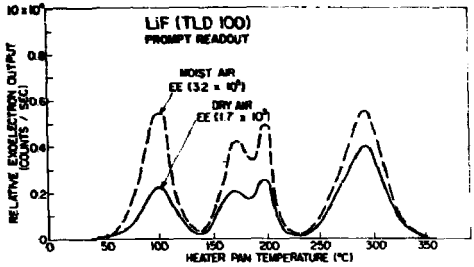

15A. Exoelectron emission from LiF(TLD-100), read out after annealing in air for 1 hr at 400°C, cooling to room temperature in water-saturated air, and then β-irradiating to 62 rad. Corresponding prompt dry-gas curve from Figs. 2A-2B is also shown.

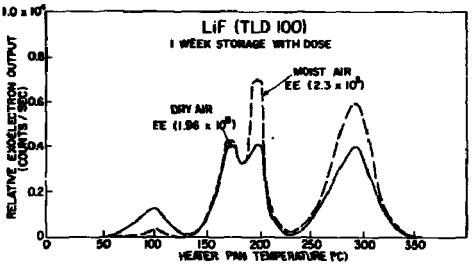

15B. Same as Fig. 15A, except that the phosphor was dosed and then stored for 1 week in wet air before readout. Corresponding dry-gas curve from Fig. 2A is also shown.

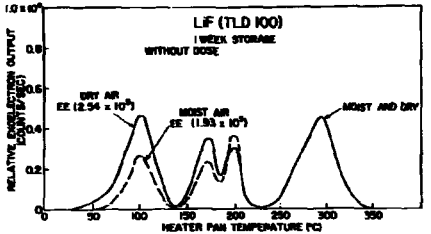

15C. Same as Fig. 15A, except that the phosphor was stored for 1 week in wet air and then dosed before readout. Corresponding dry-gas curve from Fig. 2B is also shown.

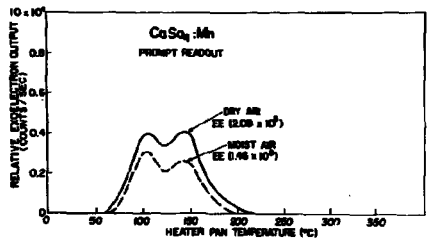

16A. Exoelectron emission from $CaSO_4$:Mn, read out after annealing in air for 1 hr at 400°C, cooling to room temperature in water-saturated air, and then β-irradiating to 1.17 rad. Corresponding prompt dry-gas curve from Figs. 6A-6B is also shown.

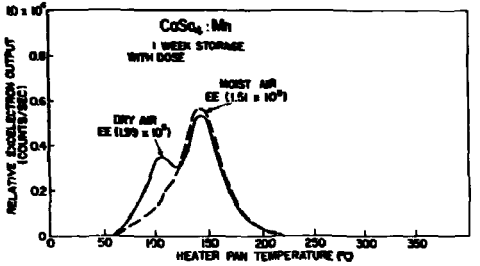

16B. Same as Fig. 16A, except that the phosphor was dosed and then stored for 1 week in wet air before readout. Corresponding dry-gas curve from Fig. 6A is also shown.

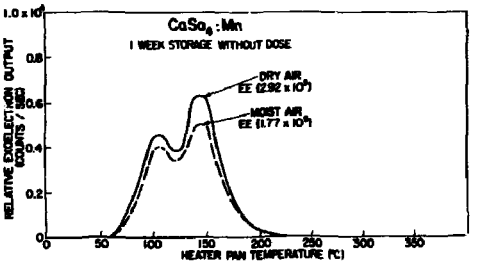

16C. Same as Fig. 16A, except that the phosphor was stored for 1 week in wet air and then dosed before readout. Corresponding dry-gas curve from Fig. 6B is also shown.

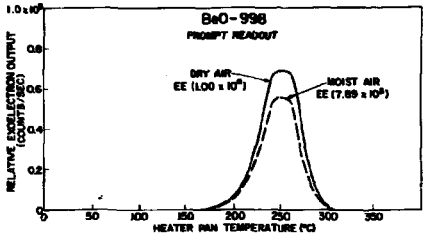

17A. Exoelectron emission from BeO-998 disc, read out after annealing in air for 1 hr at 600°C, cooling to room temperature in water-saturated air, and then β-irradiating to 2.34 rad. Corresponding prompt dry-gas curve from Figs. 7A-7B is also shown.

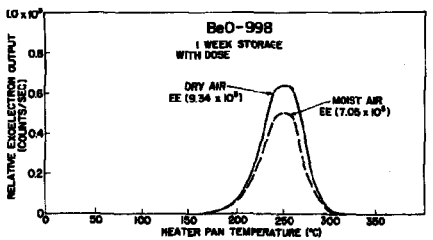

17B. Same as Fig. 17A, except that the phosphor was dosed and then stored for 1 week in wet air before readout. Corresponding dry-gas curve from Fig. 7A is also shown.

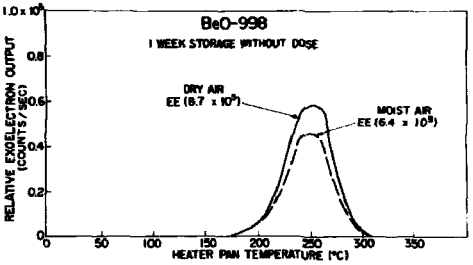

17C. Same as Fig. 17A, except that the phosphor was stored for 1 week in wet air and then dosed before readout. Corresponding dry-gas curve from Fig. 7B is also shown.

Scharmann

In the table you reported on measured exoelectrons per rad. Do you detect or count all exoelectrons?

Attix

We don't know our absolute counting efficiency, but I believe we are not missing a significant fraction. Our counter is some five times as sensitive as Dr. Becker's G-M- counter, which he has estimated as having about 20-25% counting efficiency.

Brown

You apparatus was ideal for simultaneous observation of TL and TSEE curves, and your remark that there was little correlation between TL and TSEE peaks confirmed the general impression I had formed under conditions where it was difficult to be precise about the exact peak location. Can I ask whether you feel this applied to all TSEE peaks, or whether there appears to be any exceptions to this general law?

Attix

Out of the eighteen or twenty TSEE peaks seen in these six materials, only two coincided with TL peaks, and three others were within about 10°C of TL peaks. In each of these cases the time variations were quite different in the TSEE and the corresponding TL peak. There seems to be little direct connection between TL and TSEE, although of course they are both resulting from untrapping of charge carriers. Perhaps they are simply not due to the same charge carriers.

Becker

Even if there would be complete agreement in the actual temperature of a TL and a TSEE emission peak in a given compound, no coincidence of the measured peaks would be observed for a very simple reason: TL occurs from the volume of the crystal, but TSEE takes place at the interface between the hot crystal and the cool, flowing counting gas where the actual temperature may be much lower.

Optical Absorption and ESR Properties of Thermoluminescent Natural CaF_2 after Heavy Gamma Irradiation

by

K.S.V. Nambi* and T. Higashimura

Research Reactor Institute

Kyoto University

Kumatori-cho, Sennan-gun, Osaka,

JAPAN.

Abstract

Studies have been made on the optical absorption and ESR of TLD grade natural CaF_2 after heavily irradiating with Co-60 gamma rays in the range of 10^5 - 10^9R at room temperature.

Though none of the original thermoluminescent characteristics of the phosphor changed after such heavy irradiations, new optical absorption bands were observed at about 950, 1150 and 1350 nm successively as irradiations were continued from ten to thousand megarads. Preliminary investigations indicate the formation of colloidal type centres in CaF_2 by heavy irradiations and giving rise to such near-infrared absorption bands.

---

* Permanent address : Health Physics Division, Bhabha Atomic Research Centre, Bombay - 85, India.

ESR studies with this CaF_2 powder has resulted in the identification of three distinct signals : (1) Signal P which has maximum intensity when there is no trace of TL present in the sample ; (2) Signal S which is irradiation produced and whose buildup and decay are observed to be complementary to the depletion and recovery respectively of Signal P ; and (3) A sharp doublet signal H separated by 501.25G and which saturates faster with microwave power. Arguments are presented to identify signal P with paramagnetic RE^{3+} centres, signal S with either hole centres or paramagnetic RE^{2+} centres and signal H with trapped hydrogen atoms in CaF_2 lattice.

Introduction

A sample of natural CaF_2 powder which has been successfully employed in radiation dosimetry in the dose range of 1 mR to 10^4R[1] and whose TL spectral characteristics had already been evaluated[2,3], was further investigated by observing the various effects after heavy gamma-irradiation in the range of 10^5 - 10^9R. The present paper reports the optical absorption and ESR characteristics of such a heavily irradiated sample and their association with the observed thermoluminescence.

Experimental

Thermoluminescence was measured using the conventional arrangement consisting of a heater with a fixed voltage supply to heat the sample held in a planchett, a photomultiplier (1921) to measure the light output and a d.c. amplifier coupled to a recorder to register the TL glow curve. Temperature measurements were done by a thermocouple fixed between the planchett and the heater.

Optical absorption measurements were recorded by a Shimadzu multipurpose spectrophotometer model 50L.

The ESR measurements were done in a Varian EPR spectrometer of model E-3. Weighed quantity of the powder sample was taken in a high purity quartz tube and used in the ESR cavity of the spectrometer operated in the X band.

All irradiations and subsequent optical & ESR measurements were carried out at room temperature (20°C) unless otherwise stated.

Observation

(a) Thermoluminescence

From the point of view of thermoluminescence no permanent damage effects could be observed for the irradiations carried out upto 10^9R. Such a heavily irradiated phosphor when subsequently used for low level gamma-irradiations did not show any change in the glow curve shape or TL sensitivity.

(b) Optical absorption

However, dramatic changes were observed[4] in the optical absorption spectra of the samples which were irradiated to different doses in the range of 10^6 - 10^9R. In this high dose range new absorption bands are observed in the region of 800 - 1500 nm while all the usually known bands in the visible region are flattened after saturation; the new bands appear at about 950 nm, 1150 nm and 1350 nm successively as irradiation is continued from ten to thousand megarads. (Fig. 1). The shape of these infrared bands do not change at all if measured at 77°K and are bleached selectively at their wavelength.

The behaviour of these bands is strikingly similar to extinction curves generated by colloidal particles of increasing sizes in alkali halides[5]. Eventhough colloidal particle production in fluorites by irradiation has not yet been clearly proved and understood[6], these have been extensively studied in alkali halides[7]. We think our results show for the first time, the possibility of observing colloidal centres in natural calcium fluoride under conditions of very heavy gamma irradiation.

(c) Electron paramagnetic resonance

Three distinct signals have been observed in the ESR spectra of natural CaF_2 powder samples :

(1) Signal P - a doublet which has maximum intensity in a sample which has been annealed at 600°K to remove any trace of TL already present in the sample. The g value for this signal is 2.0424 (Fig. 2a). For gamma irradi-

ations upto about 10^4R, changes are not easily detectable in the ESR spectrum. For irradiations 10^4R, this signal progressively reduces in intensity while new signals S and H are progressively built up.

Signal S : This has g value of 1.9989 (Fig. 2b) and its build up with increasing irradiations and its decay for storage at room temperature are completely complementary to the depletion and recovery respectively of signal P. (Figs. 3 & 4). The decay of signal S is completely coincident with that of TL peak I (appearing at 280°C in the glow curve).

Signal H : This has a sharp doublet separated by 501.25G with g = 2.0154 (Fig. 2b).

We interpret our ESR results as a striking revelation of the $RE^{3+} \rightleftharpoons RE^{2+}$ charge conversion processes which are known to occur in the thermoluminescence phenomenon of CaF_2. Such a model envisages irradiation induced charge reduction and thermally activated charge oxidation processes involving the triply positive rareearth ions at cubic sites present as impurities in CaF_2. The trapping centres suggested involve hole traps with configurations of F_2^- molecular ion which should be paramagnetic[9]. Since the sample of natural CaF_2 used in the present study is known to have many rareearth ions as impurities[3] our ESR results could be interpreted this way : Signal P might be associated with RE^{3+} paramagnetic centres while signal S could be associated with either a paramagnetic hole centre or RE^{2+} paramagnetic centres. The depletion of P along with the production of S on irradiation and depletion of S with the recovery of P on annealing the TL, can be associated with the irradiation induced charge reduction and thermally activated charge oxidation processes involving the RE^{3+} ions at cubic sites.

The signal H seemed to be not associated with this rareearth charge conversion processes and detailed analysis such as power saturation studies pointed out that this signal has similar characteristics of a hydrogen atom and our ESR spectral characteristics are very much in agreement with Hall et al[10]. We could not observe any hyperfine structure as is usually reported

for hydrogen atoms in CaF_2 in interstitial position. Our lines are more in comparison with those reported for U_3 centres in alkali halides[11].

Future investigations

The observation of colloidal type centres in CaF_2 unfolds an interesting field for further investigation. At least two studies could possibly be tried : (i) extension of Mie's theory and calculation of colloidal particle sizes in CaF_2 corresponding to the absorption bands observed and to check whether the sizes arrived at are compatible with the CaF_2 lattice and (ii) assignment of a role for the impurities in the formation of such colloidal centres in CaF_2.

The ESR studies need to be extended further to pinpoint exactly the nature of the centres involved in the TL process. Perhaps ENDOR measurements would be necessary especially in the case of further analysis on the hydrogen-like signals obtained in the ESR spectra. It is interesting to note that the entire irradiation-produced ESR signal S decays with the first TL peak which forms only a very small fraction of the integrated TL emission above room temperature. This and the identification of hydrogen atoms in CaF_2 lattice, might lend a new angle for the explanation of the phenomenon of TL in natural CaF_2.

References

1. K.S.V. Nambi and C.M. Sunta, Ind. J. Pure & Appl. Phys., 6, 294 (1968).
2. K.S.V. Nambi, S.P. Kathuria and A.K. Ganguly, Ind. J. Pure & Appl. Phys. 8, 280 (1970).
3. C.M. Sunta, J. Phys. C. Sol. Stat. Phys. 3, 1978 (1970)
4. K.S.V. Nambi and T. Higashimura, J. Phys. C : Sol. Stat. Phys. To be published (1971).
5. K.K. Shvarts, Sov. Phys - Sol. Stat. 12, 679 (1970).
6. K. Przibram, Irradiation colours and luminescence, Pergamon Science Series pp. 189-191 (1956).
7. W.D. Compton, Phys. Rev. 107, 1271 (1957).
8. K.S.V. Nambi and T. Higashimura, Rad. Eff. To be published (1971).
9. J.L. Mertz, Ph.D. Thesis, Harvard University, 1966. Available as Technical Report No. 514, Office of Naval Research, NR-372-012
10. J.L. Hall and R.T. Schumacher, Phys. Rev., 127, 1892 (1962).
11. Y.P. Virmani, Chem. Phys. Lett., 6, 508 (1970).

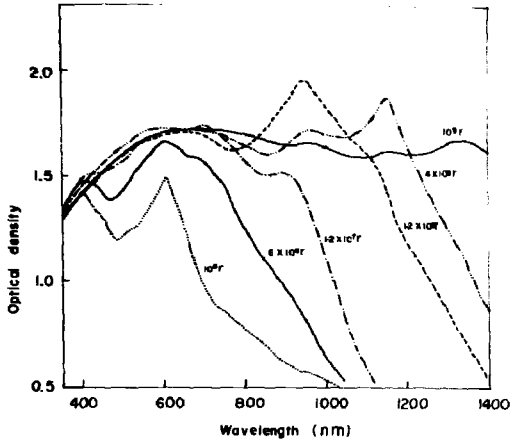

Fig. 1. Optical absorption of natural CaF_2 after heavy gamma irradiation.

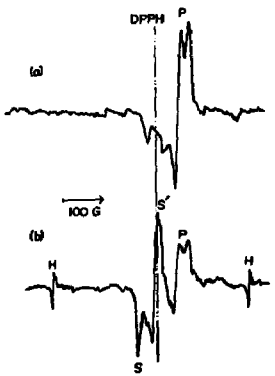

Fig. 2. ESR spectra of natural CaF_2 :

a) unirradiated, 600°C annealed powder.

b) 10^6R irradiated powder.

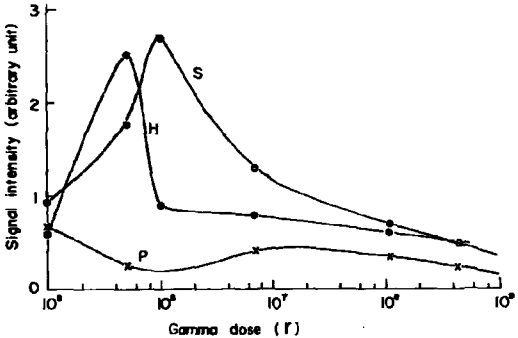

Fig. 3. ESR signal vs. gamma dose for natural CaF_2 powder.

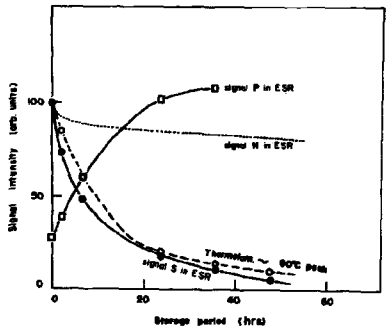

Fig. 4. ESR and TL signals of gamma irradiated natural CaF_2 powder for various storage periods at 20°C.

Methodological aspects on measurements of steep dose gradients at interfaces between two different media by means of thermoluminescent LiF

by

Gudrun Alm Carlsson and Carl A. Carlsson

Radiation Physics Department,
Linköping University
S-581 85 Linköping, Sweden

Abstract

0. 1 mm thick LiF-detectors have been used for dose measurements in a low Z-material irradiated with 100-200 kV X-rays adjacent to different high Z-materials. The detectors were thin for the photon radiation but infinitely thick for the electrons generated in the high Z-material. In the transition region, i.e. within the range of the most energetic electrons generated in the high Z-material, the dose distribution was derived by interposing a varying number of mylar films between detector and the high Z-material. The dose in these experiments varied heavily with depth in the detector, so that induced and inherent efficiency variations with depth in the detector must be considered. Evidence for a dead surface layer of LiF was observed.

Introduction

This report is based on an investigation[1] of dose gradients in a low Z material close to different metals irradiated with 100-200 kV roentgen radiation. The investigation was performed by means of thermoluminescent LiF. Some of the methodological problems are discussed here.

The measurements included the dose gradient within the region of electronic nonequilibrium (the transition region) as well as the dose gradient outside the transition region (region of electronic equilibrium) caused by characteristic roentgen rays.

Dose measurements in the region of electronic equilibrium

Fig. 1 shows depth doses in teflon close to metal foils of Al, Cu, and Pb, outside the transition region when irradiated with 100 kV roentgen radiation. Dose contributions from the K-radiation of Cu ($\bar{E}_K$=8.14 keV) and the L-radiation of Pb ($\bar{E}_L$=11.67 keV) are clearly verified. The mean free paths of the K-fluorescence photons of Cu and of the L-fluorescence photons of Pb are 0.4 mm and 1.1 mm respectively. In an absorbed dose measurement the detection of the low energy fluorescence photons is favoured by a high energy absorption in LiF per incident photon. The absorbed dose in LiF per incident photon is about 35 times higher for the K-fluorescence photons of Cu than for the primary photons. ICRU[2] recommends the absorbed dose from low energy photons to be determined from a measurement of the fluence of the low energy photons. Figure 1 shows an example of how the opposite can be done: A small fluence of low energy fluorescence photons in the presence of a large fluence of photons with higher energy can be determined from an absorbed dose distribution measurement with high spatial resolution.

The observation of the escape of L-fluorescence photons of Pb from the Pb-metal foil initiated an investigation of the origin of the emitted L-fluorescence photons. This investigation resulted in a correction of the mass energy transfer- and mass energy absorption coefficients in existing tabulations[3].

Dose measurements in the transition region

Fig. 2 shows the relative depth doses in mylar within the transition region close to metal foils of Al, Cu, Sn and Pb irradiated with 100 kV roentgen radiation. The depth doses are normalized to the electronic equilibrium absorbed dose. The dose gradients are mainly due to photoelectrons emitted from the metal foils. The transition region extends over a depth of < 10 mg/cm^2 from the metal foils.

Methods of measurement

The detectors, 0.13 mm thick LiF-teflon discs, are thin compared to the mean free paths of the photons but are infinitely thick compared to the range of the photoelectrons generated in the metal foils.

Region of electronic equilibrium

When situated within the region of electronic equilibrium the absorbed dose in the detectors is constant or slightly varying with depth in the detector. The detectors were calibrated and used as dosemeters following a technique described by Carlsson et coll.[4]

Transition region

The most direct method of dose measurements is to use detectors thin compared to the gradient of interest. In this case most of the energy is absorbed within 2 mg/cm^2 (Fig. 2). A spatial resolution better than 1 mg/cm^2 was needed.

Attempts have been made in our group as well as by others[5,6] to cut out thin slices of LiF-teflon from a LiF-teflon rod by means of a microtome. We found that slices with thicknesses less than 10 µm (≈2.2 mg/cm^2) are difficult to handle and above all do not have a well defined thickness.

Another method is to use a detector which totally absorbs the electrons, that cause the dose gradient, and then resolve the dose distribution by successively adding an increasing number of thin films between the metal foil and the detector. This method was chosen using mylar films of a well defined thickness of 0.486 mg/cm^2 and 30 mg/cm^2 thick LiF-teflon discs.

If the differences in radiation absorption and electron scattering properties of mylar and LiF-teflon are neglected the mean absorbed dose, $\bar{D}_i$, in the ith interposed mylar film is given by

$$\bar{D}_i = \frac{\{E_D\}_{i-1} - \{E_D\}_i}{A \cdot \Delta t} + D_{eq} \quad \ldots\ldots\ldots \quad (1)$$

where $\{E_D\}_i$ is the absorbed energy in the detector when i mylar films are interposed between the metal foil and the detector, A is the detector area, Δt is the thickness of the interposed films expressed in mass per unit area, D_{eq} is the absorbed dose under electronic equilibrium conditions in the detector material.

Dosimetry problems due to different radiation absorption and electron scattering properties of mylar and LiF-teflon are discussed elsewhere[1].

Methodological problems

Efficiency variations with depth in the detector

When the absorbed energy in the detector is E_D, the detector signal, M, is ideally given by

$$M = \eta \cdot E_D \quad \ldots\ldots\ldots\ldots \qquad (2)$$

where η is the efficiency of the detector.

If η varies with depth, t, in the detector, $\eta = \eta(t)$ and Eq 2 must be replaced by

$$M = \int_0^T \eta(t)\, D(t)\, A\, dt \quad \ldots\ldots\ldots\ldots \qquad (3)$$

where D(t) is the absorbed dose at depth, t, in the detector (assumed to vary with depth only), A is the detector area, and T is the detector thickness in mass per unit area.

In a LiF-teflon detector the efficiency, η, may for the following 5 reasons vary with depth, t, in the detector.

(1): Supralinearity

D(t) varies heavily with depth, t, in the detector. In the actual experiments D(0) is in some cases about 50 times more than D_{eq} (Fig. 2).

(2): Sensitizing or radiation damage

Either sensitizing or radiation damage occur in repeated use of a detector. As the radiation history varies with depth in the detector a varying degree of sensitizing or radiation damage occurs at different depths in repeated use.

(3): LET-distribution of the absorbed radiation

The efficiency, η, may vary with depth, t, in the detector due to variations in the LET-distribution of the absorbed radiation. It seems proved [7,8,9,10] that there exists a dependence of the efficiency on the LET within the actual LET-interval. The LET-variation with depth is, however, supposed to be small due to the smoothing effect of broad LET-spectra at each depth.

(4): The construction of the LiF-teflon discs

A random distribution of LiF-grains within the teflon matrix gives rise to random variations in the efficiency η with depth, t. Furthermore, there may exist systematic differences in the concentration and efficiencies of the LiF-grains at different parts of the detector, e.g. at the surface compared to the bulk of the detector.

(5): Dead layer of LiF-grains

An eventual nonthermoluminescent (dead) layer at the surface of the LiF-grains causes a correspondingly thick dead layer at the surface of the detector. This dead layer can be regarded as introducing an extra thin film between the metal foil and the active detector.

Lack of transparency for the TL-light

The LiF-teflon detector is not quite transparent for the thermoluminescent light. The light collection is better for the side of the detector viewing the photomultiplier. A correction for this lack of transparency is necessary with a steep dose gradient within the detector. The transparency increases when the detector is stored at 340-350° C for 24 hours, Fig. 3.

Normalizing depth doses measured in transition and equilibrium regions

The absorbed energy in a detector with i films interposed between the metal foil and the detector can be regarded as composed of two components, one giving the absorbed dose in the whole detector under electronic equilibrium conditions, the other giving an extra dose contribution in the surface layers of the detector, Fig. 4.

$$\{E_D\}_i = \{E_D\}'_i + \{E_D\}_{eq} = \frac{M'_i}{\bar{\eta}'} + \frac{M_{eq}}{\bar{\eta}} \quad \ldots\ldots \quad (4)$$

Here $\bar{\eta}'$ is a weighted mean efficiency of the surface layers, $\bar{\eta}$ is the mean efficiency over all depths (bulk) of the detector. When increasing the number, i, of interposed films, the penetration depth of the dose gradient in the detector is reduced. Any change in the efficiency $\bar{\eta}'$ due to this changing penetration depth of the dose gradient in the detector is neglected here and in the following.

Evidently a difference between $\bar{\eta}'$ and $\bar{\eta}$ must be corrected for (the extra dose contribution is determined with $\bar{\eta}'$ while D_{eq} is determined with $\bar{\eta}$). Moreover systematic errors are introduced if $\bar{\eta}'$ varies relative to $\bar{\eta}$ for the different num-

ber, i, of interposed films. These variations can be caused by supralinearity, sensitizing and radiation damage.

The supralinearity effect was avoided by using sufficiently small doses of D_{eq}, $D_{eq} \approx 10$ rad LiF. Sensitizing and radiation damage can in principle be avoided by using different and virgin detectors for each value, i, of interposed films. The first term in Eq 4 is independent of the thickness of the detector but the second term is proportional to this thickness, Fig. 4. Therefore, the values of the E_D:s in Eq 1 must be corrected for these thickness variations when different detectors are used.

Calibrations

The bulk efficiency of detector j relative to the average of the detectors, $\bar{\eta}_j/\bar{\eta}$, was determined by a metod described elsewhere[4]. The equilibrium absorbed dose is determined with this efficiency, $\bar{\eta}$.

The corresponding efficiency of the surface layers of detector j, $\bar{\eta}'_j/\bar{\eta}'$, was determined as follows. The detectors were all irradiated close to a metal foil of gold. The detectors thus absorbed the same energy $\{E_D\}'_o$ but did not yield the same partial signals M'_o. These signals varied witin about 5 % of the mean value. The extra dose contribution in the transition region is determined by $\bar{\eta}'$.

After the surface calibration the radiation history of a detector varies with depth. All the detectors are, however, affected equally, so that the same efficiency relation $\bar{\eta}'/\bar{\eta}$ is valid for all numbers, i, of interposed films. The relation $\bar{\eta}'/\bar{\eta}$ was studied before and after the experiment. With an appropriate annealing method[1] this realtion did not vary more than ± 1 %.

A dilemma in comparing $\bar{\eta}'$ and $\bar{\eta}$

A problem which could not be solved experimentally is whether there exists a difference between the efficiency, $\bar{\eta}'$, of the surface layers and the bulk efficiency, $\bar{\eta}$.

This problem can be tackled in two ways.

1. By analysis of the detector at different depths.
2. By comparison of measured dose distributions with theory and results obtained by other experimental methods.

.. Analysis of the detector.

A lower efficiency of the surface layer is introduced if, during the production process, grains are stripped off from the surface or are ground down.

As the individual surface efficiencies, $\bar{\eta}_j$, did not vary by more than ± 5 % it does not seem likely that whole grains are stripped off.

2. Comparison with theory and other experiments

The measured dose distributions within the transition region have been compared with calculated dose distributions using a theory originally set up by Spiers[11] and later modified by other investigators[12,13]. This theory gives result in good agreement with experiments[14] for atomic numbers up to about 15. The experimental results[1] presented here and obtained with Al are also in a reasonable agreement with theory. The precision in the measurements is, however, not better than ± 15 % with aluminium but increases considerably with increasing atomic number (± 4 % with lead). For higher Z there is no experiment that can be used for comparison with our dose distributions. For this reason the comparison with theory was extended to atomic numbers where the validity of the theory has not been verified.

In Fig. 5 the quotient between the calculated absorbed dose close to a metal foil and the experimentally determined absorbed dose close to the same metal foil is plotted as a function of the atomic number and with the quality of the primary radiation as a parameter. The quotient increases with increasing atomic number from just below 1 with Al to just above 2 with Pb. It can be shown[1] that, due to the neglect of electron scattering in the theory, the theory yields an overestimate of the absorbed dose with increasing atomic number. By introducing electron scattering in the theory[1], the experimental and theoretical results are again in reasonable agreement. This indicates that there is no great difference between $\bar{\eta}$ and η.

Dead layer

The different quotients, D_{cal}/D_{exp} , obtained with 100 kV and 204 kV roentgen radiation, Fig. 5, can be explained as an effect of a dead surface layer. The presence of a dead layer means that experimentally determined doses should be displaced to a greater depth. The steeper the dose gradient the more the experimentally determined doses are underestimated. If a dead layer of ≈ 0.07 mg/cm^2 (≈ 0.3 µm LiF) is assumed the quotients, D_{calc}/D_{exp} , coincide for both radiation qualities. A dead layer of this size is in accordance with results presented by Zanelli[15,1].

References

1. G. Alm Carlsson: Dosimetry at interfaces. A theoretical analysis and measurements at plane interfaces of Al, Cu, Sn and Pb irradiated with 100-200 kV roentgen radiation by means of thermoluminescent LiF. Accepted for publication as a Supplementum of Acta Radiologica.

2. ICRU Report 17. Radiation dosimetry: X rays generated at potentials of 5 to 150 kV.

3. G. Alm Carlsson: A criticism of existing tabulations of mass energy transfer- and mass energy absorption coefficients. Hlth Phys. 20, 653-655 (1971).

4. C.A. Carlsson, B.K.A. Mårtensson, and G. Alm Carlsson: High precision dosimetry using thermoluminescent LiF. Proc. Sec. Int. Conf. Lum. Dosimetry, Gatlinburg, Tenn., USA. September 1968. USAEC Rept. CONF 680920 (1969), pp. 936-943.

5. R.J. Schulz: Interface dosimetry with LiF-Teflon microdosimeters. Proc. Symp. on Microdosimetry. E.A.E.C., Publ. Eur 3747 d-f-e, Jan. 1968, pp. 643-668.

6. B.E. Bjärngard and D. Jones: Thermoluminescent dosimeters of LiF and CaF_2: Mn incorporated in Teflon. Proc. Symp. on Solid State and Chemical Radiation Dosimetry in Med. and Biol., IAEA, Vienna 1967, pp. 99-106.

7. S.G. Gorbics and F.H. Attix: LiF and CaF_2: Mn thermoluminescent dosimeters in tandem. Int. J. appl. Radiat. 19, 81-89 (1968).

8. E. Tochilin, N. Goldstein, and J.T. Lyman: The quality and LET dependence of three thermoluminescent dosimeters and their potential use as secondary standards. Proc. Sec. Int. Conf. Lum. Dosimetry, Gatlinburg, Tenn., USA. September 1968. USAEC Rept. CONF 680920 (1969), pp. 424-437.

9. N. Suntharalingam and J.R. Cameron: Thermoluminescent response of Lithium Fluoride to radiations with different LET. Phys. in Med. Biol. 14, 397 - 410 (1969).

10. C.A. Carlsson and G. Alm Carlsson: Proton dosimetry: measurement of depth doses from 185- MeV protons by means of thermoluminescent LiF. Radiat. Res. 42, 207-219 (1970).

11. F.W. Spiers: The influence of energy absorption and electron range on dosage in irradiated bone. Brit. J. Radiol. 22, 521-533 (1949).

12. J.L. Howarth: Calculation of the absorbed dose in soft-tissue cavities in bone irradiated by X-rays. Radiat. Res. 24, 158-183 (1965).

13. D.E. Charlton: Energy dissipation near an interface: a more realistic approach to electron range and stopping power. Radiat. Res. 44, 575-593 (1970).

14. C.L. Wingate, W. Gross, and G. Failla: Experimental determination of absorbed dose from X-rays near the interface of soft tissue and other material. Radiology 79, 984-1000 (1962).

15. G.D. Zanelli: Thermoluminescence methods applied to dosimetry in trabecular bone. Proc. Symp. on Microdosimetry. E.A.E.C., Publ. Eur 3747 d-f-e, Jan. 1968, pp. 527-549.

Acknowledgement

This work was supported by Riksföreningen mot cancer.

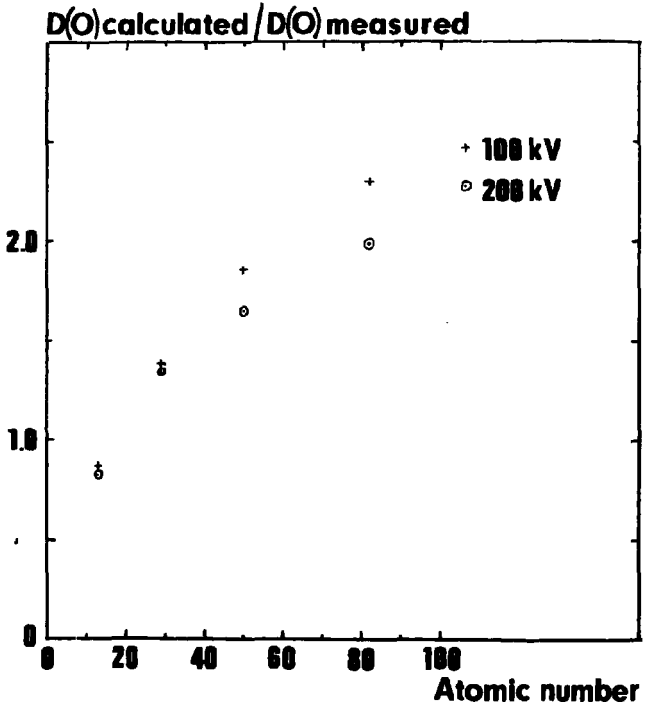

Figure 1: Depth doses in teflon beyond the transition region. The upper solid curve gives the depth doses with a beam of primary photons generated at 100 kV potential. The lower solid curve gives the corresponding depth doses with the primary photons additionally filtered by one of the indicated metal foils. The other curves give the depth doses with the indicated metal foils on the surface of the phantom.

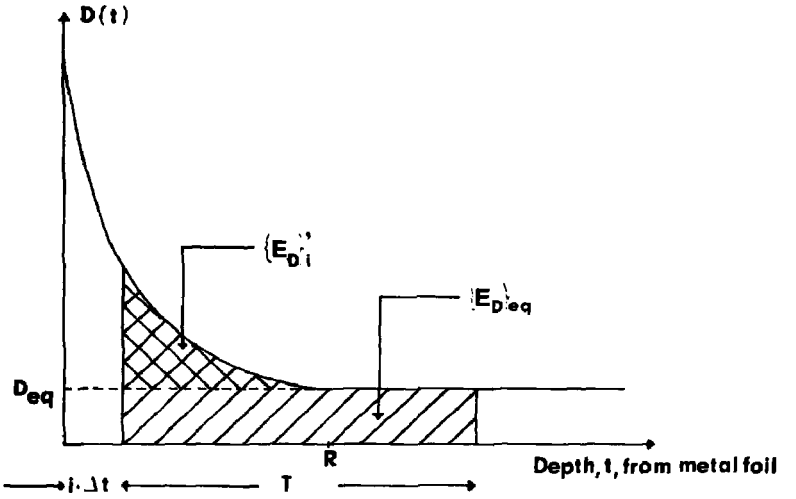

Figure 2: Depth doses in mylar from photoelectrons generated in an adjacent metal foil of Pb, Sn, Cu, and Al, irradiated with 100 kV roentgen radiation. The depth doses are normalized to the electronic equilibrium absorbed dose in LiF. The continuous curves are fitted to the experimentally obtained histograms.

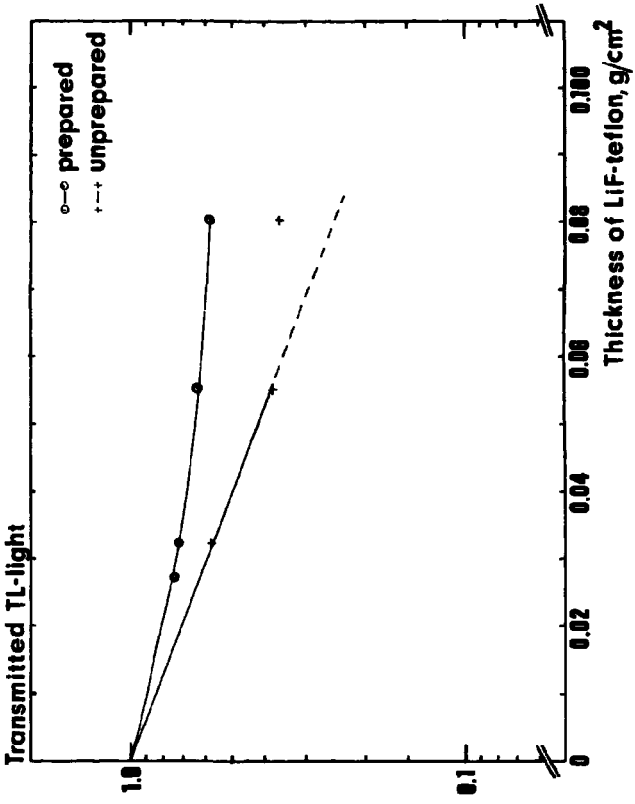

Figure 3: The fraction of thermoluminescent light transmitted through layers of LiF-teflon of varying thickness. The transparency increases when LiF-teflon is stored (prepared) at 340-350° C for 24 hours. The thickness of one LiF-teflon detector = 0.03 g/cm^2.

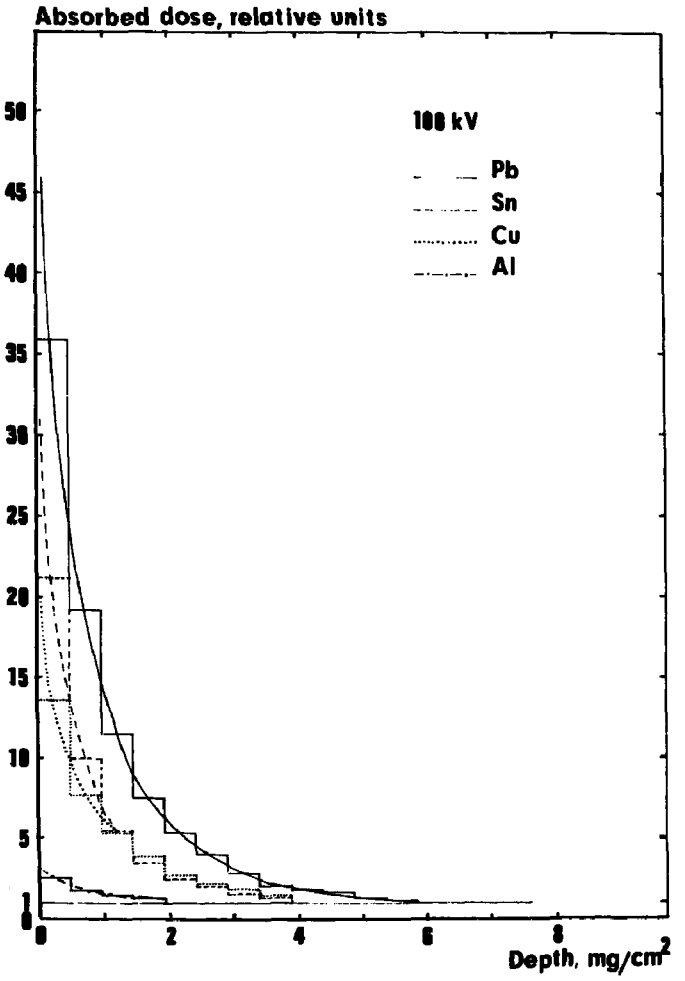

Figure 4: Division of the absorbed energy, $\{E_D\}$, in the detector into two components $\{E_D\}_i$ and $\{E_D\}_{eq}$.

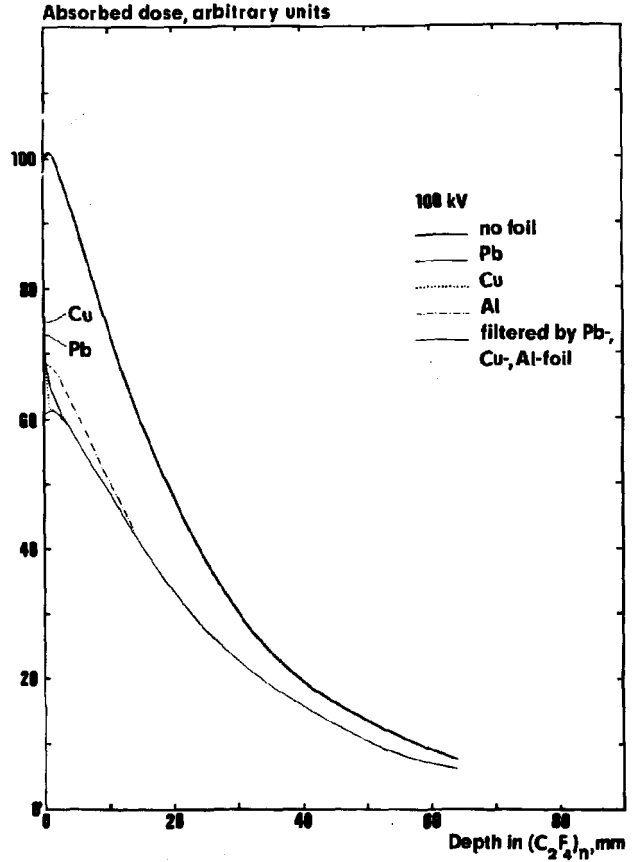

Figure 5: The quotient between the calculated and the experimentally determined absorbed doses in mylar adjacent to metal foils of Al, Cu, Sn, and Pb, represented as a function of the atomic number with the quality of the primary radiation as a parameter.

KAPIS AS A THERMOLUMINESCENT DOSIMETER

by

N.T. Bustamante, R. Petel
and
Z.M. Bartolome
Health Physics Department
Philippine Atomic Research Center

ABSTRACT

Naturally occuring kapis shells (Placuna placenta Linnaeus) were studied as possible thermoluminescent dosimeters. They grow in muddy, blackish waters from the shallow coasts to depths of even 20 fathoms. Chemical analysis showed the composition to be essentially $CaCO_3$. The kapis shells were cut into small discs (6 mm. dia.) and the response to different sources like Co^{60}, Ra^{226}, and x-ray of various energies were determined. The response to Co^{60} and Ra^{226} was linear from 50-10^4R with a precision of ±10%. The response to low energy x-ray was higher than the response to Co^{60} which showed the energy dependence of the kapis. However, the precision was lower mainly because of the heterogeneity of the beam. Fading was observed to be exponential with an average decay constant of .0043 units/hr. The highest response and best reproducibility was observed when kapis discs were placed normal to the beam. It was observed

that irradiation increased the sensitivity of kapis, thus indicating the possibility that new traps were created - a property observed also in LiF.

No definite relationship between the thermoluminescence and the weights nor the thickness of kapis shells could be seen in this study. It is possible that other factors (namely the age of the shell, geographical location of origin, climatic conditions as well as weight and thickness) are parameters that affect the thermoluminescence of kapis. The effect of pre-irradiation and post-irradiation annealing on the sensitivity of kapis are also shown.

INTRODUCTION

A number of anhydrous iron-metallic rock minerals including calcite, dolomite, aragonite, magnesite, anhydrite, and quartz are thermoluminescent.[1] Impurity ions and other defects in these minerals provide trapping centers which are characteristics of thermoluminescent materials. The possibility that these characteristics of the minerals can be utilized for measuring dose is being studied.

Kapis shells (Placuna placenta Linnaeus) was selected for the initial study of thermoluminescence of Philippine minerals because of its accessibility and low cost. Chemical analysis showed that it is essentially $CaCO_3$. Kapis shells are being used presently for

---

[1] W.L. Medlin. "Thermoluminescent Properties of Calcite." Journal of Chemical Physics, Vol. 30, No.2 (1959), p.451.

making placemats, handbags, lampshades, and many other items. They grow best in muddy, blackish waters from the shallow sea coasts to depths up to 20 fathoms and they are abundant in Bacoor Bay, Bataan, Bohol, Negros Provinces, Capiz, Iloilo, Pangasinan, Quezon, and several parts of Mindanao.[2]

The response of kapis shells to different sources like - gamma, x-rays, and neutrons - was studied. Other parameters like reproducibility, fading, energy-dependence, and re-usability were investigated to determine the possibility of using kapis shells as radiation dosimeter.

EXPERIMENTAL METHOD

The reader used for measuring the thermoluminescence was Con-Rad TLD Reader Model 7100. The characteristics of this equipment has been fully discussed in previous work.[3] The kapis shells were cut into small discs (6 mm. dia.) and then washed carefully with detergent followed by ethyl alcohol. The heater current used was 0.4 A for the heating cycle which lasted approximately 30 seconds. This gave the lowest ratio of second/first TL reading of 0.136.

---

[2] S.R. Berconio. "Shellcraft Production in the Philippines." Philippine Fishing Journal, January 1967.

[3] N.T. Bustamante and E.M. Bartolome. "TLD Studies in the Philippine Atomic Research Center." IAEA Symposium on New Development in Physical and Biological Detection. Vienna, Nov. 23-29, 1970.

Operating voltage of 925V was selected as the optimum setting since, at this setting, no appreciable change in light output can be observed with fluctuations in voltage.

EXPERIMENTAL RESULTS

a. Reproducibility

Using carefully selected discs of more or less uniform weights (±2%) and thickness (±5%), the precision of the light output was within ±7%. (See Table I). To study the effect of weight and thickness on the reproducibility of the readings, kapis discs of variable weights (ranging from 70 mg. to 220 mg.) and variable thickness (ranging from 15 mils to 35 mils) were exposed to the same dose. The result of this study shows that the reproducibility was reduced to ±25% by using kapis of variable weights and thicknesses. However, no definite relationship between the thermoluminescence and the weights or thickness could be perceived in this study. It is possible that other factors - e.g. - age of the shell, geographical location, climatic conditions as well as weights and thickness - are parameters which singly or collectively, contribute to the overall reduction in reproducibility.

b. Response of Kapis to Various Sources

1. Gamma sources -

The response of kapis to Co^{60} was linear from 50-10^4R (see Fig.1) and fits the model of thermoluminescence versus dose for LiF as suggested by Cameron, et. al.[4] The model assumes an ini-

---

[4] J.R. Cameron, et. al. "Thermoluminescence Versus Dose in LiF: A Proposed Mathematical Model." Inter. Conf. on Luminescence Dosimetry. June 21-23, 1965.

tial number of filled traps (N_o), the probability of creation of new traps by irradiation (α), the probability of filling of traps by irradiation (β), and a maximum number of traps (N_p). The relationship between the observed thermoluminescence (L) as a function of dose (D), is shown by the following mathematical relationship:

$$L = \frac{N_o \beta}{\alpha - \beta} (e^{-\beta D} - e^{-\alpha D}) + \frac{N_p}{\alpha - \beta} \left[\alpha (1 - e^{-\beta D}) - \beta (1 - e^{-\alpha D}) \right]$$

where: N_o = initial number of traps

N_p = maximum number of traps

α = probability for creation of traps

β = probability for filling of traps

N = number of traps (filled and unfilled) at any D

L = number of traps at any D assumed directly proportional to the thermoluminescence

For the response of kapis to Co^{60}, the value of the parameters that would fit the equation of the curve is as follows: $\alpha = 2 \times 10^{-5}$; $\beta = 1.3 \times 10^{-5}$; $N_o = 1 \times 10^{13}$; $N_p = 1 \times 10^{13}$; f (proportionality constant) = 2.32×10^{8}. (See Table II). Exposing the used disc to Co^{60} showed a marked increase in sensitivity. (See Figure 1). The observed thermoluminescence as a function of dose however still follows the above relationship

with the following parameters: $\alpha = 2 \times 10^{-5}$; $\beta = 1.3 \times 10^{-5}$; $N_o = 1.8 \times 10^{13}$; $N_p = 2 \times 10^{13}$, and $f = 2.76 \times 10^{8}$. Comparing the values of the parameters for the first and second irradiation shows an increase in the initial number of traps (N_o) and the maximum number of traps (N_p) for the second irradiation but the probability constants α and β remain the same for this particular radiation source. The response to Ra^{226} is the same as Co^{60} within an error of $\pm 10\%$.

2. X-ray -

Kapis discs were irradiated with different doses of x-rays of various energies: 20, 30, 80, and 180 KV. The response of kapis to x-ray is higher than that of Co^{60}. (See Figure 2). This shows the energy-dependence of this dosimeter especially at low energies. (See Figure 3). At 20KV, the sensitivity is 30X higher than the sensitivity to Co^{60}. While at 180KV, the sensitivity is 7X higher. Due to the heterogeneity of the x-ray beam, however, the precision is poor.

Using the same mathematical model for the relationship between thermoluminescence and dose, the values of α, β, and N_o are the same for all energies of the x-ray used: $\alpha = 9 \times 10^{-3}$; $\beta = 1 \times 10^{-3}$; $N_o = 1 \times 10^{13}$. Only the maximum number of traps (N_p) increased with the energy of the beam from $N_p = 1 \times 10^{12}$ for 20 and 30 KV x-ray; $N_p = 1.3 \times 10^{13}$ for 80KV x-ray, and $N_p = 1.78 \times 10^{13}$ for 180KV x-ray.

3. Neutrons -

Kapis discs were irradiated in fast and thermal neutrons using Pu-Be source. Neutrons were thermalized using 6" of H_2O. No response to Pu-Be source was observed.

OBSERVATIONS AND DISCUSSIONS

The result of the study showed that carefully selected kapis disc can be used as a thermoluminescent dosimeter with a precision of ±10%. Optimum response can be obtained when the kapis discs were placed normal to the beam. The fading of the radiation induced thermoluminescence was observed to be exponential with an average decay constant of .0043 hr^{-1}. (cf. Figure 4).

The study of the effect of heat treatment on the thermoluminescence of kapis showed that pre-irradiation heat treatment at 80°C for 1 hr. to remove natural thermoluminescence reduced the precision of carefully selected disc by ±16%. (See Table III). Studies were also made on the proper post-irradiation annealing procedure for used kapis discs to restore their original precision and sensitivity. All the annealing temperature used: 150°C, 250°C, and 300°C at various intervals of time failed to bring the kapis back to their original sensitivity and precision.

Carefully selected kapis disc can be used as a thermoluminescent dosimeter with a precision of ±10%. If the kapis discs were selected at random, the precision is reduced from ±15% to ±20%. Although the

this precision is still satisfactory considering the low cost and accessibility of kapis, efforts will be exerted to explore the possibility of improving the rather poor statistics of the results. Furthermore, studies on the parameters which might affect the reproducibility of the kapis discs will be undertaken.

BIBLIOGRAPHY

(1) MEDLIN, W.L., "Thermoluminescent Properties of Calcite.", Journal of Chemical Physics, vol. 30, No.2 (1959), p. 451.

(2) BERSOMIN, S.V., "Shellcraft Production in the Philippines.", Philippine Fishing Journal, (January 1967).

(3) BUSTAMANTE, N.T. & BARTOLOME, Z.M., "TLD Studies in the Philippine Atomic Research Center.", IAEA Symposium on New Developments in Physical and Biological Detectors, Vienna, November 23-27, 1970.

(4) CAMERON, J.R. et. al., "Thermoluminescence Versus Roentgens in Lithium Fluoride: A Proposed Mathematical Model.", International Conference on Luminescence Dosimetry, June 21-23, 1965.

ACKNOWLEDGMENT

The authors would like to thank Miss Margaret McIlvaine for assisting in the calculations and Mr. Alejandro J. Mateo for preparing the graphs.

TABLE I

Reproducibility of Kapis Shells

TL (Arbitrary Units)	Weight (mg.)	Thickness (mils)
703	141.5	236
816	143.5	233
829	143.6	236
508	144.05	266
728	145.3	244
715	147.75	257
734	148.65	250
377	148.7	253
696	149.45	242
800	149.95	270
$\bar{X}$ = 752.6 ± 53.6	$\bar{X}$ = 146.21 ± 3.04	$\bar{X}$ = 248.7 ± 1.28

TABLE II

Values of the Parameters for Different Sources

Parameters	X-ray				Co-60	
	20 KV	30 KV	80 KV	180 KV	First Irrad.	Second Irrad.
α	9×10^{-3}	9×10^{-3}	9×10^{-3}	9×10^{-3}	2×10^{-5}	2×10^{-5}
β	1×10^{-3}	1×10^{-3}	1×10^{-3}	1×10^{-3}	1.3×10^{-5}	1.3×10^{-5}
N_o	1×10^{13}	1×10^{13}	1×10^{13}	1×10^{13}	1×10^{13}	1.8×10^{13}
N_p	1×10^{12}	1×10^{12}	1.3×10^{13}	1.78×10^{13}	1×10^{13}	2×10^{13}
f	4.1×10^{8}	7.3×10^{8}	1.45×10^{9}	2.32×10^{8}	2.32×10^{8}	2.76×10^{8}

TABLE III

Effect of Pre-irradiation
Annealing at 80°C for 1 Hour on Thermoluminescence

Unannealed Kapis	Annealed Discs
502	476
446	683
512	484
448	541
478	607
506	476
570	437
$\bar{X}$ = 508.8 ± 59.2 (11.6%)	$\bar{X}$ = 529.1 ± 87.5 (16.5%)

TABLE IV

Fading of Thermoluminescence of Kapis

Time (Hr.)	TL
0	4714 ± 1390
24	4246 ± 1340
48	3048 ± 1122
72	3623 ± 1110
192	2752 ± 0373
360	694
528	505

Fig. 1 IRRADIATION OF CAPIZ DISCS USING Co-60

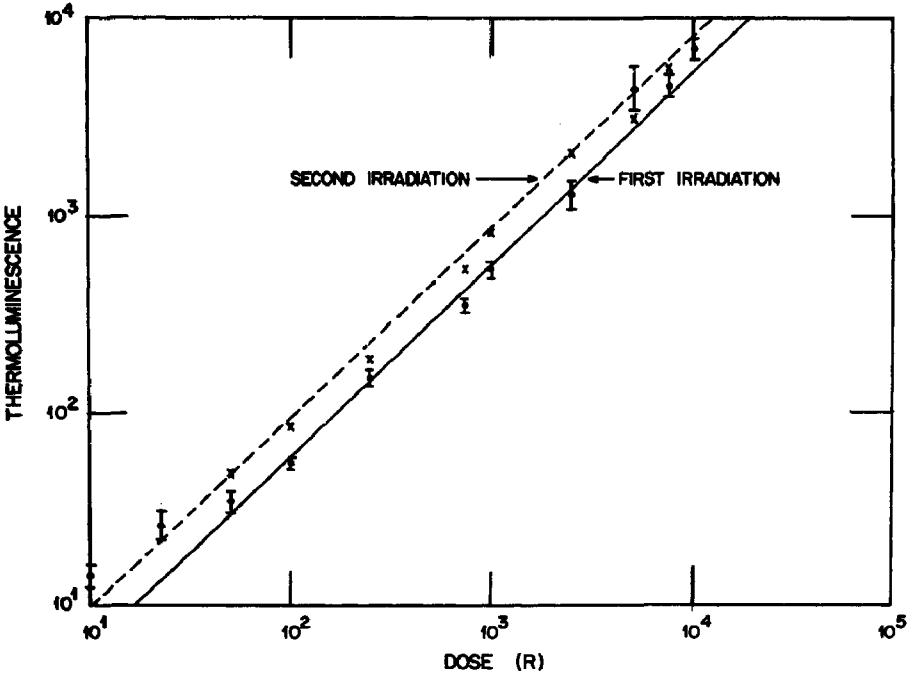

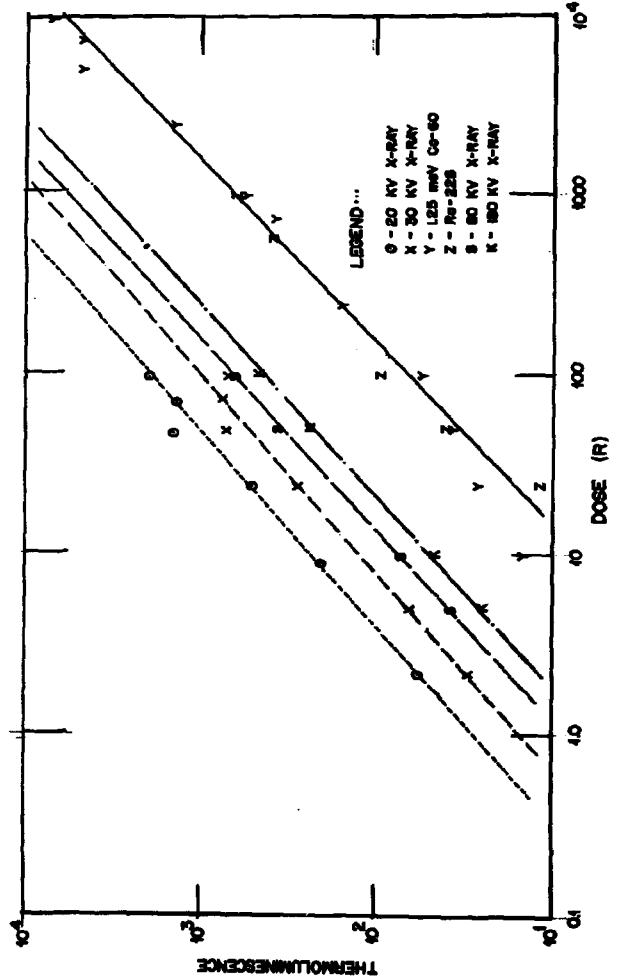

Fig. 2 RESPONSE OF CaPiZ TO VARIOUS SOURCES

Fig. 3 ENERGY DEPENDENCE OF CAPIZ

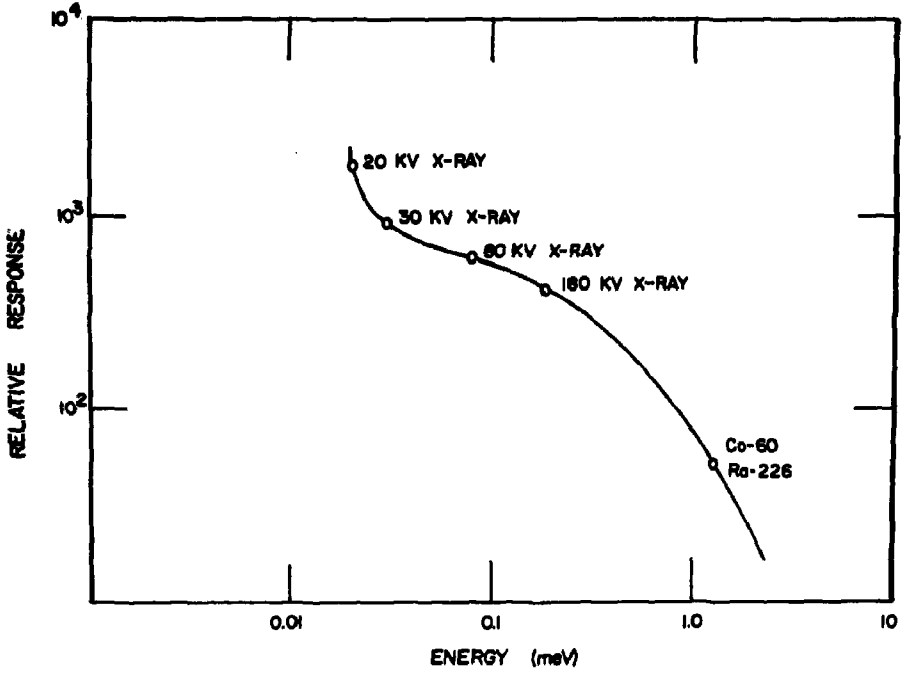

Fig. 4 FADING OF THERMOLUMINESCENCE OF CAPIZ

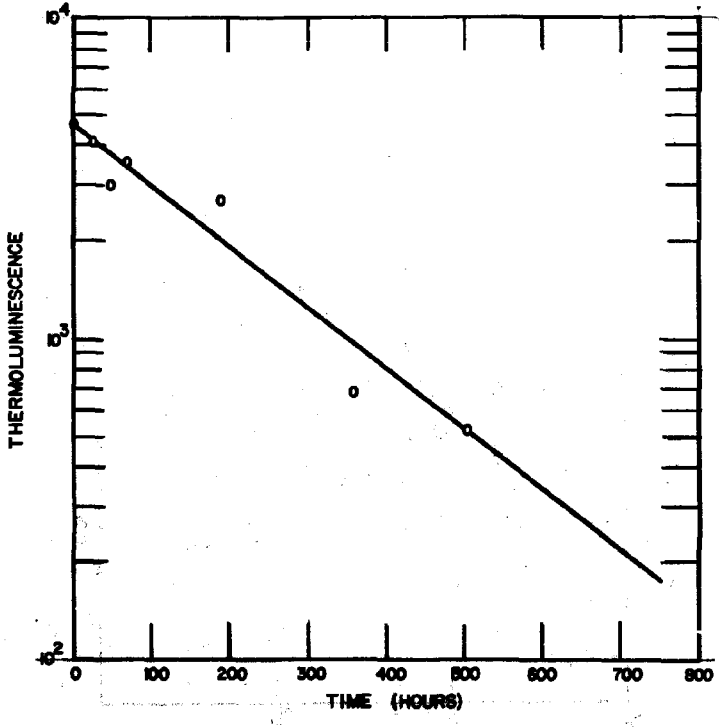

Experimental Modification of Thermoluminescence by Static and Explosive Deformation

David J. McDougall
Loyola College
Montreal, Canada

Numerous examples have been found in rock units where deformational strain appears to have been an important factor in either increasing or decreasing the thermoluminescence response of crystals and crystal aggregates. Variations in impurity elements, natural radioactivity and natural heating do not appear to have been of the proper order of magnitude to have brought about the observed changes.

A series of experiments on the deformation and rupturing of crystals have been conducted which include: crushing and grinding of crystalline material; packing of glass beads in sample holders; formation of pellets from powders under high pressure; loading of slices of crystalline aggregates; and explosive deformation of bars of crystalline aggregates. These experiments demonstrate that three, and possibly five, deformational processes may be involved in modifying the thermoluminescence (i.e., microcracking, formation and annihilation of crystal dislocations, inter-granular gliding and rupturing of crystals, intra-granular gliding and formation of pressure twins). Additional studies have been made of possible relationships between thermoluminescence and (a) stress-strain curves, and (b) dislocation concentrations as revealed by etch-pits. Further investigations are in progress.

In summary, it is clear that moderate deformation may immediately increase certain glow-curve peak heights by as much as several hundred percent without any additional radiation dose. Greater amounts of deformation may

cause an increase in one peak and a decrease in another. Rupture of crystal lattices by fine grinding or explosive shock greatly reduces or destroys the thermoluminescence properties of crystals.

Some Dosimetric Properties of Sintered Activated CaF_2 Dosimeters

D. Uran, M. Knežević, D. Sušnik and D. Kolar
Institute J. Stefan, Ljubljana, Yugoslavia

Abstract

The influence of the preparation and sintering conditions of CaF_2 : Mn powder on the characteristics of sintered thermoluminiscent dosimeters was investigated. Special care was taken to develop the material with a modified glow curve with only one symmetrical peak. Useful sintered dosimeters were prepared and checked at doses of 10^{-3} - 10^{3} R, at γ-rays energies 0.1 MeV - 2 MeV and dose rates of 1 mR/h - 1 kR/h.

The measuring instrument developed for this work is briefly discussed. Due to the slow decay of the thermoluminiscent response, the great reproducibility, and other useful properties, the described dosimeter and reading instrument may be used for personal dosimetry.

Some Dosimetric Properties of Sintered Activated CaF_2 Dosimeters

D. Uran, M. Knežević, D. Sušnik and D. Kolar
Institute J. Stefan, Ljubljana, Yugoslavia

1. Introduction

Thermoluminiscent dosimeters on the basis of Mn activated CaF_2 are well known. It is also well known that the thermoluminiscent properties of dosimeters of this kind greatly depend on the impurity content, method of preparation and on the reading conditions (1,2,3,4,8).

In the present work, some parameters were studied which influence the properties of sintered CaF_2 (Mn) dosimeters. To study the thermoluminiscent properties, an improved reading instrument was developed. The aim of the work was to develop an accidental personal dosimeter with corresponding instrumentation (10,11).

2. Material preparation

Mn activated CaF_2 was prepared by coprecipitation of CaF_2-MnF_2 from the chloride solution with ammonium fluoride. The precipitate was dried and fired up to 1200°C in an inert atmosphere in the usual way (5,6,7). The sintered mass was finely ground to a particle size below 60 μ. Spectral analysis confirmed the high purity of the material, whereas chemical analysis showed the Mn content in CaF_2 to be 1 w/o.

From the CaF_2(Mn) powder and appropriate additions (see below) discs were pressed and sintered in a protective atmosphere at 1100-1200°C. The density of the fired discs

(ϕ = 8 ± 0.1 mm, h = 1.5 ± 0.05 mm) was above 93 % of the theoretical value.

3. Influence of preparation conditions on the properties of CaF_2 : Mn pellets

For the use of CaF_2 : Mn sintered pellets as thermoluminiscent dosimeters, three main problems have to be solved:

1) CaF_2 pellets show very poor thermal shock resistance due to the high thermal expansion coefficient.

2) Mn^{+2} ion in CaF_2 matrix is susceptible to oxidation on heating. The oxidation rate depends, other factors being equal, on the density of the sintered pellets. Gradual deterioration of the CaF_2 : Mn sintered dosimeters is therefore observed after repeated measurements.

3) Glow curve of CaF_2 : Mn tends to be composed of several peaks which appear successively during heating.

Several techniques are known which avoid the difficulties listed above. In our laboratory, best results were achieved by the addition of a small amount (below 10 %) of inorganic binders, mostly glasses, to the CaF_2 : Mn powder prior to sintering.

It was found that the inclusion of glassy phase into the CaF_2 : Mn matrix greatly increases the thermal shock resistance, probably due to lowering of the expansion coefficient. At the same time, the sintering rate was increased and higher density was obtained. As a result, better oxidation resistance during repeated heating in air was achieved. Several glass compositions were tried as additives to CaF_2, for example covar, pyrex, Na_2SiO_3, soda-lime glass etc, and good results regarding the thermal

shock resistance improvement and oxidation resistance were achieved. However, the glow curve was not satisfactory since it was composed of several peaks, probably due to the inclusion and interaction of impurities in CaF_2 : Mn solid solution. The best results, as far as glow curve is concerned, were obtained by the addition of SiO_2. Therefore, this addition was chosen for further experiments in spite of the fact that the thermal shock resistance improvement was not so pronounced as compared with other additions.

The shape of the glow curve depends on the composition of the samples and preparation conditions as well. For example, the heating and cooling rate are found to be critical. Fig.1 shows several emission curves of different samples. Curve No.1 is a typical curve of natural CaF_2 as obtained on our reading instrument and is comparable with published results (3). Curve No 2 is the heating response of a CaF_2 (1 % Mn) pellet containing SiO_2 as an additive. Curve No 3 is a typical curve for a CaF_2 : Mn sample sintered without additions. Curves No 4 and 5 are from a sample with the same composition as No 2, but with faster heating and cooling rates.

It is known that the shape of the glow curves of the TL dosimeters based on CaF_2 : Mn may be changed after annealing at lower temperatures. Therefore it was interesting to note that the glow curve of sample No 2 did not essentially change during heating for 30 minutes at 100°C, whereas the glow curves of other samples were influenced by heating.

4. Reading instrumentation

Two types of readout instruments were developed. The first one is intended for universal laboratory measurements of powdered samples and dosimeters of different shapes. The

second instrument serves for routine measurements of TLD pellets to monitor accident doses.

The measured signal flow sheet in the laboratory reader is shown in the block scheme of Fig.5. Sample S is mounted on the heater H and pushed under the window of the photomultiplier P. Anode and dynodes of the photomultiplier tube are supplied by a high voltage stabiliser. The voltage can be adjusted between 700 and 1200 V.

During the heating of the sample, a light signal is emmitted which is transformed into an electrical signal and amplified with the photomultiplier and amplifier stage A. The signal C is displayed on the plotter.

The second input of the plotter is supplied with a time base signal chosen on the programmer PR. The same programmer also controls the heater H by comparing the signal from the thermal sensor mounted close to the heater, with the preseted heating rate. The programmer enables a choice to be made between 11 different heating rates, from 30°C/sec to 3°C/sec. The upper temperature limit may be continously changed from 100°C to 400°C. The light sensitivity of the instrument may be periodically checked before the measurements by the help of stabilized β light source.

The range of the instrument, using the thermoluminiscent CaF_2 : Mn pellets is between 1 mR and a few KR.

The routine reader is adapted for accident dosimetry. Therefore, a high dose level between 1 R and 999 R is chosen. The instrument is transportable and power supplied by a 12 V battery. It may be operated by unskilled personnel. The whole operation except the inserting of the pellets is automatized. No calibration during measurement is needed and the readout is digital.

This instrument contains the same components as the laboratory version except that instead of an x-y plotter a peak measuring device with an analog to digital converter and nixie display is used. The heater programme is set to a constant heating rate and is trigged by the slider serving to insert the dosimeters into the instrument. When the sample achieves the annealing temperature, the heating programme is reset and the result is transferred to the display.

The measuring head contains an element for preheating the sample to the initial temperature and a device for the exact positioning of the sample before the measurement.

The built-in calibration system automatically adjusts the amplification of the photoelectrical system. The whole measurement is done in 30 seconds.

5. Some dosimeter properties

In following, the characteristic properties of CaF_2 (1 % Mn) sintered dosimeters containing 5 % SiO_2 are given.

5.1. Reproducibility

Table 1 shows thermoluminiscent responses of 100 pellets prepared in 10 separate experiments and irradiated with 230 R (Co-60 source). The measurements were made after 2 hours storage at 20°C in a dark room. The average measured value (229 R) is extremely close to the given value. The standard deviation δ = 2.76 %.

5.2. Linearity

The dosimeters may be used in the range from 10^{-3} R to 10^{3} R. Fig. 2 shows the linear relationship between reader response and exposed dose in the range from 1 R to 1000 R.

5.3. Fading

Fig. 3 shows the reader response in the time interval of the first 6 hours after exposure. The pellets were stored at 20°C and 65°C. After the initial faster decay (4 % in the first 2 hours) the curves descend slowly, reaching 7 % decrease after 24 hours.

It is interesting to note that the temperature in the measured interval (25-65°C) does not influence the fading.

5.4. Energy dependance

It is known that the sensitivity of CaF_2(Mn) dosimeters increases at low energies of irradiation (max. at about 80 KeV). To reduce the sensitivity of the dosimeter at lower energies, a perforated Pb filter was used (Fig. 4). By this means the maximum diference between measured and received doses in the energy range 0.1-2 MeV was lowered to 15 %.

6. Conclusion

The tests confirm that the CaF_2(Mn) dosimeters, prepared with some additions, may be used in connection with the described improved reading instrument for personal dosimetry with high reliability.

References

1. H. Adler, Zur Thermolumineszenz der Seltenen Erden in CaF_2, Acta Physica Austriaca, 12, 4, 357-399, 1959
2. J.H. Schulman, Survey of Luminiscence Dosimetry, in the book: Luminiscence Dosimetry F.H. Attix, ed., USAEC 1967
3. R. Schayes et al, Thermoluminiscent Properties of Natural Calcium Fluoride, in the book: Luminiscence Dosimetry F.H. Attix, ed., USAEC 1967
4. K. Frank, L. Herforth, Zur Thermolumineszenzmetrie mit CaF_2:Mn, Kernenergie 5, 3, 573-176 (1962)
5. T. Niewiodomski, Doping method and some thermoluminiscent and dosimetric properties of LiF:Cu, Ag and CaF_2:Mn, Nukleonika 12, 4, 281-301 (1967)
6. R.J. Ginther, R.D. Kirk, The Thermoluminiscence of CaF_2:Mn, J. Electrochem. Soc. 104, 365-369 (1957)
7. R.C. Palmer, E.F. Blase, V. Poirier, A Coprecipitation Technique for the Preparation of Thermoluminiscent, Manganese Activated Calcium Fluoride (CaF_2:Mn) for use in Radiation Dosimetry, Int. J. Appl. Radiat. Isotop., 16, 11, 737-745 (1965)
8. M. Mihailović, Properties of an Enamel-coated CaF_2:Mn Thermoluminiscent Dosimeter, Conf. Solid State and Chem. Rad. Dosim. in Med. and Biol., Vienna 1967
9. D. Sušnik, D. Kolar, D. Uran; Influence of sinthesys conditions on the properties of thermoluminiscent CaF_2:Mn powders. V. Yug. Symp. on Rad. Prot., P/3/11, Bled 1970
10. D. Uran, A Thermoluminiscent Reading Automate, Symp. on New Developments in Physical and Biological Radiation Detectors, SM/143/18, Vienna 1970

11. D. Uran, F. Kolenko, The TLD Reader 7008, Proc. V. Yug. Symp. on Rad. Prot., P/3/12, Bled 1970.

T A B L E 1

Sample	Charge number									
	1	2	3	4	5	6	7	8	9	10
1.	226	234	232	231	236	227	225	229	238	227
2.	233	238	226	237	236	223	225	234	234	232
3.	235	233	222	230	233	230	230	224	211	240
4.	231	238	228	222	227	221	211	229	216	234
5.	220	240	221	216	236	223	233	230	231	236
6.	226	241	229	231	233	234	223	231	226	230
7.	236	243	225	238	232	228	231	233	227	231
8.	224	230	222	229	237	220	228	230	226	230
9.	231	231	227	220	235	235	231	225	221	223
10.	236	212	225	218	227	228	226	223	222	232
$\bar{D}_{10}$	229,8	234,0	225,7	227,2	233,2	226,9	226,3	228,8	225,2	231,2

$\sigma_{[\%]}$ = 2,76% $\bar{D}_{100}$ = 229

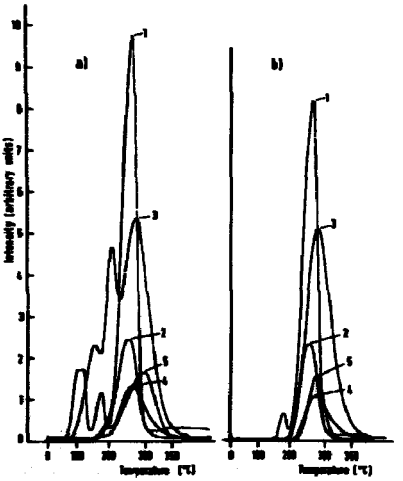

Fig.1 a) Glow curve of various TL materials stored after irradiation at room temperature.

b) Glow curve of the same samples stored at 100°C.

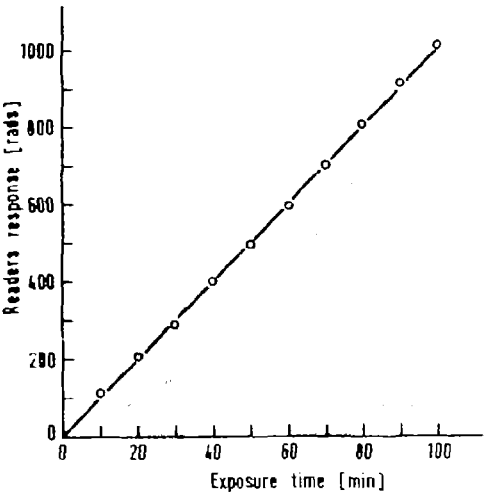

Fig.2: Readers response, corresponding to the peak height vs. exposure time (Co^{60} source).

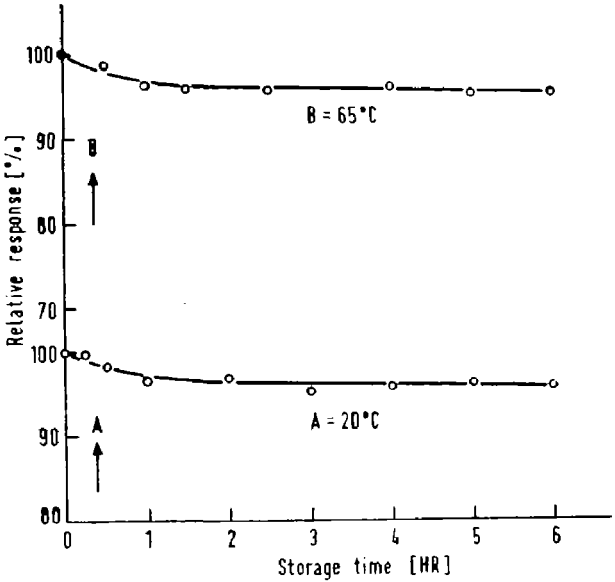

Fig.3: Loss of stored signal in TLD. (A) at room temperature, (B) at temperature 65°C.

Fig.4: Dosimeter badge with perforated shield.

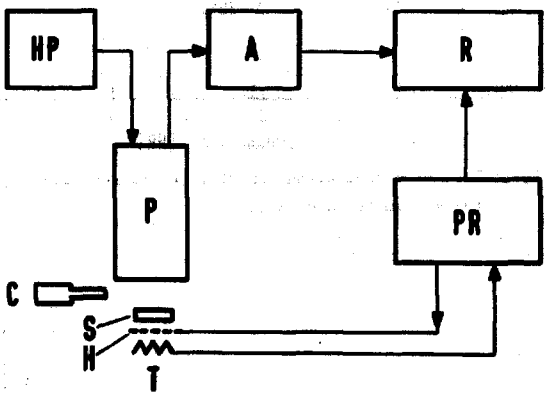

Fig.5: Schematic diagram of thermoluminiscence reader.

Panel Discussion

K. Becker

Ladies and gentlemen, the Third International Conference on Luminescence is now coming to an end. I would like to thank all those who have contributed to the success of this meeting, the speakers, the participants in the discussions, and most of all Vagn Mejdahl and his coworkers for their excellent organization. Twenty-seven countries and three international organizations have been represented, and I think that those of you who attended the first two conferences will agree that the contributions have not only grown in number, but also in quality since our first conference in Stanford. Perhaps there have been too many papers, and as chairman of the program committee I apologize for the crowded schedule. It would probably have been better to have a little more time for Jack Fowler's jokes and other important things, in particular for discussions. The large number of contributions seems to imply that the interest in this area is really so strong that we should not wait another three years for another fourth conference on this topic; but perhaps the interest in this area has reached a peak and will decline in the future. We will have to find that out, and it has been suggested by Jim Schulman, who unfortunately could not attend, that a "Standing Committee" should be formed which should decide if we should have another conference, and if so, where and when it should take place. I would like to propose that Herb Attix, Arthur Scharmann and Vagn Mejdahl should become first members of this committee.

We have already received three invitations for the next conference, namely Mexico City, Jerusalem, and Paris. The choice will be among the topics to be discussed by the standing committee, but it seems to me that Paris may be most easily accessible from East and West. One might also consider to have a next Luminescence Dosimetry Conference (assuming there will be one) in connection with another international meeting on a similar subject, thus simplifying attendance for those who come from very far away.

Now let us begin the discussion with Dr. Scharmann, who will briefly look into some of the more basic aspects of our work and try to summarize his impressions.

A. Scharmann

In this lecture hall there are two groups of persons, a bigger one who may ask: Do these methods work or not? and a smaller group, who is also interested in the basic facts of things going on in the phosphors and the crystals. I would like to mention that all kinetic models which have been

presented at all these conferences had nearly nothing to do with the physics of the crystals. If you speak of frequency factors 10^{30}, these are parameters depending on a special model, not on physics in the substance. If you believe in first-order kinetics without retrapping, you will get the Randall and Wilkin's model. Then you determine in this model trap depths and the frequency factor, and if you use this model, since most processes are not of the Randall and Wilkin's type, you find frequency factors which have nearly nothing to do with physics going on. Frequencies of 10^{30} are not reasonable to a solid-state physicist, and if you investigate TL and thermally stimulated or optically stimulated EE, you cannot explain all the effects only by measuring TL or EE; you have to investigate conductivity, colour centres or absorption, you have to make some EPR or ESR measurements, etc., and the combination of all these measurements leads to a better picture of things. I hope that at the next conference, if there should be one, there will be introductory lectures on basic methods and on basic models. Perhaps some of you don't read the Physical Review and Physica Status Solidi. There have in the last years been about four or five papers concerned with the validity of these kinetic models; two papers are by my former students, Peter Brückalich and Paul Kelly: this is in the Physical Review. Some papers of my group have been published in the Physica Status Solidi.

The explanation of such effects is not dosimetry that is correct, but this type of papers should also be at such a conference because a solid-state physicist can learn a lot from a physicist in dosimetry, and dosimetrists can learn something from the thinking of a solid-state physicists.

Becker

Our next panel member is Dr. Maushart who will, I think, look into some of the practical aspects and may also say a few more friendly words about RPL.

R. Maushart

Ladies and gentlemen. With regard to RPL you are now placed on a steep gradient between theory and practice. I did not know the results of Herb Attix's survey which he showed just before lunch. I was most impressed, and if I could believe that Herb Attix's figures were really representative, I would be compelled to say that RPL dosimetry doesn't exist, and that it has no future. Nevertheless, if I should make a guess, I would say that within five years or so the relation between TLD and TLD and RPL dosimetry would not be

50 to 50 to 0, but about 40 to 40 to 20 at the least. However, I am tempted to wonder what would have happened, and what the picture would have looked like today if Schulman had invented the Yokota glass in the early fifties instead of the Schulman glass.

Otherwise there is some work in progress with the phosphate glass dosimeters, some important work I think. The first we should mention is the laser excitation; we have heard some papers about this at this conference. Several people are working on it: Kastner at Argonne, Regulla at Munich, Yokota has been working on it too, I think, and this should give us an opportunity to go down with measurable doses in the phosphate glass and to distinguish the dirt effect. Secondly we have the scanning of the glass to evaluate the distribution of the fluorescence intensity in the glass and to see from this the radiation quality and the direction of radiation in the glass, that is the original work by Kiefer and Piesch in Karlsruhe and Yokota is working on it too, and we have heard that Toivonen is working on it as well. This may present some interesting aspects; I have heard a proposition from Aurand in Berlin that one could make sort of a phosphate glass brick mosaic and place it in the beam of an X-ray machine, and then by the distribution of the fluorescence intensity in the brick you could with this one measurement see the regularity of the beam, you could see the distribution of the energy quality of the beam. A brick like this could be sent to the users of the X-ray machine and could then be sent back to some central office for evaluation, that is perhaps a quite interesting aspect. The third thing is the low-energy measurements with the glasses. You have two possibilities: you can work on the glass composition to have a lower inherent energy dependence, and you can work on the evaluation method as Piesch and also Yokota did; that is mentioned in our paper, or you can combine both methods, you can have glasses with lots of compositions and with suitable evaluation methods that perhaps would give you the possibility to go lower down in energy measurements. Fourthly we have the uses of the glasses as neutron dosimeters by means of the activation of the glass components; again Piesch has worked on this, mainly on the aspects of accident dosimetry that could be covered by this. We further have the possibility of direct indication of the absorbed dose in a critical organ from the form of the filtering of the glass, this work is done again at Karlsruhe by Piesch. Finally I would like to mention the ease of evaluation by automation of the process and by use of more computerised data evaluation, and I think that all these things together give a future to the phosphate glass dosimeters even in spite of the fact that much more TL dosimeters are used now at the moment for the routine personnel dosimetry than phosphate glasses.

Becker

I think Jack Fowler does not need any introduction. I think he will focus more on the biomedical aspects - or on jokes - I don't know.

J.F. Fowler

Klaus has offered me spare time as long as the jokes are good. I have a joke or two appropriate to end of conferences. I won't tell you whether this one is true or not, but on the first day I arrived in Copenhagen I went walking in that nice little park down by the Mermaid, and I saw a number of very beautiful Danish girls, but in particular, one of them was wearing purple trousers, I smiled at her and she smiled back, but not very much. On the next day I went walking in the same park, and there was the same girl, and this time she was wearing a very pretty white miniskirt. I smiled at her, she smiled back - a big grin. On the next day I went back again hoping to meet her; there she was wearing some very attractive red hot pants and I said hello, and she winked and passed me a note. I couldn't wait to get back to the hotel room to open it, and I got back and I opened it and it said: "I am very patient with tired scientists".

Biomedical applications. Well - if you want another joke - biomedical applications is not a joke: Neil Armstrong, the first astronaut on the moon, met a dosimetry expert and they got talking, and the dosimetry expert said he had been to meetings in Copenhagen and Japan, Stanford, Germany, Czechoslovakia, Italy, Spain, Taiwan, and so on; then he said: Oh I mustn't talk like this - tell me about your trips. And Neil Armstrong said: I have only been to one place - Neil Armstrong was the first man on the moon.

Medical and biological applications. Obviously useful, obviously going strong, continuing well and progressing, obviously these will appear as papers or as parts of papers at all future radiological congresses; there is no problem at all of getting these dispersed. I think even perhaps improvements in technique will appear at all sorts of congresses, whether we have any future meetings devoted to solid-state dosimetry or not. The big advantage of the solid-state methods, whatever they are, are in their shape and small size, and this seems to be equally true in human applications and in mouse dose measurements. Now, the precision and reliability can be remarkably good, but only in skilled hands - it seems to me that no less skill is required still to run a first-class TLD system as described by Suntha and by others, than otherwise required for a system based on ionisation chambers. We all keep hoping that it

is going to become easier - and perhaps it will - but it hasn't yet become all that much easier, except I think it's clear that the commercial manufacturers have moved much more solidly and usefully into solid-state devices than they have done into ionisation chambers, and again the various shapes are easy to do with the solid systems.

Now the solid-state systems are still not really quite precise enough for the really precise measurements, and I mean here the basic calibrations of a cobalt machine the first time you get it; it is rather a special application that doesn't apply to everybody's use. Also for example the distribution of the field of a treatment machine for treating cancer for feeding into a computer. And I will repeat again what I said the other night giving you the proper reference: L.J. Shukovsky in the American Journal of Roentgenology 108, 27 (1970) reported results on treatments by external beams of about a hundred cases of head and neck, and when they had surveyed a change in dose, which they actually achieved accidentally: when they surveyed this across a twenty per cent change in dose it made a difference of sixty extra patients in a hundred patients cured of cancer. I think this is a particularly interesting result because there are so few, perhaps only one other in the literature - not so well written up; this means that a 3% drop in dose right in the region where the cancer is believed to be, means ten patients not cured, and correspondingly too much dose means you burn them a little bit. Now, these 3% is a smaller change than can be detected by a clinician looking at normal tissue, he might pick up 5%, he might pick up 7%, but after all that's what we have got dosimetry for, to be a little bit better than clinicians looking at reactions in patients. But it sounds to me an encouragement for these methods to push for an even better precision than can be achieved by experienced persons working in this field. We don't just have to sit and be satisfied with the 2 or 3% precision that has been available I think from John Cameron's early work, it's not that much better with most solid-state systems already unless you are very skilled at it, and ionization chambers of course are difficult to beat - except where dose rate is high, a few tens of rads per minute, or where a size of 3-5 mm diameter does matter - because these can give a reproducibility of 0.2-0.3%, and the quality correction factors are quite comparable with those shown for example by paper 71 (S.K. Dua et al.) which we just heard about this morning for various TLD systems, so don't neglect ionization chambers. Maybe we should arrange to have a little session including what they can do in some future solid-state plus other types of dosimetry meetings. Nevertheless, much bigger errors than this high-precision measurement creep in very easily if you don't take care about it, and in clinical applications TL dosimetry, even at

the 2 or 3% precision level, is very useful for avoiding the 7 or 10% errors that you can easily get by failure to check frequently or by some carelessness in setting up. And I am left with one question which I hope someone in the room will answer. Does it look as if BeO with its remarkably constant TL temperature peak even with different impurities, does it look as if this substance will be less liable to artifacts, and I mean things that need less skill to avoid trouble, than the lithium fluoride or lithium borate systems?

Becker

Dr. Carlsson did not attend our briefing before this panel discussion so I have not the slightest idea what he will talk about.

C.A. Carlsson

I must thank Dr. Fowler. He has just talked about most of the things I had prepared. For this reason I will only give some aspects on the complex behaviour of all the solid-state dosimeters we work with. If a dosimeter shows effects such as supralinearity, radiation-induced sensitization and damage, temperature effects and so on, it requires no doubt skill to use it for meaningful dosimetry. Those effects are, however, not only a disadvantage. They carry a lot of information about the radiation as well as about the dosimeter material. From supralinearity or sensitising effects we can make conclusions about LET-distributions, interacting tracks of primary particles or delta rays, specific energy-imparted distributions, etc. In a program conducted by Dr. van de Voorde to determine the absorbed dose in water in an unknown radiation field around the big proton accelerator at CERN in Geneva, a lot of different dosimeters have been placed in the same positions and their readings compared. From knowledge of energy absorption properties and LET-dependence of the different dosimeter systems, some conclusions of the radiation field can be made. We have contributed with a LiF-tandem dosimeter, one sensitized, the other not. The ratio of their readings gives information of the dose average LET necessary for estimating the absorbed dose.

Then I want to mention the difference in working with a naked dosimeter such as many solid-state dosimeters and a dosimeter with a wall like the ionization chamber. We have to be more cautious about basic dosimetry principles such as charged-particle equilibrium or cavity theory.

Becker

Finally we will have Herb Attix with some philosophical remarks, I guess.

F.H. Attix

First let me respond to Dr. Maushart's remarks about my survey not showing any future for RPL dosimeters in personnel monitoring. That survey ("A Current Look at TLD in Personnel Monitoring," in press, Health Physics) unfortunately did not address itself to the future of RPL, but only to TLD. Even so it was a rather long questionnaire, requiring considerable patience on the part of those filling it out. Therefore it is not possible for me to make any realistic estimate of the portion of personnel monitoring which will be done by RPL dosimeters, say, 5-10 years from now. My guess would be less than the 20% prediction of Dr. Maushart, however.

Among the papers presented here there were a number which interested me greatly, but it would be impossible to mention all these now. The paper by Sunta, Bapat, and Kathuria, however, contained a very satisfying verification of the interacting-track model, as opposed to the deep-trap-saturation model, for explaining supralinearity and radio-sensitization effects in LiF(TLD-100) and perhaps other TL materials as well. These findings seem to fit together nicely with the work of Podgorsak, Moran, and Cameron, who find that the degree of supralinearity observed in the glow peaks was proportional to the cube of the absolute glow-peak temperature over the range from -128°C to +186°C (the latter being the usual dosimetry peak). This suggests to me that the number of luminescent centers (including those in other charged-particle tracks) available to a charge-carrier after its release from a trap is proportional to the volume of a sphere having its radius equal to the charge-carrier's migration range, and that the migration range is approximately proportional to the absolute temperature. I believe this kind of temperature dependence would be more characteristic of a hole than of a electron, incidentally, so the issue of hole-vs-electron release may not yet be dead. Along this line, Dr. Rossiter's paper on LiF doping has verified earlier reports that titanium was an essential co-activator in LiF(TLD-100); according to Block at the Gatlinburg conference the Ti ion has a trapped electron associated with it, and serves as the luminescence center, which again points to holes as the TL charge-carriers. This, of course, does not dispose of the argument favoring electrons as TL charge carriers, based on the regeneration of glow peaks by F-center optical excitation. We have been arguing about

models for thermoluminescence in LiF since the 1965 meeting, and I expect we will continue to do so for some time to come.

Which brings me to a general comment about future meetings of this series. I think we should objectively examine the need for such meetings each time we have one, and terminate the series when it ceases to fulfill a worthwhile purpose. However, I am not suggesting that we have already reached that point in time.

After a discussion that has not been recorded, the conference was closed by Dr. Scharmann.

AUTHOR LIST

LIST OF PARTICIPANTS

AUSTRIA

Aiginger, H.	Atominstitut der Österreichischen Hochschulen, Schüttelstrasse 115, A-1020 Wien
Naba, K.	Österreichisches Studiengesellschaft für Atomenergie, Institut für Strahlenschutz, Lenaugasse 10, A-1082 Wien

BELGIUM

Eggermont, G.	Central Department for Radiation Protection, Institute for Nuclear Sciences of the Gent State University, Proeftuinstraat 86, B-9000 Gent
Ghoos, Leo	Controle-Radioprotection, c/o Laboratories du C.E.N., B-2400 Mol-Donk
Jacobs, R.	Central Department for Radiation Protection, Institute for Nuclear Sciences of the Gent State University, Proeftuinstraat 86, B-9000 Gent
Pendurkar, H.K.	Laboratoires du C.E.N./S.C.K., Boeretang 200, B-2400 Mol
Piron, Auguste	Service Radiotherapie, Institut Jules Bordet, 1 Rue Heger-Bordet, B-1000 Bruxelles
Segaert, O.	Central Department for Radiation Protection, Institute for Nuclear Sciences of the Gent State University, Proeftuinstraat 86, B-9000 Gent

BRAZIL

Mayhugh, M.R.	Instituto De Energia Atômica, Cidade Universitaria, CX. Postal, 11.049 - Pinheiros, São Paulo SP 5508
Okuno, Emico	Instituto De Energia Atômica, Cidade Universitaria, CX. Postal, 11.049 - Pinheiros, São Paulo SP 5508
Teixeira da Cruz, M.	Instituto De Energia Atômica, Cidade Universitaria, CX. Postal, 11.049 - Pinheiros, São Paulo SP 5508
Watanabe, Shigueo	Instituto De Energia Atômica, Cidade Universitaria, CX. Postal, 11.049 - Pinheiros, São Paulo SP 5508

BULGARIA

Mishev, Ilija	Institute of Physics and Nuclear Research, Bulgarian Academy of Sciences, 72 Bul. Lenin

CANADA

Jones, A. R.	Health Physics Branch, Atomic Energy of Canada Limited, Chalk River Nuclear Laboratories, Chalk River, Ontario
Lévesque, R.	Division of Physics, National Research Council of Canada, Ottawa 7
McDougall, D. J.	Loyola College, 7141 Sherbrooke St. W., Montreal 262, Quebec
Saunders, J. E.	The Ontario Cancer Foundation, Hamilton Clinic, Henderson General Hospital, Hamilton 53, Ontario

CZECHOSLOVAKIA

Knittl, Miroslav	Monokrystaly - Turnov, Leninova 175, Turnov
Mánek, Břetislav	Monokrystaly - Turnov, Leninova 175, Turnov
Spurný, Z.	The Nuclear Research Institute of Czechoslovak Academy of Sciences, Prague 8

DENMARK

Bøtter-Jensen, Lars	Danish Atomic Energy Commission, Research Establishment Risø, DK-4000 Roskilde
Christensen, P.	Danish Atomic Energy Commission, Research Establishment Risø, DK-4000 Roskilde
Ennow, Klaus	Radiation Hygiene Laboratory, National Health Service of Denmark, Frederikssundsvej 378, DK-2700 Brønshøj
Hjortenberg, Per	Danish Atomic Energy Commission, Research Establishment Risø, DK-4000 Roskilde
Kooy, Peter van der	Radiofysisk Laboratorium, Odense Sygehus, DK-5000 Odense
Lassen, Erling	Radiation Hygiene Laboratory, National Health Service of Denmark, Frederikssundsvej 378, DK-2700 Brønshøj
Majborn, Benny	Danish Atomic Energy Commission, Research Establishment Risø, DK-4000 Roskilde
Mejdahl, Vagn	Danish Atomic Energy Commission, Research Establishment Risø, DK-4000 Roskilde
Onsgaard, Jens	Odense Universitet, Niels Bohrs Alle, DK-5000 Odense
Radak, B.	Danish Atomic Energy Commission, Research Establishment Risø, DK-4000 Roskilde

FINLAND

Toivonen, M. J.	Institute of Radiation Physics, Box 268, SF-00100 Helsinki 10

FRANCE

Carpentier, S.	Carbonisation Entreprise et Ceramique, Département Nucléare N°469, B.P. 60-92 Montrouge
Chapuis, A.M.	Commissariat a l'Energie Atomique, Centre d'Etudes Nucléares, Fontenay-aux-Roses, B.P. N°6
Cluchet, J.	Commissariat a l'Energie Atomique, 29-33 Rue de la Fédération, B.P. N°510, Paris - XV^{e}
François, H.	Résidence de l'Observatoire, 8, Rue du Bel-Air, 92 - Meudon-Bellevue
Guiho, J.P.	Laboratorie de Métrologie des Rayonnement Ionisant, C.E.N. Saclay, B.P. N°2, Gif-sur-Yvette
Monnin, M.	Laboratoire de Physique Corpusculaire, Universite de Clermont, 34, Avenue Carnot, F 63 - Clermont-Ferrand
Parmentier	Commissariat a l'Energie Atomique, 29-33 Rue de la Fédération, B.P. N°510, Paris - XV^{e}
Petel, M.	Commissariat a l'Energie Atomique, Centre d'Etudes Nucléares, Fontenay-aux-Roses, B.P. N°6
Portal, G.	Commissariat a l'Energie Atomique, Centre d'Etudes Nucléares, Fontenay-aux-Roses, B.P. N°6
Tabardel-Brian, R.	Commissariat a l'Energie Atomique, 4 Rue Meyne-Claire, Orange 84
Vetillard, P.	Saphymo, 51 Rue Amiral Mouchez, Paris 13
Zara, J.	Bureau National de Métrologie, 1 Rue Mongolfier, Paris 3^{e}

GERMANY, DDR

Hafke, P.	Radiologische Klinik, Universität Rostock, Rostock
Herrmann, D.	Staatliche Zentrale für Strahlenschutz der Deutschen Demokratischen Republik, Naturwissenschaftlich-Technischer Bereich, Abteilung Physik und Technik, 1162 Berlin-Friedrichshagen, Müggelseedamm 336
Herzog, G.	Universität Greifswald, Section Chemie, Uhlenhustr. 2, 22 Greifswald
Hübner, K.	Sektion Physik/GDR, Technische Universität Dresden, 8027 Dresden, Zellescher Weg 19
Weber, Karl-Heinz	VEB RFT Messelektronik "Otto Schön", Dresden, DDR 8010 Dresden, Postschliessfach 14, Fetscherstrasse 70

GERMANY, Fed. Rep.

Becker, M.	I. Physikalisches Institut der Universität Giessen, Leigesterner Weg 104-108, 63 Giessen
Dade, M.	Frieseke und Hoepfner GMBH, 852 Erlangen, Schliessfach 72
Fängewisch, G. L.	I. Physikalisches Institut der Universität Giessen, Leihgesterner Weg 104-108, 63 Giessen
Hillenkamp, F.	Abteilung für Kohärente Optik, Gesellschaft für Strahlen- und Umweltforschung, D-8042 Neuherberg/München, Ingolstädter Landstr. 1
Hoegl, A.	Frieseke und Hoepfner GMBH, 852 Erlangen, Schliessfach 72
Holzapfel, G.	Physikalisch-Technische Bundesanstalt Institut Berlin, 1 Berlin 10, Abbestrasse 2-12, Berlin
Jähnert, Bernd	Abteilung Strahlenphysik, Hahn-Meitner-Institut für Kernforschung, Berlin, 1 Berlin 39, Glienicker Strasse 100, Berlin
Kramer, J.	Physikal.-Techn. Bundesanstalt, 33 Braunschweig, Bundesallee 100
Kriegseis, W.	I. Physikalisches Institut der Universität Giessen, Leihgesterner Weg 104-108, 63 Giessen
Maushart, R.	Berthold/Frieseke GMBH, Postfach: 76, Bergwaldstrasse 30, 7500 Karlsruhe-Durlach
Nink, R.	Physikalisch-Technische Bundesanstalt Institut Berlin, 1 Berlin 10, Abbestrasse 2-12, Berlin
Pychlau, P.	Physikalisch-Technische Werkstätten, 7800 Freiburg, Lörracherstrasse 7
Regulla, D.F.	Institut für Strahlenschutz, Gesellschaft für Strahlen- und Umweltforschung, D-8042 Neuherberg/München, Ingolstädter Landstr. 1
Scharmann, Arthur	Physik. Inst. der Universität Giessen, Leihgesterner Weg 104-108, 63 Giessen
Tumbrägel, Gerd	Erprobungsstelle 53 der Bundeswehr, Postfach 342, 3042 Munster

GREECE

Karaoulani, E.	Greek Atomic Energy Commission, Nuclear Research Center "Democritos", Athens

HUNGARY

Bóros, László	Radiological Clinic of Med. University, Budapest, VIII. Üllői-út 78

INDIA

Dua, S. K.	Health Physics Division, Bhabha Atomic Research Centre, Trombay, Bombay-85
Sunta, C. M.	Health Physics Division, Bhabha Atomic Research Centre, Trombay, Bombay-85

ISRAEL

Adam, G.	Nuclear Research Centre Negew, P.O.B. 9001 Beer - Sheva
Avni, A.	Israel Atomic Energy Commission, Soreq Nuclear Research Centre, Yavne
Schlesinger, Tuvia	Israel Atomic Energy Commission, Soreq Nuclear Research Center, Yavne
Yerushalmi, A.	The Weizmann Institute of Science, P.O. Box 26, Rehovot

ITALY

Busuoli, G.	Comitato Nazionale Per l'Energia Nucleare, Centro Di Calcolo, 40138 Bologna, Via Mazzini 2
Carfi, Nicola	Centro Informazioni Studi Esperienze, Casella postale 3986, 20100 Milano
Rimondi, O.	Comitato Nazionale Per l'Energia Nucleare, Centro Di Calcolo, 40138 Bologna, Via Mazzini 2
Rotondi, Ettore	Comitato Nazionale per l'Energia Nucleare, CSN Casaccra, C.P. 2400, 00100 Roma
Scarpa, G.	Comitato Nazionale per l'Energia Nucleare, P.O. Box 2400, 00100 Roma

JAPAN

Higashimura, Takenobu	Research Reactor Institute, Kyoto University, Kumatori-cho Sennan-gun, Osaka-fu
Nakajima, Toshiyuki	Division of Physics, National Institute of Radiological Sciences, 9-1 4-chome, Anagawa, Chiba-shi

MEXICO

Moreno, A. y Moreno	Institute of Physics, University of Mexico

THE NETHERLANDS

Broers-Challiss, J.E.	Radiobiological Institute of the Organization for Health Research TNO, 151 Lange Kleiweg, Rijswijk
Julius, H.W.	Radiologische Dienst van de Gezondheidsorganisatie, Utrechtseweg 310, Arnhem
Puite, K.J.	Institute for Atomic Sciences in Agriculture, 6 Keyenbergseweg, P.O. Box 48, Wageningen
Weber, J.	Interuniversitair Reactor Instituut, Berlageweg 15, Delft

NORWAY

Gravdahl, Trygve	Institutt for Atomenergi, Box 40, Kjeller
Omsveen, Per	Helsefysisk Avdeling, Rikshospitalet, Oslo
Storruste, Anders	Fysisk Institutt, Universitetet i Oslo, Postboks 1048, Blindern, Oslo 3
Strickert, Trond	Statens Institutt for Strålehygiene, Montebello, Oslo 3

POLAND

Niewiadomski, Tadeusz	Institute of Nuclear Physics, Cracow 23, Radzikowskiego 152

PORTUGAL

Vaz Carreiro, João Jose	Junta de Energia Nuclear, Laboratorio de Fisica e Engenharia Nucleares, Estrada Nacional N° 10, Sacavém

SWEDEN

Berggren, E.	Centrallasarettet, S-631 88 Eskilstuna
Bertilsson, Gudrun	Radiofysiska Institutionen, Lasarettet, 221 85 Lund
Carlsson, Carl A.	Department of Radiation Physics, Linköping University, The Medical School, S-581 85 Linköping
Carlsson, Gudrun Alm	Department of Radiation Physics, Linköping University, The Medical School, S-581 85 Linköping
Forslo, Hans	Department of Radiation Physics, Linköping University, The Medical School, S-581 85 Linköping
Käsoffsky, L.	Department of Radiation Physics, Linköping University, The Medical School, S-581 85 Linköping
Rudén, Bengt-Inge	National Institute of Radiation Protection, Fack, S-104 01 Stockholm 60
Samuelsson, Christer	Radiofysiska Institutionen, Lasarettet, 221 85 Lund
Spanne, Per	Department of Radiation Physics, Linköping University, The Medical School, S-581 85 Linköping
Westerholm, Lars	Umeå Universitet, Institutionen för Radioterapi och Radiofysik, Avdelningen for Radiofysik, 901 85 Umeå
Widell, C.-O.	Aktiebolaget Atomenerg., Studsvik, 611 01 Nyköping 1

SWITZERLAND

Hunzinger, W.	c/o Public Health Administration, Falkenplatz 11, CH-3012-Bern
Rottenberg, W.	c/o Public Health Administration, Falkenplatz 11, CH-3012-Bern

UNITED KINGDOM

Aitken, M. J.	Research Laboratory for Archaeology and The History of Art, 6 Keble Road, Oxford OX1 3QJ
Alldred, J. C.	Research Laboratory for Archaeology and The History of Art, 6 Keble Road, Oxford OX1 3QJ
Brown, L. D.	Edwards Radiation Laboratories, North East London Polytechnic, Romford Road, London E15 4LZ
Burgess, C. D.	HM Factory Inspectorate, Industrial Hygiene Section, Baynards House, 1 Chepstow Place, London W. 2
Fleming, S. J.	Research Laboratory for Archaeology and The History of Art, 6 Keble Road, Oxford OX1 3QJ
Fowler, J. F.	Research Unit in Radiobiology, Mount Vernon Hospital, Northwood, Middlesex HAG2RN
Göksu, Yeter	Department of Physics, The University of Birmingham, P. O. Box 363, Birmingham B15 2TT
Harvey, J. R.	Central Electricity Generating Board, Research and Development Department, Berkeley Nuclear Laboratories, Berkeley, Gloucestershire GL13 9PB
Marshall, M.	Atomic Energy Research Establishment, Harwell, Bldg. 364, Didcot, Berkshire
Marshall, T. O.	National Radiological Protection Board, Clifton Avenue, Belmont, Sutton, Surrey
Mason, E. W.	National Radiological Protection Board, Scottish Centre, 11, West Graham Street, Glasgow C. 4.
Pratt, P. L.	Imperial College of Science and Technology, Department of Metallurgy, Prince Consort Road, London SW 7
Robertson, M. E. A.	D. A. Pitman Limited, Mill Works, Jessamy Road, Weybridge, Surrey
Rossiter, M. J.	National Physical Laboratory, Teddington, Middlesex
Shearer, D. A.	Medway and Gravesend Hospital Management Committee, Radiotherapy Centre, St. William's Hospital, Rochester, Kent
Smith, J. W.	Atomic Energy Research Establishment, Harwell, Didcot, Berkshire
Stoneham, D.	Research Laboratory for Archaeology and The History of Art, 6 Keble Road, Oxford OX1 3QJ

Tite, M.S.	Department of Physics, University of Essex, Wivenhoe Park, Colchester, Essex
Wintle, A.G.	Research Laboratory for Archaeology and The History of Art, 6 Keble Road, Oxford OX1 3QJ
Yorke, A.V.	Department of Nuclear Science and Technology, Royal Naval College, Greenwich, London SE 10

USA

Attix, F.H.	US Naval Research Laboratory, Nuclear Sciences Division, Code 6603A, Washington D.C. 20390
Becker, Klaus	Health Physics Division, Oak Ridge National Laboratory, P.O. Box X, Oak Ridge, Tennessee 37820
Claffy, E.W.	Code 6062, Central Materials Research Activity, US Naval Research Laboratory, Washington D.C. 20390
Ehrlich, Margarete	Dosimetry Section, National Bureau of Standards, Washington, D.C. 20234
Gooden, David S.	Saint Francis Hospital, 6161 South Yale Avenue, Tulsa, Oklahoma 74135
Han, Mark	Museum Applied Science Center for Archaeology, 33rd and Spruce Streets, Philadelphia, Pennsylvania 19104
Jarrett, R.D.	Dosimetry Section, Radiation Sources Division, Food Laboratory, US Army Natick Laboratories, Natick, Massachusetts 01760
Jones, D.E.	University of California, Lawrence Radiation Laboratory, Box 808, Livermore, California 94550
Landauer, R.S.	Glenwood Science Park, Glenwood, Illinois 60425
Markow, B.	United States Army Material Command, Scientific and Technical Information Team-Europe, I.G. Hochhaus Bremerstrasse, Room 750, 6 Frankfurt am Main, West Germany
Moran, P.R.	University of Wisconsin, Department of Physics, 475 North Charter Street, Madison 53706, Wisconsin
Stoebe, Thomas G.	University of Washington, Department of Mining, Metallurgical and Ceramic Engineering, Seattle, Washington 98105
Suntharalingam, N.	Jefferson Medical College of Thomas Jefferson University, Philadelphia 19107
Webb, G.A.M.	Teledyne Isotopes, Westwood Laboratories, 50 Van Buren Avenue, Westwood, New Jersey 07675

YUGOSLAVIA

Knežević, M.	Institute J. Stefan, 61001 Ljubljana, Jamova 39

Mihailović, Mirjana	Institut za Fiziko, Medicinska Fakulteta, Lipiceva 2, 61000 Ljubljana
Uran, D.	Institute J. Stefan, 61001 Ljubljana, Jamova 39

ORGANISATIONS

CERN

Schönbacher, H.	CERN, European Organization for Nuclear Research, 1211 Geneve 23
Voorde, M. H. van de	CERN, European Organization for Nuclear Research, Div. ISR, 1211 Geneve 23

IAEA

Abedin-Zadeh, R.	International Atomic Energy Agency, Dosimetry Section, Division of Life Science, Kärntner Ring 11, P.O. Box 590, A-1011 Vienna
Balamutov, V.	International Atomic Energy Agency, Division of Life Sciences, Kärntner Ring 11, P.O. Box 590, A-1011 Vienna
Labarthe, Jean-Pierre	International Atomic Energy Agency, Division of Health, Safety and Waste Management, Kärntner Ring 11, P.O. Box 590, A-1011 Vienna

WHO

Waldeskog, B.	World Health Organization, Radiation Health, 1211 Geneva 27

LIST OF EXHIBITORS

D. A. Pitman L.T.D.
Mill Works, Jessamy Road, Weybridge, Surrey, England

Teledyne Isotopes
50 Van Buren Avenue, Westwood, N.J. 07675, U.S.A.

Victoreen Instrument Company, Cleveland, Ohio 44104, U.S.A.

Ekco Instruments L.T.D., Southend-on-sea, Essex, England SS2 6PS

Physikalisch-Technische Werkstätten
Dr. Pychlau KG, 7800 Freiburg, Lörracherstrasse 7, Western Germany

Harshaw Chemie mv. De Meern, Holland

VEB R.F.T. Messelektronik, 8016 Dresden, Postschliessfach 14, DDR

Saphymo, 51 Rue Amiral Mouchez, Paris 13, France